System Level Dispersion Analysis Examining Program Benefits to a Low-Thrust Interplanetary CubeSat from Autonomous Guidance and Navigation

by

Dianna M. Velez

B.S., Aerospace Engineering
Worcester Polytechnic Institute (2013)

Submitted to the Department of Aeronautics and Astronautics
in partial fulfillment of the requirements for the degree of

Master of Science in Aeronautics and Astronautics
at the
MASSACHUSETTS INSTITUTE OF TECHNOLOGY

September 2016

Author: Signature redacted
Department of Aeronautics and Astronautics
September 2016

Certified by: Signature redacted
Philip D. Hattis, Ph.D.
Laboratory Technical Staff
The Charles Stark Draper Laboratory, Inc.
Technical Supervisor

Certified by: Signature redacted
Jeffrey A. Hoffman, Ph.D.
Professor of Aeronautics and Astronautics
Thesis Advisor

Accepted by: Signature redacted
Paulo C. Lozano, Ph.D.
Associate Professor of Aeronautics and Astronautics
Chair, Graduate Program Committee

System Level Dispersion Analysis Examining Program Benefits to a Low-Thrust Interplanetary CubeSat from Autonomous Guidance and Navigation

by

Dianna M. Velez

Submitted to the Department of Aeronautics and Astronautics
On August 18, 2016, in partial fulfillment of the
requirements for the degree of
Master of Science in Aeronautics and Astronautics

Abstract

Ground based measurements through the Deep Space Network (DSN) are unlikely to be available as often for CubeSats as for prior deep space programs because higher priority missions will take precedence for access to the limited and expensive DSN resource. Consequently, to make the most of CubeSats in deep space, dependence on the ground must be minimized. In this research a closed-loop Linear Covariance (LinCov) analysis was performed to quantify the effects of the guidance and navigation (GN) system on trajectory dispersions for a low-thrust CubeSat in route to entry-interface conditions at Mars. Applicable mission plan concepts, appropriate analysis settings, as well as required mission performance used in the analysis were based on input collected from industry as well as criteria from prior Mars missions and the Deep Space 1 mission. Information was gathered regarding expected ground-derived orbit determination accuracy levels as a function of decreased DSN use. Optical navigation based on line-of-sight measurements of Mars was then investigated as a means to maintain onboard navigation accuracy despite reduced DSN coverage. The ability of onboard optical navigation to reduce needed ground tracking frequency and associated costs was found practical for interplanetary cruise. The expected resulting financial benefits from decreased DSN were quantified. Recommendations for onboard GN system capabilities and mission goals are made. LinCov was also explored as the core of a basic onboard mission planner that could enable more autonomous CubeSat interplanetary trajectory management.

Thesis Supervisor: Jeffrey A. Hoffman
Title: Professor

Thesis Supervisor: Philip D. Hattis
Title: Laboratory Technical Staff, CSDL

Acknowledgements

Above all others I thank my immediate family for their love and support. My mother for being an amazing example of perseverance and hard work, my father for sharing with me his wonder for space, my siblings for their friendship which is the deepest I know, and all of our dogs for being dogs.

The United States of America and the activists since its founding which have pushed and continue to push for progress and opportunities for all. The principles of this country not just allow but encourage people to speak out for a better way and participate to make such goals a reality. As a woman, person of Puerto Rican heritage, 2nd generation (mainland) American, 1st generation college graduate the philosophies of the U.S.A. make my life better than it could be in any other place or time in history. I will work to keep the spirit of this country, of progress and opportunity due to liberty and justice for ALL, safe to assure that future generations of American can also be in the best place and time in history.

Pine Bush Central School District for a great start to my education. The Hudson Valley and the lifelong friends I grew up with there for my first and best adventures. Worcester Polytechnic Institute for the best education, both formal and informal, a person could receive while also finding themself. My best friend for always being down for a show, be it a concert or television. Draper Laboratory for the coop positions during my time at WPI which gave me inspiration, opportunities, and amazing mentors such as Peter Kachmar, Linda Fuhrman, Donna Jean Kaiser and too many more to name. My dear MIT friends - your comradery made it possible to reach the end of this long journey.

The Charles Stark Draper Laboratory, Inc. for the Draper Fellowship which funded my time at MIT. My MIT advisor Dr. Jeff Hoffman for asking in-depth questions which showed me where I should focus my studies. My Draper supervisor Dr. Phil Hattis for providing more context and lessons of GNC and space exploration, process advice, and moral support. My Draper technical advisor Dr. Dave Woffinden for the expert linear covariance lessons, analysis program scoping, and endless optimism. Dr. Chris D'Souza of NASA for discussions on mathematical representations of guidance algorithms, EI, B-Plane, and STM propagation. Dr. Shyam Bhaskaran of JPL for vital details on DS1, DSN, OD, and AutoNav.

The Lord of the Rings movie trilogy, enjoyed numerous times while I stayed in to work, for showing that the hard trial is worth it in the end and that the support of one great friend makes anything possible.

"Yet it is not our part to master all the tides of the world, but to do what is in us for the succor of those years wherein we are set, uprooting the evil in the fields that we know, so that those who live after may have clean earth to till." – Gandalf [The Return of the King – 1954 book]

"It's all wrong. By rights, we shouldn't even be here...but we are. It's like in the great stories Mr. Frodo; the ones that really mattered. Full of darkness and danger they were. And sometimes you didn't want to know the ending. Because how could the end be happy? How could the world go back to the way it was when so much bad had happened? But in the end, it's only a passing thing... a shadow. Even darkness must pass. A new day will come and when the sun shines it will shine out the clearer. Those are the stories that stayed with you, that meant something. Even if you were too small to understand why. But I think, Mr. Frodo, I do understand. I know now. Folk in those stories had lots of chances of turning back only they didn't. They kept going." – Samwise Gamgee [The Two Towers – 2002 movie]

Thank you to all of my Gandalfs, but especially to all of my Sams. To the former for the knowledge needed to pick the right paths, to the latter for the heart to keep going.

Table of Contents

List of Figures

List of Tables

List of Acronyms

3D	Three Dimensions
4-MSPA	4 Multiple Satellite Per Antenna
6U	6-Unit
ACS	Attitude Control System
AF	Aperture Fee
AGNC	Automated Guidance Navigation and Control
AMMOS	Advanced Multi-Mission Operations System
AU	Astronomical Unit
AutoNav	Autonomous Navigation
BCT	Blue Canyon Technology
BLS	Batch Least Squares
B-Plane	Body Plane (also known as the miss distance plane)
BR	B-Plane triad direction unit vector
BT	B-Plane equatorial direction unit vector
BWG	Beam Wave Guide
CCD	Charged Couple Device
COTS	Commercial Off-the-Shelf
DDOR	Delta-Differenced One-way Ranging
DI	Deep Impact
DS1	Deep Space 1
DSN	Deep Space Network
E-48	Entry Minus 48 Hours
EDL	Entry, Descent, and Landing
EI	Entry-Interface
EM-1	Earth-Moon 1
EMTG	Evolutionary Mission Trajectory Generator
ESA	European Space Agency
EXEC	Executive
FBLT	Finite-Burn Low Thrust
FDIR	Fault Detection Isolation and Recovery
FPA	Flight Path Angle
FPGA	Free Programmable Gate Array
FTOA	Fixed Time of Arrival
GEO	Geosynchronous Orbit
GN&C	Guidance Navigation and Control
GNC	Guidance Navigation and Control
HEF	High Efficiency
HSB	High-Speed Beam Waveguide
ICAP	IND Customer Assistance Package
IND	Interplanetary Network Directorate

INSPIRE	Interplanetary NanoSpacecraft Pathfinder In Relevant Environment
IPS	Ion Propulsion System
Isp	Specific Impulse
ISSC	Interplanetary Small Satellite Conference
JPL	Jet Propulsion Laboratory
L1	Lagrangian 1 Point
L5	Lagrangian 5 Point
LEO	Low Earth Orbits
LinCov	Linear Covariance
LQG	Linear Quadratic Gaussian
LQR	Linear Quadratic Regulator
MarCO	Mars CubeSat One
MC	Monte Carlo
MGALT	Multi Gravity Assist with Low-Thrust
MGSS	Multi-Mission Ground Systems and Support Program Office
MIR	Mode Identification and Recovery
MM	Mission Manager
mN	milliNewton
MRO	Mars Reconnaissance Orbiter
MSPA	Multiple Spacecraft Per Antenna
NASA	National Air and Space Administration
NEAScout	Near-Earth Asteroid Scout
NEO	Near-Earth Objects
OANM	Onboard Autonomous Navigation and Maneuvering
OD	Orbit Determination
OMP	Onboard Mission Planner
OpNav	Optical Navigation
PDR	Preliminary Design Review
Ph.D	Philosophical Doctorate
PS	Planner/Scheduler
PSD	Planetary Science Division
RA	Remote Agent
RSS	Root Sum Squared
S/C	Spacecraft
SDRE	State Dependent Riccati Equation
SMD	Science Mission Directorate
SNOPT	Sparse Nonlinear OPTimizer
SOI	Sphere of Influence
SSC	Small Satellite Conference
SSI	Solid-State Imaging Subsystem
STK	Satellite Tool Kit
SW	Software
TCM	Trajectory Correction Maneuver

TRL	Technology Readiness Level
VTOA	Variable Time of Arrival
XATM	Crossing into of the Mars Atmosphere
XSOI	Crossing into of the Mars Sphere of Influence
ΔV	Delta Velocity

1 Introduction

1.1 Problem Statement

CubeSats have been used in Earth orbit for over two decades now. Their missions have progressed from simple technology demonstration to Earth science applications with increases in mission complexity and duration. There is interest in having CubeSats move from low earth orbits (LEO) to interplanetary trajectories. This is a new concept with a few programs coming online over the next several years. NASA, ESA, and private organizations are looking to CubeSats to support upcoming lunar, near-earth objects (NEOs) and Mars missions for the first time. As such, there is not much heritage for engineers to base their plans on.

This thesis will go over a method to provide system level information for the guidance and navigation system of a CubeSat mission to Mars. The overarching goal of this thesis is to define baseline strategic guidelines to support development decisions and design concepts for CubeSats that can reach entry-interface conditions after interplanetary transit with confidence that onboard capability meets mission needs. In doing so, it is explained how to reduce DSN usage by application of a method onboard a CubeSat that can increase autonomy, and why that method is reasonable.

1.2 Relevant Background

The Deep Space Network (DSN) is used to monitor the progress of interplanetary spacecraft and provide command updates to their trajectory plans. Guidance solutions are calculated on the ground and then uplinked to the craft. DSN is a limited and in-demand resource that is generally overbooked. It is expensive to use, with an initial setup cost with subsequent costs for each use. Limiting the use of DSN would provide a cost-saving measure, which is especially critical for CubeSats. To do so it must be assured that any onboard system can successfully perform the operations typically performed on the ground.

The Deep Space 1 (DS1) mission was a major demonstration for onboard decision making. While the demonstration was limited due to hardware issues, the algorithms were considered proven and the mission an overall success. Since then, advancements in those algorithms have been used as the basis for subsequent missions. That autonomy has typically only been applied when updates to the craft operations plan needed to occur on a time scale shorter than the delays associated with ground control (which included communication delay times due to distance).

CubeSats are significantly less costly than most satellite types. As such, they have been used to try out new technologies with less financial risk. Because of this, they are categorized into a class that is supposed to take on more mission risks. Onboard decision making demonstrations have been limited due to the expense of larger satellite classes and the lack of heritage to provide confidence in its abilities. This makes the CubeSat class ideal for investigating methods for onboard mission planning.

EI is an extremely critical point for any landing mission. EI occurs at an altitude of interest with limited velocity and flight path angle (FPA) variations acceptable. While typically not referred to as entry-interface, aerobraking to put a craft into orbit about a body with an atmosphere involves skimming the atmosphere at specific altitudes with specific velocity and flight path angles as well. As deep space CubeSats is a new mission type, it is not understood how such a system needs to be set up to meet EI conditions of interest. Related to this is an alternate method of placing a craft into orbit about a body with an atmosphere, aerocapture. It only passes through the atmosphere deeply once where as aerobraking barely skims the atmosphere numerous times. Aerocapture's benefit is that it requires significantly less fuel; its drawback is that it requires the most stringent of EI conditions and has not been demonstrated. A CubeSat mission to demonstrate aerocapture technology could increase confidence that a full demonstration on a larger platform is warranted. In general, increased EI management capabilities for onboard flight platforms would be beneficial for small payload delivery regardless of whether it was used for landing or orbit insertion.

On CubeSats, as with all space missions, efficient use of propellant is mandatory. Currently, the most efficient thrusting systems used electric propulsion. There have been limited applications to date of low-thrust electric propulsion on standard satellite platforms. Use of electric propulsion on CubeSats is of extreme interest. Multiple manufacturers are developing electric propulsion thrusters suitable for CubeSat use, including private companies and universities. [1] Electric propulsion is a viable option for long-duration mission CubeSats.

Linear Covariance (LinCov) is an analysis tool that provides insight into the divergence of a system from its nominal performance. The relationships between system model parameters are set and the statistics of their relationships are updated and propagated along a trajectory. This feature means LinCov can be used to quantify the effects of various system design decisions. With the emerging technologies for CubeSats and new use cases, LinCov can be helpful in determining whether a particular mission is viable. It is possible that, in conjunction with other onboard features, LinCov can be used to support increased autonomy and therefore lower mission costs.

1.3 Thesis Overview

CubeSats are first examined. This includes an overview of their history, and new frontiers for their use. The motivation for onboard autonomy will be discussed next. This involves gaining an understanding of traditional navigation and orbit determination (OD) techniques. Some detail will be provided on the different ways to use DSN. Then, some historical mission use of DSN will be shown and an estimate of the associated cost for such use will be calculated. The limitations associated with the traditional methods will serve to conclude why onboard autonomy is of interest.

With the motivation for increasing onboard autonomy understood, autonomy to date is reviewed. This includes analyses completed about the state of Guidance, Navigation, and Control (GNC) autonomy in space and recommendations for how to move forward. Some terminology will be clarified to show the different type of onboard needs that can be filled. Deep Space 1 will be used as a case study to show the planned onboard intelligence mission planner and the actualized autonomous subsystem planner. Overall mission planning will be discussed as well.

Needed mission autonomy features will then focus heavily on optical navigation. This includes how it works at a fundamental level, a historical overview of some of the high profile missions which have used it in deep space settings, and the advantage it produces. Onboard autonomy is examined in this section as well. A few missions have experimented with different levels of onboard autonomy. These missions will be noted, including the conditions under which onboard autonomy was actually used.
Methods and assumptions for simulating the focus areas are explained. The operation of a tool for deriving a nominal trajectory is summarized as well as a trajectory dispersion analysis tool. An investigation of a variety of deep space missions was performed to provide a deeper understanding of deep space navigation and guidance. This included the analyses performed during planning for possible

missions, the preflight analyses used to make system decisions, and post-flight analyses of successful missions. The preflight analyses were used to find information about the type of considerations that have been a part of deep space mission characterization. The flight experience analyses summarize the effects of actualized plans. For all, the navigation and dispersion requirements at the destinations were tracked. When available, information on the requirements along the trajectory was tracked as well, especially the dispersions accepted at various points. LinCov, the simulation used for the dispersion analysis, is thoroughly explained. This includes the generic mathematical expressions used in the analysis and their flow such as the state variables, covariance propagation, and observation model features.

Various attributes of the navigation portion of the simulation are detailed. The observation models include optical measurements and ground updates. The simulation's guidance features are also detailed with different guidance algorithms characteristics explained, including the conditions for their use.
The baseline nominal trajectory basis, as well as it navigation and guidance design options are explained. The navigation options fall into two categories: 1) a version that use ground-derived updates only; and 2) a version reliant on ground-derived updates and optical line-of-sight measurements. The navigation performance requirements, cost considerations, and results are summarized for each of the options. Afterwards, alternate guidance methods are explored against the same baseline missions.

Finally, variations to the system performance are explored. This includes consideration of the effects of modified navigation measurement schedules, modified trajectory correction schedules, and thruster errors. There is also an overview of the need for a backup onboard mission planning capability.

2 Beyond LEO CubeSats

A review of advances in CubeSat technology, recent missions, and upcoming missions enabled a determination of the areas where headway has been made and some important holes that still need to be filled. This included a review of material from two conferences; the Small Satellite Conference (SSC) and the Interplanetary Small Satellite Conference (ISSC). Many of the projects addressed at these conferences involve the advancement of components. Control oriented projects were generally focused on maintaining formation flight, increased pointing accuracy, or attitude determination and control. Determination of the optimal trajectory was also of frequent interest. More recently, several CubeSat missions beyond LEO have been announced, which shows faith in the viability of CubeSats for this mission class.

2.1 Missions Planned

One such mission is MarCO, for which two CubeSats will be perform a flyby of Mars to provide communication support to the InSight mission. This program was supposed to launch in March 2016 providing a relevant example of the capabilities of CubeSats in deep space, but has been delayed because of issues with the InSight spacecraft. The 6U MarCO CubeSats use cold-gas propellant to enable up to four impulsive-class trajectory correction maneuvers. "During cruise, navigation and tracking will be performed by DSN several times per week, and operators will continue to monitor health and prep for the EDL flyby." [2] It is important to note the research areas it still leaves open. One is that it uses an impulsive propulsion system, and the other is that the navigation is going to be performed solely from the ground. In addition, the CubeSats are performing a flyby as opposed to achieving an entry-interface goal.

Another relevant mission which was briefly mentioned above was Near-Earth Asteroid Scout (NEAScout), which will use a solar-sail for propulsion and will investigate near-Earth asteroids after launch in 2018. During the cruise and initial approach phase NEAScout will take images of the target with reference stars in the background to support navigation. The images will be cleaned up onboard with "frame co-adding color and ephemeris determination" [3]. The optical software onboard will be used exclusively to take images and improve their quality. Among those images, the best would be selected to be sent to the ground team. The ground team would use the optical images as an additional data source for their orbit determination work. During the approach phase of its operations, NEAScout would have limited ability to decide asteroid features to investigate. This is to be done based on searching the processed images for features scientist deem to be of interest. [4]

The INSPIRE mission, developed in 2014 with launch likely in 2017, may provide some important information for NEAScout. INSPIRE will take images of the Moon [5] or Earth [6] [7] to identify the body in a star field. While the images could be processed in the way that is planned for NEAScout (to provide orbit determination from the ground) it does not appear that will be the case. "An advancement of this technique [image sequencing with time tags to determine location], enabled by the large computing capacity available on board with solutions such as the Field Programmable Gate Array (FPGA) and its memory... bring the possibility of loading an ephemeris of viewable natural objects into memory and performing some fraction of navigation onboard with a degree of autonomy" [5].

2.2 Missions Desired

An area of development that was found to be lacking at both SSC and ISSC was guidance and navigation software for the cruise and approach portions of trajectories. This was likely due to programs assuming that they would be able to utilize DSN as needed. Section 4.1.1 and especially Section 4.1.1.3 provide information for why this assumption is not just unlikely but dangerous to a program's prospect for success. The limited availability of DSN resources also makes it very expensive. Most CubeSat programs have limited budgets so the ability to afford classic levels of DSN use is questionable.

DSN is used to track crafts to provide navigation information and then uplink guidance solutions calculated on the ground. As such, a lack of research into how programs should compensate for the inability to use this resource as desired is a major hole in the path to realizing interplanetary CubeSats. Because of this, there is significant desire for a CubeSat capability with a higher degree of onboard autonomy than previously experienced. The desired mission capability would minimally be able to perform some of its navigation analysis to be aware of its inertial position and then make some guidance decisions for localized path planning. These two features would both lessen the amount of DSN tracking required and also reduce the time spent by the ground time.

A proposed, representative mission concept is a 6U CubeSat starting at the Earth-Sun L1 point, about 1.5 million km from Earth, and targeting the Earth-Sun L5 point about 1 AU away [7]. The desired mission goal would be a full demonstration of AutoNav, the onboard autonomous guidance and navigation program first implemented on Deep Space 1, onboard a CubeSat. Orbit determination accomplished onboard would be possible with optical navigation data. Optical navigation data would be used, as opposed to DSN providing Doppler and range information. Onboard the craft the navigation data would be processed for orbit determination, which would then be used to autonomously solve and execute a guidance solution. The use of AutoNav would occur throughout the trajectory. This is a key difference from the missions described in the prior section: NEAScout and Inspire will use a subset of AutoNav features once they are close to their targets, but not for the duration of their missions.

3 Thesis Focus Areas and Rationale

The prior section showed that the deep space CubeSat research performed so far has not focused on guidance and navigation needs. Planned, near-term deep space CubeSat missions have little to no autonomy, and there is a stated desire for an autonomous guidance and navigation demonstration on a deep space CubeSat. This shows that the system-level guidance and navigation investigation addressed in this thesis is a contribution to the field in general, with the focus areas selected to maximize the usefulness of its results for interplanetary CubeSat development.

3.1 Navigation Contributions

Prior interplanetary missions were primarily dependent on DSN. It is of interest to lessen the dependence on the ground for navigation and guidance solutions through onboard autonomy. This begins with the use of onboard navigation techniques. Optical navigation can provide the position information needed for orbit determination.

First and foremost an understanding of a navigation regime that can provide accurate information capable of meeting interplanetary mission knowledge requirements is needed. An examination of various navigation regimes was performed to determine their resulting accuracies. The navigation contributions include: a proposed alteration to the ground team responsibilities to decrease the man hours associated with DSN use, an examination of the effects caused by decreasing DSN usage compared to similar prior missions, and an examination of the benefits of including optical data in determining the navigation solution.

3.2 Guidance Contributions

Once navigation data has been collected mission staff currently use it to solve for a maneuver sequence to uplink to the craft. The vast majority of spacecraft have effectively been blind to the desired inertial state trajectory requirements. Historically, onboard determination and control responsibilities have been limited to orienting the craft's body to assure the proper pointing of solar panels, science instruments, etc.

The second portion of desired onboard autonomy is to use the navigation solution to determine the path needed to meet mission requirements. In this investigation it is assumed that an acceptable nominal trajectory was determined on the ground and that waypoints with desired state details would be stored onboard the craft. These waypoints would be used by the onboard guidance program to solve for the desired path in real time based on the craft's current state.

The primary guidance contribution is the resulting information concerning the relationship between the knowledge accuracy provided by navigation and the corresponding physical dispersion when a particular guidance algorithm is used. An understanding of this relationship for an interplanetary CubeSat case provides several benefits for the field.

One benefit is the ability of a program to consider the expected level of dispersions at the start of the program during the concept of operations. Since the use of CubeSats on interplanetary trajectories is a new field, details about the relationship between guidance, navigation, and expected dispersion are not readily available. There are two main scenarios where an understanding of the navigation and guidance relationship for interplanetary CubeSats is beneficial in this way. The first involves the needs of science instruments for which the combined navigation regime and guidance algorithm would be used to assure that the experiments' dispersion limits are met. The second involves selection of a science mission that can still obtain useful data given the expected dispersions. In the former case the results of research in this thesis would provide information about the resources needed to finance use of instruments defined for a mission; in the latter case the findings of this thesis research would provide information about what science it can accomplish with the resources it expects to have. The second case, in which a science mission is selected based on expected dispersions, is especially exciting because it may enable an interplanetary CubeSat with onboard autonomous features to occur sooner than it might otherwise. This is due to the opportunity this research provides to match a science instrument having autonomy needs with projected onboard autonomy technology capability. Such a resulting mission would enable a flight demonstration to move forward and increase the Technology Readiness Level (TRL) of onboard CubeSat navigation and guidance.

Another benefit of an understanding of the relationship between the combined navigation and guidance selections' resulting dispersions is to provide information about when a new reference trajectory may be required for a mission. The nominal reference trajectory and its defined waypoints at the start of the mission may become unsustainable for a variety of reasons. A new nominal trajectory may need to be uplinked to the craft or, depending on the onboard resources available, solved for in real time. Having the ability to quantify the dispersions caused by the current reference trajectory, navigation plans, and guidance capability can show a point along the trajectory where switching to a more up to date reference trajectory would be necessary. This could be, for instance, when the current dispersions are considered too large for the prior reference trajectory to remain valid or when the predicted, resulting dispersion at a point of interest does not meet science requirements. With this dispersion knowledge, rooted in an understanding of the relationship between navigation and guidance, a new reference trajectory can be determined and made available beginning at a predefined point with it and its waypoints stored onboard. If a ground team is needed to define a new reference trajectory due to limitations in processing and algorithmic capabilities available onboard the spacecraft, under this paradigm they could have a new reference trajectory ready at a predefined point, only needing to uplink waypoint state information. The determination of detailed maneuver sequences would not be the responsibility of the ground team, as the onboard guidance system would take care of that portion of the work. As lessons were learned from the initial onboard guidance experiments more automated systems could be integrated onto a platform and further lessen the work required of a ground team.

3.3 Low Thrust Focus

The majority of interplanetary missions to date have used impulsive chemical thrusters as opposed to continuous low-thrust electric propulsion. Because low-thrust electric propulsion is very efficient, it is of interest for deep space exploration in general and especially for CubeSats which have limited available mass and volume allocation. There are various developers of low-thrust technology, but it has seen very limited experience as the primary means of propulsion for interplanetary trajectories. The nominal trajectory for a spacecraft using low-thrust electric propulsion was defined for this analysis. The low-thrust focus of the dispersion analysis provides insight into the potential performance of a new propulsion option still under development. The results can be used to help define requirements for thruster capabilities and scoping of missions which use them.

3.4 CubeSat Focus

As previously mentioned, high DSN usage gets expensive fast. Despite this, few programs are willing to risk larger, more expensive missions due to potential issues from attempting use of onboard autonomy when ground oversight is tried and true.

There are a multitude of reasons why people are interested in using CubeSats for deep space exploration, the main one being that the platform is relatively inexpensive compared to traditional satellite platforms. This makes CubeSats a natural test bed for deep space missions with increased autonomy. The CubeSat platform provides a method to try onboard autonomy to increase experience with its use and guide future improvements. With the lessons learned from CubeSat demonstrations of deep space onboard autonomy, researchers can use the resulting flight experience to justify its use on more expensive missions.

With a focus on CubeSats, there are some resulting guidelines for the initial flight experiments on deep space missions. The reference trajectory, on top of being defined with low-thrust electric propulsion, was also defined with consideration of CubeSat-class volume, mass, and onboard resources constraints. The finding is that the needed onboard capability is not very computationally demanding. Currently, there is not a standard autonomous system design for CubeSat guidance and navigation. Because the processing needs to quantify dispersions is not computationally demanding, it would be possible to use some version of it as an onboard mission planner for a CubeSat. Onboard a craft the dispersion results for a variety of scenarios could be computed. The results could then be checked against a set of program goals to determine which result is most desirable and thus should be implemented. An onboard mission planner with low computational needs is desirable in general. It is a benefit to the CubeSat platform especially because one of the currently applicable resource limits is processing capability.

4 Onboard Autonomy

4.1 Motivation

4.1.1 Past and Current Satellite Position Determination, State Estimation and Guidance Methods

DSN was developed to provide a means for deep space mission communication and navigation. By tracking spacecraft transmissions, DSN can provide Doppler, range, and range rate information. There are three DSN complexes spaced around the world so that as the world turns a spacecraft will be able to stay in communication with the network. These DSN complexes each have one 70-meter antenna, one high-efficiency 34-meter antenna, and one or more beam waveguide antenna, which is 34m for deep space tracking. For tracking Earth-orbiting spacecraft each complex has a 26-meter dish.

With DSN, three types of measurements can be produced: Doppler, range, and Delta-Differenced One-way Ranging (DDOR). Doppler data provides range-rate information by tracking the transmitted and received frequencies from the spacecraft to the ground antennas; this provides line of sight velocity information. Range data provides the line of sight position information by analyzing the round-trip light time between radio signals. DDOR uses two DSN stations at once and a reference radio source (quasars) to determine the angular separation between the spacecraft and the quasar. The in plane-of-the-sky spacecraft position is known with the DDOR measurement. When only Doppler and range measurements are used additional dynamic models are needed to know all of the position coordinates. When DDOR is also used all three position coordinates are known, as DDOR is orthogonal to the Doppler and range measurements. More details on the specifics for how each measurement type works can be found in [8].

Missions reliant on DSN utilize many tracking passes. The tracking data is analyzed on the ground and decisions are made about needed trajectory updates. Once trajectories updates are finalized, they are uploaded to the spacecraft in the form of command sequences. How frequently DSN passes occur to collect trajectory data and to provide command sequence uplinks is affected by the phase of the mission. In Table 1 the use of DSN Doppler and range tracking by mission phases are detailed. Table 1 and Table 2 note the use of DSN for DDOR measurements.

Table 1: DSN Doppler and Range Tracking Comparison by Mission Phase for Various Missions

Phase	Time Period	Tracking Frequency
	Pathfinder [9]	
Launch	L+0 d to L+30 d	3 passes/day
Cruise	L +30 d to M-45 d	3 passes/week
Approach	M -45 d to M-0d	3 passes/day
TCM Coverage	TCM-3 d to TCM+3 d	1 pass/day
	Surveyor [10]	
Launch	L+0 d to L+30 d	3 passes/day
Cruise	L +30 d to M-45 d	3 passes/week
Approach	M-45 d to M-0d	3 passes/day
TCM Coverage	TCM-3 d to TCM+3 d	1 pass/day
	Spirit – Mars Exploration Rover [11]	
Launch	L+0 d to L+30 d	L+0 d to L+30 d
Cruise	L +30 d to M-45 d	L +30 d to M-45 d
Approach	M-45 d to M-21 d	M-45 d to M-21 d
Final Approach	M-21 d to M-0 d	M-21 d to M-0 d
TCM Coverage	TCM-3 d to TCM+3 d	TCM-3 d to TCM+3 d
	Opportunity – Mars Exploration Rover [11]	
Launch	L+0 d to L+30 d	3 passes/day
Cruise	L +30 d to M-45 d	3 passes/week
Approach	M-45 d to M-35 d	~2 passes/day
Final Approach	M-35 d to M-21 d	~2.5 passes/day
End Approach	M-21 d to M-0 d	~3 passes/day
TCM Coverage	TCM-3 d to TCM+3 d	1 pass/day
	Phoenix [8]	
Launch	L+0 d to L+14 d	3 passes/day
Cruise	L+15 d to M-60 d	3 passes/week
Approach	M-60 d to M-0 d	3 passes/day
TCM Coverage	TCM-4 d to TCM+4 d	3 passes/day
	Curiosity - Mars Science Laboratory (MSL) [12]	
Launch	L+0 d to L+30 d	3 passes/day
Cruise	L+30 d to M-67 d	3 passes/week
Approach	M-67 d to M-0d	3 passes/day
TCM Coverage*	TCM-4 d to TCM+4 d	3 passes/day

Table 2: DDOR Tracking Mission Comparison

Time Period	Tracking Frequency
Mars Exploration Rovers – Spirit & Opportunity [11]	
L+21 d to M-45 d	1 pass/week
M-45 d to M-28 d	2 pass/week
M-28 d to M-8 d	1 every other day
M-8 d to M-0 d	1/day
Phoenix [8]	
L+36 d to L+42 d	1 pass/day
L+64 d to M-60 d	1 pass/week
M-60 d to M-18 d	3 pass/week
M-18 d to M-0 d	2-3 passes/day
Curiosity - Mars Science Laboratory (MSL) [12]	
L+30 d to M-67 d	1 pass/week
M-67d to M-28 d	2 passes/week
M-28 d to M-0 d	2 passes/day

Tracking measurements performed with DSN is the primary method of navigation for missions historically. Some missions have incorporated different levels of optical navigation for additional support. When optical navigation was introduced the images were returned to the ground for processing. A few missions have processed images onboard to make their own guidance decisions. The specifics of optical navigation and the missions which used it are in Section 5.1.

4.1.1.1 DSN Usage Cost

To setup the use of the DSN there is an initial standard fee. Then there are costs dependent on the number of tracking stations used, the frequency of their use, and the length of time they are used. These are referred to as the DSN aperture fee. While NASA missions do not pay for this directly (it is part of institutional overhead), other missions need to do so. DSN costs include engineering support as well as space communication and navigation data services.

Among the DSN-user fee factors applicable to all paying users are the following: first use; telemetry; mission-specific tracking and commanding; mission-specific services; DSN operations; special/unique requirements; ground communications; and radio frequency compatibility testing. There are a variety of standard services, but there are also tailored services available for specialized missions. Tailored services have additional costs which must be negotiated. [13]

For Aperture Fee estimation the following formula is provided [14] with the variables defined in Table 3.

$$\mathbf{AF} = \mathbf{R_B}[\mathbf{A_W}\left(\mathbf{0.9} + \frac{\mathbf{F_C}}{\mathbf{10}}\right)] \tag{1}$$

Table 3: Aperture Fee Equation Variables [14]

Variable	Definition
AF	Weighted Aperture Fee per hour of use
R_B	Contact-dependent hourly rate, adjusted annually ($1057/hr. for FY09)
A_W	Aperture weighting = 0.8 for 34-meter High-Speed Beam Waveguide (HSB) station = 1.00 for all other 34-meter station (i.e. 34 Beam Wave Guide (BWG) and 34-meter High Efficiency (HEF)). = 4.00 for 70-meter stations
F_C	Number of station contacts, (contacts per calendar week)

Using Figure 1, below, an aperture fee approximation can be determined. The red line is the 70-meter antenna, the blue line is the 34-meter BWG and HEF antennas, and the green line is the 34-meter High-Speed Waveguide antenna.

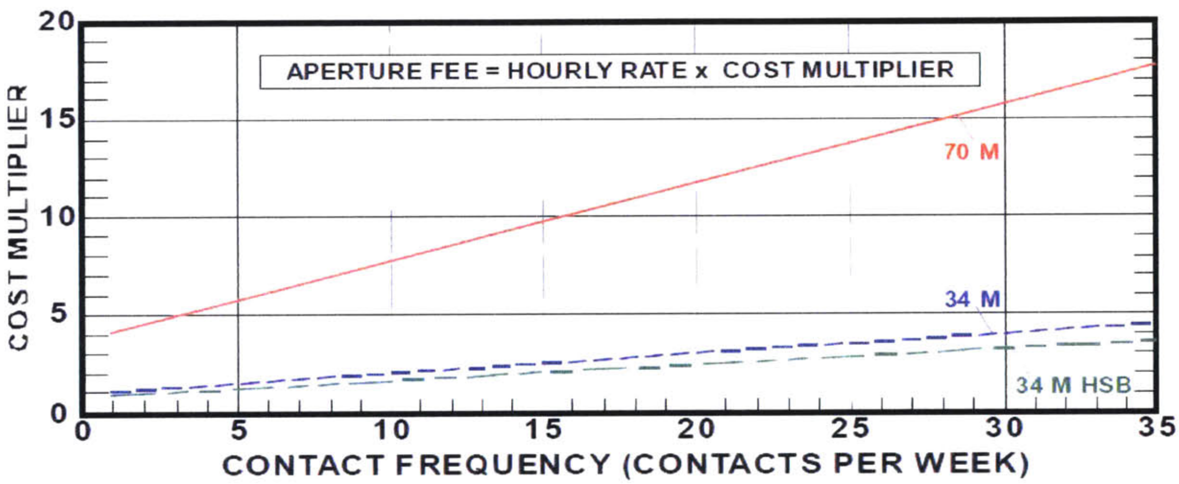

Figure 1: Aperture Fee Approximation [14]

To determine the cost by hour using Figure 1 take the number of contacts per week, go to the antenna of interest to find the cost multiplier, then use the multiplier on the current fiscal year per hour cost. If it was known that 28 contacts per week were desired with the 70m antenna, a cost multiplier of approximately 15 is used. With the Aperture Fee (AF) estimate of $1057/hr and this cost multiplier, an hour of DSN use would be $15,855. Following the AF equation results in a similar cost of $15643.6/hr compared to the graph estimate with the same conditions. It needs to be noted that one hour's cost must be added to each DSN track pass (regardless of its duration) to account for DSN link connection and removal time.

With the data from Table 1 and Table 2 along with the Aperture Fee equation, (1), an estimate of the tracking cost for each mission was determined. Two sets of assumptions were made, as seen in Table 4 and Table 6, with their corresponding cost estimates in Table 5 and Table 7, respectively.

Table 4: Antenna and Duration Assumption 1

Phase	Launch	Cruise	Approach	TCM	DDOR
Antenna	34m	70m	70m	70m	34m
Time	8	8	8	8	4

Table 5: Cost Estimates from the Assumptions of Table 4

Mission	Launch	Cruise	Approach	TCM	DDOR	Total
Pathfinder	\$2,283,120	\$3,522,528	\$13,698,720	\$1,217,664	N/A	\$20,722,032
Surveyor Orbiter	\$2,283,120	\$3,522,528	\$13,698,720	\$1,217,664	N/A	\$20,722,032
Surveyor Lander	\$2,283,120	\$3,522,528	\$13,698,720	\$1,522,080	N/A	\$21,026,448
Spirit	\$2,283,120	\$3,522,528	\$11,770,752	\$1,217,664	\$514,608	\$19,308,672
Opportunity	\$2,283,120	\$3,522,528	\$11,085,816	\$913,248	\$514,608	\$18,319,320

Table 6: Antenna and Duration Assumption 2

Phase	Launch	Cruise	Approach	TCM	DDOR
Antenna	34m	34m	70m	70m	34m
Time	8	8	8	8	4

Table 7: Cost Estimates from the Assumptions of Table 6

Mission	Launch	Cruise	Approach	TCM	DDOR	Total
Pathfinder	\$2,283,120	\$880,632	\$13,698,720	\$1,217,664	N/A	\$18,080,136
Surveyor Orbiter	\$2,283,120	\$880,632	\$13,698,720	\$1,217,664	N/A	\$18,080,136
Surveyor Lander	\$2,283,120	\$880,632	\$13,698,720	\$1,522,080	N/A	\$18,384,552
Spirit	\$2,283,120	\$880,632	\$12,988,416	\$1,217,664	\$514,608	\$16,666,776
Opportunity	\$2,283,120	\$880,632	\$11,085,816	\$913,248	\$514,608	\$15,677,424

While NASA missions do not have to directly pay aperture fees, an externally sponsored mission would have to pay the estimated price. The other DSN related costs are assumed not to be hour-dependent but are incurred if DSN is used at all.

4.1.1.2 Analysis and Staffing Time

When using DSN, after spacecraft data is obtained on the ground, time is needed for its analysis. Generally large teams work together to accomplish both the initial data analysis and application. The associated cost of the highly skilled engineer work-hours is significant. While the analysis is being completed the craft would continue on its path; therefore, the orbit determination results based on the measurement data would be a projection of where the craft is expected to be without the latest data. This section deals with the use of measurement information on the ground to make command decisions.

It will cover both the analysis methods to turn the measurement data into trajectory information and the support personal needed to do so. It will primarily use the Cassini mission as a case study but will point out common processes and those that were needed specifically for Cassini due to the nature of its mission. The Cassini-Huygens Mission used traditional Doppler and range tracking through DSN and optical navigation images, all of which were analyzed on the ground followed by uploads of new maneuver plans.

Before a mission launches, a navigation team helps plan a trajectory. In the planning stages conservative estimates are used for the accuracy of the measurement devices, actuator performance, and other error sources. The end result becomes the reference trajectory that the mission attempts to keep to; the measurements taken of the spacecraft are used to verify the reference trajectory will likely be kept, and if not, action plans are made for corrections. While a maneuver may have been part of the nominal/reference trajectory, the analysis of the measurements (described below) helps fine tune what commands will be sent to the spacecraft.

The process of using measurements to determine the trajectory of a spacecraft is known as orbit determination (OD). "In general, orbit determination is the process of estimating the spacecraft's state (position & velocity) by minimizing (in a least squares sense) the residuals of tracking data observables (relative) to the computed observables based on a dynamic model of the [spacecraft's] motion" [15]. Typically speaking, some version of an epoch state estimation filter is used to estimate the spacecraft's state and to correct details of the environment and targets. When necessary, the output from the filter is used to update the reference trajectory. The necessity of an update is determined in part by covariance studies that show the different dispersions which will occur or can occur based on what is currently happening (based on the best available knowledge), compared to what may happen if certain changes are made. Before the nominally planned maneuvers there is inherently a data cutoff time and then an analysis cutoff time so that the final maneuvers can be approved and implemented. Depending on the program and the phase of the mission, the cutoff time could vary from less than a day to almost a week before the planned maneuver. The orbit determination informs the planned maneuver, which is then fed back into the orbit determination for analysis. Once the maneuver is executed, more data is taken to form an updated orbit determination of what actually occurred by fitting over the prior/expected result. There is handshaking and feedback between different portions of a program to make this possible. An overview of the analysis team relationships is shown in Figure 2.

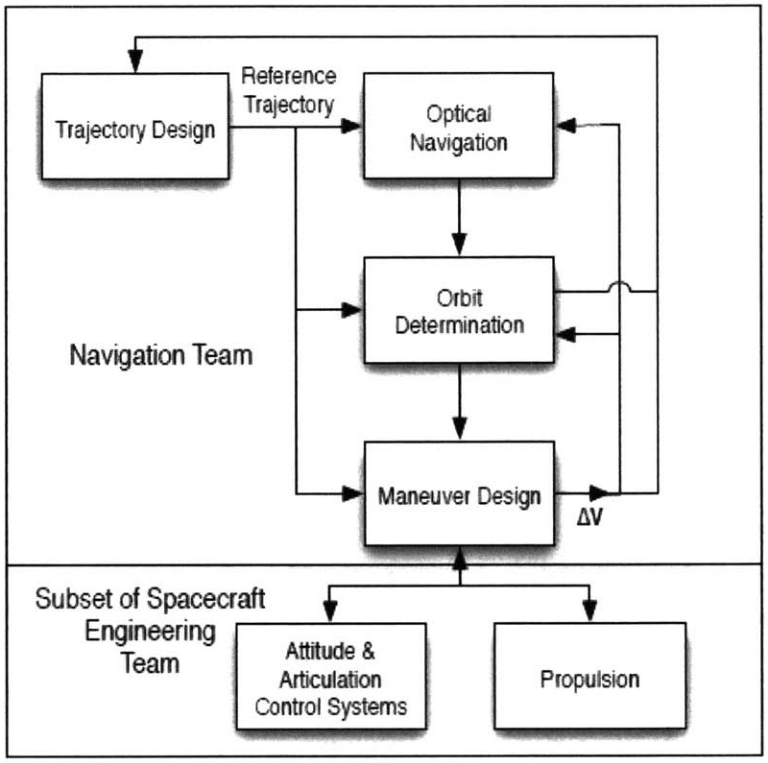

Figure 2: Cassini Navigation Analysis Team Interactions [15]

The Cassini program broke down the OD team's responsibilities into four phases: planning, going online, going into operations, and going offline. These phases would be applicable to any program but the frequency of the need to do so would be mission dependent. "Planning" occurs first and involves using the covariance analysis the program has been enhancing during flight from the conservative pre-flight covariance analysis to improve expectations. "Going online" occurs just as the data arc segment is beginning and is done so the maneuver team can plan ahead to better define the arc for operations. "Going into operations" occurs throughout the arc segment and involves frequent determination of the spacecraft and target conditions. "Going offline" means a new arc segment has begun and the arc segment which was just completed must be analyzed. This provides other teams the ability to make more accurate plans and provides a verification point to check that the orbit determination analysis is functional. [15] These phases are summarized below in Figure 3.

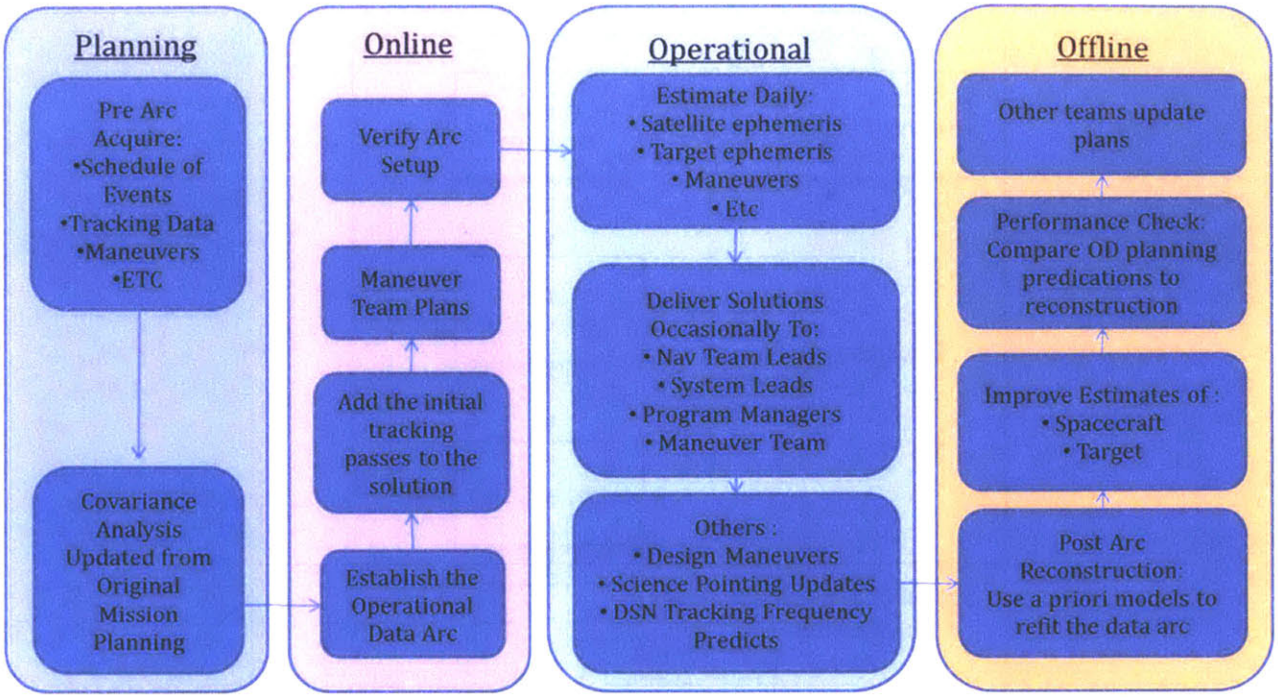

Figure 3: Summary of Orbit Determination Phases

The OD process, for the establishment of an arc is iterative. As new inputs about the condition of the spacecraft and target are provided, and measurement information is applied, the filters are run numerous times "until the corrections in the estimated parameters are very, very small and the pre-fit tracking residuals sum-of-squares closely match that of the post-fit residuals" [15]. This occurs with the reconstructed data from the last offline arc as the *a priori* covariances for the new arc become operational. When operational, the maneuver designs and their accuracy are included into the analysis. The effects of the planned maneuver are projected to points of interest along the current arc, to the next expected maneuver point, and frequently to the desired target. When the planned maneuver meets mission criteria as indicated by orbit determination covariance analysis, it is accepted by program leads, who can define a new reference trajectory.

Staffing needs for orbit determination can be significant depending on the program. As described above, OD is an intensive process that has far-reaching implications for other teams and overall mission success. Cassini's OD team was "relatively large" with "six to seven members and a team manager" [15]. A redundant staff schedule was made, but there was still an expectation that nontraditional business hours would be required with holidays and weekends lost. Advanced degrees, including Ph. D's, were common on the team with several years of experience with astrodynamics and OD as well. With its many arc segments for the many flybys by Cassini of the moons of Saturn, two-member teams rotated responsibility so the orbit determination phase responsibilities could be shared by all. All planned maneuvers required the OD team to support minimally five meetings with the stakeholders, such as the maneuver design and science team.

Cassini used a legacy Jet Propulsion Laboratory (JPL) OD program for its work. "Deep space navigation, particularly the OD operations of Cassini at Saturn, cannot easily be automated due to the complex dynamical environment in which the S/C flies; however, several of the sub-processes are automated"

[15]. There are multiple areas the user interfaces and automated features help to input some data and report outputs. The OD team is responsible for reporting information such as: the converged trajectory, spacecraft ephemeris, target ephemeris, planetary ephemeris, solution parameters, "[spacecraft] state mappings at the first and second encounter target B-Planes and the tracking data used in the fit", "dynamical events important to OD during the arc with a diagram showing the orbital [spacecraft] locations of these events and a table listing them chronologically", and much more. [15] These outputs are shared with other teams. For the OD team's own needs an extensive file management system must be maintained by members so that all have easy access to inputs they need for their segment of analysis. Because of the complexity of the Cassini mission, daily comparisons of experienced and expected dispersions through covariance analysis were considered essential.

4.1.1.3 Resulting Limitations

DSN is in extremely high demand and is a limited resource. Schedules for its use are set extremely far in advanced and are challenging to alter. Should there be any issue with a facility there would be far reaching implications for numerous programs. Should a satellite require the reworking of its scheduled DSN use for any reason, many stakeholders would need to be brought in to reassess how the changes might be accommodated.

Only high priority missions can afford frequent DSN contact. The specific features that DSN can offer for technical support to a given mission have to be negotiated and not all are likely to be within a CubeSat program's budget. Reliance on DSN means coordination between many users for any program using it. This is especially true for CubeSats because of how it is expected for them to interface with DSN. Planned use of DSN requires a program to begin interfacing with its operators very early for scheduling, compatibility, and many other usage requirements. Also, applicable spacecraft-ground communication links demand onboard power allocations.

Because of its heritage and accuracy, combined with the high-costs of the current deep space mission paradigm, all deep space missions make use of DSN. There are currently 28 missions supported in some capacity by DSN and 12 additional missions already planned for future support. [16] While a beyond LEO mission would be extremely important to the program running it, in the larger scheme of things, CubeSats are generally considered to be Class D missions, meaning they have lower budgets, must accept more risk, and are a lower priority than a Class A mission. The lower priority status applies to DSN access. The Orion EM-1 mission will deploy CubeSats as secondary payloads, with many having their own deep space capability demonstration missions. While it is likely all of these missions have planned/scheduled DSN use, "supporting EM-1's primary mission will be the DSN's priority." [17] In addition, "DSN is an oversubscribed resource. Contention levels [disagreement over access rights] for antenna resources can range from 30% - 70% [of those desiring access]. [18]" It can and should be expected that if any Class A, high-priority mission requires DSN in a critical moment, or unexpectedly, then a CubeSat program DSN schedule would be altered.

Depending on the location of two spacecraft, DSN may be able to track and communicate with them over the same aperture pass. This can be used as a cost saving measure for the aperture fee for a multi-craft mission. This type of DSN usage is referred to as Multiple Spacecraft Per Antenna (MSPA). Reference [14] has several examples of how this can work and the cost savings that can be associated with it for the AF. Currently, this is limited to two spacecraft at a time, which split the first and second half of a pass. To support the emerging deep space CubeSat programs that are beginning to come on line, adding in the capability to support 4 satellites at a time, known as 4-MSPA, is being investigated.

This is in part due to CubeSats being secondary payloads which might be released at the same time, subsequently flying relatively close to one another. The more immediate plans for 4-MSPA involve serial uplink between the spacecraft on a shared pass. This would take place on one frequency and coordination among the spacecrafts would be needed for successful DSN usage. Not all spacecraft that would consider shared DSN usage would necessarily be from the same mission, but this method would necessitate careful coordination between the different programs. [19] For example, the communication frequency band selections must avoid usage of common or too-closely-space frequencies during a shared MSPA pass. "The spectrum management for CubeSats is more complicated than (for) most major space systems [20]." This model of use requires CubeSat programs to interface with more stakeholders than a regular program in order to have DSN access.

If a CubeSat part of MSPA experiences any issues, it would have to be skipped over for the next spacecraft scheduled during the pass. A program would need to negotiate with others sharing MSPA serial uplinks if it needs more DSN support to help recover from an issue, and the other programs would be under no obligation to yield their time slots. [21] Initial state knowledge accuracy has propagated effects with respect to navigation errors and dispersions for the duration of the mission. Decreased state knowledge accuracy upon initial acquisition could be catastrophic to a mission. The current plans for DSN shared use by CubeSats could compound a program's troubles should the DSN link schedule work against them.

To deal with the short communication windows made available to CubeSats and other low-budget program, DSN operators are working on different methods to minimize the need for such programs to interact with them over the course of a mission and to decrease costs. The Multi-Mission Ground Systems and Support Program Office (MGSS) manage multiple mission ground support programs. One example is the IND (Interplanetary Network Directorate) Customer Assistance Package (ICAP). ICAP includes Advanced Multi-Mission Operations System (AMMOS), which enables ground system engineers to have a compatible command/telemetry system, a command sequence generator, and some additional features at no cost. In addition, some amount of consulting time is included so the program can learn to use the ICAP without the DSN engineers needing to be called on repeatedly. Not included are navigation and mission design, DSN scheduling, and additional program required capabilities that can be taken care of on their own or purchased from DSN for additional fees. More information on the plans for how to include low priority/low budget CubeSat missions into the DSN schedule may be found in reference [18].

4.2 Benefits of Increased Onboard Autonomy

When taking into account what has been done with guidance, navigation, and control and the desired future path of space missions, some major holes are found in the ability to achieve them. "GNC has progressed in the 60 years of space flight but not enough to perform upcoming missions. Technology investments need to be made in onboard GNC to accomplish the missions proposed for the next decade." [22]

Because of the level of ground dependence in current methods, future missions with more complex navigational needs would be unable to accomplish their goals in the same way. "Onboard autonomous navigation and maneuvering (OANM) techniques are critical for improving the capabilities and reducing the support requirements for many future space missions, and will reduce the dependence on routine position fixes from the Earth, freeing the communication network for other tasks." [23] The benefits of this technology are not limited to one type of mission. Manned missions typically require some level of onboard autonomy as a backup in case of communication failure. Robotic science missions could benefit by allowing more to be supported or by accomplishing new types of missions. Planetary missions can also benefit from increased autonomous GNC by improving the chance of entering the atmosphere with the appropriate conditions and/or by dealing with atmospheric conditions that are unable to be compensated for remotely from Earth. As such, increased onboard autonomy would greatly align with NASA's goals.

There are multiple areas and types of autonomy and intelligent reasoning which can be utilized. Some do relatively simple tasks and do not interface with more than one subsystem. Multiple functions can be integrated together by using some data onboard to make a decision about what to do next. It has been found that the majority of missions which have integrated functional autonomy have occurred primarily in LEO. This is despite the fact that GEO and interplanetary missions would benefit the most from increased autonomy. [24]

4.3 Autonomy to Date

There have been limited example cases of onboard autonomy use on interplanetary space vehicles to date. As described in Section 4.1 significant mission support work is now done on the ground. This involves the orbit determination, maneuver sequencing, task planning, etc., that requires much effort from the ground teams. Onboard autonomy is a way to decrease a mission's needs for DSN usage, as less ground intervention would be required. It would also free up personnel to work on additional missions.

Before continuing it is useful to define the features of an autonomous system versus an intelligent system. "An autonomous system reacts to its external inputs and takes some action without operator control... An intelligent system uses some internal algorithms to emulate a human expert in determining its course of action... If the input is generated automatically by the operational environment and fed into an intelligent system, then you have both an autonomous and intelligent system. [24]" With respect to this work, the majority of the focus is on what may be possible with an autonomous guidance and navigation system. Recommendations and examples of a rudimentary intelligent system applicable to CubeSats are provided in addition.

This section goes over the various reasons to increase onboard autonomy in general, the areas that could benefit from onboard autonomy the most, and some ways that it might be accomplished.

4.3.1 Accomplishing Onboard Autonomy

Multiple reviews on industry progress with respect to increased autonomy use have found "that the majority of implementations take an evolutionary, rather than a revolutionary approach" [24]. Missions with higher levels of autonomy or intelligent reasoning primarily had point solutions for their very specific cases. While researchers can develop different onboard autonomy systems, turning them into black boxes with standard interfaces would allow programs to easily select from different autonomy solutions. The ability to reuse an onboard autonomy program across multiple platforms would allow more examples of its use and increase industry confidence in its ability. Program specific mission inputs would need to be accepted to a software code that would be the same regardless of the mission for a program to be considered reusable. "The onboard navigation software can be a compact, simplified version of the ground software." [22] "Part of the executive system responsibility will eventually need to extend to mission planning, when changes in the environment, the status of onboard components or the forecast trajectory requires changes in the mission plan." [23]

The needs for onboard autonomy development based on the needs of the scientific community most relevant to this paper have been summarized in Table 8.

Table 8: Relevant Findings from Autonomous GNC Industry Survey [23]

Finding	Recommendation
"Advancement in spacecraft autonomous GN&C capability, i.e., the ability to manipulate spacecraft trajectory and attitude autonomously on board in reaction to the *in situ* unknown and/or dynamic environment, is broadly required for next-generation [Science Mission Directorate] SMD [Planetary Science Division] PSD missions aimed to reach and explore scientific targets with unprecedented accuracies and proximities "	"Invest in autonomous GN&C capability, with parallel investments in innovative architectures, innovative and optimized algorithms, advanced sensors and actuators, and system-level demonstrations with relevant physical dynamics and environment conditions."
"Onboard GN&C is performed by systems and not just components. As more complex systems with stringent performance requirements are pursued, the interplay across components, flight dynamics, and physical environment increases. System-level physical test and demonstration systems are necessary"	"Invest in system-level demonstration systems, such as end-to-end GN&C system test-beds, aerial field tests, sounding rockets tests, and free-flying-vehicle-based, closed-loop GN&C system tests."
"Testing capabilities are critical and need to be improved. End-to-end system-level modeling, testing, and simulation are required to flight-qualify newly developed system-level capabilities achieved through incorporation of new technology elements"	"Continue to advance integrated modeling and simulation at the mission capability level, with increasing fidelity matching advancements in component technologies."
"There is substantial commonality in GN&C technology needs across missions. GN&C components and *systems* can be developed and deployed across multiple mission types more effectively and economically than point-design solutions engineered for individual mission scenarios."	"Attention should be paid to GN&C *systems*, not just the individual algorithms, hardware, and software subsystems, because this will allow for reasoned crosscutting trade across functions and missions. SMD provides incentives in the structure of announcements of opportunity such that feed-forward of developments for one project to the next can be maximized."

As can be seen from Table 8, the focus area of this investigation encompasses some of the major needs of the field for deep space exploration dependent on the advancement of autonomous guidance and navigation. This is a broad ranging system level demonstration of guidance and navigation capabilities so that deep space missions have guidelines for onboard autonomous development. In addition, the demonstration of the system level covariance analysis tool for onboard mission planning would meet the need of a reusable program able to intake mission specific parameters without changing the structure of the software setup for different types of missions.

4.3.2 Onboard Autonomy to Date

Unlike optical navigation, onboard mission planning has rarely been demonstrated. The most complete demonstration was Deep Space 1. Subsets of DS1's onboard mission planner were incorporated into the subsequent generations of AutoNav to allow the near-target final approach of asteroid missions to take place without ground in the loop. Another area which has demonstrated limited onboard mission planning has been autonomous rendezvous and docking, such as with the Orbital Express mission. This section will look at Deep Space 1's onboard mission planner and focus primarily on the planning segment. This is due to the extended cruise phase in which DS1 was to utilize autonomous guidance and navigation coupled with onboard mission planning.

4.3.2.1 Deep Space 1 – Intelligence Onboard Demonstration Plan

An artificial intelligence control system was to be central to ensuring DS1 was robust to a variety of on orbit issues. Known as Remote Agent (RA), it was comprised of the Planner/Scheduler (PS), Executive (EXEC), and model-based Mode Identification and Recovery engine (MIR). Together, the RA was designed to allow the ground to send high-level goals as opposed to command sequences, provide failure robustness onboard, and enable better subsystem performance based on awareness of failure. Such features were meant to lower mission costs by decreasing ground intervention in response to failure. These capabilities were meant to decrease DSN usage so that it may be planned to have DSN coverage "only one pass every two weeks." [25]

The PS "provides responses [to failures] that require the ability to look ahead and deliberate about global interactions, whereas the rest of the RA handles real-time failures requiring only local reasoning but quick reactions" [25]. The PS is commented on more thoroughly than the other two portions of RA here; the other two segments will be addressed as needed to provide clarity to PS responsibilities as needed. EXEC and MIR were designed to send low-level commands to device drivers and determine if the devices followed commands so that a fault could be identified and recovery could be made from its effects. PS, on the other hand, worked at a higher mission level. Its purpose was to choose between multiple goals, decide how each should be altered, and set the methods needed to achieve the goals based on the information available at a particular point in time.

PS was to be responsible for two-week segments of cruise. A database of potential actions was provided which PS searched through to fill up the timeline as needed. All actions accounted for needs of the devices utilized, for example antenna pointing before uplinking. While defining a plan, inconsistencies would be identified so any issues could be found early and rectified. This process was base lined to take 8 hours, so the initial conditions PS used were a projection of a future state expected when the new plan was set to begin.

A Mission Manager (MM) feature of RA provided waypoints along the mission timeline, as opposed to the PS two-week timeline. These waypoints set conditions for the PS plan to satisfy so that it did not optimize a two-week segment to the detriment of the overall mission. At the beginning of a planning cycle, the AutoNav system, detailed in the next section, provided navigation and trajectory needs to the PS. The PS coordinated goals from the onboard systems such as AutoNav and the MM using a preset prioritization scheme. [25]

Because PS was meant to respond in real time, the ground would not need to worry about sending extremely detailed actions plans. To ensure fault protection, such plans could be very complex. With PS, "when execution conditions differ so much from initial assumptions that local failure recovery is insufficient, execution of the plan stops and PS is asked for a new plan that takes into account the new situation. Dealing with fault conditions on an as-needed basis simplifies the solution of the fault protection problem." [25] Failures were to be dealt with in two ways "an immediate reactive response and a longer deliberative response. This is typical of many autonomy architectures." [25] The reactive response handled immediate and/or potentially fatal issues and then deliberated a response. During deliberation, impact on goals was assessed to decide how to move forward. The deliberative response information decided if the PS plan was broken, and at which point the PS should replan as needed. If the failure was catastrophic and PS could not meet the goals as prioritized, it placed the spacecraft into a standby mode until the next DSN pass.

The actual flight use of the full Remote Agent on DS1 was extremely limited, but the overall concept definition was important for providing details of an intelligent program worthy of a flight demonstration.

4.3.2.2 Deep Space 1 – Onboard Autonomy Actualized

DS1 provided a significant and successful demonstration of the benefits of onboard autonomous guidance and navigation. The program is referred to currently as AutoNav, short for Autonomous Navigation, though this name is a slight misnomer. AutoNav performs both navigation and limited guidance. Unlike prior missions with optical navigation, AutoNav allowed for the raw images to be processed onboard. The images were edited and their details weighed so that data could be fed into the least squares filter. The filtered results then made OD possible. A conservative scheme was applied for optical data inclusion, where the data was not immediately included for calculation, but instead a representative set was first stored and outliers were removed. The paradigm was that it was better to execute maneuvers based on good data, even if it was old, than to attempt maneuvers based on recent but possibly bad data. Determination of how many images are needed for statistically relevant data to produce the accuracies required involved testing of expected in-flight scenarios prior to launch.

Based on the OD solution, AutoNav then computes and executes maneuvers. The dynamics used for determining interplanetary spacecraft orbital parameters are nonlinear, but can be linearized about a reference trajectory. Linearization solves for the orbital parameter deviations. A spherical model of the spacecraft can be used in the equations of motion despite solar radiation pressure if the solar panel area is much larger than the craft and are generally fixed relative to the sun.

Thrusting events are obviously accounted for in the equation of motion. The method used to incorporate the effects of low-thrust electric propulsion, the type of propulsion which DS1 used, was dependent on whether AutoNav was inspecting the data arc from its past or predicting a future state of the spacecraft. Past events were tracked by "measured voltages across the ion acceleration grid" [26] and saved to file for integration. Account for future events was dependent on available power, which for DS1 was based on the distance to the sun because of the dependence on solar power. Both are important capabilities of DS1, because this allowed it to refine its estimate of the prior spacecraft state to be used as the starting point for the guidance analysis to determine future actions.

The filtering technique used to solve for state parameters about the reference trajectory was from linear estimation theory and known as epoch state batch filtering. This was acceptable and beneficial because "[if] the nominal values are reasonably close to the truth, then the corrections should be linear over the batch time span, and the corrections at the epoch state can be linearly mapped to any other time using the state transition matrix" [26]. Areas that need to be analyzed to properly use this method are as follows: the number of planning cycles which affect the number of differential equations used in the state transition matrix, the values in the *a priori* covariance matrix which should allow the filter to adjust the spacecraft initial position and velocity while maintaining acceptable thrust and acceleration limits, and the optimal batch length which has enough data for a proper solution but does not keep unnecessary data.

4.3.3 Mission Planning

The camera used for optical navigation imaging and then later for the star tracking on DS1 experienced in-flight issues. Because of these issues the cruise portion of the autonomous capability demonstration was only able to take place for about a month. The realized demonstration of AutoNav during cruise operations was considered to achieve validation. The mission segments addressing autonomous approach to an asteroid were considered more successful than the cruise segment. This is in part because the hardware components for approach did not experience the failures of the components needed for cruise. It must be kept in mind that the software for autonomous operations during both cruise and approach were deemed to be valid based on realized flight usage experience.

Stardust, a mission launched in the late 90's, used AutoNav for an asteroid flyby starting 30 minutes prior to the encounter. Since then, multiple missions have used updated versions of AutoNav, including Deep Impact. [27] The use of AutoNav in each of these cases was exclusively for mission phases when remote ground control is not feasible due to communication delays compared to the rate at which actions had to be implemented.

Without a fully successful demonstration of cruise flight autonomy available on DS1, subsequent missions to date have not been willing to utilize such features. Here, the suggested autonomous guidance and navigation setup for intelligent onboard mission planning is defined. It is based on the needs of the industry, validated AutoNav features, and a subset of the PS responsibilities for decision making.

1. Optical Navigation – Available for primary navigation data and/or as a backup should expected ground-based navigation capability not be available when expected.
2. Ground updates –Intervention from the ground may be needed due to unacceptable deviations from the reference trajectory that endanger mission success. Ground intervention may take the form of providing state information based on DSN observations which has a higher accuracy than optical navigation; the inclusion of state information provided from the ground would take precedent over the onboard estimates, resetting the navigation filters. Another ground intervention that may be needed is a new reference trajectory for the autonomous system to use for its guidance decisions. The reason such ground updates are included as a resource in the current definition of an onboard mission planner is three fold. The first is that because an extended cruise onboard mission planning demonstration has not occurred since DS1, it is highly possible that some sort of refinement may be needed. The second is to assure that the linear region about the nominal trajectory is adhered to so that solutions from the onboard mission planner are valid. The third is that the current iteration of an onboard mission planner may not have all the features of a fully fleshed-out, all-encompassing mission planner as was planned for the intelligent decision system of DS1.
3. Guidance – Guidance algorithms valid over the linear region of a trajectory can be utilized. Orbital dynamics make linearization about a nominal trajectory valid in most cases. Linearization was an essential assumption and characteristics of multiple facets of the DS1 algorithms which

were validated and used in subsequent missions. This creates further support for a linear guidance algorithm to be used.

4. Thrust Event Tracking – As was done on DS1, when low-thrust electric propulsion is used, the measured voltage across the ion grid would be saved to file for integration to improve smoothing of prior data arcs of the trajectory. It is likely that the measured voltage across the ion grid had to be saved to file so that the acceleration experienced could be calculated because the acceleration is too low to be measured accurately.
5. Limited Planner/Scheduler – The attempted PS of DS1 was broad in scope but the Remote Agent was unable to complete a full demonstration. A limited set of the originally planned PS responsibilities would provide an interesting and useful demonstration for an onboard mission planner. While it would be valid to consider any number of subset of Planner/Scheduler features, the ones which will guide this demonstration are summarized here. The focus is achieving higher-level mission goals without considering failure responses. Alteration of mission goals is also not considered, but instead exclusively performing deliberations so that the methods needed to achieve goals can be determined. A database of potential actions is also assumed, was the case for PS. Unlike DS1's PS, the actions will be limited to those related to guidance and navigation. This would involve using data from forward predictions on the state of the spacecraft under various conditions and comparing the cases to see which best meets the set mission goals. The scenario which best meets mission goals over the current PS segment would be the one which sets the schedule for the guidance and navigation activities. One example of how this may work includes joining different combinations of guidance algorithms and navigation regimes, analyzing them over the nominal trajectory, comparing the outputs to the relevant mission goals of which the PS is aware, and then implementing the combination by sending commands to the relevant components. As with DS1 if the set of potential actions cannot meet the desired mission goals, the craft could be placed in a standby mode. Such a standby mode could be removed by the ground in several manners; the most relevant for this discussion would include: providing increased actions to be considered, providing a new reference trajectory, or a reset of the navigation filters.
6. LinCov Analysis – Because of the computational efficiency of this method, it would be used to analyze the different combinations of guidance algorithms and navigation regimes of interest. The results for each case would be saved for the PS to consider.

Ideally an onboard mission planner would be coupled with extensive Fault Detection Isolation and Recovery (FDIR) capabilities. The other two portions of DS1's RA were to track components for faults and to mitigate the resulting issues as needed. The PS was provided with updated information concerning the state and capabilities of the components by the segments of RA that were more closely involved with FDIR. Including such information in a planning segment increases the accuracy of those plans. If an onboard FDIR program is not available for direct consideration by the onboard mission planner, such capabilities would need to be provided by the ground.

Simplified component information could be made available to the onboard mission planner. For example, DS1 predicted its future state with consideration to the power available based on the distance to the Sun. Similarly, the thrusting data saved to improve prior state information could be compared to what was expected based on the commands sent. The differences between the implemented and the expected conditions can be used to determine changes that have occurred to the thrusting capabilities for consideration in subsequent onboard mission planner analysis. While this would not be as accurate as detailed information from an FDIR program it would be improvement over not updating component status information at all.

5 Needed Mission Autonomy Features

Implementation of autonomy in space missions has been limited to date. Instances of autonomy in space have frequently been technology demonstrations to prove a concept is a viable option. Primarily, the use of autonomy occurred because of limitations caused by communication delays which made ground control infeasible for what was trying to be accomplished. This was typically during the final approach phase to a target, when maneuvers occur very rapidly and need extreme precision.
There are some common features of autonomy when utilized in space. One aspect previously mentioned is optical navigation. It has been used to varying degrees. The imager's relative position to a target can be determined without needing to know the inertial position of the target. When the target's inertial position is known the relative position to the target can be used to find the imager's inertial position as well. This method for inertial position determination has been used for hundreds of years during nautical navigation. The concept is easily applied in the space setting. Using a camera image to obtain usable data for inertial position information is much more complex than the general concept. Both the concept and some of the specifics for using optical navigation will be outlined in the subsequent sections. Historical cases where optical navigation has been used are also provided. Important notes regarding those cases are outlined to show multiple ways that optical navigation has been implemented and to provide confidence in its viability.

While previously only nation states performed space projects, there has been a rapid shift in recent years which has allowed more players to enter the market. The advent of CubeSats has enabled more organizations to experiment with what is possible in space. The ground-based resources that have been traditionally used for state information and mission planning are limited and typically focused on highly critical programs.

Additional experimentation helps to increase understanding of space itself but also what is possible in space in a broader sense. As mentioned in Section 2 the various limitations of the CubeSat platform combined with the methods required to use ground based navigation systems detailed in Section 4.1 have made it so there are only several deep space CubeSat programs planned for launch over the next few years. The use of optical navigation on deep space CubeSats is a necessity if such programs are to become commonplace.

"There is strong motivation to create navigation systems that allow CubeSats to determine their locations for themselves, without the aid of Earth-based systems that require two-way data transmission, the power for which is difficult to generate on a small spacecraft. Autonomous navigation technology would remove one of the greatest barriers to entry for deep-space CubeSat missions by reducing the costs of navigation. A system like this would help enable the type of science, research, and commercial development occurring in LEO to take place in deep space" [28].

5.1 Optical Navigation

"Orbit determination is the process by which the spacecraft's state (position and velocity) and other parameters relevant to the trajectory, such as nongravitational accelerations acting on the spacecraft are estimated." [26]

Typically orbit determination occurs on the ground with DSN tracking data. The methods used by the ground team for orbit determination analysis are found in Section 4.1.1.2. Optical navigation can be used as the only source of navigation data but has more often been used along with DSN. It has been used as an additional data source by the ground team as well as the primary data source for onboard orbit determination. The methods behind optical navigation will be discussed along with some details about how various missions have utilized this alternative sensing method to benefit orbit determination. This section does not go deeply into the mathematics needed to fully integrate optical navigation into a system. Instead, it provides an overview of the various responsibilities which must be integrated. References to algorithm nuances are made as appropriate.

5.1.1 Methods

Optical navigation uses a camera to view space objects with respect to stars in the background. Stars provide an inertial reference compared to the object being viewed. The time when the image is taken must be known. An object's ephemeris information provides its inertial position. With knowledge of the imaged object's ephemeris, the inertial position of the craft can be determined.

5.1.1.1 Application Concepts

Measurement of relative position information is obtained by processing the image. An estimate of where an object is expected to appear in the image is calculated prior to the measurement. That object image position estimate is based in part on the estimate of the craft's inertial position. Another part of the image position estimate is from the object's ephemeris data. The difference between the object's observed location in the image and the calculated location corrects the estimate of the relative position from the craft to the object. The correction to the relative position information combined with the object's ephemeris details is used to update the craft's inertial position estimate.

Imaging two objects at the same time can instantly provide a complete fix on the craft's current inertial position. Imaging one object multiple times in a series can provide that same information so long as there is an understanding of the expected vehicle state changes over that time span. The mathematics for each of these aspects of optical navigation, including geometry effects, camera calibration, image processing, optics fundamentals, camera type effects, etc. can be found in [29].

"By its nature, optical data are not as precise as radio systems, but have the distinct advantage of being self-contained onboard the spacecraft. DS1 system was enriched with a completely autonomous centerfinding procedure of the objects used to determine its position and, as a consequence, the position of the spacecraft using an ephemeris database." [30]

5.1.1.2 Application Implementation

Methods for interplanetary optical navigation have been investigated for some time. It has been found that three-degree-of-freedom navigation can be performed when multiple objects with known ephemeris are imaged "without modeling any spacecraft attitude position dynamics" [28].

The needed geometry for an object with available ephemeris information and other celestial bodies to be used in a series of time-tagged photos has also been researched. Reasonable assumptions about the spacecraft trajectory over a short span of time of an image series have also been noted. The minimum number of images required over the span with these assumptions has been quantified. The resulting optical navigation solutions with these assumptions applied were found to be highly accurate and along the lines of less simplified cases. Error sources which degraded solution quality have also been tracked. [31]

Combining attitude measurements of the craft and object line of sight information from images has been found to provide enough details for orbit determination in deep space. "[One algorithm] is a simple Batch Least Squares (BLS) filter," another "is composed of two sequential sub-modules: a measurements preprocessing gives a first estimation of a portion of the state, and then a filter refines that estimation and reconstructs the overall state" [30]. The assumptions needed to use the OD algorithm along with image quality issues which affect OD quality have been provided. "It should be noted that image processing and optical characteristics of the sensor plays a fundamental role, therefore either an adequate processing of the image prior to the filtering algorithm is required or a model of the error due to optics is to be included in the filter. [30]" These algorithm applications assumed a type of camera known as a Charged Couple Device (CCD). Cameras were used to provide navigation data for orbit determination before the development of CCDs; algorithms developed without the CCD assumptions are readily available. In either case the "image processing and optical characteristics of the sensor plays a fundamental role, therefore either an adequate processing of the image prior to the filtering algorithm is required or a model of the error due to optics is to be included in the filter" [30].

5.1.2 Use Cases

This section shows how optical navigation use in space missions has advanced over the years. It has improved from very basic demonstrations, to an integral part of decreasing uncertainty, to being vital for mission success. Different components for imagery will be mentioned along with variant methods for processing the images in context of the missions which utilized them. Ironically, since feasibility of optical navigation was demonstrated it has been used in more demanding situations than simple ones. Deep Space 1 (DS1) will be examined more thoroughly than the other cases for two reasons: 1) the first set of missions detailed provide a reference for development and use cases of optical navigation;2) a thorough examination of DS1 will allow the reader to have a better idea of all the different pieces of optical navigation working together.

5.1.2.1 Mission Overviews

Described here is the progression of optical navigation use in space. Table 9 provides an overview of the most relevant detail from each mission. The year noted in Table 9 for each mission is not the launch date but when optical navigation processes began.

Table 9: Optical Navigation Mission Overview

Mission	Viking	Voyager	Galileo	Cassini	Deep Space 1
Optical Navigation Demonstration	Simple demo [32]	at Saturn [33]	Single Frame Mosaic Method [33]	at Saturn's satellites [34]	Full validation for Approach and Cruise [27]
Year	1978	1981	1991	2002	1999
Mission	**Stardust**	**Mars Reconnaissance Orbiter**	**Deep Impact**	**Dawn**	**NEAScout**
Optical Navigation Demonstration	New scanning technique [27]	Conceptual Validation for Mars Approach [35]	w/AutoNav comet landing [27]	w/Low thrust propulsion [27]	On a CubeSat [27]
Year	2002	2008	2010	2011	~2018

Detailed are the specifics of how of each mission showed how useful optical navigation could be for increasing orbit determination accuracy and how optical navigation was physically implemented. This is to provide confidence that the overall scheme has been well tested and to show a few very relevant cases for the CubeSat platform.

The Viking orbiters demonstrated some optical navigation using Phobos and Deimos. [32]. It was rudimentary and was to show the feasibility of using optical navigation. Voyager used some optical navigation at Saturn to image its satellites. [33] At the time, the ephemeris information of Saturn's satellites was very poor. "Radio plus optical OD is a means of combining both radio tracking data and onboard satellite imaging observations into an orbit solution which is more accurate than that obtainable by using either type alone." [36] "This method improves navigation performance over conventional radio by factors of 2 to 20" [32]. In addition to improving Voyager's navigation solution, the ephemeris details of Saturn's satellites could be improved as well.

Galileo used a charge couple device (CCD) camera to take the images as part of the solid-state imaging subsystem (SSI) for optical navigation. A new technique to use fewer images was developed due to an antenna downlink capacity issue. The resulting Galileo method is known as "single-frame mosaic" that built "up a series of Gaspra [asteroid] and star images in a single picture by moving the scan platform while the shutter of the SSI camera remained open." [33] The Galileo mission incorporated optical navigation because "earth-based radio measurements could not provide the desired navigation accuracy" [33]. The processing of the images for orbit determination was performed on the ground. The single-frame mosaic method is important to note because it can have implications for other missions with limited downlink capabilities that would benefit from optical navigation. The accuracy on the B-Plane, described in Section 7.4.2, was higher with the combined optical data with earth-based radio than anticipated for the encounter. Details on the single-frame mosaic image processing algorithm can be found in [33].

Cassini has been in operation since 2002. Its prime mission included 45 targeted Titan flybys. Its first mission extension involved gravity assists from Titan and from Saturn's other satellites, and its current mission extension is slated to go through 2017 for more Titan exploration. It too uses optical navigation to increase accuracy. For the prime mission and the first extension optical navigation was very important. The increased accuracy of ephemeris information of Saturn's satellites from the use of optical navigation justified reducing the number of optical navigation (OpNav) measurements during the second mission extension planning. [34]

The Mars Reconnaissance Orbiter (MRO) contained an optical navigation experiment. "From 30 days to 2 days prior to Mars Orbit Insertion, the spacecraft collected a series of images of Mars' moons Phobos and Deimos. By comparing the observed position of the moons to their predicted positions relative to the background stars, the mission team was able to accurately determine the position of the orbiter in relation to Mars. While not needed by Mars Reconnaissance Orbiter to navigate to Mars, the data from this experiment demonstrated that the technique could be used by future spacecraft to ensure their accurate arrival. Accuracy will be important to future landers and rovers in need of extremely precise navigation to safely reach their landing sites." [35]

Stardust "capture[d] images of [the] Comet Borrelly" [32]. Launched in Feb 1999, Stardust performed multiple asteroid flybys, focusing on the Wild 2 comet. It used an updated version of AutoNav from DS1 "with the primary difference being that [Stardust] used a unique camera/scan mirror combination for imaging" [37]. Its method meant the spacecraft did not need to reorient its attitude while taking optical measurements of the comet. For the Wild 2 encounter AutoNav was used 30 minutes before the encounter using "the best ground-based target relative trajectory solution at E-48 hours" [37] AutoNav was used when ground-control was not really an option for Stardust but showed a high level of accuracy possible and importantly demonstrated use of planning features.

Deep Impact (DI) was launched in January 2005 on a mission to impact a comet. "DI used standard ground radiometric and optical navigation techniques for the cruise and approach phases of the mission. AutoNav was used only in the hours prior to the impact event and had dual roles. On the Impactor, AutoNav needed to use its own onboard calculated maneuvers to guide the spacecraft to a sunlit area on the comet nucleus, and bias the impact site towards the side where the flyby spacecraft had its closest approach. On the Flyby spacecraft, no maneuvers were computed but AutoNav needed to maintain camera lock on the nucleus and predict where the Impactor would hit, as well as determine the time of closest approach and initiate a high-rate imaging sequence." [37]

Dawn was launched in 2007 to orbit the asteroids Vesta and Ceres. This mission uses low-thrust ion propulsion. Dawn uses optical navigation along with ground-based navigation. It demonstrated using landmarks to improve navigation information.

The above list of examples does not encompass all optical navigation events which have occurred in space or even within the missions detailed above. Each was chosen for discussion here because of the significance they played in showing the benefits of optical navigation, because optical navigation was critical to their success, and/or because of the clarity the chosen example could provide to methods of optical navigation implementation. Most important for potential CubeSat users to be aware of were: the Galileo mission, because it showed how to use optical navigation when the analysis is performed on the ground and there is limited downlink capability; Stardust, because it shows a physical layout which limits the use of onboard resources; and NEAScout, where optical navigation will actually be used on a CubeSat on approach to a NEO and during the flyby.

5.1.2.2 Deep Space 1 – Optical Navigation Case Study

DS1 used optical navigation, sighting multiple nearby asteroids sequentially and using their ephemeris details to provide heliocentric information. Had two cameras been available on DS1, concurrent sightings of two asteroids would have been sufficient for a heliocentric fix with the ephemeris information and the camera inertial pointing both known. The pointing information was improved by least-square fitting when at least three stars were available. Multiple asteroids were used to average the information together so that individual asteroid ephemeris errors could be ignored in an effort to keep the onboard orbit determination (OD) simple. Centroiding the asteroids is of great importance to the autonomous navigation. "because of its importance, the centerfinding algorithms (and the associated pointing solution) used during cruise when asteroids are distance point sources have had the most testing." [26] One trade that must be considered is the time and resources it takes to slew between the asteroids needed for state determination. "The accuracy of this type of data is dependent on several factors, including the angular separation, brightness, and distance to the imaged asteroids, the resolution of the camera, the ability to pinpoint the location of asteroid in the camera frame (centerfinding), the accuracy of the camera pointing information, and the knowledge of the asteroid ephemerides." [26]

Between the various factors that affect orbit determination, the ability to centerfind and remove bad data is of paramount importance to autonomous operations. Centerfinding algorithms which use point sources during cruise for navigation need extensive testing. "Pattern finding" based on the spots for bodies and known stars also in sight were used. An initial guess of the direction to point the camera was provided to the Attitude Control System (ACS). The star information was taken from the European Space Agency's Hipparcos satellite's catalogue for the DS1 mission. Given the unknown shape of the asteroids used for navigation, only the brightness center can be used when the spacecraft is considered close to it. For distant, unresolved asteroids the observation uncertainty was 0.1 pixel but when closer to an asteroid the error could be large as the asteroids' radius. An additional important error was uncertainty in the ephemeris of the asteroids. For simplicity, the observations of 12 asteroids were averaged together to remove an individual asteroid's ephemeris errors, effectively allowing this error source to be ignored. Prior to launch, the asteroids to be used were selected based on an analysis that "propagated the spacecraft state and asteroid states using either conic elements or numerical integration" [26]
The amount of time in which interplanetary cruise was performed autonomously on DS1 was limited due to the failure of the star tracker, the time it took to program the use of a different onboard camera to include some star tracking functions, and issues with the onboard camera that was reprogrammed. One of the main issues with the camera that remained functional and had to be reprogrammed was its ability to characterize the brightness of objects not in the planned range. Only very bright objects could be used effectively. Specifically, the camera "pictures corrupted by stray light, sensitivity of camera not at the expected level, camera distortions were unusual and proved difficult to model." [27] The camera had been set to use the clear filter for navigation which allowed "max throughput, highest signal with shortest integration time [and] reduced smear caused by motion." [27] Despite these limitations, the amount of interplanetary cruise time was enough for that aspect of AutoNav to be validated. The functionality for the relative navigation flight phase, the portions of missions spent closer to asteroids, was also validated.

The onboard steps for using unresolved bodies, as was the case for asteroids while DS1 was in the cruise phase, involved using the *a priori* location of the objects. The brightness of an object was used to find the centroid location in the vicinity set, followed by using a Gaussian fit to fine tune the location. Typically, this would result in "0.05 to 0.2-pixel accuracy" but was not possible with the degraded performance experienced. The camera filter used the (x,y) coordinates of the location determined for the detected object and the line coordinates in the camera frame. The filter digitization utilized "8-12 bits per pixel". The spacecraft was not able to maintain a stable attitude for the duration of the needed image exposure time so “smear” resulted. To deal with smear the camera filter used a “multiple cross-correlation method to determine pixel/line coordinates of target relative to stars,” a method also used on the Galileo mission. [27]

6 Analysis Considerations

There is interest in having CubeSats move from Low Earth Orbit (LEO) to interplanetary trajectories. This is a new concept; as such, the desired and planned missions detailed in Section 2 do not have a heritage on which to base their plans. The CubeSat programs generally have very limited financial resources, and the platforms have many constraints. This analysis goes over a method to provide system-level design information for the guidance and navigation system of a low-thrust CubeSat mission to Mars that will accommodate both the financial and physical constraints.

6.1 Investigation Goals

The overarching goal of this thesis is to define baseline strategic guidelines to support development decisions and design concepts for CubeSats that can reach entry-interface conditions after interplanetary transit with confidence that onboard capability meets mission needs. In doing so, it is explained how to reduce DSN usage by application of a method onboard a CubeSat that can increase autonomy, and why that method is reasonable.

6.2 Supporting Information

The DSN is already oversubscribed, and high-cost deep space missions will always have DSN usage priority over CubeSats. It is expected that the number of DSN-supported spacecraft will increase by ~30% after the EM-1 CubeSats are released. [19] Consequently, deep space CubeSats need to be robust because sequential/shared DSN passes intended for CubeSats may be skipped to accommodate needs of other missions. The plans for DSN support of CubeSats are detailed in Section 4.1.1.3.

Traditionally, deep space missions use DSN to track spacecraft so analysis can be performed on the ground to determine the needed maneuver sequences in detail that are then uplinked to the vehicle. DSN use in this manner can get very expensive very quickly in Section 4.1.1.1. Consequently, the desire for autonomy has increased with the needed features detailed in Section 5.

Deep Space 1 (DS1), part of NASA's New Millennium program, demonstrated low-thrust propulsion, autonomous navigation, and an onboard mission planner. Trajectory Correction Maneuvers (TCMs) took the form of linearized course corrections and were valid so long as the Ion Propulsion System (IPS) performed as expected. An intelligent onboard mission planner had a portion called the Planner/Scheduler (PS), which chose between multiple goals and set methods to achieve them based on current information. The autonomous navigation program on DS1 which had subsystem localized planning capabilities is AutoNav. AutoNav takes optical navigation images and processes the images onboard to provide position data. With that position data its onboard guidance determines the maneuver plan, then it directs the craft to execute that plan. The AutoNav demonstration was extremely successful; the program has since been refined and used on subsequent missions, detailed in Section 4.3.

So far it has been shown that CubeSats will not be DSN's priority and need to be robust with respect to navigation: If CubeSats do not address these issues, then extremely high expenses to use DSN will be incurred. Desired design features for an interplanetary CubeSat include: low-thrust propulsion, an optical-enabled navigation aiding system, an onboard mission planner that that can successfully manage mission trajectory dispersions with respect to a reference trajectory. This leads to specific key questions to be addressed when examining guidance and navigation needs for interplanetary CubeSats.

6.3 Key Questions

There are many design considerations that need to be addressed when developing guidance and navigation systems. Most important are the required types of input information, the needed frequency of the input information, and the required accuracy of that information. The resulting system must be able to overcome the effects of plausible in-flight dispersions. Characterizing these requirements provides program managers with the information needed to logically determine the available design choices for a mission. The key questions are correlated to the thesis analysis topics and their action plans in Table 10.

Table 10: Thesis Key Question Correlation to Analysis Topics and Action Plans

Analysis Topic	Overarching Question	Action Plan
Navigation	How does my navigation plan affect my dispersions?	Determine where ground support is most useful and if optical navigation can be used as the primary information source.
Trajectory Dispersion	Are my dispersions acceptable?	To meet Mars entry-interface conditions, determine the acceptable dispersion profile for a low-thrust system.
Onboard Mission Planning	How well can the Planner/Scheduler of DS1 be replicated so high-level mission goals can be met with onboard decisions?	Apply the developed tool to enable TCM selection.

7 Methods and Assumptions

7.1 Overview

The proposed CubeSat GNC design contains features that free up ground personnel time, free up DSN resources, use an ancient method of navigation already shown useful in deep space, and can utilize commercial off-the-shelf (COTS) HW. Table 11 tracks the top-level assumptions of the proposed platform used in analysis.

Table 11: GNC Feature Assumptions and Descriptions

Assumption Areas	Description
"Ground Update": Occasional ground supplied state update	Limited DSN tracks applied to limited ground-determined orbit determination
Optical Navigation with Ephemeris Information	Repeated sightings of Earth and/or Mars for inertial state determination
Simple Guidance Algorithms	Applicable over the linear perturbation region of a reference trajectory
Linear Covariance Onboard Mission Planner	Rapidly determines maneuver points, guidance choice, etc. based on preset capabilities

Given these assumptions the methods used for the analysis are explained below. This includes an overview of Linear Covariance (LinCov) analysis for guidance and navigation purposes as well as the settings applied to the specific LinCov tool used. As LinCov needs a reference trajectory, the desirable features of a reference trajectory as well as an overview of the tool which generated the one used for analysis in this thesis are provided.

7.2 Ground Operation Assumptions

What follows is the modified ground operations approach for deep space CubeSats as compared to prior deep space missions as depicted in Figure 3. In the current baseline approach to deep space missions, the ground team provides most if not all of the guidance, navigation, and maneuver analysis as shown in the underlying process of Figure 4. For CubeSats, the ground function is recommended to be reduced as indicated by the crossed-out ground support activities. The decreased ground responsibilities are considered reasonable because in the proposed CubeSat paradigm, onboard guidance and navigation capabilities perform some of the work that the ground team traditionally does. Nominally, the state information of the onboard mission planner would be acceptable for mission operations. When needed to supplement the navigation information used by the onboard mission planner, the ground team would provide more accurate state information than can be realized with the onboard resources; this would be treated as a measurement update by the navigation filter. Interfacing with program managers is still required by ground support personnel to discuss the results of their work so program managers can decide if a new reference trajectory needs to be uplinked to the craft.

A summary of the ground operation assumptions which produced Figure 4 is provided in Table 12.

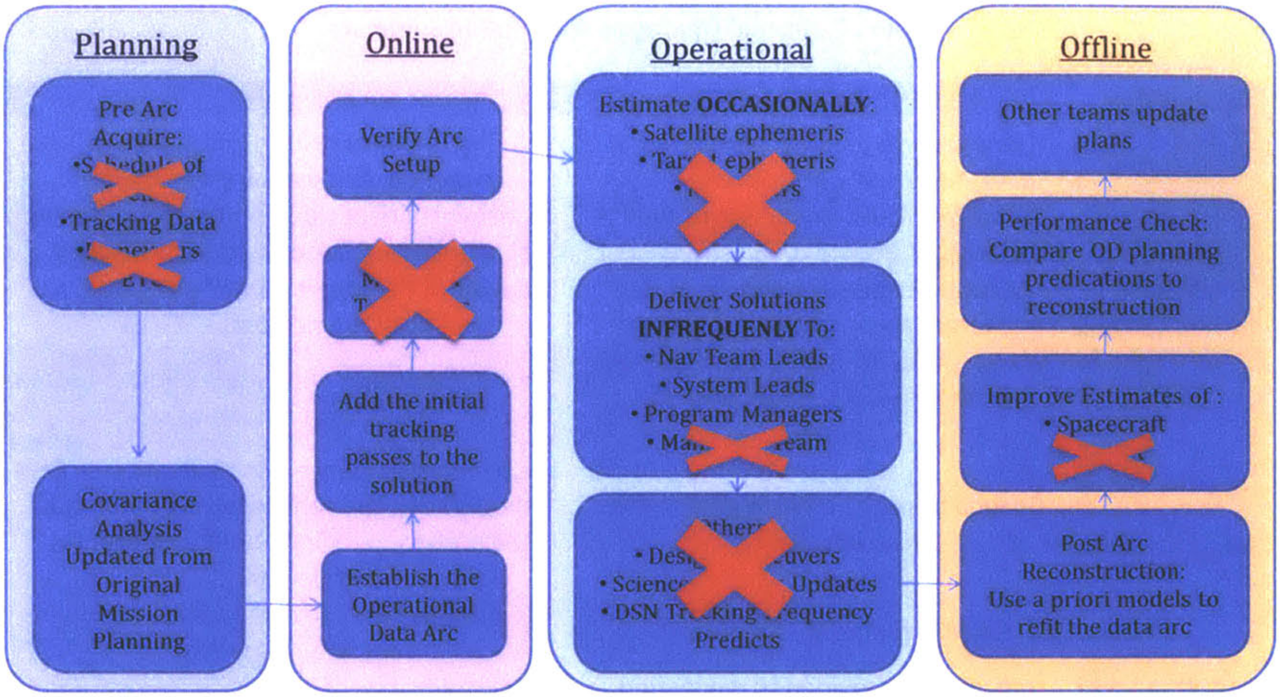

Figure 4: Modified Ground Team Responsibilities

Table 12: Ground Operation Assumption Summary

Assumption	Details	Reasoning
1	Less ground based analysis steps need to be performed.	The onboard system has guidance, navigation, and planning capabilities.
2	Iterations with the maneuver team would not need to be performed.	Maneuvers are decided onboard; maneuver sequences are not uplinked to the craft.
3	Accurate ephemeris details of the target are readily available.	Analysis of the target ephemeris would not be needed.
4	Vehicle state information is uplinked to reset the navigation filters as needed.	The state accuracy onboard is inferior to DSN based ground analysis.
5	Ground based analysis is performed less frequently.	The onboard guidance and navigation system should keep the vehicle within the linear perturbation region about a reference trajectory.
6	Smaller teams are acceptable.	Ground Operation Assumptions 1 - 5 means there is less work.
7	Results are provided to navigation team leads, system leads, and program managers only when needed.	The onboard system has decision making capabilities so high ranking decision makers need to be tapped less frequently.
8	Some vehicle information is downlinked.	High ranking decision makers need such information for planning.
9	A new reference trajectory can be uplinked to the craft.	Program leads may determine the analysis results and downlinked information shows the reference trajectory is no longer valid.
10	The development of a new reference trajectory is not considered part of nominal operations.	Assumption 5 is valid so long as the system performs as expected a new reference trajectory means extenuating circumstances may have occurred.

7.3 Optical Navigation Assumptions

Optical Navigation (OpNav) views space objects with respect to stars in the background. Stars can provide an inertial reference if the time of the viewing is well known. Ephemeris information provides the true location of the object while the measurement update provides relative position information. Onboard, the line of sight to the object is compared to what was expected at the time of observation and a derived onboard estimated inertial state error determination is used to correct the estimate as detailed in Section 5.1. This section will go through some of the features of optical navigation and the assumptions made for this thesis research.

When using optical navigation, it is possible, depending on the location of the vehicle at a given time, to image any number of bodies and use their ephemeris information to determine the inertial state of the vehicle. The quality of the optical navigation solution derived by this method is influenced by the following effects: the nature of the observed bodies; the accuracy of their ephemeris information; the vehicle pointing control precision during sightings; and the ability to correlate those details in one sighting segment. The benefit of sighting multiple bodies in one segment, assuming the conditions to do so accurately are available, is that a 3D fix of the craft's state is available immediately afterwards. The time to rotate between the bodies within a segment must be factored into the solution. Another sighting option is to look at only one body multiple times over a trajectory and correlate the multiple observations to provide a 3D fix over time. In each optical navigation option, the time when a sighting occurs must be known so the proper ephemeris information can be used. In the second setup less maneuvering is required to perform the imaging as the craft does not have to reorient to image multiple bodies. The maneuvering required to rotate to multiple bodies for one sighting segment is traded against the additional navigation accuracy benefits of doing so. That trade is not investigated in this work; it is assumed here that only one body and its surrounding stars are used to provide inertial information.

The measurements (azimuth, elevation angle, pixel location) are used by the navigation filter to update the vehicle position and velocity. When near the target the apparent angular diameter of the body is used as part of the calculations. For the majority of cruise, the craft would be far enough from the target that it is effectively a point source. When far from the target the apparent distance is used instead, as show in Figure 5.

The selected optical navigation setup assumptions are summarized in Table 13.

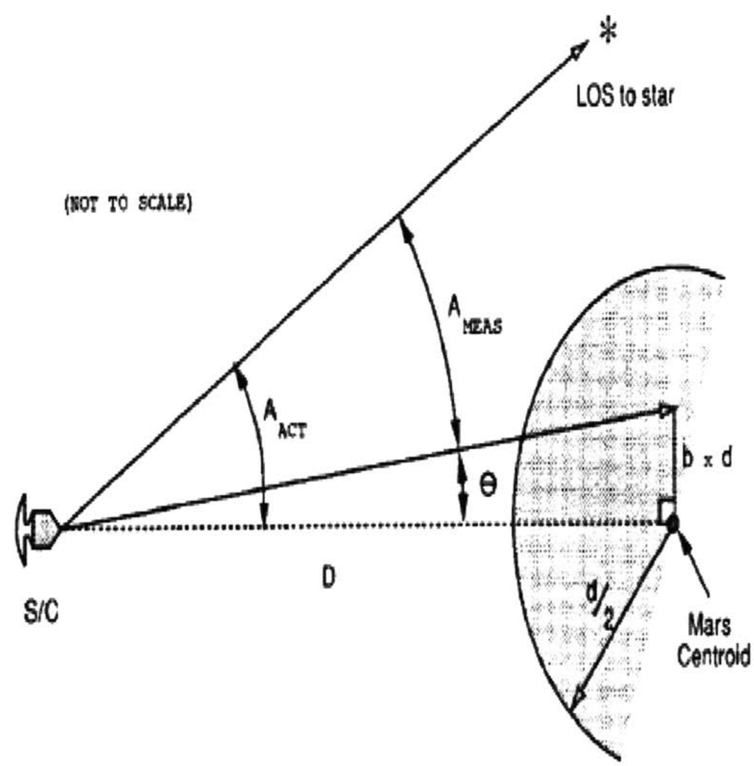

Figure 5: Point Source Optical Navigation [38]

Table 13: Optical Navigation Assumption Summary

Assumption	Details	Reasoning
1	The cameras were well calibrated and their operation well understood.	Inaccurate camera assumptions have crippled prior missions.
2	The image processing, specifically centerfinding when an object is a point source, received significant testing.	Centerfinding is critical to autonomous navigation; during cruise the bodies will be a point source; DS1 tested centerfinding capabilities the most.
3	Accurate ephemeris information of planets and asteroids of interest is available onboard the spacecraft.	Ephemeris details are critical to the inertial state update of the craft. Using bodies where accurate details are already available minimizes a calculation error source
4	An accurate star catalogue is available onboard.	Star trackers already have star catalogues; many different catalogues are available.
5	The cameras centerfind to the bodies and stars in an image.	Stars provide an inertial reference. When a body has star information in the image the inertial fix is more accurate.
6	Only one body will be viewed at a time.	The geometry can make it difficult to view multiple bodies well at once. Only one camera may be available on a CubeSat.
7	Multiple observations of one body are used to provide a 3D fix overtime.	Rotation and pointing control are needed to view multiple bodies. To do this in a time frame suitable for an immediate 3D fix may be too demanding for a CubeSat, and is not likely needed for long duration trajectories.

7.4 Past Mission Requirements and Dispersions

A precedent was required to have a sense of what settings and results could be considered reasonable. Prior Mars missions were used to provide this, especially those which landed on the surface. Information about prior mission dispersions came from two distinct mission phases. Preflight analyses determine whether a mission would meet its requirements and to identify any areas that might need modification before launch. Flight experience analyses present the performance understood during the missions and the corrected performance values after the missions were completed. The available information is presented with the two analyses phases separated. Preflight analyses tend to keep conservative estimates as a safety factor to increase success assurance. Flight experience analyses can make comments concerning how and why the performance was better or worse than the preflight analyses. It was found that, generally speaking for the Mars missions examined, the flight experience was much better than the preflight expectation.

As this report focuses on the preflight analyses of a new platform the available dispersion information is used in a slightly different manner depending on whether it represents preflight or flight experience analyses. Preflight plans and results represent the upper bounds (worst case) of expectations while flight experience results provide a lower bound of expectations. Of interest for each was: The entry interface requirements and how well they were met; when a data cutoff had to occur for ground team orbit determination analysis needed to enable a timely maneuver sequence uplink to the vehicle; and the acceptable dispersions along the cruise portion of the trajectory that enabled the desired trajectory end conditions to be met.

7.4.1 Requirement Summary

The requirements for the various Mars missions and how well they are met are summarized in Table 14 and Table 15 from preflight analyses and flight experience analyses, respectively. Also included are comments about the results. For preflight analyses this includes factors which may have degraded the results shown and whether it is expected that the requirements will be met. For flight experience analyses this includes notes about the dispersions at important points and what caused them.

Table 14: Mission Requirements and Preflight Analyses Results

Mission	Requirements	Analyses Results and Comments
Pathfinder [9]	The error in the flight path angle at atmosphere entry will be no greater than 1°	The final FPA error was within requirements.
Surveyor Orbiter [10]	The variation in capture orbit periapsis altitude is no greater than ± 20 km	The analysis was performed before accurate momentum wheel desaturation maneuver models were available. The analyses results did not meet requirements but it was expected that once more accurate models were available requirements would be met.
Surveyor Lander [10]	Lander's FPA error upon atmospheric entry < 0.25°	The projected lander FPA error was expected to be less than 0.27 degrees and 0.24 degrees upon completion of the fourth and fifth midcourse maneuvers, respectively.

Table 15: Mission Requirements and Flight Experience Analyses Results

Mission	Requirements	Results and Comments
Spirit [11]	The maximum allowable errors in FPA following TCM-5 at Entry (E) – 2 days were ±0.12° (3σ).	At the navigation data cutoff for the TCM-5 final design, the orbit determination FPA knowledge error was ±0.028° (3σ). The amount of the landing position offset caused by navigation-only errors was only 3.3 km (uptrack).
Opportunity [11]	The maximum allowable errors in FPA following TCM-5 at Entry (E) – 2 days were ±0.14° (3σ)	At the navigation data cutoff for the TCM-5 final design, the orbit determination FPA knowledge error was ±0.035° (3σ). The amount of the landing position offset caused by navigation-only errors was only 9.7 km (downtrack).
Phoenix [8]	Entry Requirement: 20 km wide position error limit band, FPA 3σ uncertainty – 0.21°	Due to the OD accuracy the position error limit band was < 2 km wide The data cutoff of TCM-3 was 6 days prior to the maneuver. TCM-3 placed Phoenix within the FPA requirements. The data cutoff of TCM-5 was 21 hours prior to the maneuver. TCM-5 corrected the error parallel to the entry corridor but none of the FPA error. TCM-5 immediately satisfied the required landing site safety criteria.
Odyssey [39]	Encounter periapsis altitude accuracy of ± 25 km, with an inclination accuracy of ± 0.2°.	Arrival conditions were well within the 1σ design.
	If the TCM-4 solution ± 50 km uncertainty goes below 200 km at second periapsis pass (P2), then execute TCM-5.	The TCM-4 estimate was within 1 km of the target, no TCM-5.

The above missions had specific landing sites for their missions. Their requirements for an entry corridor were set with several factors in mind, a subset of which are the downrange deceleration needed, the landing accuracy desired, and staying within thermal and dynamic pressure bounds for the landing system. Keeping to the thermal and dynamic pressure bounds greatly reduces corridor size compared to the other entry, descent, and landing factors.

Earlier missions, such as Pathfinder, had much larger acceptable flight path angle dispersions compared to later missions. Both the earlier and later missions were able to meet their requirements. The later missions achieved dispersions notably smaller than their requirements. The difference between the experienced dispersions versus the requirements for later missions is significant when compared to the minor differences between experienced dispersions versus requirements of earlier missions.

There are several reasons why the dispersions of the later missions were set with much more stringent requirements and they were able to be met so easily. Besides the advancements in hardware and the experience gained by the earlier missions, the later missions were able to take advantage of DDOR measurements for navigation information. As in Section 4.1.1, DDOR involves two antennas to take measurements simultaneously, and both must be paid for.

The defined orbit determination data cutoff times prior to the trajectory correction maneuvers for some past missions are provided in Table 16. The values represent the amount of time before a maneuver after which measurement data for orbit determination stopped being collected. In the days between the data cut off and the maneuver the ground teams refined the vehicle state estimate based on previously collected data to finalize the measurement sequence for uplink.

Table 17 shows when the TCMs occurred with respect to the start of the trajectory (S) to the end of the trajectory (E).

Table 16: Orbit Determination Data Cutoff Points Prior to Maneuvers

Mission	Phoenix [8]	Spirit [11]	Opportunity [11]	Odyssey [39]	MSL [12]
TCM-1	-5 days	–5 days	–5 days	-13 days	-7 days
TCM-2	-6 days	–5 days	–5 days	-11 days	-7 days
TCM-3	-5 days	–5 days	–5 days	-7 days	-7 days
TCM-4	-3 days	–13 hours	–13 hours	-5 days	-13 hours
TCM-5	-5 hours	–13 hours	–13 hours	-9.5 or -4.5 hours	-13 hours
TCM-6	-5 hours	–4.6 hours	–4.6 hours	N/A	-5 hours

Table 17: Planned and Implemented TCM Schedule

Mission	Pathfinder [9]	Surveyor [10]	Spirit [11]	Opportunity [11]	Phoenix [8]	Odyssey [39]	MSL [12]
TCM-1	S+30 d	S+15 d	S+10 d	S+10 d	S+7 d	S+47 d	S+15 d
TCM-2	S+60 d	S+45 d	S+52 d	S+62 d	S+81 d	S+87 d	S+120 d
TCM-3	E-60 d	E-60 d	E-50 d	E-65 d	E-45 d	E-38 d	E-60 d
TCM-4	E-10 d	E-10 d	E-8 d	E-8 d	E-14 d	E-13 d	E-8 d
TCM-5	N/A	N/A	E-2 d	E-2 d	E-7 d	N/A	E-2 d
TCM-6	N/A	N/A	E-4 h	E-4 h	E-3 d	N/A	E-9 h

The information in Table 16 and Table 17 is important for understanding when information must be finalized to define a critical maneuver and when critical maneuvers occur along a trajectory, respectively. The closer to the target, the shorter the amount of time between the data cut off point and its maneuver. Later missions, with more stringent entry requirements, had planned for potential maneuvers much closer to the target than earlier missions. For preliminary investigation purposes the data cut off points and TCM schedule for missions are used to set important navigation and guidance events. Taken as a whole, the prior missions' requirements, results and analysis, data cutoff points, and TCM schedules provide a guideline for reasonable inputs to and results from the analysis.

7.4.2 Prior Mission Preflight and Flight Experience Analyses Results

It is important to clarify certain terminology before discussing the dispersion results of the prior missions that are used as guidelines for this report. OD uncertainty is the knowledge uncertainty in the spacecraft state that the ground used to make planning decisions. Navigation uncertainty, guidance uncertainty and delivery uncertainty are all different terms for the physical dispersions that a vehicle is expected to experience. These are computed prior to the performance of the maneuver. Achieved uncertainty is the uncertainty in state relative to the target during the flight based on maneuver reconstruction. Based on achieved uncertainty, the error is the difference from the desired target to what occurred. It is also referred to as post-event condition uncertainty.

Another important concept is the plane over which the dispersion results are detailed. Whether an object will impact or flyby a planet is determined by the impact parameter which results from the vehicle trajectory and the planet's physical characteristics. Defined by the radius of the planet, its escape velocity, and the V_∞ of the trajectory, the impact parameter is typically symbolized with "b". Physically, the distance from a line parallel to the V_∞ from the center of the planet to a line perpendicular with the V_∞ is the magnitude of the impact parameter, b. The relationship between the impact parameter and the object's approach distance to a planet determines whether the object will flyby the planet, impact the planet, or would skim the planet's surface if there were no interferences such as atmosphere. [40] The B-Plane "passes through the center of the target body and perpendicular to the incoming asymptote of the hyperbolic flyby trajectory" [34]. This is shown in Figure 6. It is on this plane that the error along the trajectory is referenced. "The B-Plane is a convenient coordinate frame for expressing guidance and navigation results for interplanetary missions... The guidance uncertainty is expressed by a two-dimensional ellipse in the B-Plane with semi-major axis, semi-minor axis and orientation angle theta, and the uncertainty in the time of arrival [10]." Expressing the error of an incoming or outgoing hyperbola along the B-Plane is standard for interplanetary guidance and navigation uncertainty analysis. Figure 7 shows the errors in the B-Plane.

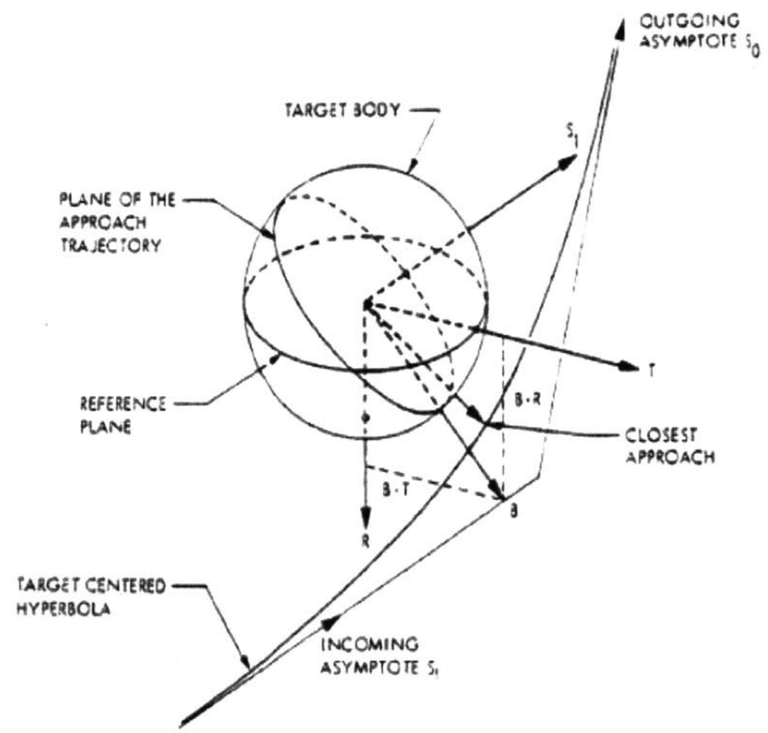

Figure 6: Vectors Defining B-Plane Geometry [41]

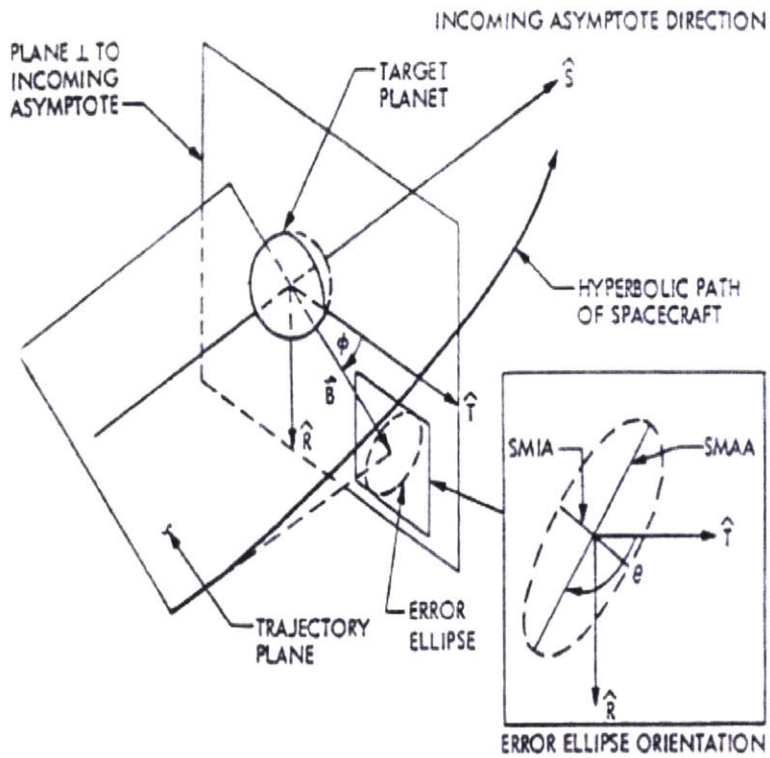

Figure 7: Error Ellipse Along the B-Plane [41]

Tables 18-22 provide the expected B-Plane uncertainty information for Pathfinder, Surveyor, Spirit, Opportunity, and Odyssey, respectively. This information is used to provide a basis of comparison for dispersions experienced along the trajectory which allowed the final target requirements to be met. The B-Plane dispersion of the Surveyor orbiter in Table 19 is compared to its 3σ periapsis requirement in Figure 8. Similarly, Figure 9 shows the Surveyor lander B-Plane dispersions compared to its 2σ FPA requirement. The lines within Figure 8 and Figure 9 represent the relevant requirements, and an ellipsis within the bands that satisfies the requirements.

Table 18: Pathfinder Preflight Analysis-Based B-Plane Expected Uncertainties

Event	Semi-Major Axis (km)	Semi-Minor Axis (km)	ToF (s)	FPA Error (°)
3σ OD Uncertainty [9]				
TCM1	870	90	210	N/A
TCM2	255	88	54	10
TCM3	63	43	9.6	2
TCM4	22	16	1.3	0.76
3σ Navigation Uncertainty [9]				
TCM1	68,760	2,367	24,819	N/A
TCM2	3,045	1,971	1,197	N/A
TCM3	275	255	5.4	12.1
TCM4	23	17.4	1.8	0.83

Table 19: Surveyor Preflight Analysis-Based B-Plane Expected Uncertainties

Event	BR (km)	BT (km)	ToF (s)	Periapsis (km)	FPA (°)
3σ Orbiter Guidance Uncertainty [10]					
Injection	1,635,000	166,800	1,472,256	N/A	N/A
TCM-1	73,950	8,151	51,420	N/A	N/A
TCM-2	5,493	698.1	2,992	N/A	N/A
TCM-3	385.8	324.6	47.5	276	N/A
TCM-4	41.46	20.88	6.5	35.3	N/A
2σ Lander Guidance Uncertainty [10]					
Injection	3,470,000	101,100	275,616	N/A	N/A
TCM-1	38,800	1,391	3,396	N/A	N/A
TCM-2	2,596	58.82	171.5	N/A	N/A
TCM-3	57.48	39.02	9.178	N/A	0.27
TCM-4	6.052	2.262	0.408	N/A	0.24

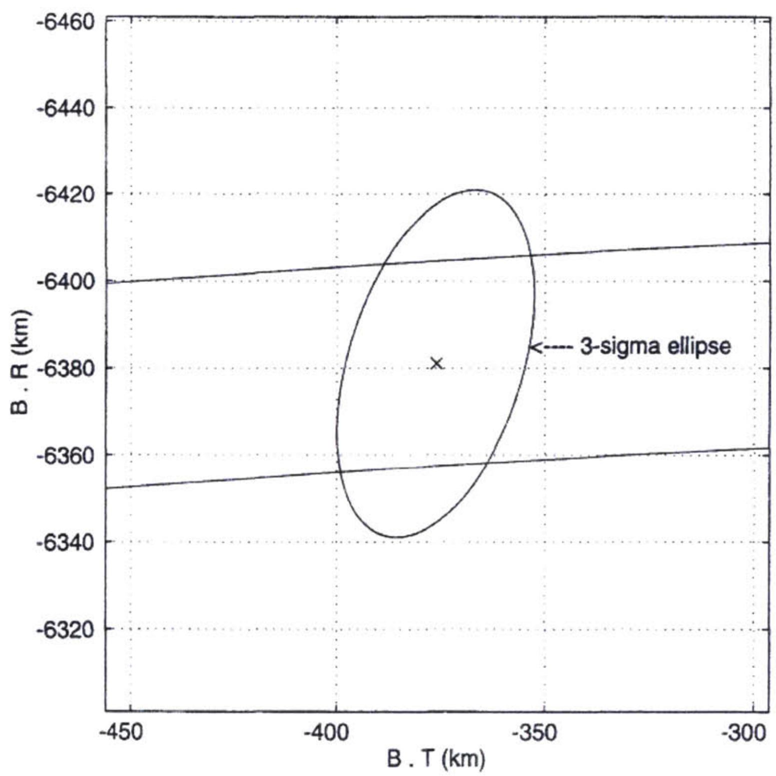

Figure 8: Surveyor Orbiter 3σ Dispersion and Periapsis Requirement along the B-Plane [10]

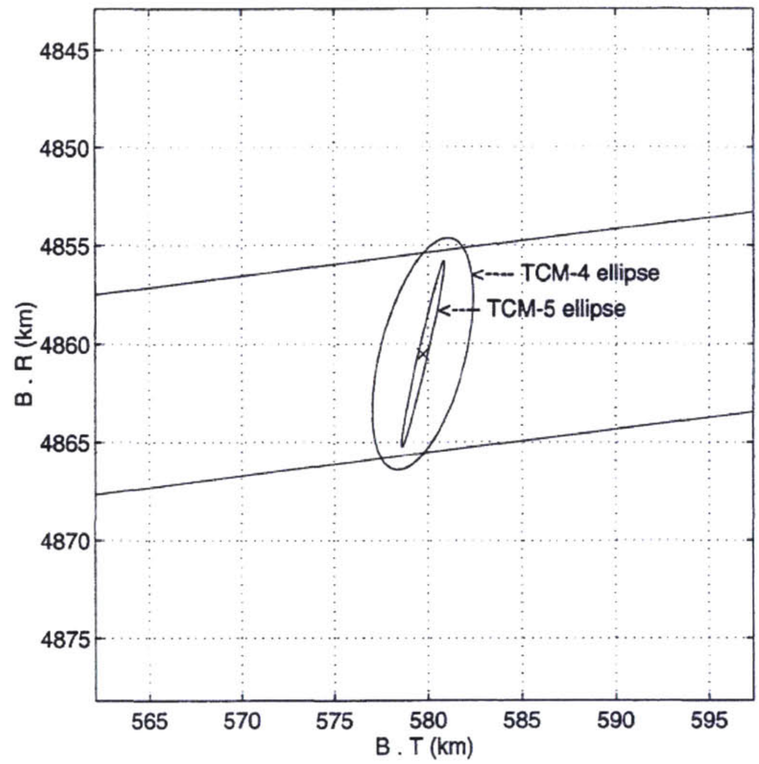

Figure 9: Surveyor Lander 2σ Dispersion and FPA Requirement along the B-Plane [10]

Table 20: Spirit Flight Experience Analysis-Based Navigation Performance Errors

Event	BR (km)	BT (km)	ToF (s)	FPA (°)
1σ Achieved Uncertainty [11]				
TCM-1	380	528	230	N/A
TCM-2	12.6	13.9	4.8	N/A
TCM-3	0.57	0.35	0.16	0.013
TCM-4	0.48	-0.05	0.011	0.0033
1σ Error [11]				
TCM-1	2,348.3	293.9	2,673.4	N/A
TCM-2	425.7	643.6	994.6	N/A
TCM-3	13.1	-11.3	15.2	-0.2283
TCM-4	-0.05	-0.18	0.1	-0.0072
1σ Delivery Uncertainty [11]				
TCM-1	5,519	7,102	3,788	N/A
TCM-2	1,340	2,037	710	N/A
TCM-3	44	50.7	16.1	2.02
TCM-4	1.53	1.5	0.53	0.056

Table 21: Opportunity Flight Experience Analysis-Based Navigation Performance Errors

Event	BR (km)	BT (km)	ToF (s)	FPA (°)
1σ Achieved Uncertainty [11]				
TCM-1	79	116	36	N/A
TCM-2	0.51	0.29	0.15	0.0095
TCM-4	0.44	0.2	0.015	0.007
1σ Error [11]				
TCM-1	3,122	4,771.8	2,792.7	N/A
TCM-2	-46.9	-55.7	-13.8	-2.1791
TCM-4	1.07	0.68	1	0.0301
1σ Delivery Uncertainty [11]				
TCM-1	5,112	8,799	2,388	N/A
TCM-2	148	222	36.2	N/A
TCM-4	2.49	2.38	0.82	0.096

Table 22: Odyssey Flight Experience Analysis-Based OD Pre-Event and Post-Event Errors

Event	BR (km)	BT (km)	TOF (s)	Altitude (km)
1σ Delivery [39]				
Injection	75,000	190,000	N/A	N/A
TCM-1	904	1977	730	N/A
TCM-2	518	998	214	N/A
TCM-3	38	53	14	N/A
TCM-4	5.3	8.3	1.7	5
1σ Post Event Conditions [39]				
Injection	693	1291	404	N/A
TCM-1	652	1061	356	N/A
TCM-2	363	480	145	N/A
TCM-3	4.2	5.6	1.3	N/A
TCM-4	0.04	0.06	0.004	0.043

The results shown in Tables 18-22 should be kept in context of whether the analysis occurred preflight or after the flight experience. It was important to have a concept of the dispersions along the trajectory, but of primary interest were the dispersions experienced at the target point. The final TCM dispersion for each mission in Tables 18-22 were compared by mission type, navigation uncertainty, achieved uncertainty, or delivery error, and were standardized into 3σ values for easy comparison. Table 23 has the lander navigation uncertainties, Table 24 has the orbiter navigation uncertainties, Table 25 has lander-achieved uncertainty, and Table 26 has the orbiter-achieved uncertainty. None of these missions publicly disclosed navigation and achieved uncertainty information. For Phoenix only the final TCM delivery error could be found and is shown in Table 27. Despite this, enough information was available to establish upper and lower bounds for reasonable requirements and navigation uncertainty. In addition, the achieved uncertainty values provide a concept of what would likely be the best case scenario for final target dispersions.

Table 23 : Lander 3σ Requirement for Entry-Interface and Final TCM Navigation Uncertainty

Mission	FPA Requirement (°)	FPA (°)	BT (km)	BR (km)
Pathfinder	1	0.83	23	17.4
Surveyor	0.25	0.25	2.363	6.323
Spirit	0.12	0.082	2.19	2.24
Opportunity	0.14	0.140	3.48	3.64

Table 24: Orbiter 3σ Requirement for Periapsis and Final TCM Navigation Uncertainty

Mission	Altitude Requirement (km)	Altitude	BT (km)	BR (km)
Surveyor	20	35.3	20.88	41.46
Odyssey	25	7.3	8.3	5.3

Table 25: Lander 3σ Requirement for Entry-Interface and Final TCM Achieved Uncertainty

Mission	FPA Requirement (°)	FPA (°)	BT (km)	BR (km)
Spirit	0.12	0.0048	0.073	0.701
Opportunity	0.14	0.0102	0.292	0.643

Table 26: Orbiter 3σ Requirement for Periapsis and Final TCM Achieved Uncertainty

Mission	Altitude Requirement (km)	Altitude	BT (km)	BR (km)
Odyssey	25	0.063	0.088	0.058

Table 27: Phoenix Requirement and Final TCM 5 Delivery Error

Parameter	Requirement	Design and Achieved Difference [8]
Position Error (km)	20	2.002
BT (km)	N/A	1.038
BR (km)	N/A	1.712
FPA (°)	0.21	0.0675

The later landing missions showed a wider margin between the navigation uncertainties and their requirements than the earlier landing missions as seen in Table 23. This was also the case with the navigation uncertainty of the orbiter missions as shown in Table 24. The achieved uncertainty was only available from the later missions for both the lander and orbiter as shown in Table 25 and Table 26, and they were significantly more accurate than their requirements. This was also in the case for the delivery error of Phoenix as shown in Table 27.

Recall that the measurement types and frequencies used for the OD analyses, were shown in Table 1 and Table 2 of Section 4.1.1. During the approach phase of later missions, the DSN measurement frequency was greatly increased. Extremely accurate DDOR measurements were available for later missions, which in turn greatly increased the OD accuracy.

7.5 Basis for Assumed Low-Thrust Propulsion

In the early days of space operations, low-thrust guidance algorithms were of theoretical interest only. There was no hardware on which to test the theories until relatively recently. With limited low-thrust flight demonstrations, an area of active research are methods to increase their reliability. This is not limited to just hardware advancement but also software to mitigate risks. "Planetary protection requirements and the need for robustness to unplanned temporary loss of control is a significant design concern for low-thrust missions in highly perturbed orbital environments." [42]

7.5.1 Deep Space 1 – Low-Thrust Guidance Example Case

DS1 demonstrated an autonomous low-thrust guidance scheme using a terminal controller. The scheme linearized its states to solve for the characteristics of the needed thrust profile. Lagrange multipliers were used to determine the needed conditions of the controller. In addition, achieving desired waypoints along approach trajectories was used for as a basis for low-thrust propulsion autonomous guidance. [43]

DS1 had a solar powered low-thrust Ion Propulsion System (IPS). The electrically controlled IPS "has about 100 throttle levels, with a thrust range of 20 to 90 mN" [26] achieved by varying the voltage supplied to the IPS. The thrust level available is dependent on the electric power available, which decreases as the distance to the sun increases. Unlike chemical propulsion system trajectories, low-thrust trajectories have extremely long active thrusting periods and intermittent coast arcs with no thrusting.

TCM took the form of linearized coarse corrections based on the navigation information. The linearized corrections were valid so long as the IPS performed close to what was expected. "However, if there are very large deviations in the IPS performance from its design, or if frequent outages occur during mission burns, a redesign of the reference trajectory will be done on the ground and uplinked to the spacecraft." [26] The TCM could occur every few weeks and were broken into two parts separated by several hours to ensure that all attitude requirements were followed.

7.6 Hardware Assumptions

CubeSat platforms have been accomplishing increasingly complex missions over the years. There are numerous hardware suppliers for applicable Commercial Off-the-Shelf (COTS) products. A sample of some of the products most relevant to CubeSat navigation and control is provided in Table 28. The included vendors were chosen because they are held in high regard by CubeSat consumers. Each of the components highlighted have either been chosen or were considered for inclusion in the first demonstration missions of deep space CubeSats.

NEAScout, detailed in Section 5.1.2.1 uses the Malin Space Science Systems camera for both its science mission as well as optical navigation. Blue Canyon Technology (BCT) control products come packaged as shown or as individual components. BCT star trackers are commonly used, including by NEAScout. [3] Sinclair Interplanetary focuses on extremely high performance components, especially star trackers, for guidance, navigation, and control.

Table 28: Commercial Off-the-Shelf CubeSat Navigation and Control Components

Blue Canyon Technology (BCT) XACT [44]	BCT Extended Baffle Nano Star Tracker [45]	Sinclair 2nd Gen. Star Tracker (ST-16RT) [46]	Malin Space Science Systems ECAM-M50 [47]
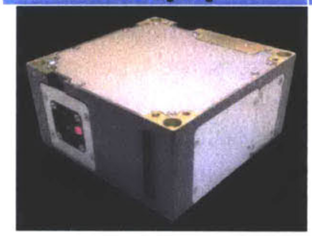	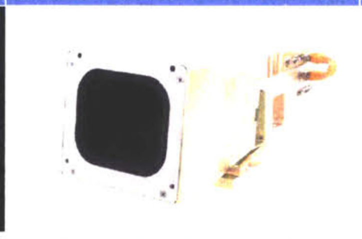		
0.91 kg	1.30 kg	0.158 kg	0.256 kg
10x10x5 cm (0.5u)	25x10x10 cm	6.2x5.6x3.8 cm	7.8x5.8x4.4 cm
3.23 W peak	<= 1.0 W peak	1.0 W peak	2.5 W peak
± 0.003° (1σ) 2 axis, ± 0.007° (1σ) 3rd axis	6 arcsec (1σ), 40 arcsec (1σ) (boresight, roll axis)	< 4 arcsec RMS, < 30 arcsec RMS (cross, around)	5 Megapixel

To accomplish a deep space CubeSat mission, the showcased hardware would not need to be altered in any fundamental way. Star trackers software already performs centerfinding for the objects in the image field. Only a subset of the objects, the stars, are currently used for attitude purposes based on the stars in their available catalogues. Catalogues with the ephemeris information for the bodies of interest for optical navigation can be easily joined with the software already in use for these components. The cameras which do not come off-the-shelf as star trackers can be programmed for optical navigation as was done with NEAScout. With the fundamental GNC hardware already developed, it is expected that as time goes by more accurate and capable components will be available off-the-shelf. In the meantime, processing algorithms for optical navigation have been refined for use in support of the prior missions discussed in Section 5.1.2.

7.7 Linear Covariance (LinCov) Analysis

7.7.1 LinCov Overview

Often used through Preliminary Design Review (PDR) to evaluate GNC design concepts, LinCov also has the potential to be used onboard for mission planning as part of orbit determination for CubeSats - "it is often the case that the expected operational range of a system falls within a narrow band that can be accurately described by linear equations. This is especially true for orbital dynamics where the expected envelope of trajectories about the nominal is often very small." [48]

As DS1 remained close to its nominal trajectory it used linear methods to make mission planning decisions, especially for those related to thrusting. However, to date LinCov has typically been used on programs only during the preliminary design review phase to offer information relevant for the first cut at requirements definition.

LinCov can show the dispersion differences which result from more complex algorithms and simplified algorithms simultaneously if desired. The results from more complex algorithms typically represent the system plans as the ground team would be aware of them. Onboard the spacecraft some of the capabilities that the ground team has may be simplified or not required. This means that LinCov can show the dispersions which would result if the planned flight software was used to make maneuver selections along a trajectory. [48]

Based on the results LinCov analysis, the program can have informed discussions about how to refine the mission plans. Topics can include, but are not limited to, whether the flight software should be more complex, whether the sensors used should be more accurate, the timing of maneuvers, the types of maneuvers performed, if different actuators are needed, and more. Because once a LinCov program is completed it shows the statistics of different options much more quickly than other GNC analysis methods given the same computational capabilities used, there has been interest in using its methods as part of an onboard mission planner.

After a nominal maneuver has been performed the flight computer could determine if it will meet its end requirement. If it will not, the flight computer can use LinCov to determine the "best" location to perform additional maneuvers. "Best" is in quotes because it is subjective to the capabilities provided onboard and the desires of the program managers. "Best" can be to minimize fuel use while meeting the requirement, the time to get there, or a weighted combination of desired characteristics. One maneuver option could be derived from one style of targeting the flight computer has to use for analysis with specific locations and/or maneuver durations selected along the nominal trajectory. Another option could be derived from multiple targeting or guidance options to be compared at one or multiple locations along the nominal trajectory. The subjective features for the criteria of the "best" maneuver to compare to the other maneuver options available onboard can be preloaded into the flight computer or, depending on the amount of available onboard autonomy, decide fully onboard to match real time conditions. This is exactly how LinCov is used during PDR, except that the ground team has more resources for decision making based on the results. Once a linear covariance tool has been developed, it can perform analyses rapidly. This speed allows reaction in near-real time. Very importantly, it does not take much computational ability, an important consideration for CubeSats.

7.7.1.1 LinCov Output Details

When assessing the overall performance of a GNC system, key parameters such as trajectory dispersion, navigation errors, and timing of critical events are analyzed. This is typically performed by Monte Carlo (MC) analysis over hundreds or potentially thousands of runs. LinCov does not replace MC but complements it for top-level analysis, and its big picture view untangles the complex interdependencies of a closed-loop system. This is done by augmenting the analyzed state to include the true and navigation dispersions and analyzing those statistics directly. A MC run sums the dispersion of all the runs completed, but both methods yield the same results. [48] Figure 10 shows the states used to quantify the dispersions which are described in Table 29.

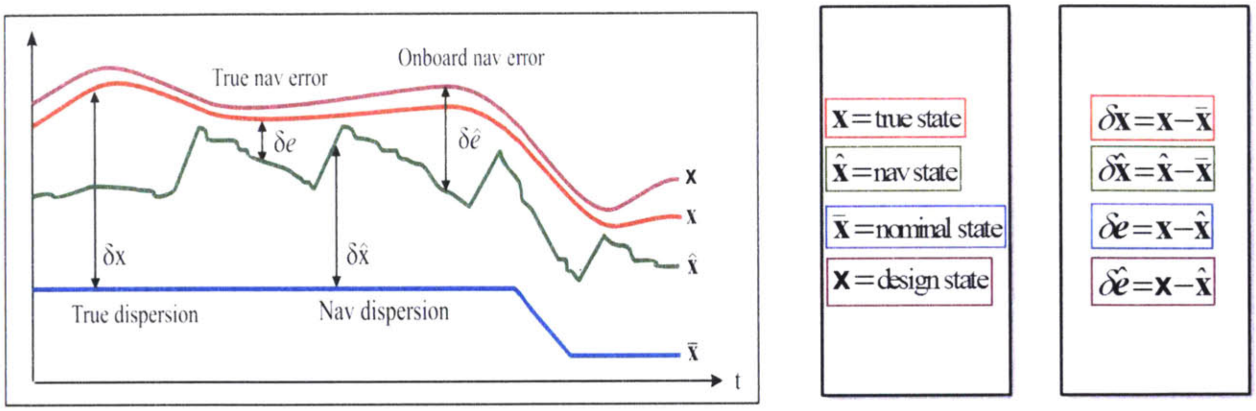

Figure 10: Linear Covariance States for Dispersion and Error Analysis [49]

Table 29: Covariance Detail Summary

Covariance Type	Description	Equation
True Dispersion Covariance	How precisely the GNC system can follow the desired trajectory	$\mathbf{D} = E\left[\delta\mathbf{x}\,\delta\mathbf{x}^{\mathrm{T}}\right]$
Navigation Dispersion Covariance	How precisely the flight computer can follow the nominal trajectory	$\hat{\mathbf{D}} = E\left[\delta\hat{\mathbf{x}}\,\delta\hat{\mathbf{x}}^{\mathrm{T}}\right]$
True Navigation Covariance	The actual navigation performance	$\mathbf{P} = E\left[\delta\mathbf{e}\,\delta\mathbf{e}^{\mathrm{T}}\right]$
Onboard Navigation Covariance	The flight computer's predicted navigation accuracy	$\hat{\mathbf{P}} = E\left[\delta\hat{\mathbf{e}}\,\delta\hat{\mathbf{e}}^{\mathrm{T}}\right]$

7.7.1.2 Process

With LinCov analysis, the same statistical information for a closed-loop GN&C system can be produced with a single simulation run. For this reason, the LinCov tool is ideal for top-level analysis because it produces Monte Carlo-like results rapidly. Figure 11 shows the alternate form of the true dispersion, navigation dispersion, true navigation covariance, and onboard navigation covariance.

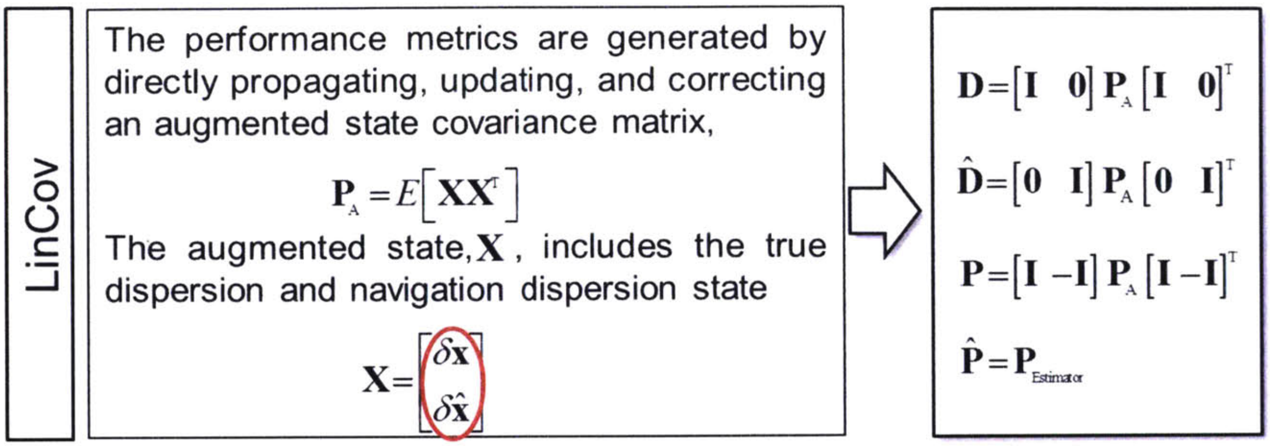

Figure 11: Augmented States for Linear Covariance Relationship Analysis [49]

Overall performance information includes the effects of the errors on both navigation and trajectory dispersions in one run. Figure 12 shows the flow of information in a Linear Covariance analysis where the states and errors are initiated and propagated, sensor information updates the navigation error, and maneuvers correct the trajectory dispersions.

Table 30 identifies the correlation of states needed in LinCov analysis to affected events.

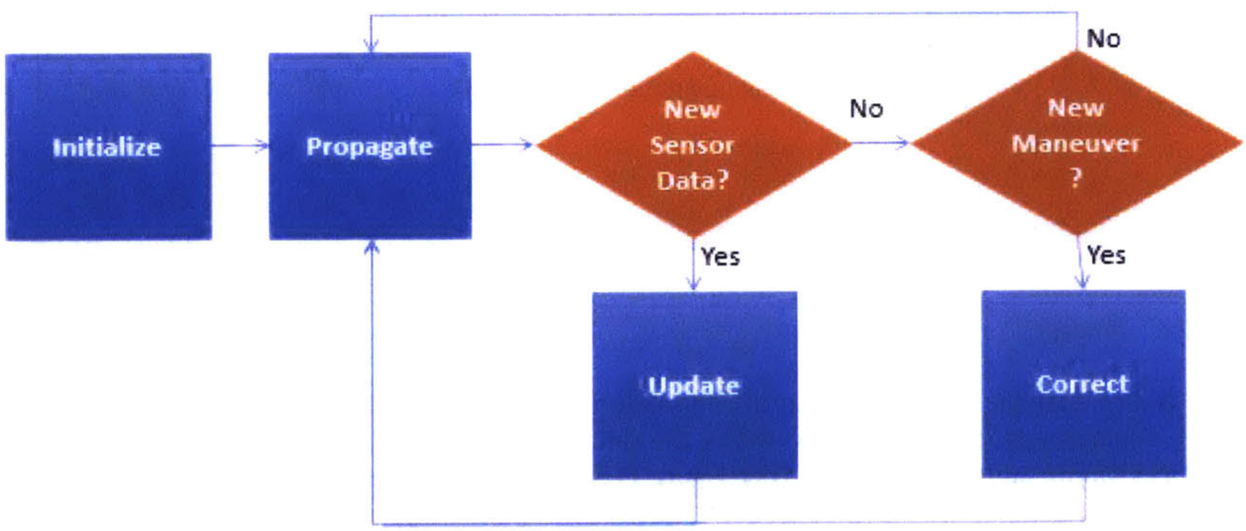

Figure 12: Linear Covariance Analysis Data Flow

Table 30: Correlation of Needed States Analyzed by LinCov to Affected Events

Needed States	Affected Events
True State	Maneuvers
Onboard State	Measurements
Trajectory Dispersion	Maneuvers & Trajectory Corrections
Navigation Error	Measurements & Updates

7.7.1.3 General Mathematic Formulation

This section provides the generic mathematic equations to set up a linear covariance analysis. First, the nomenclature is defined for the variable types of interest in Table 31. With the states to considered determined, Table 32 defines their covariances. The standard form of their covariance based on the expectations of the dispersion and errors of the states considered separately. By augmenting the state considered to include the state dispersions directly, equivalent forms of the covariances can be used so the dispersions do not have to be calculated separately. [48] [49]

Table 31: Considered States

Symbol	Description	Details
x	Design state	The design's expected state
x	True state	The actual state of the system
$\hat{\mathrm{x}}$	Navigation state	The state according to instruments and filters
$\bar{\mathrm{x}}$	Nominal State (modeled state)	The baseline approximation of the state

The differences between the various state options define the errors and dispersions of interest:

$$\delta\mathbf{x} = \mathbf{x} - \bar{\mathbf{x}} \tag{2}$$

$$\delta\hat{\mathbf{x}} = \hat{\mathbf{x}} - \bar{\mathbf{x}} \tag{3}$$

$$\delta\mathbf{e} = \mathbf{x} - \hat{\mathbf{x}} \tag{4}$$

$$\delta\hat{\mathbf{e}} = \mathbf{x} - \hat{\mathbf{x}} \tag{5}$$

$$\mathbf{D} = E\left[\delta\mathbf{x}\delta\mathbf{x}^{\mathrm{T}}\right] \tag{6}$$

$$\widehat{\mathbf{D}} = E\left[\delta\hat{\mathbf{x}}\delta\hat{\mathbf{x}}^{\mathrm{T}}\right] \tag{7}$$

$$\mathbf{P} = E\left[\delta\mathbf{e}\delta\mathbf{e}^{\mathrm{T}}\right] \tag{8}$$

$$\widehat{\mathbf{P}} = E\left[\delta\hat{\mathbf{e}}\delta\hat{\mathbf{e}}^{\mathrm{T}}\right] \tag{9}$$

Table 32: Covariance Details

Equation	Description	Details
(6)	True Dispersion Covariance	How precisely the GNC system can follow the desired trajectory
(7)	Navigation Dispersion Covariance	How precisely the flight computer can follow the nominal trajectory
(8)	True Navigation Covariance	The actual navigation performance
(9)	Onboard Navigation Covariance	The flight computer's predicted navigation accuracy

The difference between equations (6) and (7) is the actual overall system performance versus the flight computer's characterization of the system's performance. The difference between equations (8) and (9) is the navigation performance versus the flight computer's characterization of the navigation's performance.

To propagate, update and correct the values of equations (6) and (9), an augmented state is defined with equations (2) and (3), which is in turn used to define an augmented state covariance matrix, as seen below.

$$\mathbf{X} = \begin{bmatrix} \delta\mathbf{x} \\ \delta\hat{\mathbf{x}} \end{bmatrix} \tag{10}$$

$$\mathbf{P}_{\mathrm{A}} = E[\mathbf{X}\mathbf{X}^{\mathrm{T}}] \tag{11}$$

$$\mathbf{D} = [\mathrm{I} \quad 0]\mathbf{P}_{\mathrm{A}}[\mathbf{I} \quad \mathbf{0}]^{\mathrm{T}} \tag{12}$$

$$\hat{\mathbf{D}} = [\mathbf{0} \quad \mathbf{I}]\mathbf{P}_{\mathrm{A}}[\mathbf{0} \quad \mathbf{I}]^{T} \tag{13}$$

$$\mathbf{P} = [\mathbf{I} \quad \mathbf{-I}]\mathbf{P}_{\mathrm{A}}[\mathbf{I} \quad -\mathbf{I}]^{T} \tag{14}$$

$$\hat{\mathbf{P}}=\mathbf{P}_{\mathrm{Estimator}} \tag{15}$$

7.7.1.3.1 Initialization and Propagation

To initialize (11) the augmented covariance matrix is defined in terms of the initial true dispersion and initial navigation dispersion, δx_0 and $\delta \hat{x}_0$ respectively.

$$P_{A_0} = E[X_0 X_0^T] = E\begin{bmatrix} \delta x_0 \delta x_0^T & \delta x_0 \delta \hat{x}_0^T \\ \delta \hat{x}_0 \delta x_0^T & \delta \hat{x}_0 \delta \hat{x}_0^T \end{bmatrix} \tag{16}$$

Rearranging equations (4), (10), and (16) shows the initial augmented state covariance in terms of the initial dispersions and navigation error.

$$P_{A_0} = E\begin{bmatrix} \delta x_0 \delta x_0^T & \delta x_0(\delta x_0 - \delta e_0)^T \\ (\delta x_0 - \delta e_0)\delta x_0^T & (\delta x_0 - \delta e_0)(\delta x_0 - \delta e_0)^T \end{bmatrix} = \begin{bmatrix} D_0 & D_0 \\ D_0 & D_0 + P_0 \end{bmatrix} \tag{17}$$

To propagate (17) involves taking the partial derivatives of the true state dynamics, navigation state dynamics, true control input, and commanded control input. The following equation series shows the general relationships required to propagate the augmented state covariance.

$$\dot{\boldsymbol{x}} = \boldsymbol{a}(\boldsymbol{x}, \boldsymbol{u}, \boldsymbol{w}) \tag{18}$$

$$\dot{\hat{\boldsymbol{x}}} = \hat{\boldsymbol{a}}(\hat{\boldsymbol{x}}, \hat{\boldsymbol{u}}) \tag{19}$$

$$\boldsymbol{u} = \boldsymbol{b}(\boldsymbol{x}, \hat{\boldsymbol{x}}, \boldsymbol{v}) \tag{20}$$

$$\hat{\boldsymbol{u}} = \hat{\boldsymbol{b}}(\hat{\boldsymbol{x}}) \tag{21}$$

$$\delta\dot{\boldsymbol{x}} = \boldsymbol{A}_x \delta\boldsymbol{x} + \boldsymbol{A}_u \delta\boldsymbol{u} + \boldsymbol{A}_w \boldsymbol{w} \tag{22}$$

$$\delta\dot{\hat{\boldsymbol{x}}} = \hat{\boldsymbol{A}}_{\hat{x}} \delta\hat{\boldsymbol{x}} + \hat{\boldsymbol{A}}_u \delta\hat{\boldsymbol{u}} \tag{23}$$

$$\delta\boldsymbol{u} = \boldsymbol{B}_x \delta\boldsymbol{x} + \boldsymbol{B}_{\hat{x}} \delta\hat{\boldsymbol{x}} + \boldsymbol{B}_v \boldsymbol{v} \tag{24}$$

$$\delta\hat{\boldsymbol{u}} = \hat{\boldsymbol{B}}_{\hat{x}} \delta\hat{\boldsymbol{x}} \tag{25}$$

The partials are taken about the nominal trajectory and are defined as follows in Table 33 and Table 34.

Table 33: State Variables Linearized about the Nominal Trajectory

Variable	$\boldsymbol{A}_x$	$\boldsymbol{A}_u$	$\boldsymbol{A}_w$	$\hat{\boldsymbol{A}}_{\hat{x}}$	$\hat{\boldsymbol{A}}_{\hat{u}}$
State Partial	$\left.\frac{\partial \boldsymbol{a}(\boldsymbol{x},\boldsymbol{u},\boldsymbol{w})}{\partial \boldsymbol{x}}\right\|_{\bar{x}}$	$\left.\frac{\partial \boldsymbol{a}(\boldsymbol{x},\boldsymbol{u},\boldsymbol{w})}{\partial \boldsymbol{u}}\right\|_{\bar{x}}$	$\left.\frac{\partial \boldsymbol{a}(\boldsymbol{x},\boldsymbol{u},\boldsymbol{w})}{\partial \boldsymbol{w}}\right\|_{\bar{x}}$	$\left.\frac{\partial \hat{\boldsymbol{a}}(\hat{\boldsymbol{x}},\hat{\boldsymbol{u}})}{\partial \hat{\boldsymbol{x}}}\right\|_{\bar{x}}$	$\left.\frac{\partial \boldsymbol{a}(\boldsymbol{x},\boldsymbol{u},\boldsymbol{w})}{\partial \boldsymbol{w}}\right\|_{\bar{x}}$

Table 34: Control Variables Linearized about the Nominal

Variable	$\boldsymbol{B}_x$	$\boldsymbol{B}_u$	$\boldsymbol{B}_v$	$\hat{\boldsymbol{B}}_{\hat{x}}$
Control Partial	$\left.\frac{\partial \boldsymbol{b}(\boldsymbol{x},\hat{\boldsymbol{x}},\boldsymbol{v})}{\partial \boldsymbol{x}}\right\|_{\bar{x}}$	$\left.\frac{\partial \boldsymbol{b}(\boldsymbol{x},\hat{\boldsymbol{x}},\boldsymbol{v})}{\partial \hat{\boldsymbol{x}}}\right\|_{\bar{x}}$	$\left.\frac{\partial \boldsymbol{b}(\boldsymbol{x},\hat{\boldsymbol{x}},\boldsymbol{v})}{\partial \boldsymbol{v}}\right\|_{\bar{x}}$	$\left.\frac{\partial \hat{\boldsymbol{b}}(\hat{\boldsymbol{x}})}{\partial \hat{\boldsymbol{x}}}\right\|_{\bar{x}}$

Joining equations (22)and (24) produces the true state dispersions as a function of the true state, navigation state, process noise and measurement noise.

$$\delta\dot{\boldsymbol{x}} = [\boldsymbol{A}_x + \boldsymbol{A}_u \boldsymbol{B}_x]\delta\boldsymbol{x} + [\boldsymbol{A}_u \boldsymbol{B}_{\hat{x}}]\delta\hat{\boldsymbol{x}} + [\boldsymbol{A}_w]\boldsymbol{w} + [A_u B_v]\boldsymbol{v} \tag{26}$$

Similarly, equations (23) and (25) together define the navigation state dynamics as a function of the navigation state.

$$\delta\dot{\hat{\boldsymbol{x}}} = [\hat{\boldsymbol{A}}_{\hat{x}} + \hat{\boldsymbol{A}}_{\hat{u}} \hat{\boldsymbol{B}}_{\hat{x}}]\delta\hat{\boldsymbol{x}} \tag{27}$$

With both equations (26) and (27) and defined the augmented state dynamics can be defined as

$$\begin{bmatrix} \delta\dot{x} \\ \delta\dot{\hat{x}} \end{bmatrix} = \begin{bmatrix} (A_x + A_u B_x) & (A_u B_{\hat{x}}) \\ 0 & (\hat{A}_{\hat{x}} + \hat{A}_{\hat{u}} \hat{B}_{\hat{x}}) \end{bmatrix} \begin{bmatrix} \delta x \\ \delta\hat{x} \end{bmatrix} + \begin{bmatrix} A_w \\ 0 \end{bmatrix} w + \begin{bmatrix} A_u B_v \\ 0 \end{bmatrix} v \tag{28}$$

Which can be represented as

$$\dot{X} = \mathbf{AX} + \mathbf{Ww} + \mathbf{V}v \tag{29}$$

When recalling equations (11) and (17)using equation (29) the augmented state covariance propagation is

$$\dot{P}_A = AP_A + P_A A^T + WS_w W^T + VS_v V^T \tag{30}$$

Where the variables are as defined in Table 35.

Table 35: State Propagation Variable Summary

Variable	Equivalence
A	$\begin{bmatrix} (A_x + A_u B_x) & (A_u B_{\hat{x}}) \\ 0 & (\hat{A}_{\hat{x}} + \hat{A}_{\hat{u}} \hat{B}_{\hat{x}}) \end{bmatrix}$
$\mathbf{W}$	$\begin{bmatrix} A_w \\ 0 \end{bmatrix}$
V	$\begin{bmatrix} A_u B_v \\ 0 \end{bmatrix}$
S_w	$E[w(t)w(t')^T]\delta(t-t')$
S_v	$E[v(t)v(t')^T]\delta(t-t')$

7.7.1.3.2 Update and Correct

Updates to the covariance come from new measurement information. The following shows the relationships involving discrete measurements to form an update.

$$x^+ = x^- \tag{31}$$

$$\hat{x}^+ = \hat{x}^- + \hat{K}[\tilde{z} - \hat{z}] \tag{32}$$

$$\hat{K} = \hat{P}^- \hat{H}\left[\hat{H}\hat{P}^- \hat{H}^T + \hat{R}\right]^{-1} \tag{33}$$

$$R = E\left[\eta_k \eta_{k'}^T\right]\delta_{kk'} \tag{34}$$

$$\tilde{z} = h(x^-, \eta) \tag{35}$$

$$\hat{z} = h(\hat{x}^-) \tag{36}$$

Discrete measurements do not affect the true state, which is reflected in (31) as it is only a function of the prior state. The navigation state is affected both by the prior state, the measurements taken, the measurements expected, and the Kalman gain, shown in (32). The Kalman Gain in (33) is based on the prior covariance, the measurement matrix and the noise expectation. The measurement matrix, H, captures the type of information a sensor provides. For example, if a sensor's measurement is only a reflection of position and not velocity, only the position columns would have elements as appropriate and the velocity portion of the measurement matrix would be empty. The actual measurement in (35) will differ from the expected measurement, (36), based on the algorithms used onboard to set the navigation predictions.

As expected, the dispersions of the true state and navigation dispersions have the same relationship to measurement updates as the true state and navigation state. The linearized functions form the augmented state and covariance updates, seen below.

$$\delta \boldsymbol{x}^{+} = \delta \boldsymbol{x}^{-} \tag{37}$$

$$\delta \widehat{\boldsymbol{x}}^{+} = [\widehat{\boldsymbol{K}}\boldsymbol{H}_{x}]\delta \boldsymbol{x}^{-} + [\boldsymbol{I} - \widehat{\boldsymbol{K}}\widehat{\boldsymbol{H}}_{\hat{x}}]\delta \widehat{\boldsymbol{x}}^{-} + [\widehat{\boldsymbol{K}}]\boldsymbol{\eta} \tag{38}$$

$$\begin{bmatrix} \delta \boldsymbol{x}^{+} \\ \delta \widehat{\boldsymbol{x}}^{+} \end{bmatrix} = \begin{bmatrix} \boldsymbol{I} & \boldsymbol{0} \\ (\widehat{\boldsymbol{K}}\boldsymbol{H}_{x}) & (\boldsymbol{I} - \widehat{\boldsymbol{K}}\widehat{\boldsymbol{H}}_{\hat{x}}) \end{bmatrix} \begin{bmatrix} \delta \boldsymbol{x}^{-} \\ \delta \widehat{\boldsymbol{x}}^{-} \end{bmatrix} + \begin{bmatrix} \boldsymbol{0} \\ \widehat{\boldsymbol{K}} \end{bmatrix} \boldsymbol{\eta} \tag{39}$$

$$\boldsymbol{X}^{+} = \boldsymbol{M}\boldsymbol{X}^{-} + \boldsymbol{N}\boldsymbol{\eta} \tag{40}$$

$$\boldsymbol{P}_{A}^{+} = \boldsymbol{M}\boldsymbol{P}_{A}^{-}\boldsymbol{M}^{T} + \boldsymbol{N}\boldsymbol{R}\boldsymbol{N}^{T} \tag{41}$$

The measurement partials are taken about the nominal trajectory and are defined as follows in Table 36.

Table 36: Update Variables

Variable	$\boldsymbol{H}_{x}$	$\widehat{\boldsymbol{H}}_{\hat{x}}$	$\boldsymbol{M}$	$\boldsymbol{N}$
Equivalence	$\left.\frac{\partial \boldsymbol{h}(\boldsymbol{x}^{-}, \boldsymbol{\eta})}{\partial \boldsymbol{x}^{-}}\right\|_{\bar{x}}$	$\left.\frac{\partial \widehat{\boldsymbol{h}}(\widehat{\boldsymbol{x}}^{-})}{\partial \widehat{\boldsymbol{x}}^{-}}\right\|_{\bar{x}}$	$\begin{bmatrix} \boldsymbol{I} & \boldsymbol{0} \\ (\widehat{\boldsymbol{K}}\boldsymbol{H}_{x}) & (\boldsymbol{I} - \widehat{\boldsymbol{K}}\widehat{\boldsymbol{H}}_{\hat{x}}) \end{bmatrix}$	$\begin{bmatrix} \boldsymbol{0} \\ \widehat{\boldsymbol{K}} \end{bmatrix}$

Correcting the covariance is done to reduce the uncertainty which is implicit in the covariance magnitude. It is done with targeting of some sort to alter what was originally planned to consider what may currently be needed. It is very similar to the original covariance flow seen in (18) through (25) with features used to update the covariance.

$$\boldsymbol{x}^{+c} = \boldsymbol{x}^{-c} + \boldsymbol{d}(\boldsymbol{x}^{-c}, \Delta \boldsymbol{u}) \tag{42}$$

$$\delta \boldsymbol{x}^{+c} = \delta \boldsymbol{x}^{-c} + \boldsymbol{D}_{x}\delta \boldsymbol{x}^{-c} + \boldsymbol{D}_{\Delta u}\delta \Delta \boldsymbol{u} \tag{43}$$

$$\widehat{\boldsymbol{x}}^{+c} = \widehat{\boldsymbol{x}}^{-c} + \widehat{\boldsymbol{d}}(\widehat{\boldsymbol{x}}^{-c}, \Delta \widehat{\boldsymbol{u}}) \tag{44}$$

$$\delta \widehat{\boldsymbol{x}}^{+c} = \delta \widehat{\boldsymbol{x}}^{-c} + \widehat{\boldsymbol{D}}_{\hat{x}}\delta \widehat{\boldsymbol{x}}^{-c} + \widehat{\boldsymbol{D}}_{\Delta \hat{u}}\delta \Delta \widehat{\boldsymbol{u}} \tag{45}$$

$$\Delta \boldsymbol{u} = \Delta \boldsymbol{b}(\boldsymbol{x}, \widehat{\boldsymbol{x}}, \Delta \boldsymbol{v}) \tag{46}$$

$$\delta \Delta \boldsymbol{u} = \Delta \boldsymbol{B}_{x}\delta \boldsymbol{x}^{-c} + \Delta \boldsymbol{B}_{\hat{x}}\delta \widehat{\boldsymbol{x}}^{-c} + \Delta \boldsymbol{B}_{\Delta v}\Delta \boldsymbol{v} \tag{47}$$

$$\Delta \widehat{\boldsymbol{u}} = \Delta \widehat{\boldsymbol{b}}(\widehat{\boldsymbol{x}}) \tag{48}$$

$$\delta\Delta\widehat{\boldsymbol{u}} = \Delta\widehat{\boldsymbol{B}}_{\hat{x}}\delta\widehat{\boldsymbol{x}}^{-c} \tag{49}$$

The partials of the corrected state and control are taken about the nominal trajectory and are defined as follows in Tables 37 and 38.

Table 37: Corrected State Linearized Variables

Variable	$\boldsymbol{D}_x$	$\boldsymbol{D}_{\Delta u}$	$\widehat{\boldsymbol{D}}_{\hat{x}}$	$\widehat{\boldsymbol{D}}_{\widehat{\Delta u}}$
State Partial	$\left.\frac{\partial \boldsymbol{d}(\boldsymbol{x}^{-c},\Delta\boldsymbol{u})}{\partial \boldsymbol{x}^{-c}}\right\|_{\bar{x}}$	$\left.\frac{\partial \boldsymbol{d}(\boldsymbol{x}^{-c},\Delta\boldsymbol{u})}{\partial \Delta\boldsymbol{u}}\right\|_{\bar{x}}$	$\left.\frac{\partial \widehat{\boldsymbol{d}}(\widehat{\boldsymbol{x}}^{-c},\Delta\widehat{\boldsymbol{u}})}{\partial \widehat{\boldsymbol{x}}^{-c}}\right\|_{\bar{x}}$	$\left.\frac{\partial \widehat{\boldsymbol{d}}(\widehat{\boldsymbol{x}}^{-c},\Delta\widehat{\boldsymbol{u}})}{\partial \Delta\widehat{\boldsymbol{u}}}\right\|_{\bar{x}}$

Table 38: Correcting Control Linearized Variables

Variable	$\Delta\boldsymbol{B}_x$	$\Delta\boldsymbol{B}_u$	$\Delta\boldsymbol{B}_{\Delta v}$	$\widehat{\Delta\boldsymbol{B}}_{\hat{x}}$
Control Partial	$\left.\frac{\partial \Delta\boldsymbol{b}(\boldsymbol{x},\widehat{\boldsymbol{x}},\Delta\boldsymbol{v})}{\partial \boldsymbol{x}}\right\|_{\bar{x}}$	$\left.\frac{\partial \Delta\boldsymbol{b}(\boldsymbol{x},\widehat{\boldsymbol{x}},\Delta\boldsymbol{v})}{\partial \widehat{\boldsymbol{x}}}\right\|_{\bar{x}}$	$\left.\frac{\partial \Delta\boldsymbol{b}(\boldsymbol{x},\widehat{\boldsymbol{x}},\Delta\boldsymbol{v})}{\partial \boldsymbol{v}}\right\|_{\bar{x}}$	$\left.\frac{\partial \widehat{\Delta\boldsymbol{b}}(\widehat{\boldsymbol{x}})}{\partial \widehat{\boldsymbol{x}}}\right\|_{\bar{x}}$

The state and control equations can be combined to produce the augmented state and covariance, shown below.

$$\delta\boldsymbol{x}^{+c} = [\boldsymbol{I} + \boldsymbol{D}_x + \boldsymbol{D}_{\Delta u}\Delta\boldsymbol{B}_x]\delta\boldsymbol{x}^{-c} + [\boldsymbol{D}_{\Delta u}\Delta\boldsymbol{B}_{\hat{x}}]\delta\widehat{\boldsymbol{x}}^{-c} + [\boldsymbol{D}_{\Delta u}\Delta\boldsymbol{B}_{\Delta v}]\Delta\boldsymbol{v} \tag{50}$$

$$\delta\widehat{\boldsymbol{x}}^{+c} = \left[\boldsymbol{I} + \widehat{\boldsymbol{D}}_{\hat{x}} + \widehat{\boldsymbol{D}}_{\Delta\hat{u}}\Delta\widehat{\boldsymbol{B}}_{\hat{x}}\right]\delta\widehat{\boldsymbol{x}}^{-c} \tag{51}$$

$$\begin{bmatrix}\delta\boldsymbol{x}^{+c}\\ \delta\widehat{\boldsymbol{x}}^{+c}\end{bmatrix} = \begin{bmatrix}(\boldsymbol{I} + \boldsymbol{D}_x + \boldsymbol{D}_{\Delta u}\Delta\boldsymbol{B}_x) & (\boldsymbol{D}_{\Delta u}\Delta\boldsymbol{B}_{\hat{x}})\\ \boldsymbol{0} & \left(\boldsymbol{I} + \widehat{\boldsymbol{D}}_{\hat{x}} + \widehat{\boldsymbol{D}}_{\Delta\hat{u}}\Delta\widehat{\boldsymbol{B}}_{\hat{x}}\right)\end{bmatrix}\begin{bmatrix}\delta\boldsymbol{x}^{-c}\\ \delta\widehat{\boldsymbol{x}}^{-c}\end{bmatrix} + \begin{bmatrix}\boldsymbol{D}_{\Delta u}\Delta\boldsymbol{B}_{\Delta v}\\ \boldsymbol{0}\end{bmatrix}\Delta\boldsymbol{v} \tag{52}$$

$$\boldsymbol{X}^{+c} = \boldsymbol{D}\boldsymbol{X}^{-c} + \boldsymbol{U}\Delta\boldsymbol{v} \tag{53}$$

$$\boldsymbol{P}_A^{+c} = \boldsymbol{D}\boldsymbol{P}_A^{-c}\boldsymbol{D}^T + \boldsymbol{U}\boldsymbol{S}_{\Delta\boldsymbol{v}}\boldsymbol{U}^T \tag{54}$$

Where the variables of the augmented corrected state and covariance are as defined in Table 39.

Table 39: Corrected State Variable Summary

Variable	Equivalence
$\boldsymbol{D}$	$\begin{bmatrix}(\boldsymbol{I} + \boldsymbol{D}_x + \boldsymbol{D}_{\Delta u}\Delta\boldsymbol{B}_x) & (\boldsymbol{D}_{\Delta u}\Delta\boldsymbol{B}_{\hat{x}})\\ \boldsymbol{0} & \left(\boldsymbol{I} + \widehat{\boldsymbol{D}}_{\hat{x}} + \widehat{\boldsymbol{D}}_{\Delta\hat{u}}\Delta\widehat{\boldsymbol{B}}_{\hat{x}}\right)\end{bmatrix}$
$\boldsymbol{U}$	$\begin{bmatrix}\boldsymbol{D}_{\Delta u}\Delta\boldsymbol{B}_{\Delta v}\\ \boldsymbol{0}\end{bmatrix}$
$\boldsymbol{S}_{\Delta v}$	$E\left[\Delta\boldsymbol{v}_k\Delta\boldsymbol{v}_{k'}^T\right]\delta_{kk'}$

7.8 LinCov Tool

7.8.1 Guidance Options

"The guidance function must compute an acceleration profile correction that takes the spacecraft to the desired state at a given time and produces a trajectory as close as possible to the reference trajectory." [43]

There are numerous guidance schemes that can be selected for space missions. Many have core similarities which will be discussed. The procedures applied to the impulsive case are frequently modified for optimality in the low-thrust case. Normally a trajectory correction maneuver (TCM) is impulsive. When in a heliocentric orbit, low-thrust maneuvers can be considered impulsive. This is because of the duration of the overall trajectory compared to the length of the burn. "A weeklong burn arc is small compared to the heliocentric orbit period, and the burn direction is nearly constant." [50] This section provides an overview of the guidance algorithms selected for analysis.

7.8.1.1 Time of Arrival Guidance – Terminal Controller Overview

When it comes to choosing a path, two concerns that come to mind are the effort it takes to takes to achieve that path and the time to reach the final destination. A further issue to consider is whether or not the system as designed is capable of the actions required without damaging itself. An example that comes to mind is a hiker on a mountain. A new hiker wanting to expend as little energy as possible may take a longer, less steep path to the top of the mountain regardless of the time it takes. An experienced hiker that is part of a competition might need to reach the summit by a certain time and will choose the path which will allow him to do so regardless of the effort required. Each hiker may be considering their physical capabilities when choosing their path or exclusively the effort required.

The sort of concerns described above motivate time of arrival guidance. Questions that remain are: How should a system, likely nonlinear, be modeled? What type of controller should be used to manage the system's dynamic capabilities?

"Many systems that we wish to control are already adequately described by linear dynamic models. In this case, it is possible to synthesize very satisfactory linear feedback controllers by the proper choice of quadratic performance criteria and quadratic constraints. A terminal controller is designed to bring a system close to desired conditions at a terminal time (which may or may not be specified) while exhibiting acceptable behavior on the way." [51]

As noted previously, orbital dynamics naturally keep objects within a small band about a nominal trajectory. This means the linearity required for time of arrival guidance schemes is applicable. Though low-thrust propulsion is used in the case to be examined, as it is in the heliocentric frame, a linear terminal controller will suffice.

"Over relatively short periods of time a linear compensator will effectively control the spacecraft since the linearized system matrix changes slowly over time compared to the numerical integration step size." [52]

It is desired to bring a linear time-varying system from an initial state

$$x(t_0)$$

To a terminal state

$$x(t_f) \cong 0 \tag{55}$$

using "acceptable" levels of control and not exceeding "acceptable" levels of the state errors along the way. One way to do this is to minimize a performance index made of a quadratic form in the terminal state plus an integral of quadratic forms in the state and control:

$$J = \frac{1}{2}(x^T S_f x)_{t=tf} + \frac{1}{2}\int_{t_0}^{t_f}(x^T Ax + u^T Bu)dt \tag{56}$$

"Where S_f and $A(t)$ are positive semidefinite matrices and B is a positive definite matrix. An appropriate choice of these matrices must be made to obtain "acceptable" levels of $x(t_f)$, $x(t)$, and $u(t)$." [51] The control which minimizes the performance index can be found using the Euler-Lagrange equations.

The boundary value portion of the problem can be solved using the transition matrix through linear superposition. The gain from the feedback control law through this method is then based on the current state. Another way to the boundary value solution is to use the "sweep method" based on the Riccati equations. It is called this because from the acceptable terminal conditions the coefficients of its matrix are solved by being "swept" backwards to the initial time. Doing so yields a matrix Riccati equation. The feedback control gain in this case has the same form as with the transition matrix method. The difference is the first is dependent on the transition matrix and the latter is dependent on the solution to the Riccati equation. More details on the methods to solve for a terminal controller, along with different performance index, can be found in chapter 5 of [51].

The linearization of the nonlinear dynamics has already been shown during the LinCov overview, Section 7.7.1.2. The connection of the Kalman Gain for estimation was presented, also known as the Linear Quadratic Gaussian (LQG). The true state dispersions were defined exclusively by the state by replacing the control variables with the linearized state dependent control equation. This is possible because the same can be done with the dynamics directly.

With the same cost function and linearized dynamics, a Linear Quadratic Regulator (LQR) can be defined which has state dependent feedback gains. This is also referred to as the state dependent Riccati equation (SDRE) [53]. The control equation previously defined had variables dependent on the true state. The feedback control law with the optimal gain defined by the Riccati equations results in closed loop dynamics that instead of having constant matrices have state-dependent matrices. These would be applied in the "correcting" portion of the analysis.

7.8.1.2 Variable Time of Arrival

"The objective of a variable time guidance law is to find the velocity correction to obtain a desired position with respect to the target body, disregarding the final time. This type of guidance is especially interesting when the along track navigation is poor and when the arrival time is not critical." [54] This section goes over one method to solve for a variable time of arrival terminal controller. The performance index in Equation (59) was used for the analysis in this report.

"A closed-form, easily mechanized optimal guidance law is obtained using the Pontryagin's Maximum Principle. This law is a function of the time-to-go which is also obtained in a closed form analytic solution. This guidance law, which solves the associated two-point boundary value problem, does not involve any iterations." [55]

With equations of motion

$$\dot{\boldsymbol{r}} = \boldsymbol{v} \tag{57}$$

$$\dot{\boldsymbol{v}} = \boldsymbol{a}_c + \boldsymbol{g} \tag{58}$$

where r, v, and a_c are the three-dimensional position, velocity, and commanded acceleration vectors respectively. The local gravitational acceleration is **g**, which is considered applied in the third dimension only.

Given the following performance index

$$\min \mathrm{J} = \Gamma \mathrm{t_f} + \frac{1}{2}\int_{\mathrm{t_0}}^{\mathrm{t_f}} \mathbf{a}_\mathrm{c}^\mathrm{T} \mathbf{a}_\mathrm{c}\, \mathbf{d}\tau \tag{59}$$

The minimum control effort (commanded acceleration) can be solved subject to the above dynamics from an initial time to terminal constraints. Γ is a weighting parameter on an unspecified final time and can be tuned to balance a desire to minimize time or to minimize control effort. If it is set to zero, the problem is exclusively focused on minimizing the control effort.

$$H = \frac{1}{2}\boldsymbol{a}_c^T \boldsymbol{a}_c + \lambda_r^T \boldsymbol{v} + \lambda_v^T(\boldsymbol{a}_c + \boldsymbol{g}) \tag{60}$$

$$G = \Gamma t_f + \nu_r^T \left(\boldsymbol{r}_{t_f} - \boldsymbol{r}_{fs}\right) + \nu_v^T(\boldsymbol{v}_{t_f} - \boldsymbol{v}_{fs}) \tag{61}$$

Using the Pontryagin Minimum Principle along with the transversality condition yields

$$\dot{\lambda}_r = 0 \tag{62}$$

$$\dot{\lambda}_v = -\lambda_r \tag{63}$$

With terminal conditions

$$\lambda_{rf} = \nu_r \tag{64}$$

$$\lambda_{vf} = \nu_v \tag{65}$$

With the time from the final time to the current time defined as

$$t_{go} = t_f - t \tag{66}$$

The Lagrange multipliers are

$$\lambda_r = \nu_r \tag{67}$$

$$\lambda_v = \nu_r t_{go} + \nu_v \tag{68}$$

With the commanded acceleration as

$$\boldsymbol{a}_c = -\lambda_v = -\nu_r t_{go} - \nu_v = -[I_3 t_{go}\; I_3]\begin{bmatrix}\nu_r \\ \nu_v\end{bmatrix} \tag{69}$$

Where the states can also be written as

$$\boldsymbol{r} = -\frac{1}{6}\nu_r t_{go}^3 - \frac{1}{2}\nu_v t_{go}^2 + \frac{1}{2}\boldsymbol{g} t_{go}^2 - \boldsymbol{v}_f t_{go} + \boldsymbol{r}_f \tag{70}$$

$$\boldsymbol{v} = \frac{1}{2}\nu_r t_{go}^2 + \nu_v t_{go} - \boldsymbol{g} t_{go} + \boldsymbol{v}_f \tag{71}$$

Solving the Lagrange multipliers in terms of the states yields

$$\begin{bmatrix}\nu_r \\ \nu_v\end{bmatrix} = \frac{1}{t_{go}^3}\begin{bmatrix} 12 & 6t_{go}^2 \\ -6t_{go}^2 & -2t_{go}^2\end{bmatrix}\begin{bmatrix}(\boldsymbol{r} - \boldsymbol{r}_f) + \boldsymbol{v}_f t_{go} - \frac{1}{2}\boldsymbol{g} t_{go}^2 \\ (\boldsymbol{v} - \boldsymbol{v}_f) + \boldsymbol{g} t_{go}\end{bmatrix} \tag{72}$$

So the commanded acceleration is

$$\mathbf{a}_c = -\frac{6}{t_{go}^2}(\mathbf{r} - \mathbf{r}_f) - \frac{4}{t_{go}}(\mathbf{v} - \mathbf{v}_f) - \frac{6}{t_{go}}\mathbf{v}_f - \mathbf{g} \tag{73}$$

With optimal performance index

$$\begin{aligned} J_{min} = \Gamma t_f + \frac{1}{2}t_{go}\Bigg[&\frac{v^T v}{t_{go}^2} + 12\frac{(r - r_f)^T(r - r_f)}{t_{go}^4} + 12\frac{\left(r - r_f\right)^T(v + v_f)}{t_{go}^3} \\ &+ 4\frac{v_f^T(v + v_f)}{t_{go}^2} + \frac{g^T(v - v_f)}{t_{go}}\Bigg] \end{aligned} \tag{74}$$

"If the problem were posed as a fixed final-time (terminal state) problem, the identical solution would be obtained using the sweep method (Riccati equations) and the accessory minimum problem. The variational method was used because it allows for a solution of the final time (or t_{go})". [55]

When there is no specific final time desired, the one which provides the minimum control effort for the above performance index can be solved for analytically. The above also can be shown to satisfy the second variation necessary conditions and the second variation sufficient conditions. The terminal controller has been used in numerous applications and confirmed with Monte Carlo simulations. [55]

7.8.1.3 Fixed Time of Arrival

"The objective of a fixed time guidance law is to find the nominal trim maneuver so that at a fixed final time the nominal trajectory is reached." [54] While minimum control effort is frequently desired, instances where the assurance that a required final time will be met can be easily imagined. "The entrance time to the target planet is important in some interplanetary mission." [56] This can be caused by a multitude of factors, the most obvious being that the planets themselves are also in motion.

The use of a fixed time of arrival terminal controller for interplanetary cases is fairly common. Besides assuring arrival when desired, the terminal controller is also able to include system limitations in the solution of the commanded acceleration. Frequently when used over long trajectories such as the interplanetary case, waypoints are defined along a nominal trajectory for the terminal controller guidance to solve for sequentially. The top-level terminal controller used for guidance decisions can be joined with actuator controllers to implement the solutions. One study which joined a "guidance function ...that aims to reach the next waypoint at a specific time" and a receding horizon controller to implement the solutions found "[these] qualities make them suitable for operational use even in autonomous guidance, navigation and control systems." [43]

The difference between the implemented variable time of arrival terminal controller and the fixed time of arrival terminal controller is that in the waypoints provided the variable time of arrival controller was blind to the time associated with the waypoint while the fixed time of arrival controller was not. The analytical solutions for both guidance terminal controllers were compared to numerical solution simulations with the same conditions and were verified as accurate.

7.8.1.4 Considerations for Low-Thrust Propulsion

Using a terminal controller for low-thrust propulsion guidance decisions along a heliocentric trajectory theoretically works, and DS1 showed that it works in practice as well. The low-thrust propulsion system should have variable thrust levels available. The nominal trajectory provided to the terminal controller using waypoints must account for the varying levels of electrical power available with respect to distance from the sun. The propulsion system must go through rigorous preflight checkout so that its characteristics are understood well enough and so that the applied linearized corrections are valid. Methods to correct issues with the propulsion system and/or identify changes to its performance would ideally be available onboard so that they can be taken into consideration in real time by the onboard guidance. The ability to provide a new, valid reference trajectory to the craft should also be possible.

7.8.2 Navigation Options

Different absolute and relative navigation sensors are available for use during the analysis. The absolute sensors include gyros, accelerometers, star trackers, magnetometer, GPS, altimeter, altimeter pointing and ground updates. In this report star trackers are used to provide attitude information and ground updates provide updated position and velocity information. The relative sensors available are lidar, a range sensor, and optical line of sight sensor system. Due to the platform of interest and the trajectory the optical line of sight sensor is used to determine the inertial conditions of the craft based on its relative position to a target.

The models of the sensors used are shown below as the ground update, optical navigation, and star tracker.

7.8.2.1 Ground Update Model

In the assumptions of ground operation, mentioned in Section 7.2, DSN is used to track the spacecraft and the ground orbit determination team uses the Doppler and range measurements to compute the spacecraft state. The ground update is the state information and its variance. This is treated as discrete measurement sensor update. Unlike stochastic navigation, it is not a navigation state update which instantly overwrites the navigation covariance matrix with one determined on the ground. The ground update measurement is significant in that after it is included the navigation error becomes very nearly the variance of the ground update. This is because the ground update provides information about the position and velocity in each axis with relatively small variance compared to other sensor types.

Each ground update type includes the position and velocity variance of the spacecraft measurement. The measurements occur at defined update rates, for example once a day throughout the trajectory, or at discrete points in time, such as 3 days into a trajectory then 45 days into a trajectory.

All of the ground update types use the same model. First, the model checks if it is time for an update to occur. As detailed in the LinCov Section 0, the measurement matrix, H, captures the type of information included in the measurement. There is no onboard state associated with ground updates so it is not propagated. The ground update measurement matrix and noise matrix are shown in Equations (75) and (76), respectively.

$$\boldsymbol{H}_{ground\ update} = \begin{bmatrix} 1 & 0 & 0 & 0 & 0 & 0 \\ 0 & 1 & 0 & 0 & 0 & 0 \\ 0 & 0 & 1 & 0 & 0 & 0 \\ 0 & 0 & 0 & 1 & 0 & 0 \\ 0 & 0 & 0 & 0 & 1 & 0 \\ 0 & 0 & 0 & 0 & 0 & 1 \end{bmatrix} \tag{75}$$

$$\boldsymbol{R}_{ground\ update} = diag\left(\begin{bmatrix} Variance(Position_x) \\ Variance(Position_y) \\ Variance(Position_z) \\ Variance(Velocity_x) \\ Variance(Velocity_y) \\ Variance(Velocity_z) \end{bmatrix}\right) \tag{76}$$

7.8.2.2 Optical Navigation Model

Because the optical navigation is being used in an interplanetary setting, the optical sightings are for a point source. The camera misalignment is considered but the camera bias is not. Because the target is Mars and the ephemeris information is onboard, this is a "known" situation where information of the sighted target can be considered directly in the measurements.

Each optical navigation sensor has a noise variance for the azimuth, elevation, and range of the solution. Also included is the camera misalignment amount, the quaternion of the camera, and the frequency of measurement.

The model for the optical line-of-sight effect on the linearized state is propagated onboard until it is time for a new measurement. After it has been determined that it is time for a measurement and that the target is within range of the sensor, the measurement matrix is calculated based on the optical line of sight partials from the current craft position to the current target position. The range equation is given in (77) with the variables defined in Table 40. The range equation used after the assumptions of the optical measurements are accounted for is shown in (84).

$$\boldsymbol{\rho}^O = \left[(\boldsymbol{I} - [\boldsymbol{\epsilon}_O^O \times])\boldsymbol{T}_{\hat{C}\to O}(\boldsymbol{I} - [\boldsymbol{\theta}_C^C \times])\boldsymbol{T}_{I\to C}\right]\Big[\Big(\boldsymbol{r}_T + \{(\boldsymbol{I} - [\boldsymbol{\theta}_T^T \times])\boldsymbol{T}_{I\to\hat{T}}\}^T(\boldsymbol{r}_F^T + \boldsymbol{\lambda}_{feat})\Big) - \Big(\boldsymbol{r}_C + \{(\boldsymbol{I} - [\boldsymbol{\theta}_C^C \times])\boldsymbol{T}_{I\to C}\}^T(\boldsymbol{r}_O^C + \boldsymbol{\lambda}_O)\Big)\Big] \tag{77}$$

Table 40: Optical Range Variables

Feature	Variable
Optical Misalignment	$\boldsymbol{\epsilon}_O^O$
Transformation from the Camera to the Optical Senor Frame	$\boldsymbol{T}_{\hat{C}\to O}$
Chaser Angle	$\boldsymbol{\theta}_C^C$
Transformation from the Inertial to the Chaser Frame	$\boldsymbol{T}_{I\to C}$
Target Position	$\boldsymbol{r}_T$
Target Angle	$\boldsymbol{\theta}_T^T$
Transformation from the Inertial to the Target	$\boldsymbol{T}_{I\to\hat{T}}$
Position of a Feature to the Target	$\boldsymbol{r}_F^T$
Bias for the Feature Measurement	$\boldsymbol{\lambda}_{feat}$
Chaser Position	$\boldsymbol{r}_C$
Position of the Optical Sensor to the Chaser	$\boldsymbol{r}_O^C$
Bias of the Optical Measurement	$\boldsymbol{\lambda}_O$

$$\delta\boldsymbol{T}(\boldsymbol{\epsilon}_O^O) = \left(\boldsymbol{I} - [\boldsymbol{\epsilon}_O^O \times]\right) \tag{78}$$

$$\boldsymbol{T}(q_{I\to C}) = (\boldsymbol{I} - [\boldsymbol{\theta}_T^T \times])\boldsymbol{T}_{I\to T} \tag{79}$$

$$\boldsymbol{T}(q_{T\to I}) = \left(\boldsymbol{I} - [\boldsymbol{\theta}_C^C \times]\right)\boldsymbol{T}_{I\to C} \tag{80}$$

$$\boldsymbol{T}(q_{C\to I}) = \left(\boldsymbol{I} - [\boldsymbol{\theta}_C^C \times]\right)\boldsymbol{T}_{C\to I} \tag{81}$$

$$\boldsymbol{r}_I = \boldsymbol{r}_T - \boldsymbol{r}_C \tag{82}$$

$$\boldsymbol{\rho}^O = \left[\delta\boldsymbol{T}(\boldsymbol{\epsilon}_O^O)\boldsymbol{T}_{\hat{C}\to O}\boldsymbol{T}(q_{T\to I})\right]\left[\left(\boldsymbol{r}_T + \{\boldsymbol{T}(q_{I\to C})\}^T\left(\boldsymbol{r}_F^T + \boldsymbol{\lambda}_{feat}\right)\right) - \left(\boldsymbol{r}_C + \{\boldsymbol{T}(q_{T\to I})\}^T\left(\boldsymbol{r}_O^C + \boldsymbol{\lambda}_O\right)\right)\right] \tag{83}$$

$$\boldsymbol{\rho}^O = \left[\delta\boldsymbol{T}(\boldsymbol{\epsilon}_O^O)\boldsymbol{T}_{\hat{C}\to O}\boldsymbol{T}(q_{T\to I})\right]\left[\boldsymbol{r}_T - \left(\boldsymbol{r}_C + \{\boldsymbol{T}(q_{T\to I})\}^T\boldsymbol{r}_O^C\right)\right] \tag{84}$$

The measurement matrix, below, is made of the partial of range with respect to chaser inertial position, the partial of range with respect to chaser attitude, the partial of range with respect to target inertial position, and the partial of range with respect to misalignment.

$$\boldsymbol{H}_{optical} = \begin{bmatrix} \frac{\partial\rho}{\partial\boldsymbol{r}_I}\frac{\partial\boldsymbol{r}_I}{\partial\boldsymbol{r}_C} & \frac{\partial\rho}{\partial\boldsymbol{r}_I}\frac{\partial\boldsymbol{r}_I}{\partial\boldsymbol{\theta}_C^C} & \frac{\partial\rho}{\partial\boldsymbol{r}_I}\frac{\partial\boldsymbol{r}_I}{\partial\boldsymbol{r}_T} & \frac{\partial\rho}{\partial\boldsymbol{r}_I}\frac{\partial\boldsymbol{r}_I}{\partial\boldsymbol{\epsilon}_C^C} \\ \frac{\partial a}{\partial\boldsymbol{r}_I}\frac{\partial\boldsymbol{r}_I}{\partial\boldsymbol{r}_C} & \frac{\partial a}{\partial\boldsymbol{r}_I}\frac{\partial\boldsymbol{r}_I}{\partial\boldsymbol{\theta}_C^C} & \frac{\partial a}{\partial\boldsymbol{r}_I}\frac{\partial\boldsymbol{r}_I}{\partial\boldsymbol{r}_T} & \frac{\partial a}{\partial\boldsymbol{r}_I}\frac{\partial\boldsymbol{r}_I}{\partial\boldsymbol{\epsilon}_C^C} \\ \frac{\partial e}{\partial\boldsymbol{r}_I}\frac{\partial\boldsymbol{r}_I}{\partial\boldsymbol{r}_C} & \frac{\partial e}{\partial\boldsymbol{r}_I}\frac{\partial\boldsymbol{r}_I}{\partial\boldsymbol{\theta}_C^C} & \frac{\partial e}{\partial\boldsymbol{r}_I}\frac{\partial\boldsymbol{r}_I}{\partial\boldsymbol{r}_T} & \frac{\partial e}{\partial\boldsymbol{r}_I}\frac{\partial\boldsymbol{r}_I}{\partial\boldsymbol{\epsilon}_C^C} \end{bmatrix} \tag{85}$$

The ability of the system to characterize the range, azimuth, and elevation based on the noise of each parameter makes up the variance matrix.

$$\boldsymbol{R}_{optical} = \begin{bmatrix} R_{range} & 0 & 0 \\ 0 & R_{azimuth} & 0 \\ 0 & 0 & R_{elevation} \end{bmatrix} \quad (86)$$

7.8.2.3 Star Tracker Model

The star tracker model checks if there are any outage periods of the star tracker and if it's time for an update. The frequency of the measurement can be set to any desired. The measurement matrix for the star tracker involves the partial of the star tracker measurement with respect to the attitude rotation vector and with respect to the misalignment.

$$\boldsymbol{H}_{star\ tracker} = \begin{bmatrix} \frac{\partial \emptyset}{\partial r_I} \frac{\partial r_I}{\partial \theta_C^C} & \boldsymbol{I} \end{bmatrix} \quad (87)$$

The noise matrix involves the boresight variance measurement and the boresight measurement cross correlation.

$$\boldsymbol{R}_{star\ tracker} = \begin{bmatrix} R_{boresight} & 0 & 0 \\ 0 & R_{cross\ boresight} & 0 \\ 0 & 0 & R_{cross\ boresight} \end{bmatrix} \quad (88)$$

7.8.3 Initial Condition and Propagation Options

The baseline LinCov tool has a variety of options which can be used to account for gravity perturbations, second order mass effects, and aero perturbations. These options can be turned off as needed and were in the case of this examination. The gravity models to choose from include multibody dynamics, the effects of J2, and a circular model around a point source. As the majority of the trajectory takes place in the heliocentric frame the circular gravity model is used. The gravity source to use can be set at the start of the analysis and can be switched during the analysis as appropriate.

A variety of spacecraft reference frames and properties can be set for the analysis. The basic settings for the spacecraft reference frames include the frame for the nominal vehicle position and velocity, the inertial-to-body quaternion, the body angular rate in body coordinates, and the chaser position with respect to other bodies. In addition, the spacecraft properties that can be set include its nominal mass and its moment of inertia. Besides the nominal reference frames and properties for the spacecraft, its expected trajectory dispersions and navigation errors can also be set. Initial state variances can be set for the position and velocity along with their correlation, the angular rate, attitude, attitude rate, and their correlations. The chaser process noise for the translational, rotational and correlation distance can be set as needed based on the desired maneuvers.

The target properties can be set as well. It is possible to consider a moving or nonmoving target, as well as initial state variances and process noise. In this case, the optical target is moving but the desired nominal end condition is not. Unlike a spacecraft target, there is no variance or process noise set for the target as the Mars ephemeris is considered to be known.

Nominal control partials concerning the maneuvering of both the spacecraft and the target can be input to the analysis if known ahead of time. If the nominal maneuver partials are not available to be uploaded at the start of the analysis, it is possible to select different attitude, impulsive thrusting, and continuous thrusting maneuvers to be calculated during the analysis. The start time and duration of any type of maneuver can be set as desired with options to switch between different types of maneuvers as needed. When calculating the maneuver dispersions, it is possible to do so with the analytical partials if they have been determined previously or numerically by testing small variations in state details with the same maneuvers.

With the attitude and thrusting types selected, the ability of the system to execute the maneuvers as desired can also be set. With the propulsion maneuver selected, the propulsion system maneuver biases, misalignment and scale factors are also features which can be selected. Their rotational and translational process noise, white noise level, the ΔV frame, thrust Isp and a fixed thrust value are options for the analysis as well. If desired, spacecraft attitude and position controllers can be used to alter the ideal maneuver execution further. Different triggers can be used to represent important events and different types of considerations can be applied based on the trajectory time or geometry.

With the initial conditions set and the maneuver execution capabilities selected, a fourth order Runge-Kutta (RK4) is used for integration of the covariances along the nominal trajectory. An RK4 involves fourth order Taylor series expansion to numerically integrate the third order derivatives of a function. The process is detailed in chapter 12 of [57]. The use of an RK4 is standard, with implementation details dependent on the step size desired compared to the length of the trajectory. Given a mission length along one arc for several months in the Earth-to-Mars transfer case studies, a step size of 2 hours was used.

7.8.4 Onboard Mission Planning Example

Section 4.3.1 summarized industry reviews from where the state of autonomy is currently and suggestions on where to focus investigations to reach the desired autonomous capabilities. Section 4.3.3 detailed the proposed methods to bridge the described gap which is the bases of this report. "[LinCov] can be used for mission design and planning activities or in autonomous flight systems to help determine the best trajectories, the best maneuver locations, and the best navigation update times to ensure mission success" [48].

A LinCov package has the desired features to both provide more details on the new deep space CubeSat platform as well as a computationally efficient onboard mission planner. The onboard navigation software (SW) can be a compact, simplified version of the ground SW. It could be set to allow the mission inputs to be specific of the program using it but the software code would be the same regardless of the mission

Figure 13 shows the dispersions experienced along a nominal trajectory from one orbit to a rendezvous point along a coelliptic orbit as an example of LinCov's potential as an Onboard Mission Planner.

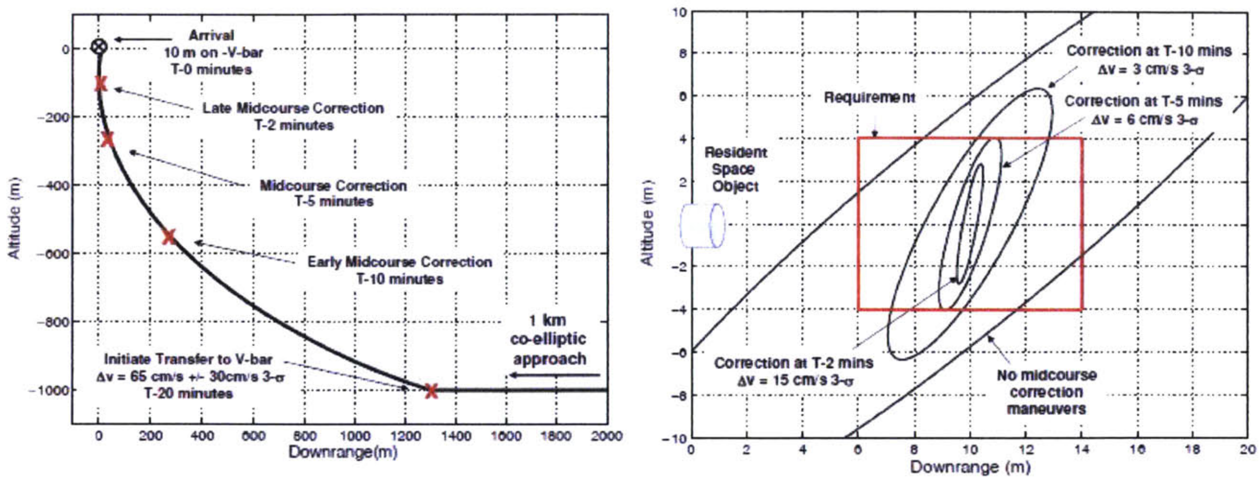

Figure 13: Onboard Mission Planning Example [48]

Understanding Figure 13 is vital to understanding not just Linear Covariance as an Onboard Mission Planner but in general. The rendezvous point has a dispersion requirement represented by the red box. The nominal trajectory uses the desired targeting method to arrive at the rendezvous point from its starting orbit. Though the spacecraft nominally arrives at the target with the original maneuver the nominal dispersions are very large. Retargeting the end point while along the nominal trajectory with an additional maneuver decreases the dispersions at the target. Within Figure 13 LinCov is used to correct and propagate the dispersions which would occur by computing the effects of performing an additional maneuver with 10 minutes to go to the target, 5 minutes to go, and 2 minutes to go. When performed at the 10-minute mark the dispersions are much smaller than without any correction but still do not meet the dispersion requirement. However, a maneuver at either the 5-minute mark or the 2-minute mark to the target meets the dispersion requirement. As such, additional mission goals would be used to select between performing the maneuver at either the 5-minute mark or 2-minute mark. Performing a maneuver closer to the target consumes more fuel than when it is performed further away with the tradeoff being that the dispersions are smaller. The 5-minute-to-go maneuver would be selected by the onboard mission planner as it meets the secondary mission goal of lower fuel consumption in additional to the primary goal of meeting the dispersion requirement. Computing the dispersions for the nominal and the three potential retargeting points would require minimally computational effort and can occur rapidly. [48]

It must be noted that the LinCov Onboard Mission Planner analysis performed does not necessarily find the optimal solution but a feasible solution based on the parameters it is set to analyze for a desired goal. It is possible that along the nominal trajectory shown in Figure 13 performing a targeting maneuver at a point other than the 5-minute mark also meets the dispersion requirements with even less fuel consumption. It is possible that using a targeting method other than that selected would achieve better results at the 5-minute mark. Depending on the mission type multiple maneuvers types and locations to perform them could be analyzed. The point is that because LinCov is computationally efficient it can check the effects of different maneuvers at different locations against mission goals rapidly. The results of the analysis are then implemented as maneuver sequences. With different onboard resources available LinCov analysis can be used to check numerous maneuver options.

Available processing capabilities is the foremost onboard resource needed to use LinCov as an onboard mission planner. Stored onboard would need to be the characteristics of the maneuver types of interest. Also stored would either be the location (or time) or frequency to perform the analysis of maneuver dispersions along the nominal trajectory. With additional processing capabilities the possibility of determining the "best" plan for the mission goals increases from the results of the additional analysis performed. Storage capacity is also needed to track the analysis results and the mission goals.

Additional, useful onboard resources would include onboard vehicle health and monitoring, as well as fault detection, isolation, and recovery. Including such information in the LinCov analysis would allow the most up to date representation of the state of the components used for navigation and maneuver execution. Minimally, LinCov as an onboard mission planner provides the ability rapidly analyze different maneuver options based on the details of the system information it is preset with preflight or which is updated by the ground team.

Within this analysis, the represented onboard mission planner would have several maneuver and navigation plans to choose from. While ground updates are used to support the mission, the onboard system only has the ability to alter its optical sightings for navigation information. The maneuver types are either Fixed Time of Arrival (FTOA) or Variable Time of Arrival (VTOA), but the onboard mission planner would have the ability to modify waypoint selection. From a list of potential waypoints which must be adhered to, the onboard mission planner would have the ability to compute the effects of targeting different waypoints based when joined with its navigation resources. It is expected that the onboard mission planner has an expectation of when it should receive ground updates and the accuracy of the update in its considerations. Should an expected ground update be missed, it is true that the prior decisions of the onboard mission planner would not have been ideal. Despite this, the onboard mission planner would be able to compute the effects of the loss of that navigation resource and choose between alternate plans that do offer the best path forward under the circumstances.

7.9 Reference Trajectory

Linear Covariance analyses occurs along a nominal trajectory and will be used to calculate the dispersions based on the statistics of the system components. To do this, it was required to obtain a suitable nominal trajectory. The fidelity of the nominal trajectory could be relatively simple with very basic assumptions, but a higher fidelity trajectory was desired. To select an appropriate nominal trajectory, the needs of the dispersion analysis were compared to the capabilities of available orbital mechanic propagators. It was found that Evolutionary Mission Trajectory Generator (EMTG) met the criteria desired.

7.9.1 Considerations for Dispersion Analysis

How the trajectory definition tool represented low-thrust propulsion was of the utmost importance. The electric thrusters available for CubeSats operate with moderate differences compared to larger electric propulsion systems and extremely differently than impulsive systems. In order that the analysis would not be overly specific to any one of the CubeSat electric propulsion thruster classes under development, generalized settings were desired. It was assumed that the propulsion system would have constant efficiency and Isp. The thruster Isp value, efficiency, duty cycle, and input power bounds would need to be set to ranges expected for the CubeSat platform. Because electric propulsion is dependent on the power available, the effects of varied distance from the sun needed to be included in the nominal trajectory as well. This should be coupled with the ability to set the assumed efficiency of the solar panels as well as the expected beginning of life power available from the solar panels at a given distance from the sun. This would allow appropriate power settings for specific CubeSat solar panels.

The objectives at the target also needed to be represented by the nominal trajectory. A common objective is to maximize the final mass of the system at the target. Important entry-interface conditions needed to be represented as well to investigate the CubeSat platforms ability to meet target conditions after an interplanetary journey. Besides approach type, this includes atmospheric interface altitude, flight path angle, and velocity along with acceptable uncertainty bounds. Representing the true location of Earth and Mars for a given date was also required, with an ability to add multibody gravitational effects as needed. This meant that true ephemeris knowledge of the planets needed to be part of the nominal trajectory definition package

The representation of the system and the boundary conditions is not sufficient in the definition of the nominal trajectory. The output of the program would not just include details about the trajectory, but the conditions of the spacecraft along the trajectory as well. Either the partials of the maneuvers used must be output directly or the maneuvers must be represented in a manner that would allow use of different guidance options in the analysis. In addition, the nominal information would need to output granularity at a frequency acceptable for use of RK4 during an interplanetary trajectory.

7.9.2 Tool Overview

NASA developed a low-thrust deep space trajectory analysis tool referred to as Evolutionary Mission Trajectory Generator (EMTG). It is meant for preliminary trajectory design and can be used as a basis for more detailed mission analysis. Multibody dynamics are included in the trajectory design by using planetary ephemeris information available from JPL. Optimization of the trajectory is performed by using the nonlinear programmer Sparse Nonlinear OPTimizer (SNOPT). Its output can interface with Satellite Tool Kit (STK) and NASA's General Mission Analysis Tool (GMAT) when additional refinement is needed.

Because it is designed for use early in a program, it allows for simplified propulsion representation. This is beneficial, as some of the new low-thrust propulsion systems for CubeSats do not have the same features as classic impulsive or low-thrust systems. EMTG factors in effects like solar power availability changes over the mission; this is important as it impacts electric propulsion performance.

The tool provides low-thrust system trajectories relevant to a desired ending target condition such as entry interface. The possible target constraints include target altitude, velocity bounds, and flight path angle constraints. With start and end conditions selected, EMTG uses a numerical solver to perform forward and background propagation simultaneously for solution determination.

There are two main methods to choose from when representing the low-thrust propulsion in EMTG. There is the Sims-Flannigan transcription in the Multi Gravity Assist with Low-Thrust (MGALT) mode; the second option is the Finite-Burn Low Thrust (FBLT) mode. Both divide the trajectory into X phases and each phase is broken into N segments. "The MGALT model approximates the continuous-thrust that could be applied over one segment as an instantaneous velocity change at the center of each segment, and utilizes Keplerian propagation, whereas the FBLT transcription continuously integrates the spacecraft's state vector" [58]. This is show in Figure 14, below.

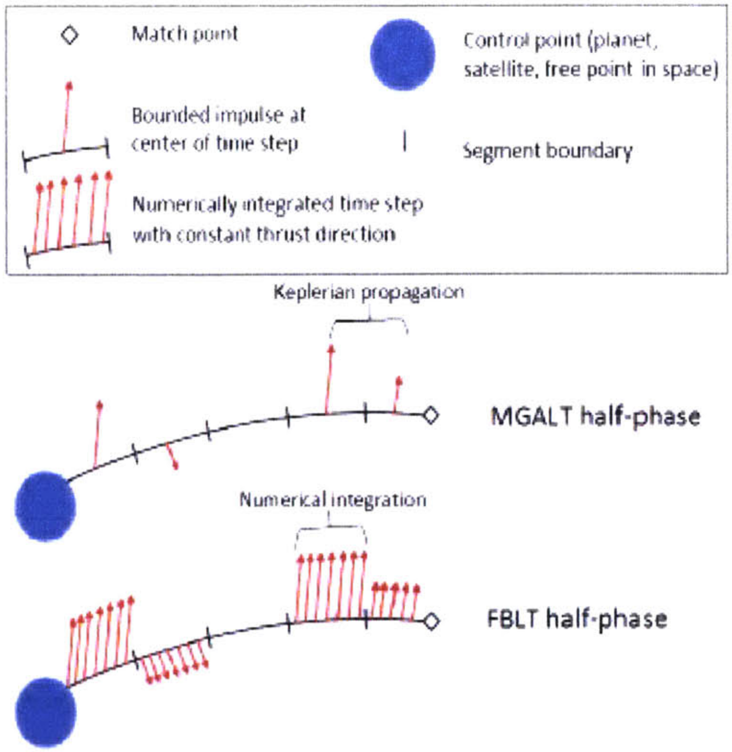

Figure 14: EMTG Thrust Representation [58]

7.9.3 Nominal Trajectory

Not all portions of the nominal trajectory require thrust. This is because EMTG produces an optimized trajectory for the given start and ending conditions desired. As such, it looks to provide a trajectory with minimal fuel use. Though a given trajectory segment may not require thrusting, the trajectory dispersions of those segments will grow in the absence of any corrections. Some level of trajectory maintenance must be performed to limit trajectory errors. Without such maintenance the trajectory end conditions may not be met with the accuracy required for mission needs.

The two options for low-thrust propulsion representation in EMTG have different trade-offs when used with a linear covariance analysis. When using MGALT for a trajectory dispersion assessment, statistics are needed regarding changes to the trajectory from small changes to each of the position and velocity elements for each instant of thrust. For a long duration mission this could mean hundreds of finite thrust events would need to be modified in a statistically significant way. Because the analytical partials of each maneuver are not available, a numerical dispersion analysis would be required if MGALT was to be used. A numerical dispersion analysis would mean that the position and velocity of the trajectory at each location that a maneuver occurred would need to be altered, the trajectory recomputed with that alteration, and then the difference in the altered results compared to the original results. This would involve running EMTG numerous times to gather the data required to compute the statistics for each maneuver. Suitable perturbation values for each condition for an interplanetary low-thrust propulsion system were unknown. The setup used for this research focused on FBLT maneuver execution exclusively. As the focus is on onboard guidance capabilities, MGALT mode is not adequate for the analysis. On the other hand, FBLT has several features which make it easier to integrate with the LinCov tool for guidance dispersion analysis. With FBLT, the determination of the required acceleration to meet the desired end conditions occurs by directly integrating with account for the multibody dynamics. Because the nominal trajectory is defined by representing thrust as continuous events, any continuous thrust guidance scheme can be used in the analysis. This allows the comparison of the dispersions caused by different guidance algorithms.

For the purpose of this analysis the nominal trajectory begins outside of Earth's sphere of influence. The nominal end conditions were set fall within a particular flight path angle and velocity range at the altitude above Mars where the atmosphere is considered to begin. The output of EMTG includes the heliocentric position and velocity information, the nominal thrust output, the mass difference, as well as other details. The nominal conditions are used as the reference trajectory within LinCov and to select waypoints for the guidance system. The Julian dates are used to look up the conditions of the target planet for the duration of the analysis using JPL ephemeris files. Table 41 notes the major points and information from the EMTG output, in addition to the determined time when the craft would cross Mars' Sphere of Influence (SOI) and atmosphere.

Table 41: Nominal Trajectory Information

Julian Date (ET)	MM/DD/YYYY	Event	Location	Duration (days)
2458970.85283288	5/1/2020	Departure	Earth	N/A
2458972.39497454	5/2/2020	Coast	Deep-Space	40.09568316
2459012.49065772	6/11/2020	FBLT Thrust	Deep-Space	80.19136632
2459092.68202410	8/31/2020	Coast	Deep-Space	160.3827326
2459245.938	1/31/2021	Cross SOI	Mars	N/A
2459248.427	2/2/2021	Cross Atmosphere	Mars	N/A
2459248.43833187	2/2/2021	Intercept	Mars	N/A

The nominal trajectory in the heliocentric inertial frame is shown in Figure 15. The trajectory of the CubeSat is shown from when it exits the Earth's sphere of influence to its end at the altitude of interest above Mars.

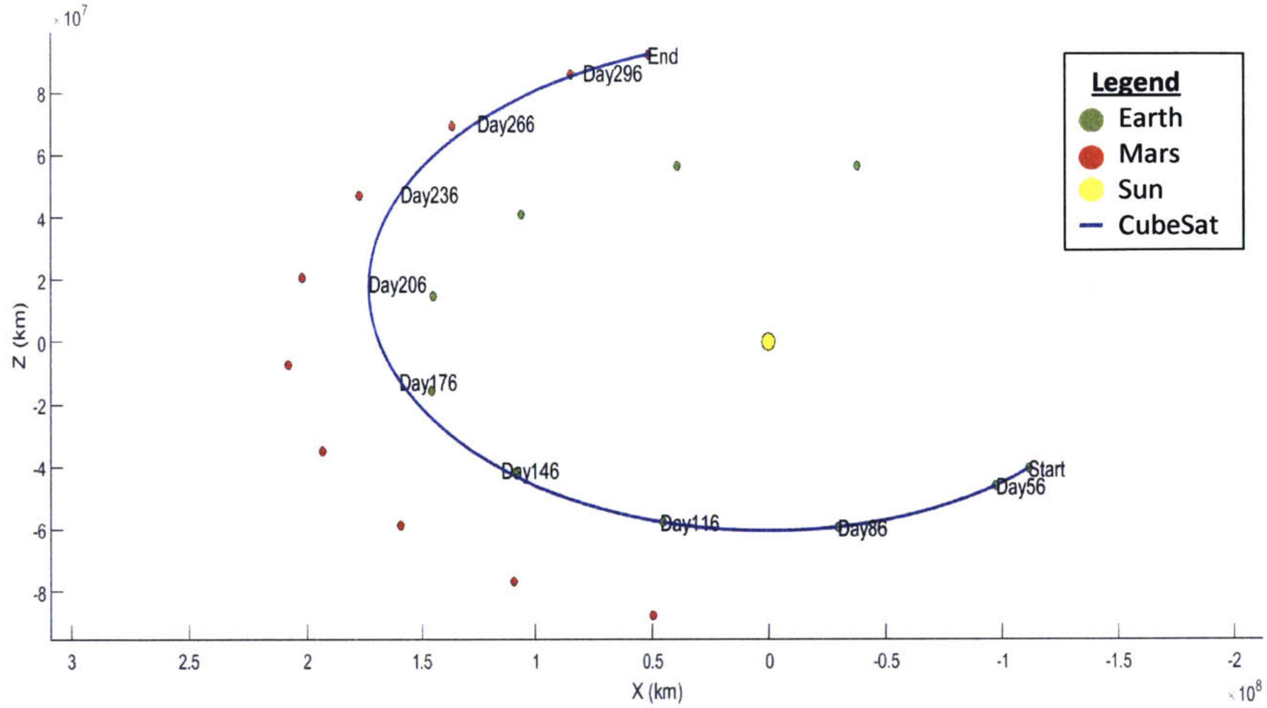

Figure 15: Nominal Trajectory in the Heliocentric Inertial Frame

7.10 Parameters of Interest

To provide useful information for the advancement of deep space CubeSats, focus was kept on several parameters which would be of the highest interest for new platform with limited capabilities as would be typical of programs of limited financial resources. These parameters include:

1. The navigation errors and trajectory dispersion for a targeted flight path angle at a specific altitude.
2. The navigation error and trajectory dispersions for a targeted altitude.
3. The navigation errors and trajectory dispersions along the B-Plane.
4. The translational process noise which alters the trajectory dispersions.
5. The accuracy of the optical navigation system effect on navigation error.
6. The accuracy and frequency of ground updates.

Accounting for the above parameters will point to the types of mission possible and the associated costs that a program needs to plan for. As interplanetary missions are new for the CubeSat platform, such details are not generally available and are important for a program to consider in the initial stages of its definition.

8 Short Guidance Segments: Baseline Results

8.1 Important Settings

Deep Space 1 used two-week planning segments during its cruise and as is the guiding example for the platform discussed in this report. Section 4.3.2, Section 5.1.2.2, and Section 7.5.1 were case studies of DS1's onboard autonomy, optical navigation, and low-thrust use.

As DS1 used two-week planning segments during its cruise, checking the nominal trajectory over the same waypoint duration was of interest. At the start of a way point segment a guidance option to the desired state two weeks away is used. 1 day before the original waypoint is reached, a new waypoint two weeks away is selected. No guidance is used during the 2 hours before the end of the trajectory.

The optical navigation system accuracy of DS1 was had a pixel accuracy between 0.05 and 0.2 once all filtering was performed after the multiple asteroid sightings were completed. This was considered much more accurate than what would likely be experienced on a CubeSat with the new optical hardware available.

The ground update schedule is based on the planned Phoenix mission scheduled since it was a Mars landing mission. As shown in Table 16, the DSN measurement data cutoff point occurs at different times before the nominal maneuver depending on the mission phase. After that point no new DSN measurement can be included in the OD analysis performed by the ground team. The data cutoff points of the Phoenix mission were used as the ground update point in the analysis.

It is assumed that the spacecraft has been fully checked out and any initial issues with actuators, sensors, and software programs have been resolved at the start of its mission. As noted in Section 7.9.3, the nominal trajectory begins outside of the Earth's SOI. It is considered that this nominal trajectory was the updated optimal trajectory provided based on the spacecraft check out and its measured location. The initial variation in the trajectory dispersion and navigation error at the start of the nominal trajectory is therefore very well known.

The nominal trajectory was detailed in Table 41 (Section 7.9). The accuracy of the ground update, which includes the craft's inertial position and velocity, along with the mission relative dates when they occur, is captured in Table 42. The accuracy defined is the OD analysis variance expected when DSN passes occur 3/week. The baseline optical navigation system target, measurement frequency, and accuracy are detailed in Table 43. The settings would result in a pixel accuracy of 2 for 5° FOV camera with 1024 pixels. The Malin CubeSat camera pixel error would be 1 with the optical navigation settings used based on the known specifications. The initial navigation error, trajectory dispersions, and translational process noise are defined in Table 44. The conditions of Tables 42-44 define the baseline input conditions.

Table 42: DS1 Baseline Case Ground Update Schedule and Accuracy

Update	Mission Relative Date	1σ Position Accuracy (km)	1σ Position Accuracy (cm/s)
1	SOI+2	15	5
2	SOI+75	15	5
3	Intercept-50	15	5
4	Intercept-16	15	5
5	Intecept-8	15	5
6	Intercept-4	15	5

Table 43: DS1 Baseline Optical System Accuracy

Parameter	Value
Optical Target	Mars
Frequency Measurement	1/day
Camera Misalignment (°)	0.01
Noise in Azimuth Knowledge (°)	0.01
Noise in Elevation Knowledge (°)	0.01
Noise in Range Knowledge (m)	0.001

Table 44: DS1 Baseline Initial Condition

Initial Condition	A
Position Dispersion (m)	(1000/3)
Velocity Dispersion (cm/s)	(5/3)
Position Navigation Error (m)	(100/3)
Velocity Navigation Error (cm/s)	(1/3)
Translational Process Noise (m/s2)	4.8020E-15

8.2 Expected Variations with Standard Ground Update

The standard cruise phase DSN tracking is 3 passes per week with no optical support. Though one of the interests of this report is in investigating whether decreasing DSN usage can be enabled, it is important to establish a baseline with the expected ground update accuracy with standard DSN use. This case is referred to as GU1. Figure 16 and Figure 17 show the resulting 3σ Position Root Sum Squared (RSS) and 3σ FPA dispersions mapped to entry-interface. Figure 18 compares the 3σ B-Plane dispersions at several points along the trajectory, specifically after the ground updates have occurred and the final TCM segment. "Mapped to entry-interface" means that the errors of the parameter at a point in time are propagated forward to provide insight as to whether the current dispersions meet the requirements at entry-interface.

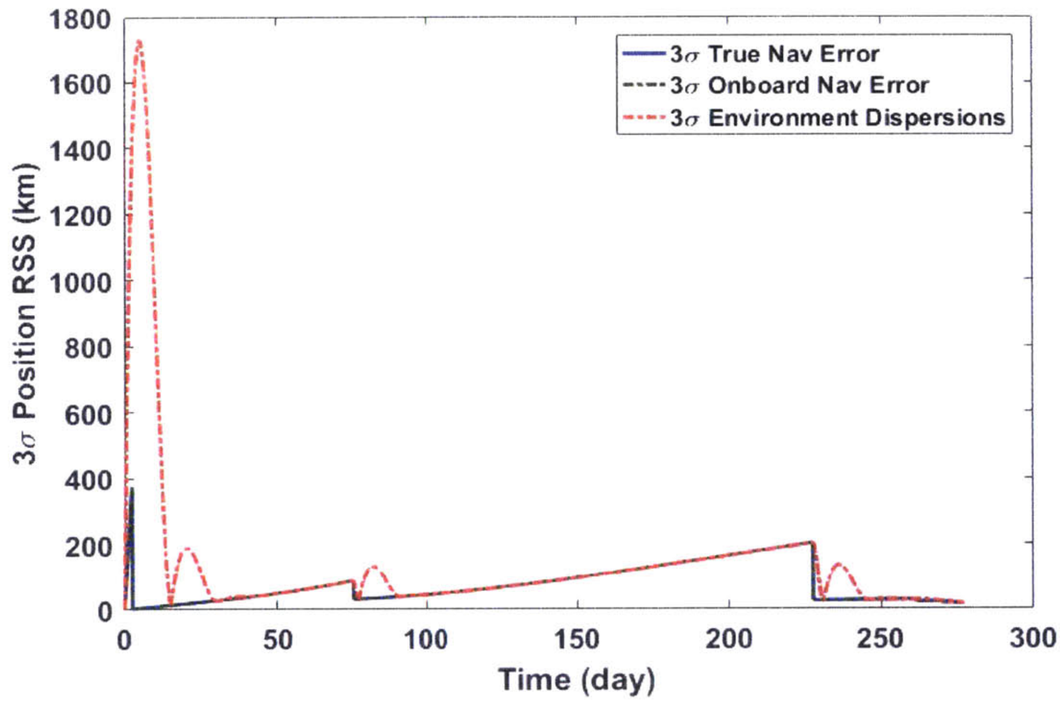

Figure 16: GU1 3σ Position RSS

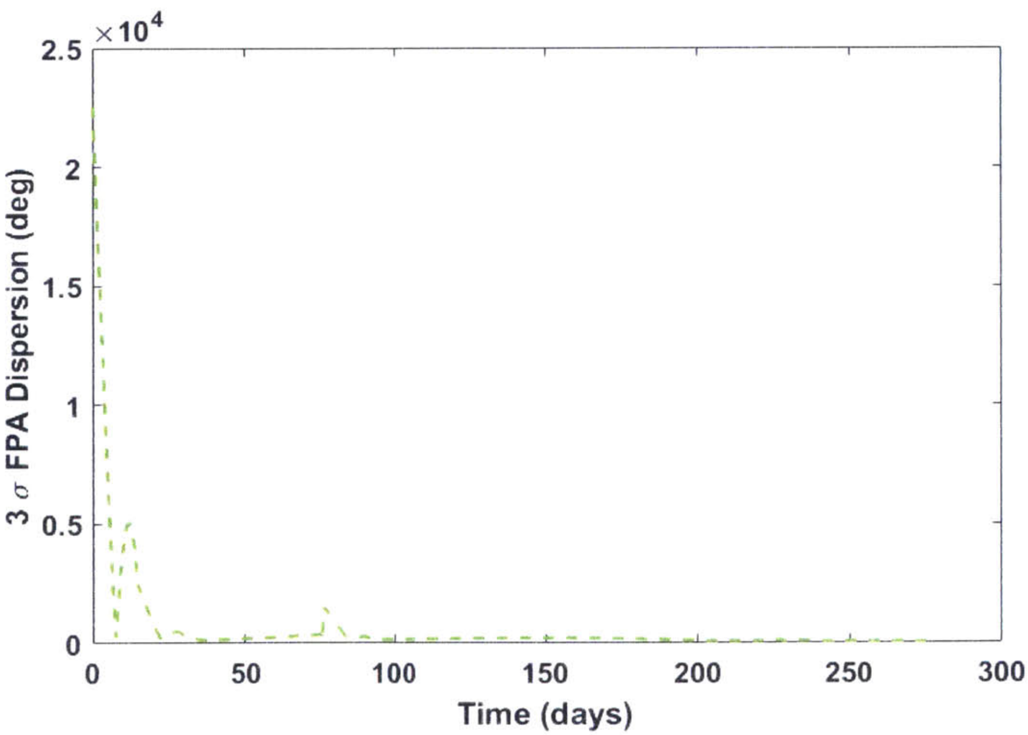

Figure 17: GU1 3σ FPA Dispersion Mapped to Entry-Interface

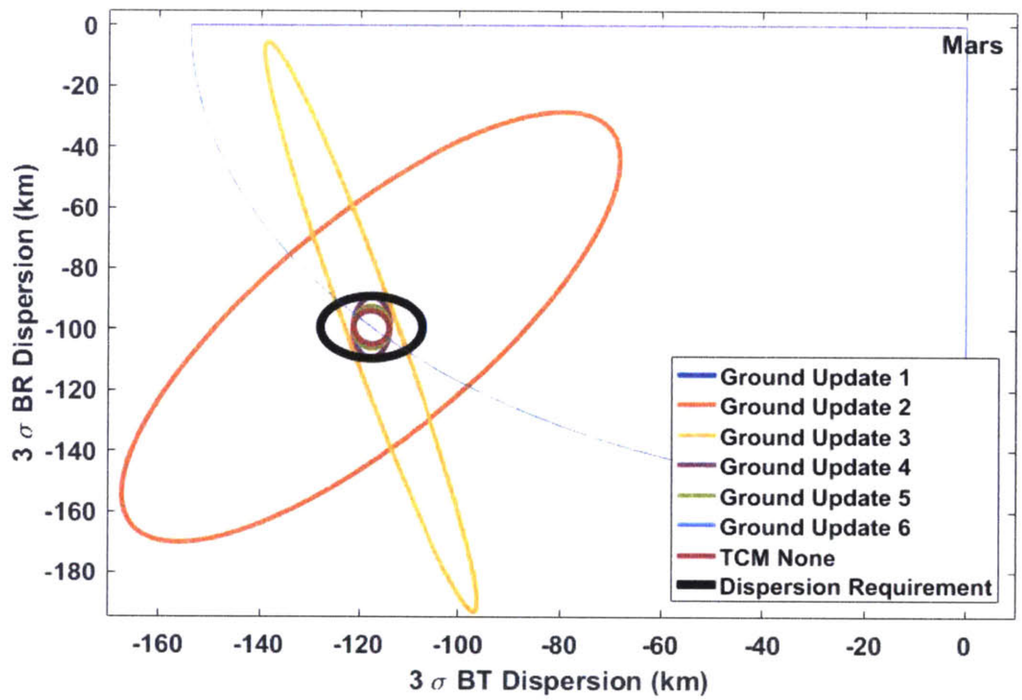

Figure 18: GU1 3σ B-Plane Dispersion Mapped to Entry-Interface

The position dispersion of Figure 16 shows that with two-week guidance segments, trajectory dispersions very nearly follow the navigation and onboard error. Only the initial segment of the cruise has drastic differences between the trajectory dispersions and navigation errors. Figure 17 shows that the mapped FPA dispersion has spikes which coordinate with the larger position dispersions shown in Figure 16. The B-Plane dispersion requirement was set to have a 20 km diameter. Figure 18 shows the B-Plane dispersions centered at the point of closest approach. As the nominal trajectory was appropriate for a landing trajectory, the point of closest approach in this case is the altitude of entry-interface. Recall that in Figure 9, though the TCM-4 was just outside of the FPA corridor limits, had only its orientation been different it could have met the requirements. In Figure 18, if the B-Plane dispersion requirement were for a 15 km diameter, though the area of the dispersions for ground update 3 would be less than the B-Plane dispersion requirement area, the shape of the dispersion would violate the requirement.

The progression of the trajectory dispersion results is tracked at the start of every other FTOA guidance segment, the final trajectory segment with no guidance, and just prior to Crossing into of the Atmosphere (XATM). Table 45, below, captures the results when the Ground Update settings of Table 42 are used.

Table 45: DS1 Baseline 3σ Results for GU1 Based on the Table 42 Ground Update Schedule

Segment	BT (km)	BR (km)	FPA (°)	Altitude (km)	Position (km)	Velocity (m/s)
TCM-FTOA2	168.2505	478.6998	2469.775	438.1384	44.16749	1.044909
TCM-FTOA4	11.09051	20.0133	171.7658	17.30536	44.13991	0.017632
TCM-FTOA6	69.26525	220.6571	1501.146	73.72796	65.2611	0.807335
TCM-FTOA8	13.29448	9.951881	168.8405	30.57855	50.58265	0.013618
TCM-FTOA10	17.56444	9.951881	222.0388	62.06373	81.84329	0.01617
TCM-FTOA12	8.097755	32.77735	206.7226	109.3625	121.4255	0.020054
TCM-FTOA14	6.277226	61.145	116.998	161.263	164.2444	0.022711
TCM-FTOA16	5.428836	102.2101	80.43058	68.24077	42.81589	0.752349
TCM-FTOA18	3.746983	10.67991	80.28183	22.87224	30.02738	0.008538
TCM-None1	3.456107	5.249946	42.59776	11.91977	18.58277	0.020586
XATM	3.565715	5.474436	42.67896	13.03609	18.6174	0.020586

The first thing that is noticed in Table 45 is that toward the start of the cruise trajectory, the dispersions do not consistently decrease. This is because the navigation and guidance are disjointed early in this scenario. Typically, guidance segments (and maneuver executions) only occur when the navigation accuracy is refined. By TCM-FTOA14 the dispersions for BT, BR, FPA, altitude, and position consistently decrease for the remainder of the trajectory. The velocity dispersions consistently decrease starting at TCM-FTOA16. What is also important is that, except for the FPA dispersions, the results of Table 45 are well within the desired bounds of the prior requirements. The dispersions results are well within the bounds of the orbiter navigation uncertainty, provided in Table 24. The results are also within the bounds of the prior lander mission preflight and flight experience navigation uncertainty, provided in Table 23, except for the FPA dispersion. Unfortunately, if entry is to be attempted, the FPA dispersions at the entry interface are critical.

8.3 Expected Variations with Standard Ground Updates and Optical Navigation

Again, though it is known that optical navigation can support mission needs very well, it is important to have a baseline for this scenario. The baseline case keeps the ground update accuracy assuming DSN tracking occurs three times a week, but is now supported with daily optical sightings of Mars. This case is referred to as Optical GU1. Figure 19 and Figure 20 show the position RSS and Mapped FPA dispersions, respectively, for the case which includes daily optical sightings of Mars. Figure 21 shows the Mapped B-Plane dispersions as the same points as Figure 18.

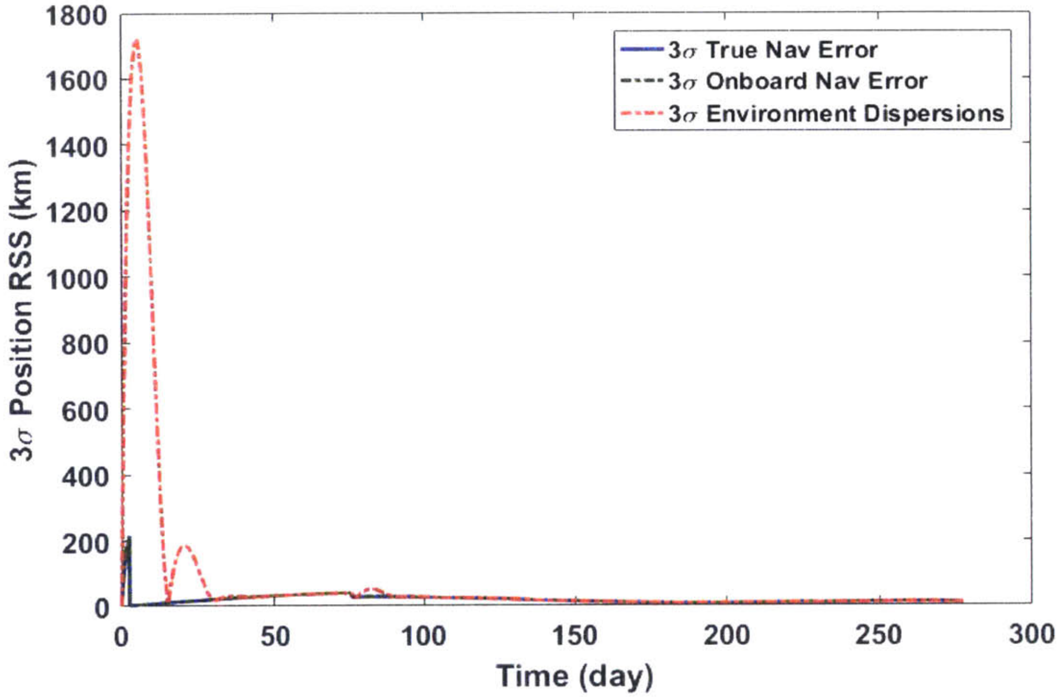

Figure 19: Optical GU1 3σ Position RSS

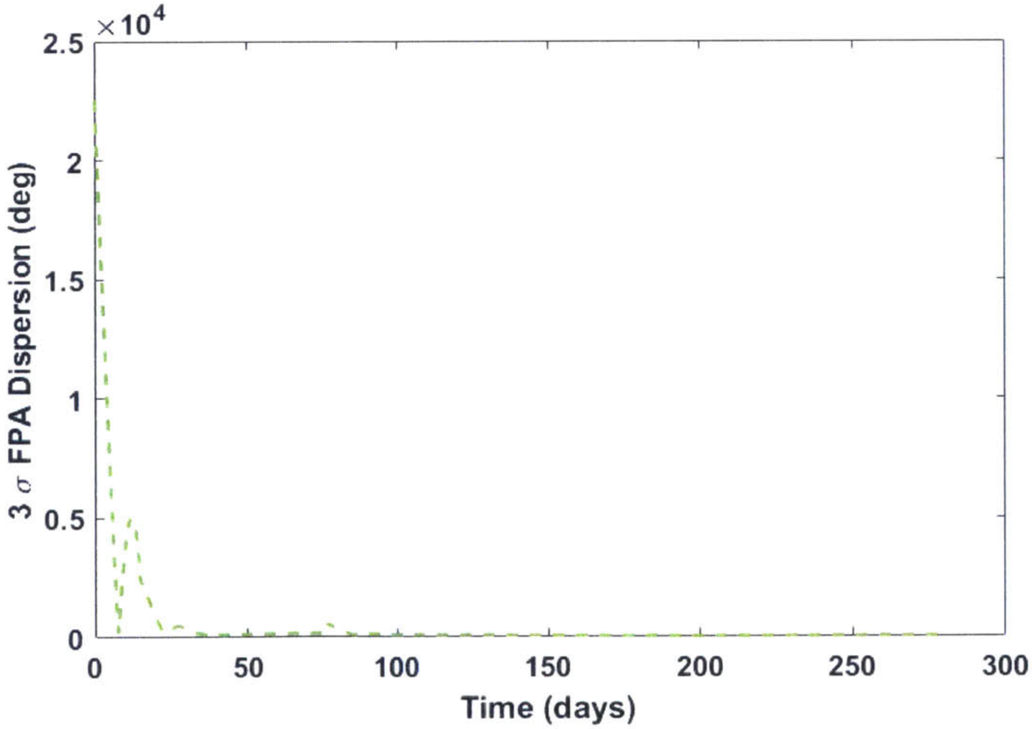

Figure 20: Optical GU1 3σ FPA Dispersion Mapped to Entry-Interface

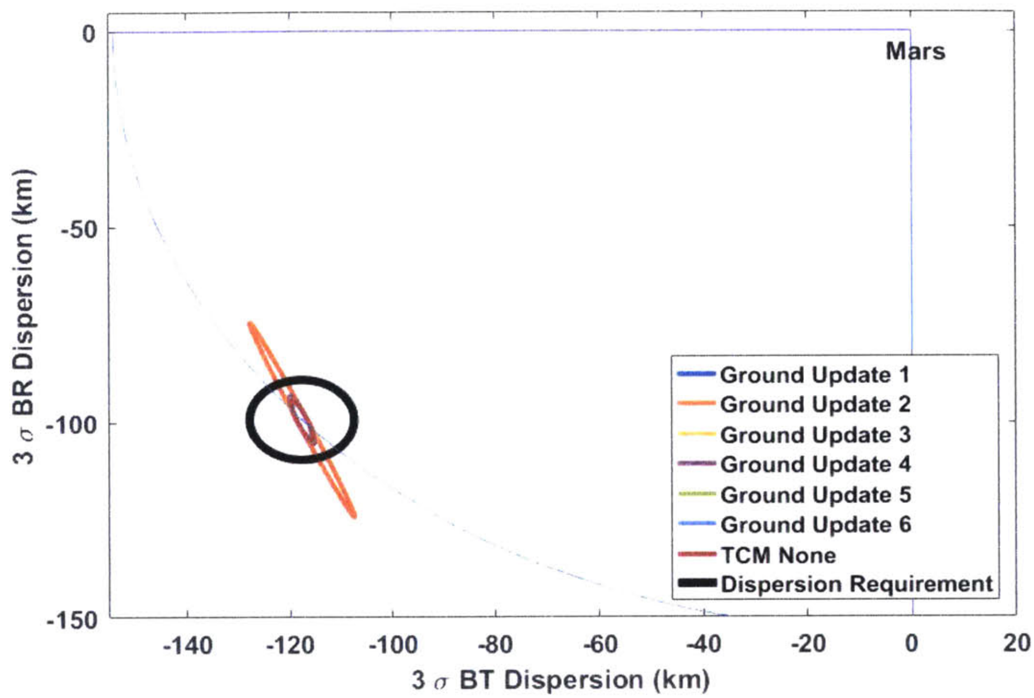

Figure 21: Optical GU1 3σ B-Plane Dispersion Mapped to Entry-Interface

The progression of the trajectory dispersion results is tracked at the start of every other FTOA guidance segment, the final trajectory segment with no guidance, and just prior to the XATM event. Table 46 below, captures the results when the Ground Update settings of Table 42 and Optical System of Table 43 are used.

Table 46: DS1 Baseline 3σ Results for Optical GU1 when Applying Table 42 Ground Updates, Table 43 Optical System Characteristics

Segment	BT (km)	BR (km)	FPA (°)	Altitude (km)	Position (km)	Velocity (m/s)
TCM-FTOA2	166.6411	476.1678	2452.549	431.5491	43.02479	1.035459
TCM-FTOA4	2.199334	22.76181	126.0963	4.007416	29.42475	0.013962
TCM-FTOA6	1.218121	133.2625	553.6882	2.310738	33.64828	0.275762
TCM-FTOA8	1.425843	22.30366	122.1526	4.223208	25.10999	0.037895
TCM-FTOA10	1.434367	14.01367	76.62793	4.685272	17.60602	0.026198
TCM-FTOA12	1.086499	5.523497	45.68301	4.991443	10.33611	0.01104
TCM-FTOA14	1.280829	3.854265	21.86154	6.142508	8.900249	0.008993
TCM-FTOA16	1.065548	7.408774	27.60477	5.64954	10.16573	0.019855
TCM-FTOA18	0.991046	9.353763	44.07873	5.692758	13.06329	0.008052
TCM-None1	0.950116	7.877375	39.39279	4.616968	10.95121	0.053518
XATM	1.11853	11.35969	39.1249	4.568715	10.89038	0.053519

As with Table 45, the dispersions of Table 46 do not consistently decrease at the start of the cruise of the trajectory. The difference between adjacent TCMs shown in Table 46 is significantly smaller than in Table 45. With optical support, the dispersions for BT are significantly reduced and the altitude and position dispersions are noticeably reduced. The FPA dispersions are marginally reduced, but are still way too large at entry-interface to be acceptable for an entry mission. The dispersions along BR are increased when optical measurements are included and grow closer to the target. The velocity dispersion is also large with optical measurements included, but they decrease along the trajectory.

8.4 Suggested Missions

As the above-discussed dispersion results for all of the parameters except for FPA were on par with prior mission navigation uncertainty, this scenario is most applicable to orbital insertion missions. The position and velocity accuracy of the ground updates for GU1 and Optical GU1 were for the standard DSN cruise tracking of 3 passes/week. As the primary interest of this report is the use of autonomous guidance and navigation to lower mission costs by decreasing the use of DSN, further cases are also investigated. The standard DSN tracking for the duration to Mars may be cost prohibitive for many programs looking to use CubeSat platforms.

9 Short Guidance Segments: Navigation Comparison

9.1 Important Settings

One of the important aspects of this study was the reduced use of DSN. The various reasons for this desire were detailed in Section 4.1. Using DSN at the traditional level of prior missions is undesirable due to the cost it would require. The portion of the trajectory where it intuitively makes the most sense to lessen the amount of DSN tracking is during the cruise portion. The prior missions had different DSN tracking frequencies based on their mission phase as shown in Section 4.1.1. Typically, prior missions used 3 passes/week were during cruise other segments, such as launch, approach, and TCMs, received increased levels of tracking as detailed in Table 1. The DSN Doppler and range measurements acquired from performing 3 passes/week during deep space cruise is used to make an orbit determination solution with a 1σ position and velocity accuracy of 15 km and 5 cm/s, respectively.

The OD accuracy produced by using the standard cruise DSN of 3 passes/week has been scaled to what is expected if the measurement rate was decreased. This scaling is shown in Table 47. The achieved uncertainty of the prior landing mission providing in Table 25 served as a guide for selecting needed approach phase ground update accuracies. This assumes that the DSN measurement frequency has been increased from the cruise phase and the tested accuracy values are shown in Table 48. The ground update cases examined are summarized in Table 49. The ground update schedule, optical navigation system, and initial conditions are the same as in Table 42, Table 43, and Table 44, respectively.

Table 47 : DSN Ground Update Accuracy

Tracks	1σ Position Accuracy (km)	1σ Velocity Accuracy (cm/s)
3 passes/week	15	5
2 passes/week	30	10
1 pass/week	45	15
2 passes/month	150	50
1 pass/month	300	100

Table 48: DSN Ground Update Approach Accuracy

Approach Case	1σ Position Accuracy (m)	1σ Velocity Accuracy (cm/s)
Coarse	300	15
Fine	15	5

Table 49: Baseline Ground Update Accuracy Cases

Updates	GU1	GU2	GU3	GU4	GU5	GU6	GU7	GU8	GU9	GU10
1-4	3/W	2/W	1/W	2/M	1/M	1/W	2/M	1/M	1/W	2/M
5-6	3/W	2/W	1/W	2/M	1/M	Fine	Fine	Fine	Coarse	Coarse

The navigation accuracy directly affects the trajectory dispersions experienced by a mission. The orbit determination state information is used to determine the maneuvers which should be performed. The less accurate the navigation information the less certain the maneuvers selected will have the desired effect. Less passes with DSN for Doppler and range measurements decreases the accuracy of the orbit determination solution. The values in Table 47 represent the accuracy of the ground update which would be uplinked to the spacecraft to be used onboard with the autonomous system. More broadly, it is the accuracy of the orbit determination used to determine maneuvers regardless if the analysis is performed by a ground maneuver team or an onboard guidance program. The difference is that a ground based maneuver team has continuous access to orbit determination details of the accuracy in Table 47 whereas an onboard system has only discrete access.

9.2 Expected Variations

The cases of Table 49 are compared during the segment when the guidance was turned off 2 hours prior to entry interface, "None1". The analysis results are compared directly with the results of the final TCM of the prior missions which were shown in Tables 23-26. The analysis dispersion results of lander-oriented missions, with and without optical support are provided in Table 52. Table 50 is the key for the results comparison to prior lander missions and are used for the BR, BT and FPA results. Table 52 and Table 53 results can be used to identify several scenarios which would warrant consideration for an Autonomous GNC (AGNC) demonstration. Scenarios where B-Plane dispersions/errors meet the requirements for landing missions also meet accuracy requirements for orbiter missions. While the FPA dispersions and navigation error are not important for orbiter missions, the altitude dispersions are. Table 51 provides the accuracy code used to compare the altitude analysis results to that of prior missions. Though a direct comparison is not available for the position and velocity dispersion and navigation error is not available, the results of the analysis for those parameters are included in Table 52 and Table 53 as well.

Table 50: Prior Lander Missions Final TCM 3σ Ground Update Comparison Codes

Code	Lander Comparison
PAN	Pathfinder Navigation Uncertainty
SUN	Surveyor Navigation Uncertainty
OPN	Opportunity Navigation Uncertainty
SPN	Spirit Navigation Uncertainty
OPA	Opportunity Achieved Uncertainty

Table 51: Prior Orbiter Missions Final TCM 3σ Ground Update Comparison

Code	Orbiter Comparison Code
ODA	Odyssey Achieved Uncertainty
ODN	Odyssey Navigation Uncertainty
SUR	Surveyor Altitude Requirement
ODR	Odyssey Altitude Requirement

Table 52: 3σ Dispersions at TCM-None1

Ground Updates Only

Case	BT (km)		BR (km)		FPA (°)		Altitude (km)		Position (km)	Velocity (m/s)
GU1	OPN	3.45611	SUN	5.24995		42.5978	SUR	11.9198	18.5828	0.02059
GU2	PAN	6.37916	PAN	10.2276		80.5853	ODR	22.8072	35.2520	0.04002
GU3	PAN	9.39194	PAN	15.2642		119.437		33.8910	52.2780	0.05972
GU4		30.8499		50.6918		394.484		112.159	172.732	0.19826
GU5		61.6032		101.351		788.299		224.135	345.117	0.39617
GU6	OPN	1.73548	SUN	4.08916		2.19701	ODN	0.62212	0.64694	0.03839
GU7	PAN	5.68661	PAN	13.6108		7.24504	ODN	2.06340	2.13256	0.12715
GU8	PAN	11.3524		27.2165		14.4731	ODN	4.12348	4.25951	0.25405
GU9	OPN	1.74712	SUN	4.11541		4.02953	ODN	0.89295	1.26423	0.03844
GU10	PAN	5.69018	PAN	13.6187		7.99417	ODN	2.16057	2.39332	0.12716

Ground Updates and Daily Optical Sightings

Case	BT (km)		BR (km)		FPA (°)		Altitude (km)		Position (km)	Velocity (m/s)
GU1	SPN	0.95012	PAN	7.87738		39.3928	ODN	4.61697	10.9512	0.05352
GU2	SPN	0.95012	PAN	7.87738		39.3928	ODN	4.61697	10.9512	0.05352
GU3	SPN	0.95316	PAN	9.66748		46.6015	ODN	5.24086	12.8603	0.07657
GU4	SPN	0.95539	PAN	12.2604		56.6233	ODN	6.14029	15.5039	0.11611
GU5	SPN	0.95555	PAN	12.5507		57.7062	ODN	6.2392	15.7882	0.12091
GU6	OPA	0.17232	SPN	1.84031	PAN	0.67841	ODN	0.07924	0.14657	0.00814
GU7	OPA	0.1725	SPN	2.12997	PAN	0.76994	ODN	0.08816	0.16522	0.00932
GU8	OPA	0.17251	SPN	2.15769	PAN	0.77883	ODN	0.08904	0.16704	0.00943
GU9	OPA	0.20779	SPN	1.87252		2.4632	ODN	0.43099	0.77284	0.00827
GU10	OPA	0.20793	SPN	2.15786		2.49003	ODN	0.43274	0.77662	0.00943

Table 53: 3σ Navigation Error at TCM-None1

Ground Updates Only										
Case	BT (km)		BR (km)		FPA (°)		Altitude (km)		Position (km)	Velocity (m/s)
GU1	OPN	3.45611	SUN	5.24995		42.5532	SUR	11.913	18.5794	0.00210
GU2	PAN	6.37916	PAN	10.2276		80.5039	ODR	22.794	35.2452	0.00373
GU3	PAN	9.39194	PAN	15.2642		119.318		33.8712	52.2677	0.00545
GU4		30.8500		50.6918		394.093		112.093	172.698	0.01779
GU5		61.6032		101.351		787.517		224.004	345.049	0.03550
GU6	SUN	1.73548	SUN	4.08916	SUN	0.20802	ODA	0.03782	0.06599	0.00020
GU7	PAN	5.68661	PAN	13.6109	SUN	0.20802	ODA	0.03782	0.06599	0.00020
GU8	PAN	11.3525		27.2165	SUN	0.20802	ODA	0.03782	0.06599	0.00020
GU9	SUN	1.74713	SUN	4.11541		3.38233	ODN	0.64089	1.08759	0.00025
GU10	PAN	5.69019	PAN	13.6187		3.38321	ODN	0.64099	1.08777	0.00025

Ground Updates and Daily Optical Sightings										
Case	BT (km)		BR (km)		FPA (°)		Altitude (km)		Position (km)	Velocity (m/s)
GU1	SPN	0.95012	PAN	7.87738		38.9459	ODN	4.56124	10.8630	0.00123
GU2	SPN	0.95012	PAN	7.87738		38.9459	ODN	4.56124	10.8630	0.00123
GU3	SPN	0.95316	PAN	9.66748		45.7992	ODN	5.14907	12.7049	0.00138
GU4	SPN	0.95539	PAN	12.2604		55.0570	ODN	5.97132	15.2044	0.00161
GU5	SPN	0.95555	PAN	12.5507		56.0353	ODN	6.05969	15.4691	0.00163
GU6	OPA	0.17232	SPN	1.84031	SUN	0.19897	ODA	0.02535	0.05334	0.00017
GU7	OPA	0.17250	SPN	2.12997	SUN	0.19897	ODA	0.02535	0.05334	0.00017
GU8	OPA	0.17251	SPN	2.15769	SUN	0.19897	ODA	0.02535	0.05334	0.00017
GU9	OPA	0.20779	SPN	1.87252		2.37309	ODN	0.42395	0.76024	0.00021
GU10	OPA	0.20793	SPN	2.15786		2.37316	ODN	0.42396	0.76027	0.00021

Figure 22, Figure 23, and Figure 24 show the B-Plane dispersions at TCM-None1 per Table 52. Figure 22 shows each of the navigation cases with only ground updates while Figure 23 shows each case with optical support as well. Figure 24 compares five of the navigation cases with and without optical support directly. This is to provide a better sense of scale of the benefits of optical navigation for individual cases.

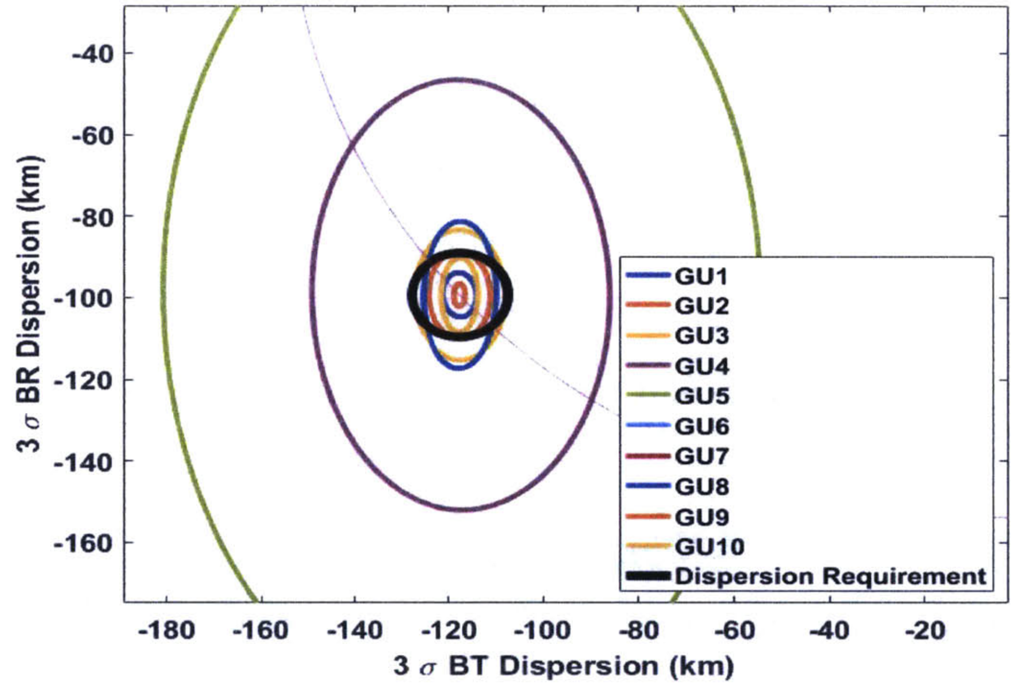

Figure 22: 3σ B-Plane Dispersion Mapped to Entry-Interface Ground Update Comparison

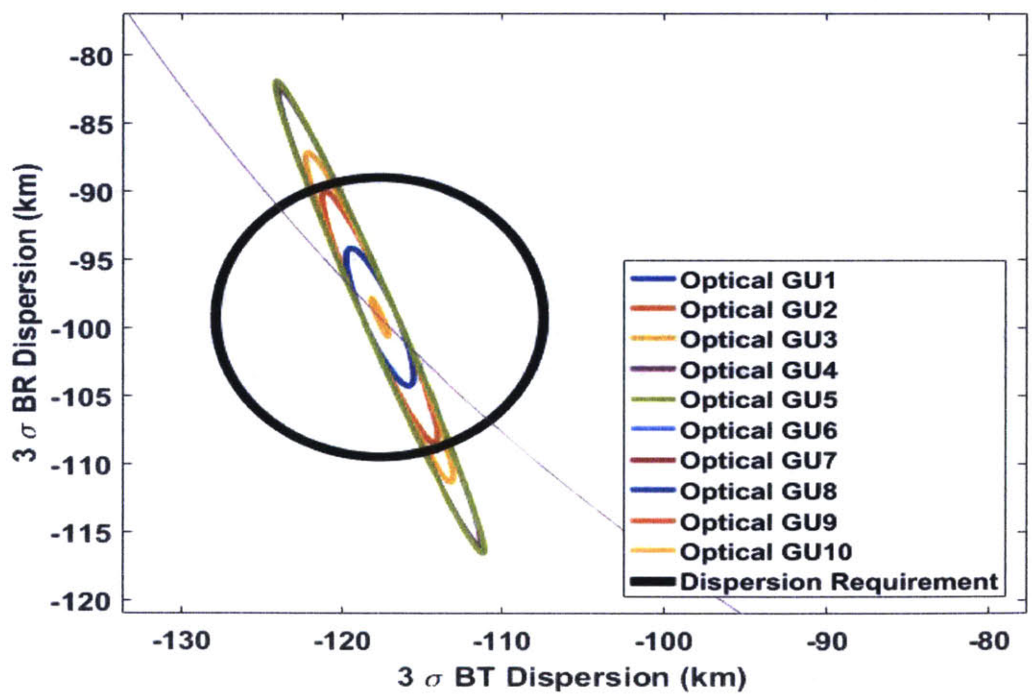

Figure 23: 3σ B-Plane Dispersion Mapped to Entry-Interface Ground Update with Optical Comparison

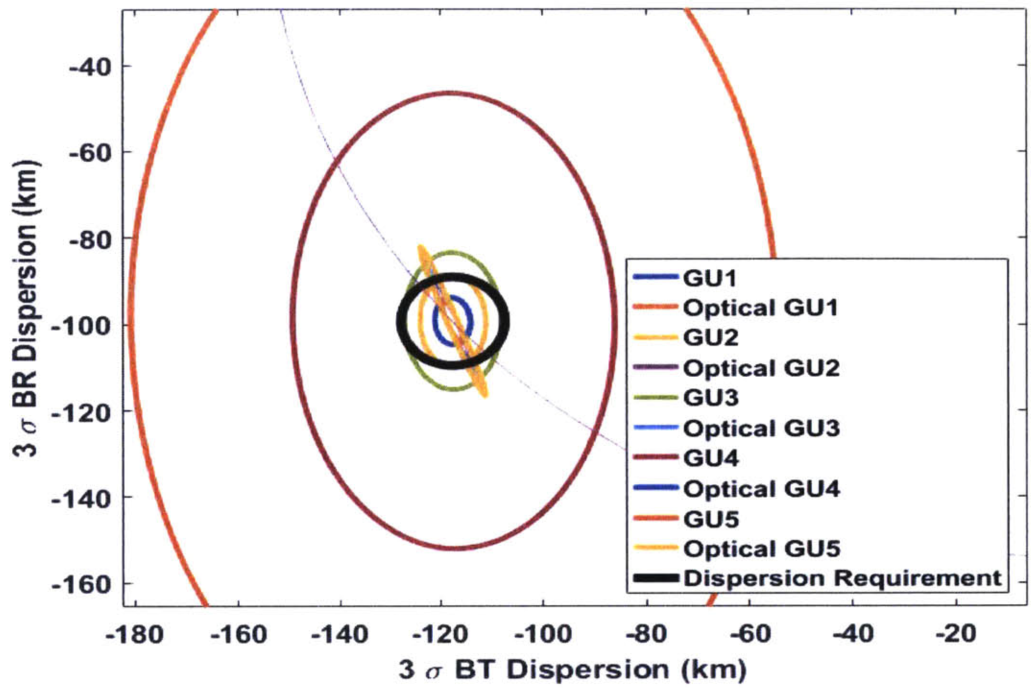

Figure 24: 3σ B-Plane Dispersion Mapped to Entry-Interface Direct Comparison with and without Optical Support

The dispersion ellipses with only ground updates, in Figure 22, are larger and rounder than the results when optical navigation is included, in Figure 23. Not only does including optical support reduce the size of the dispersions overall, the orientation of the dispersions rotate counter clockwise slightly. Though both the BR and BT dispersions are reduced compared to the ground update only cases, BT dispersions are influenced more by including optical navigation. This is consistent with the patterns shown in Section 8 with the standard 3/Week DSN tracking not just at the final TCM but throughout the trajectory.

9.2.1 BT Analysis

The accuracy of each ground update case is defined in Table 49. In Table 52 GU2, GU3, GU7, GU8, GU10 all meet the Pathfinder navigation uncertainty goals when using only ground updates for the navigation. The Pathfinder navigation uncertainty was the largest of the prior lander missions. Out of these cases, GU10 is of the highest interest as it has the least frequent DSN use throughout cruise and during approach. Also of interest is GU3 as its ground update accuracy is based on the assumption of DSN use of one pass per week through both cruise and approach. GU1, GU6, and GU9 meet the opportunity navigation results with only ground updates. This is a higher accuracy level than the Pathfinder navigation uncertainty. Out of these, GU9 would be of the most interest to explore further as its accuracy was based on the use of DSN 1/week during cruise and approach with coarse ground updates. If higher accuracy is needed at the target than that of Pathfinder or Surveyor navigation uncertainty, then the inclusion of optical navigation would be one method to do so without increasing the use of DSN. Because many of the ground update cases meet desirable BT target conditions, only the most significant cases are discussed. GU4 and GU5 meet the Spirit navigation uncertainty when daily sightings of Mars are performed; their accuracies reflect DSN passes of 2/month and 1/month, respectively. GU9 and GU10, with optical navigation, utilizing 1/week and 2/month DSN passes meet the Opportunity achieved-uncertainty.

The results shown in Table 52 are influenced by the guidance capabilities and thrusting accuracy, and Table 53 provides the navigation error results. There is effectively no difference between the trajectory dispersions of Table 52 and the navigation error of Table 53 for the BT parameter. This shows that the guidance system accurately mirrors the navigation results with respect to BT. The results of Table 52 are shown in Figure 25 for a visual comparison of the final segment BT dispersions with different levels of ground update support.

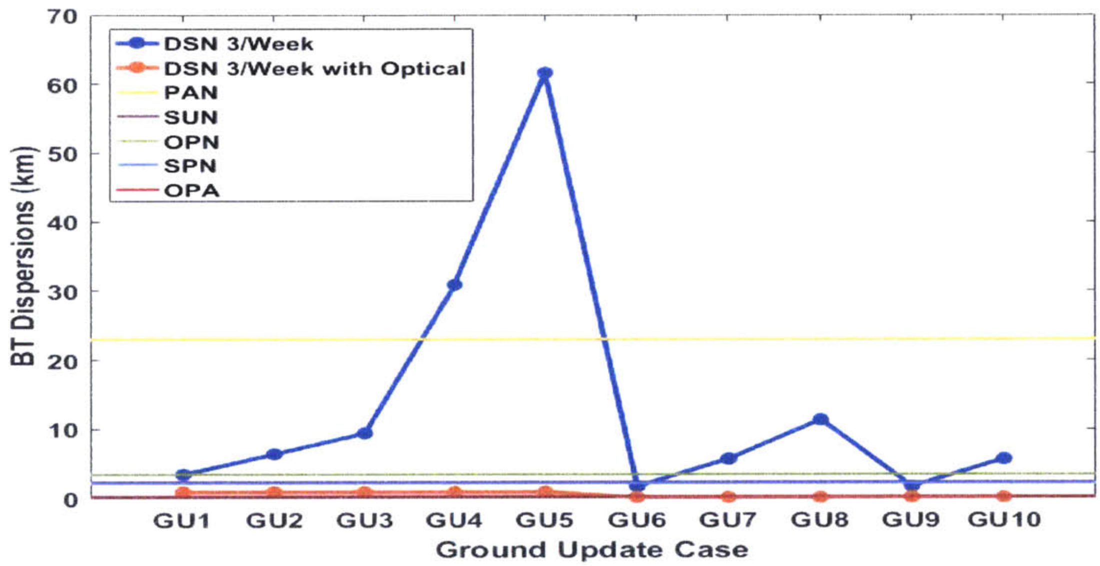

Figure 25: Ground Update 3σ BT Dispersion Comparison

9.2.2 BR Analysis

Because the focus of this report is on what can be accomplished when the use of DSN is decreased, only the cases of Table 52 most relevant to this goal are discussed further. Though both GU6 and GU9 meet the Surveyor navigation uncertainty, GU9 would have to be selected as it uses coarse DSN accuracy while GU6 uses fine DSN accuracy. The same goes for GU7 and GU10, which assume the same cruise DSN accuracy but GU10 uses coarse DSN accuracy for approach to meet Pathfinder navigation uncertainty. Using optical navigation, GU9 and GU10 can both meet the Spirit navigation uncertainty for BT dispersions.

As was the case with the BT navigation errors matching the dispersions, Table 53 shows very little difference between the BR navigation errors and the Table 52 the BR dispersions. The results between the four B-Plane dispersion and navigation error tables shows that significantly reduced DSN use supported with optical navigation can be a viable option to meet the B-Plane accuracy levels of prior landing missions. Table 52 results for the final BR dispersions are shown in Figure 26.

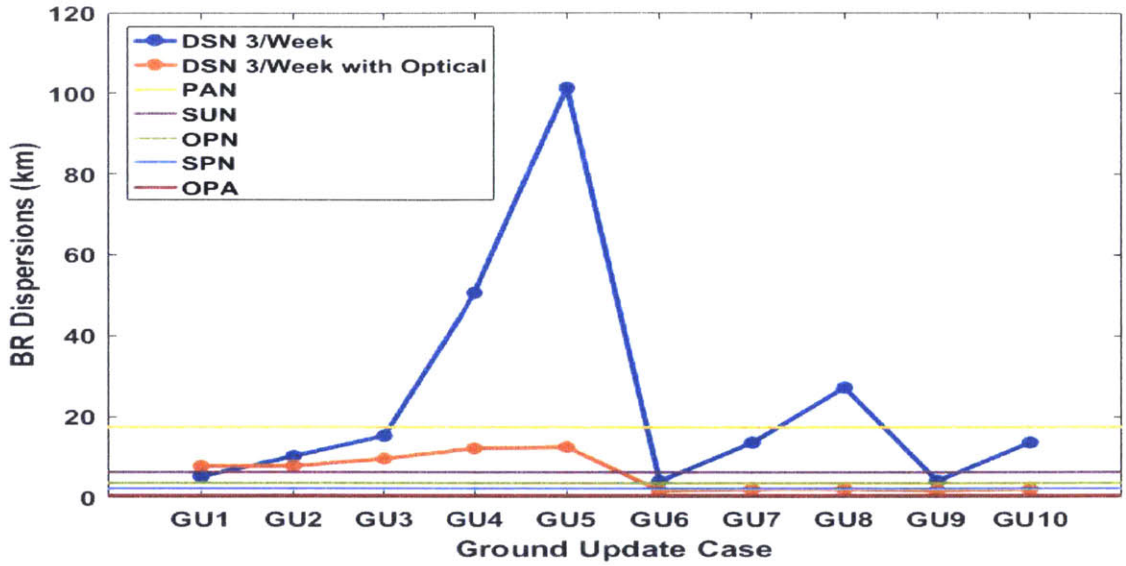

Figure 26: Ground Update 3σ BR Dispersion Comparison

9.2.3 FPA Analysis

Table 52 shows drastically reduced opportunities to meet the FPA accuracy experienced by prior missions. Only with both optical navigation and DSN fine approach accuracy can the Pathfinder navigation uncertainty be met, which used the broadest of the FPA requirements of the considered, prior landing missions.

Table 53 shows the FPA navigation error which are not affected by the guidance and thrusting capabilities, unlike the results in Table 52. These navigation error shows more cases that meet prior mission FPA values with higher accuracy than the dispersions shown in Table 52. This provides confidence in the navigation system and points to a need for either a different guidance scheme, a more accurate thrusting model which would decrease the translational process noise, or both. The FPA dispersion results of Table 52 are shown in Figure 27.

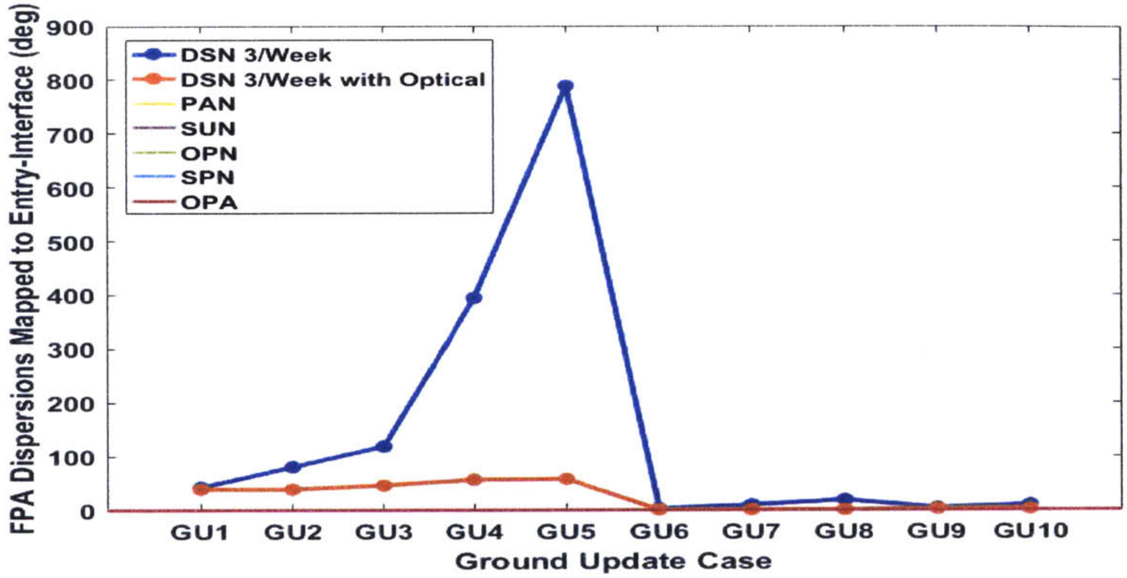

Figure 27: Ground Update 3σ FPA Dispersion Comparison

9.2.4 Altitude Analysis

Table 52 and Table 53 show that both the altitude dispersions and navigation errors have cases that meet the Odyssey-achieved uncertainty which was the most accurate of the prior orbiter missions examined. GU9 and GU10 dispersion both meet the experienced Odyssey navigation uncertainty, and are of the highest interest because of the low amount of DSN used during cruise, though it must be supplemented with an increase to coarse DSN approach accuracy. The altitude dispersion results of Table 52 are shown in Figure 28.

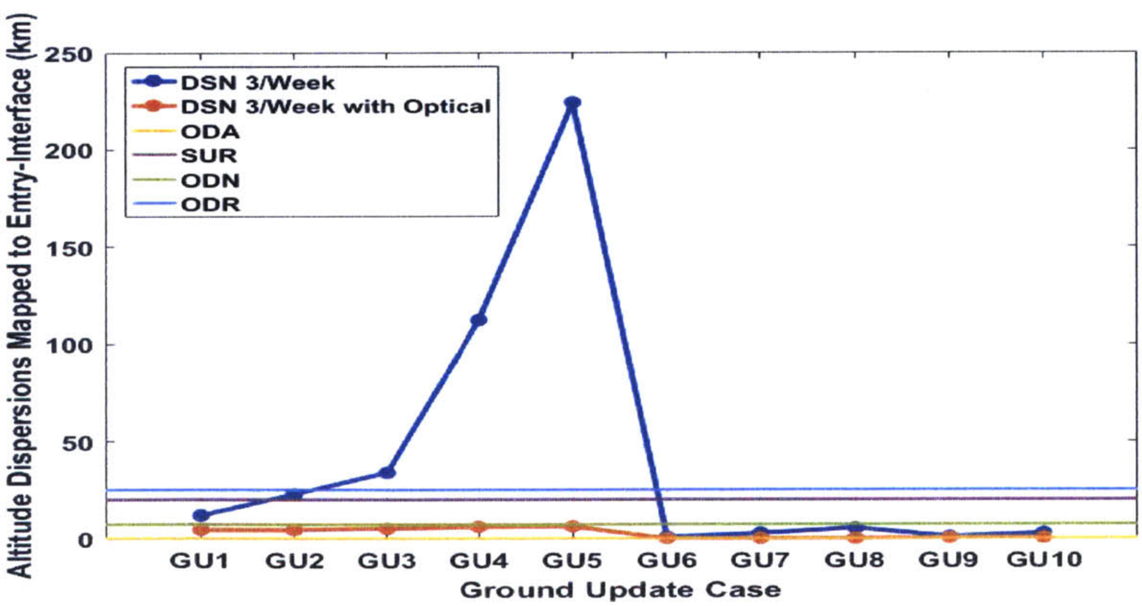

Figure 28: Ground Update 3σ Altitude Dispersion Comparison

10 Short Guidance Segments: Guidance Comparison

10.1 Initial Settings

The optical system accuracy for daily optical measurements is provided in Table 43. The baseline initial conditions are provided in Table 44. The ground update accuracy for the cases is shown in Table 49 with the specifics of the variations shown in Table 47 and Table 48. The guidance segments have two-week durations for the majority of the trajectory with no guidance for a final segment just prior to entry.

10.2 Expected Variations of Multiple Guidance Types

In Table 54, FTOA and VTOA guidance are compared for several of the ground update cases which do not experience an increase in accuracy during the approach phase, with and without optical navigation. In Table 55, FTOA and VTOA guidance are compared for several of the increased approach accuracy ground update cases.

Table 54: 3σ Dispersion for DS1 with Constant Ground Update Accuracy

Parameter	Fixed	Variable	Fixed w/Opt	Variable w/Opt
GU1 – DSN Tracking 3/Week				
BT (km)	3.456107	3.602616	0.950116	1.007521
BR (km)	5.249946	6.469928	7.877375	8.023355
FPA (°)	42.59776	42.59526	39.39279	39.02649
Altitude (km)	11.91977	13.46119	4.616968	4.973289
Position (km)	18.58277	19.5531	10.95121	11.0381
Velocity (km/s)	0.020586	0.037355	0.053518	0.045028
GU4 – DSN Tracking 2/Month				
BT (km)	30.84998191	32.62575	0.955386	1.015417
BR (km)	50.6918	62.53175	12.26035	12.5361
FPA (°)	394.4843	394.4706	56.62331632	55.27848
Altitude (km)	112.1591407	128.1996	6.140287	6.628699
Position (km)	172.7323	182.9865	15.50386	15.47828
Velocity (km/s)	0.19826	0.370679	0.116113	0.099083
GU5 – DSN Tracking 1/Month				
BT (km)	61.6032244	65.1609	0.95555	1.015606
BR (km)	101.3511	124.9917	12.5507	12.83853
FPA (°)	788.2991	788.2719	57.70616797	56.2695
Altitude (km)	224.1352722	256.201	6.239203	6.737415
Position (km)	345.1173	365.62	15.78824	15.75161
Velocity (km/s)	0.39617	0.740887	0.120912	0.103217

Table 54 shows that when only ground updates are used, FTOA guidance typically performs better than VTOA guidance for each of the ground update accuracy cases. With optical navigation included as well, VTOA guidance begins to perform better from GU1 to GU4, to GU5.

Table 55: 3σ Dispersion for DS1 with Increased Approach Ground Update Accuracy

Parameter	Fixed	Variable	Fixed w/Opt	Variable w/Opt
GU8 – DSN Tracking 1/Month During Cruise with Fine Accuracy During Approach				
BT (km)	11.35246995	0.03911	0.17251	0.010001
BR (km)	27.21651	61.30379	2.157686	1.274436
FPA (°)	14.4731	26.88612	0.778826925	0.592068
Altitude (km)	4.123477171	139.2733	0.089035	2.88532
Position (km)	4.25951	135.4737	0.167038	2.807
Velocity (km/s)	0.254048	0.8292	0.009434	0.017179
GU9 – DSN Tracking 1/Week During Cruise with Coarse Accuracy During Approach				
BT (km)	1.747126827	0.226938	0.207787	0.148384
BR (km)	4.115409	9.252191	1.872515	1.219104
FPA (°)	4.029531	5.276148	2.463196193	2.426088
Altitude (km)	0.892948351	20.98986	0.430993	2.625495
Position (km)	1.264234	20.43666	0.772838	2.632509
Velocity (km/s)	0.038442	0.124911	0.008266	0.015429
GU10 – DSN Tracking 2/Month During Cruise with Coarse Accuracy During Approach				
BT (km)	5.690187444	0.227695	0.207933	0.148392
BR (km)	13.61874	30.68008	2.157858	1.331105
FPA (°)	7.994172	13.87144	2.490025994	2.437346
Altitude (km)	2.160571019	69.69174	0.432737	2.890283
Position (km)	2.393316	67.7963	0.776621	2.883063
Velocity (km/s)	0.127162	0.41491	0.009432	0.017024

The differences between FTOA and VTOA are not as straightforward in Table 55 as they are in Table 54. Some of the parameters are better with FTOA while others are more accurate with VTOA when only ground updates are used. FPA, altitude, position, and velocity dispersions are all better with FTOA when only ground updates are used. The results of GU9, while very different between VTOA and FTOA, are still within the requirements of the earlier prior lander missions and the orbiters investigated. There are also differences between the B-Plane parameters but overall the FTOA results for the B-Plane are either more accurate or comparable to the VTOA results for the same ground update case. When the cases of Table 55 include optical navigation there is a drastic decrease in the size of the dispersions. This is significant because each of those cases had ground updates with poor accuracy during cruise but were provided fine or coarse ground updates during approach only. For each case, the VTOA B-Plane results are better than the FTOA when optical navigation is included. The FPA results for VTOA are marginally better than the FTOA with optical navigation as well. On the other hand, the altitude, position and velocity dispersions are all better with FTOA than VTOA with optical navigation. In either case though, the results all well within the requirements for orbit insertion but only GU8 is within the FPA dispersion requirement of Pathfinder. Visual comparisons of the BT, BR, FPA, and altitude dispersions in the final segment with each guidance method, are shown in Figure 29, Figure 30, Figure 31, and Figure 32, respectively. The difference between FTOA and VTOA with optical navigation is minimal compared to the differences without optical navigation for most cases. Except for FPA, VTOA without optical navigation performs noticeably worse than FTOA without optical navigation; this is especially the true for navigation cases with less DSN tracking during cruise even with the tracking is increased during approach.

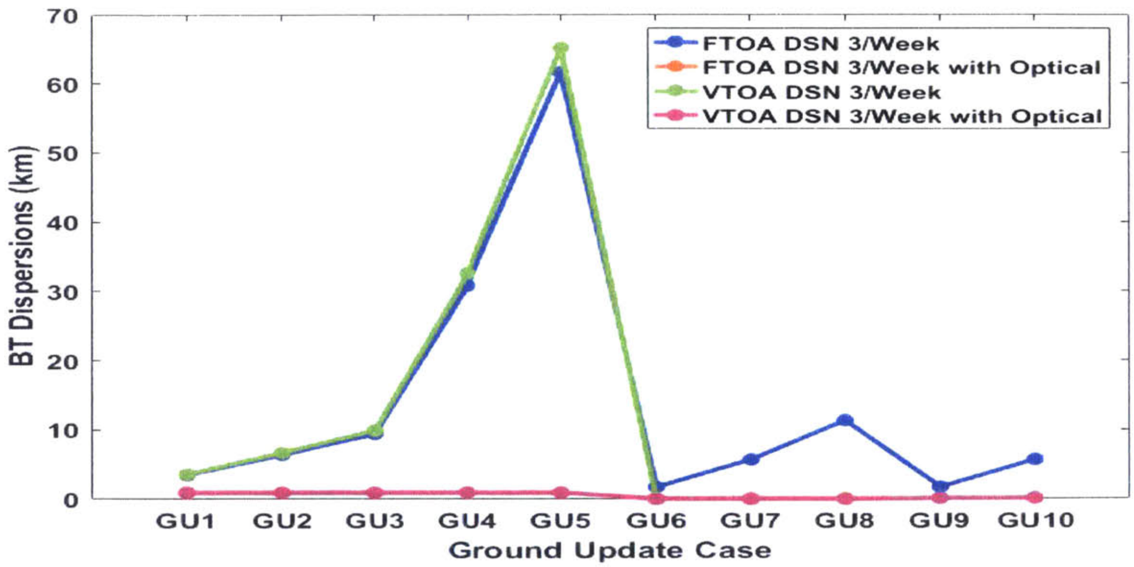

Figure 29: Guidance Scheme 3σ BT Dispersion Comparison

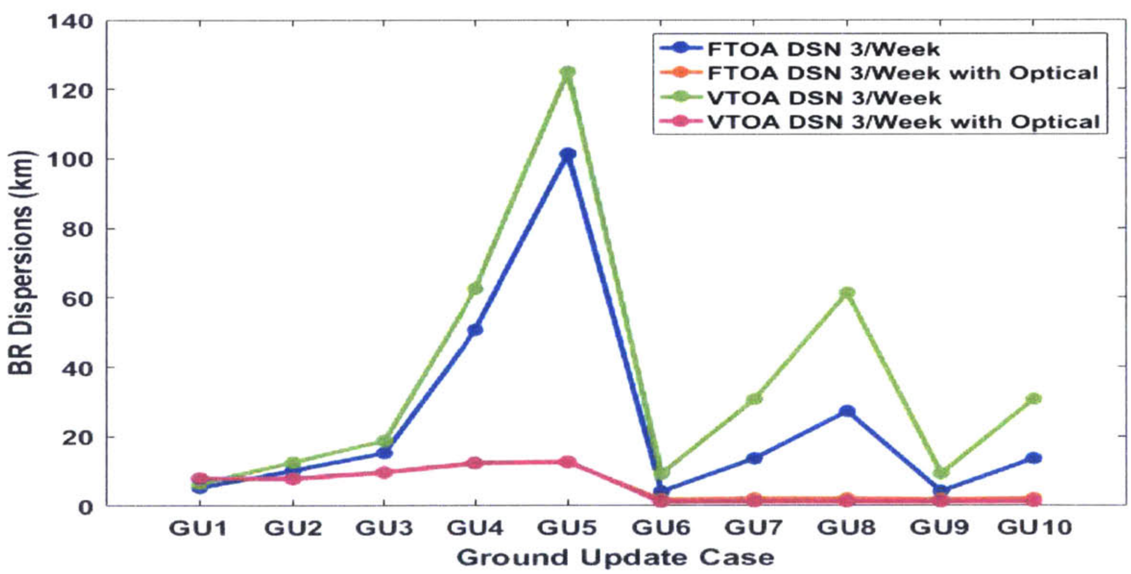

Figure 30: Guidance Scheme 3σ BR Dispersion Comparison

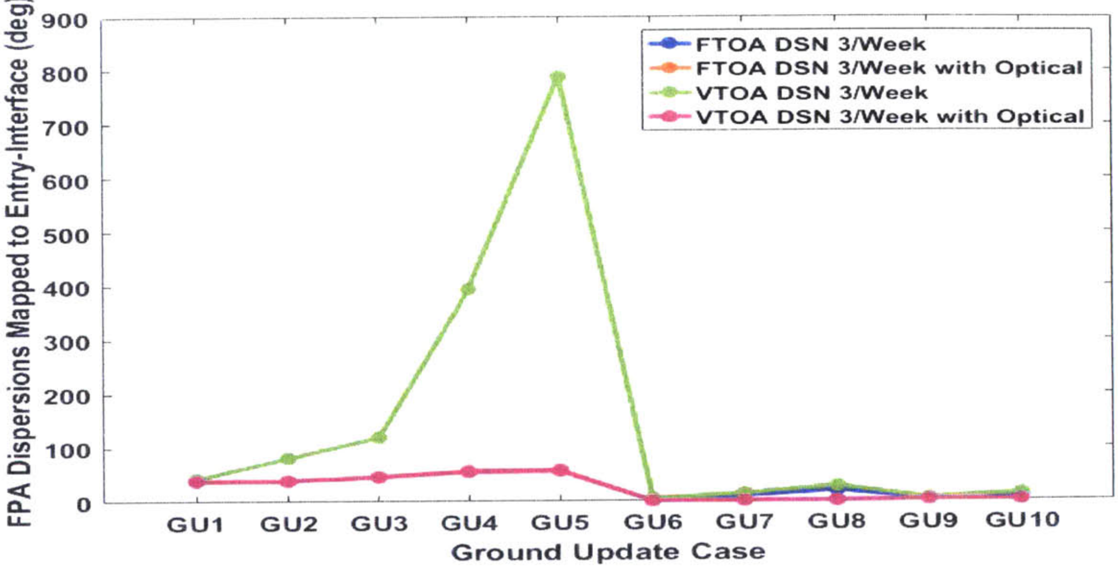

Figure 31: Guidance Scheme 3σ FPA Dispersion Comparison

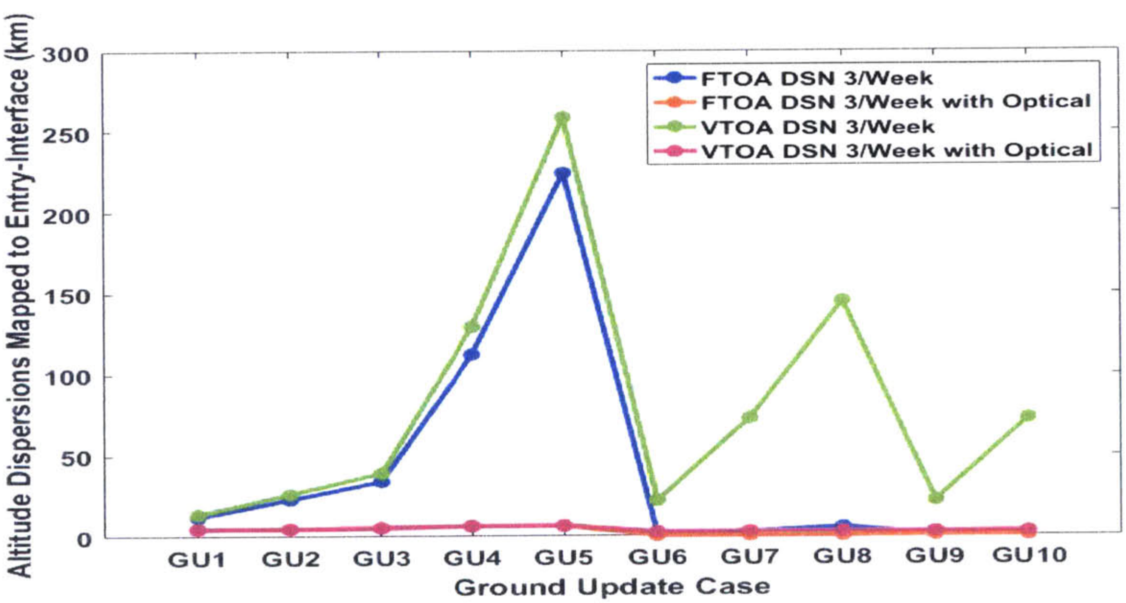

Figure 32: Guidance Scheme 3σ Altitude Dispersion Comparison

11 Short Guidance Segments: Interplanetary Cruise Highly Dependent on Optical Navigation

The prior sections have shown that so long as the ground update accuracy of the approach phase is very accurate, the ground updates during the cruise phase can be relatively inaccurate and still produce highly desirable results. The values of the ground update accuracy during the approach phase were selected based on the navigation uncertainty and achieved uncertainty of the more recent prior landing missions. Because the results from reducing the cruise phase ground update accuracy were well within the prior mission requirements, the demonstration phase requirements, and some of the prior mission navigation uncertainty it is reasonable to further investigate the use of a mission highly dependent on optical navigation during the interplanetary cruise.

11.1 Effective use of Optical Navigation Check

First an optical navigation comparison is performed to determine if it is worth sighting the target more frequently. Table 56 shows the results when the optical navigation system that was used for daily sighting of Mars in the prior sections is used to perform sightings two times a day and three times a day. Several ground update cases are compared; for each, no optical sights are performed, a daily sighting, a twice daily sighting, or thrice daily sighting.

Table 56: Optical Navigation Sighting Frequency Effects Comparison

Case	BT (km)	BR (km)	FPA (°)	Altitude (km)	Position (km)	Velocity (m/s)
DS1 FTOA						
GU1	3.565715	5.474436	42.67896	11.92183	18.6174	0.020586
GU1 O1	1.11853	11.35969	39.1249	4.568715	10.89038	0.053519
GU1 O2	1.075987	5.92038	26.73639	3.555977	7.584852	0.025339
GU1 O3	1.137316	6.463337	26.09836	3.460329	7.359095	0.034837
GU3	9.681048	16.02304	119.6243	33.89082	52.37153	0.059714
GU3 O1	1.121936	15.34604	46.01978	5.157038	12.73808	0.076569
GU3 O2	1.099026	15.33412	44.45543	4.991402	12.28822	0.077463
GU3 O3	1.163154	16.99423	40.79837	4.61287	11.15598	0.099566
GU6	1.245007	2.849033	0.567228	0.154215	0.468875	0.038389
GU6 O1	0.123593	1.319081	0.260038	0.032147	0.11288	0.008138
GU6 O2	0.122805	1.314326	0.258124	0.032082	0.112421	0.008107
GU6 O3	0.122572	1.310046	0.25644	0.032016	0.112028	0.008082
GU9	1.264907	2.892421	3.41929	0.658941	1.183133	0.038442
GU9 O1	0.180516	1.37194	2.382706	0.424641	0.766947	0.008267
GU9 O2	0.179536	1.366264	2.357833	0.424538	0.764149	0.008233
GU9 O3	0.179398	1.361961	2.348938	0.424357	0.762949	0.008211

Table 56 shows that after while there is a benefit to having an optical sighting once in a day compared to none at all, there is very little return to have more sightings included if the sightings are only of Mars. It is likely that sighting different planetary bodies with variations in their geometry at the time of the measurements would provide benefit. Because optical navigation provides state information along the line of sight, without differences in the measurement direction not all axes are likely to experience significant increases in the knowledge accuracy. This is why it is consistently seen, throughout this report, that the BT accuracy improves more significantly than the BR accuracy with optical navigation included. See Table 52 or Figure 24 for the specific BT and BR dispersion results with optical navigation measurements taken once a day compared to ground update only.

11.2 Alternate Ground Update Cases for an Interplanetary Cruise Highly Dependent on Optical Navigation

Table 56 shows, so long as Mars is the only sighting target considered in the optical navigation system, there is no reason to perform more than one optical measurement in a day. For the investigation into further decreasing DSN use, only once daily Mars sightings are performed with optical system accuracy per Table 43. New ground update cases are defined for this investigation. The basis for the ground update schedule is the Phoenix mission measurement data cutoff conditions, but with only a subset of the updates included. These are shown in Table 57. The results of the dispersions during the final segment are detailed in Table 58 while the navigation error is shown in Table 59. In both Table 58 and Table 59 the results are compared to the experiences of prior missions with codes per Table 50 and Table 51.

Table 57: Alternate Ground Update Accuracy Cases

Case	Update 2	Update 3	Update 4	Update 5	Update 6
GU11				Fine	Fine
GU12			1/W	Fine	Fine
GU13		1/W	1/W	Fine	Fine
GU14	1/W		1/W	Fine	Fine
GU15	1/W			Fine	Fine
GU16			1/M	Fine	Fine
GU17		1/M		Fine	Fine
GU18	1/M		1/M	Fine	Fine
GU19	1/M			Fine	Fine
GU20			1/W	Coarse	Coarse
GU21		1/W	1/W	Coarse	Coarse
GU22	1/W		1/W	Coarse	Coarse
GU23	1/W			Coarse	Coarse
GU24			1/M	Coarse	Coarse
GU25		1/M		Coarse	Coarse
GU26	1/M		1/M	Coarse	Coarse
GU27	1/M			Coarse	Coarse

Table 58: 3σ Dispersion Alternate at TCM-None1

Case	BT (km)		BR (km)		FPA (°)		Altitude (km)		Position (km)	Velocity (m/s)
G11	OPA	0.17252	SPN	2.16718	PAN	0.78188	ODN	0.08934	0.16766	0.00947
G12	OPA	0.17242	SPN	2.02052	PAN	0.73279	ODN	0.08465	0.15776	0.00885
G13	OPA	0.17232	SPN	1.89712	PAN	0.69556	ODN	0.08092	0.15007	0.00836
G14	OPA	0.17242	SPN	1.98504	PAN	0.72200	ODN	0.08359	0.15554	0.00871
G15	OPA	0.17251	SPN	2.12338	PAN	0.76819	ODN	0.08798	0.16485	0.00930
G16	OPA	0.17251	SPN	2.16344	PAN	0.78062	ODN	0.08922	0.16741	0.00946
G17	OPA	0.17251	SPN	2.16342	PAN	0.78070	ODN	0.08922	0.16742	0.00946
G18	OPA	0.17251	SPN	2.16243	PAN	0.78030	ODN	0.08918	0.16734	0.00945
G19	OPA	0.17251	SPN	2.16616	PAN	0.78156	ODN	0.08930	0.16760	0.00947
G20	OPA	0.20787	SPN	2.04990		2.47877	ODN	0.43203	0.77506	0.00897
G21	OPA	0.20779	SPN	1.92838		2.46798	ODN	0.43131	0.77351	0.00849
G22	OPA	0.20786	SPN	2.01494		2.47560	ODN	0.43182	0.77461	0.00883
G23	OPA	0.20794	SPN	2.15135		2.48949	ODN	0.43270	0.77655	0.00941
G24	OPA	0.20795	SPN	2.19091		2.49335	ODN	0.43295	0.77709	0.00957
G25	OPA	0.20795	SPN	2.19089		2.49338	ODN	0.43296	0.77709	0.00957
G26	OPA	0.20795	SPN	2.18991		2.49326	ODN	0.43295	0.77708	0.00956
G27	OPA	0.20795	SPN	2.19359		2.49365	ODN	0.43297	0.77713	0.00958

Table 59: 3σ Navigation Error Alternate at TCM-None1

Case	BT (km)		BR (km)		FPA (°)		Altitude (km)		Position (km)	Velocity (m/s)
G11	OPA	0.17252	SPN	2.16718	SUN	0.19897	ODA	0.02535	0.05334	0.00017
G12	OPA	0.17242	SPN	2.02052	SUN	0.19897	ODA	0.02535	0.05334	0.00017
G13	OPA	0.17232	SPN	1.89712	SUN	0.19897	ODA	0.02535	0.05334	0.00017
G14	OPA	0.17242	SPN	1.98504	SUN	0.19897	ODA	0.02535	0.05334	0.00017
G15	OPA	0.17251	SPN	2.12338	SUN	0.19897	ODA	0.02535	0.05334	0.00017
G16	OPA	0.17251	SPN	2.16344	SUN	0.19897	ODA	0.02535	0.05334	0.00017
G17	OPA	0.17251	SPN	2.16342	SUN	0.19897	ODA	0.02535	0.05334	0.00017
G18	OPA	0.17251	SPN	2.16243	SUN	0.19897	ODA	0.02535	0.05334	0.00017
G19	OPA	0.17251	SPN	2.16616	SUN	0.19897	ODA	0.02535	0.05334	0.00017
G20	OPA	0.20787	SPN	2.04990		2.37314	ODN	0.42396	0.76027	0.00021
G21	OPA	0.20779	SPN	1.92838		2.37309	ODN	0.42395	0.76024	0.00021
G22	OPA	0.20786	SPN	2.01494		2.37313	ODN	0.42396	0.76027	0.00021
G23	OPA	0.20795	SPN	2.15135		2.37316	ODN	0.42395	0.76027	0.00021
G24	OPA	0.20795	SPN	2.19091		2.37316	ODN	0.42396	0.76028	0.00021
G25	OPA	0.20795	SPN	2.19089		2.37316	ODN	0.42396	0.76027	0.00021
G26	OPA	0.20795	SPN	2.18991		2.37316	ODN	0.42396	0.76028	0.00021
G27	OPA	0.20795	SPN	2.19359		2.37316	ODN	0.42396	0.76028	0.00021

Figure 33 shows the position navigation error and trajectory dispersion throughout the cruise with the Ground Updates of GU11. To show the benefits of optical navigation, the ground update conditions of

GU11 were kept but the use of daily optical sightings of Mars was eliminated. The resulting position navigation error and trajectory dispersions are shown in Figure 34.

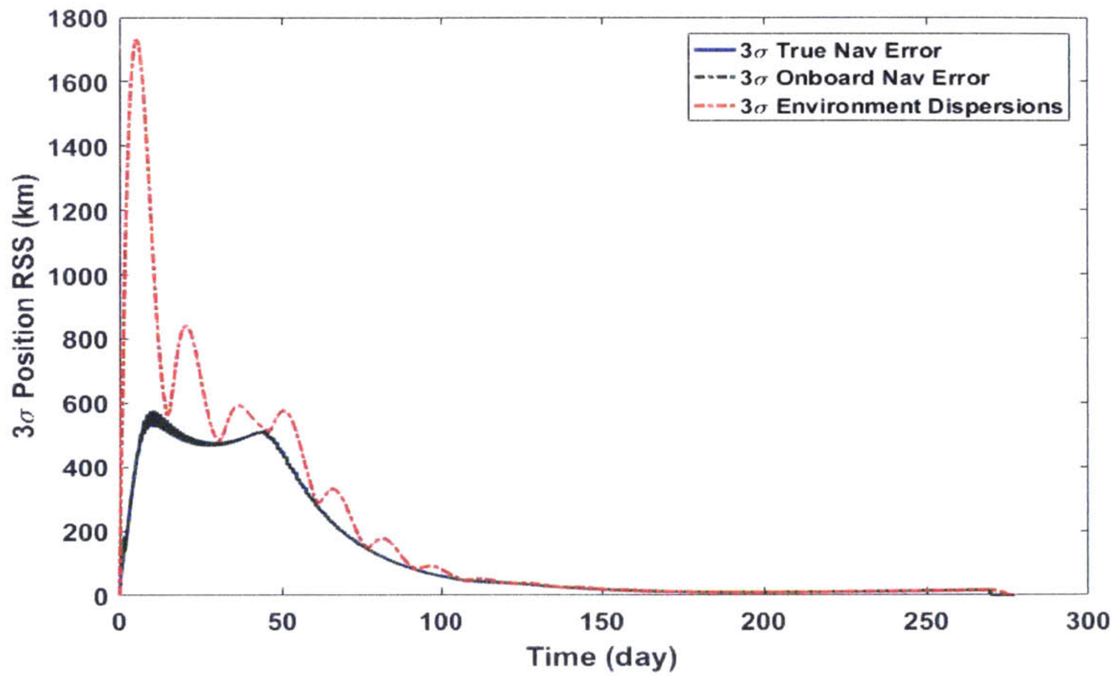

Figure 33: GU11 3σ Position RSS

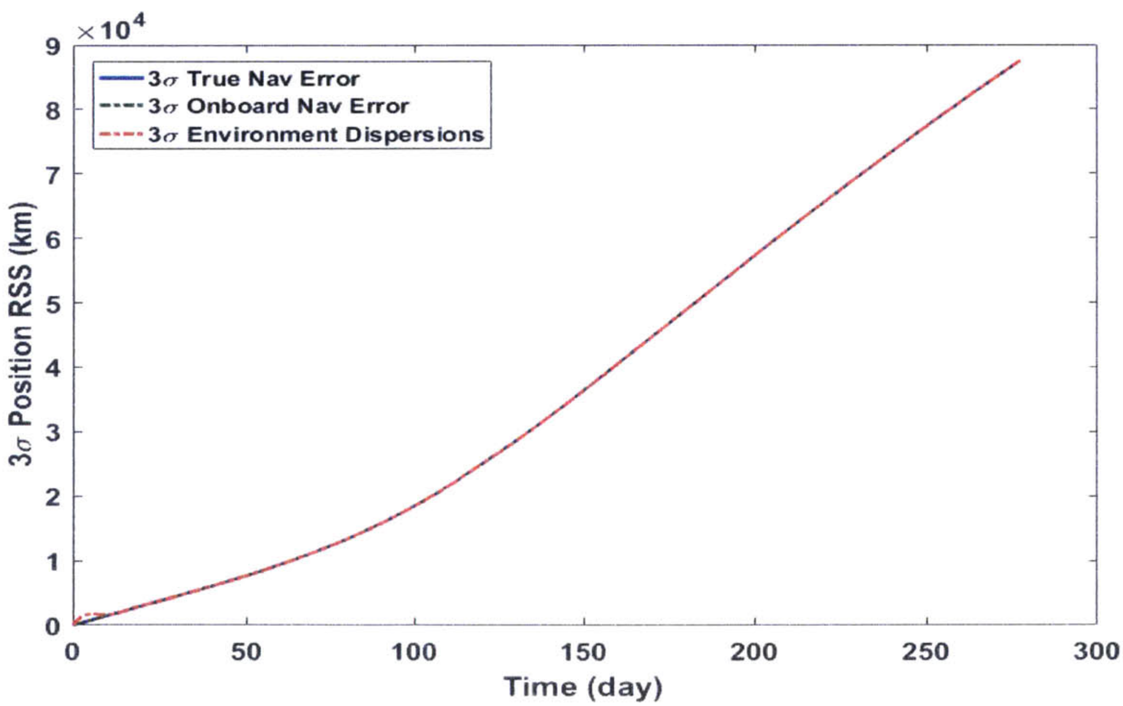

Figure 34: GU11 3σ Position RSS without Optical Navigation

11.3 Suggested Missions

The results in Table 58 and Table 59 show a step increase for all of the parameters, except BR, depending on whether the final approach uses fine ground update accuracy or coarse accuracy. The navigation error still does not meet even the widest of requirements with coarse ground updates during approach. On the other hand, with an approach significantly supported with ground updates it is possible for the dispersions to meet the Pathfinder requirement after an interplanetary cruise with minimal ground updates based on infrequent DSN tracking. Besides FPA, each of the parameters of interest meet a desirable dispersion accuracy. All of the BT dispersions meet the Opportunity achieved uncertainty, all of the BR cases meet the Spirit navigation uncertainty, and all of the altitude dispersions meet the Odyssey navigation uncertainty experienced.

Figure 16 shows the same type of results as Figure 33, position dispersions. The difference between their inputs is that Figure 16 shows the effects from 3/Week DSN measurements ground updates throughout cruise (GU1) while Figure 33 shows very accurate ground updates during approach only but optical navigation throughout cruise (GU11). Figure 16 shows GU1 outperforms GU11 for the first half of the trajectory of the trajectory but GU11 outperforms GU1 over the second half of the trajectory. GU11 performs worse for position dispersions when optical navigation is used in addition to 3/Week DSN measurement ground updates (Optical GU1) during both cruise and at the target. This can be seen by comparing Figure 19, position dispersions of Optical GU1, with Figure 33. This is not unexpected given the accuracy of the ground updates in Optical GU1 and the frequency which they are provided. The difference in dispersion magnitude after the "ground update 5" point for both Optical GU1 and GU11 is within meters. This points to using optical navigation throughout the interplanetary cruise coupled with significant improvements in ground update accuracy during approach as a promising cost savings measure. Optical navigation would need to be used throughout cruise though as to Figure 34 shows that despite the nominal trajectory reaching Mars entry-interface the dispersions diverge otherwise.

Recall that Table 48 defined the position and velocity variance levels for "fine" and "coarse" approach ground updates. GU20, with its final TCM values in Table 58 and Table 59 , also has position dispersions within meters of Optical GU1 after "ground update 5" as well. The only ground update during the cruise of GU20 was at "ground update 4" while "ground update 5" was of "coarse" accuracy. "Ground update 5" of GU11 was of "fine" accuracy, which is significantly more accurate than "coarse" approach ground updates.

This shows that attempting to meet an orbit insertion target after an interplanetary cruise heavily dependent on optical navigation, and an approach supported with ground OD accuracies seen for prior missions, is a reasonable mission concept. In addition, the use of AGNC and an Onboard Mission Planner (OMP) that performs with reasonable confidence, can meet the desirable conditions and reduce oversight required by the ground team.

12 Long Guidance Segments: Baseline Results

12.1 Important Settings

The long guidance segment baseline mission chosen for analysis was Phoenix. The important mission features are summarized in Table 60 and used as guidelines for the guidance correction schedule and the ground update navigation schedule. The asterisks on a TCM represent those which were planned before the flight but during the flight were found not to be needed. Those TCMs were still included in this analysis because the results are for preflight mission definition.

Table 60: Planned Phoenix Mission Trajectory Correction Schedule

Maneuver	Maneuver Date	Analysis Data Cutoff
TCM-1	S+7d	S+2d
TCM-2	S+81d	S+75d
TCM-3	E-45d	E-50d
TCM-4*	E-14d	E-16d
TCM-5	E-7d	TCM5-5h
TCM-6*	E-3d	TCM6-5h

Fixed Time of Arrival guidance is used as the baseline. Each of the baseline guidance segments start with planned maneuver dates that match the Phoenix plan. Except for the end point of the trajectory, each waypoint for a guidance segment is one day past the start of the subsequent segment. When a waypoint was set to be exactly at the start of the subsequent segment singularity issues occurred. This was most likely due to the granularity and required response time of the corrective control system, being too large to effectively respond at the very end of a waypoint segment. Under these conditions, use of the control system can actually exacerbate errors, so error correction attempts are ceased. The final guidance segment settings are captured in Table 61.

Table 61: Implemented Guidance Segments

Segment	Start	Waypoint
1	S = Outside Earth SOI	S+8 days
2	S+7 days	S+82 days
3	S+81 days	E-44 days
4	E-45 days	E-13 days
5	E-14 days	E-6 days
6	E-7 days	E-2 days
7	E-3 days	E = Mars end

12.1.1 Navigation

The implemented ground updates occur on the days listed in Table 62. For convenience, maneuver-relative dates are also provided. The standard DSN use during cruise is 3 passes/week with a 1σ position accuracy of 15km and 1σ velocity accuracy of 5 cm/s. The ground update date and accuracy and the optical navigation accuracy and measurement frequency is the same as the examination with the two-week guidance segments.

Table 62: Implemented Ground update Schedule

Ground update	Trajectory Date	Maneuver Relative Date
1	S+2 days	TCM-1-5 days
2	S+75 days	TCM-2-6 days
3	E-50 days	TCM-3-5 days
4	E-16 days	TCM-4-2 days
5	E-8 days	TCM-5-1 day
6	E-4 days	TCM-5-1 day

It was important to get a sense how much optical navigation affected the results when combined with the nominal ground update case. The parameters of the optical navigation system represent the resulting accuracy after all image processing and centerfinding has occurred. Resulting parameter values are captured in Table 63.

Table 63: Implemented Optical Navigation Conditions

Parameter	Value
Optical Target	Mars
Frequency Measurement	1/day
Camera Misalignment (°)	0.01
Noise in Azimuth Measurement (°)	0.01
Noise in Elevation Measurement (°)	0.01
Noise in Range Measurement (m)	0.001

12.1.2 Initial Conditions

The initial position and velocity navigation error represents the error after the spacecraft has been fully checked out by the ground team which has supplied with an initial ground update based on DSN measurements. The initial position and velocity trajectory dispersion represents the dispersions for a craft which has been supplied with an up to date optimal reference trajectory based on its post check out conditions. The knowledge of the targeted location of Mars is considered perfect due to an expectation of having high-precision Mars ephemeris information onboard. The translational process noise represents the dispersions to model of the thrusting system that impact feedback control. These conditions are detailed in Table 64.

Table 64: Baseline Initial Dispersion Conditions

Initial Condition	A	G	M
Position Dispersion (m)	(1000/3)	(10000/3)	(100000/3)
Velocity Dispersion (cm/s)	(5/3)	(50/3)	(500/3)
Position Navigation Error (m)	(100/3)	(1000/3)	(1000/3)
Velocity Navigation Error (cm/s)	(1/3)	(10/3)	(10/3)
Translational Process Noise (m/s^2)	4.8020E-15	4.8020E-15	4.8020E-15

Several initial conditions are examined and referred to as A, G, and M. TPN is kept constant across the cases but the trajectory dispersions and navigation error increases with each. This is to investigate the effect on the dispersion at the target with varying levels of characterization at the start of the interplanetary trajectory.

12.2 Expected Errors with Ground Update Accuracy from Standard DSN Tracking

Recall that as described earlier, during cruise DSN tracking typically occurs three times per week and results in ground OD of 15 km position variance and 5 cm/s velocity variance. Table 65 shows the dispersion results when the standard ground update accuracy is provided per the schedule of Table 62.

Table 65: 3σ Dispersion for Baseline Use of Standard Ground Updates

Parameter	TCM-1	TCM-2	TCM-3	TCM-4	TCM-5	TCM-6
Initial Conditions A						
BT (km)	322.8341	18.72001	4.163663	3.872269	3.983867	3.657769
BR (km)	918.824	39.29904	45.8753	11.30942	8.994601	6.076765
FPA (°)	4769.329	277.1955	72.38229	56.7957	49.26232	43.52055
Altitude (km)	846.1654	27.48002	34.84484	16.38821	13.99611	12.28974
Position (km)	83.76149	33.96033	30.23062	23.31076	20.94904	18.86285
Velocity (km/s)	1.994762	0.137191	0.339355	0.104773	0.105159	0.076893
Initial Conditions G						
BT (km)	3228.027	71.5292	4.195814	3.893706	4.004391	3.673865
BR (km)	9188.076	192.0647	45.91205	11.31329	8.997326	6.085254
FPA (°)	47691.29	939.9455	72.48785	56.82799	49.2846	43.53713
Altitude (km)	8461.429	161.4825	34.85628	16.39163	14.00145	12.29727
Position (km)	835.2295	39.51262	30.27118	23.34563	20.98212	18.895
Velocity (km/s)	19.94728	0.545394	0.339536	0.104866	0.105235	0.076949
Initial Conditions M						
BT (km)	29127.68	602.2799	5.323133	3.896575	4.004452	3.673866
BR (km)	82905.77	1713.618	46.83973	11.31954	8.997492	6.085257
FPA (°)	430360.5	8147.805	74.58195	56.82803	49.28463	43.53713
Altitude (km)	76359.23	1443.115	34.99425	16.39163	14.00145	12.29727
Position (km)	7492.91	186.061	30.36782	23.34608	20.98213	18.895
Velocity (km/s)	179.9562	4.788174	0.345343	0.104927	0.105237	0.076949

Figure 35 and Figure 36 show the position trajectory dispersions and navigation error RSS and the B-Plane dispersions for initial conditions A with DSN tracking 3/week, respectively. Figure 37 and Figure 38 show the position trajectory dispersions and navigation error RSS and the B-Plane dispersions for initial conditions G with DSN tracking 3/week, respectively. Figure 39 and Figure 40 show the position trajectory dispersions and navigation error RSS and the B-Plane dispersions for initial conditions M with DSN tracking 3/week, respectively.

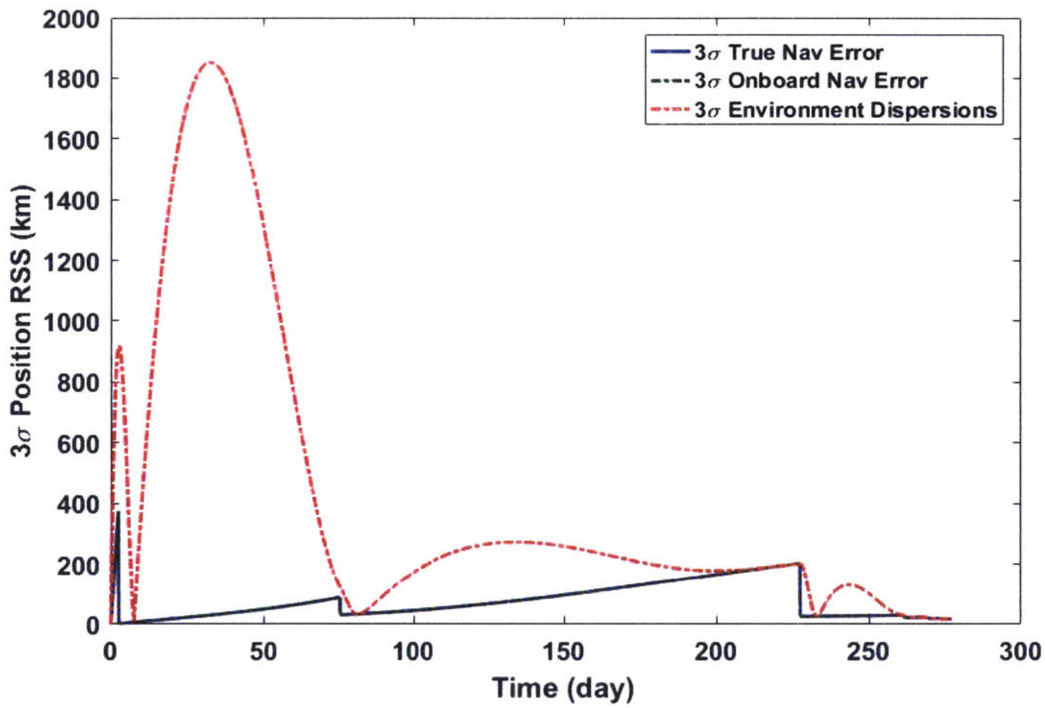

Figure 35 : Inertial Position RSS with Long Guidance Segments and Initial Conditions A

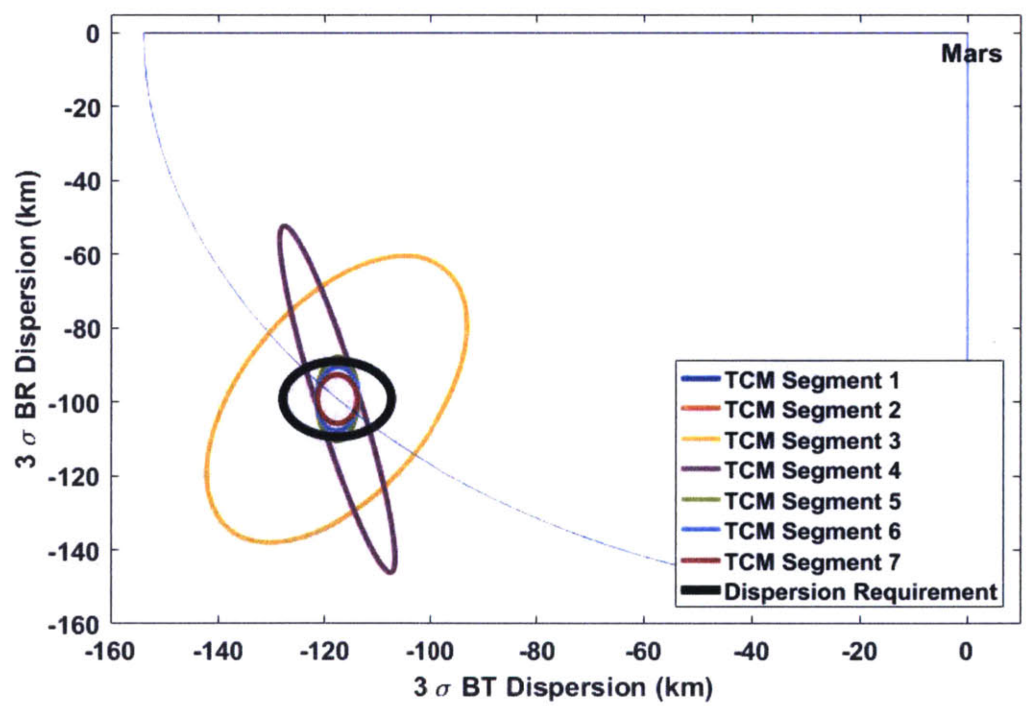

Figure 36: B-Plane Dispersions with Long Guidance Segments and Initial Conditions A

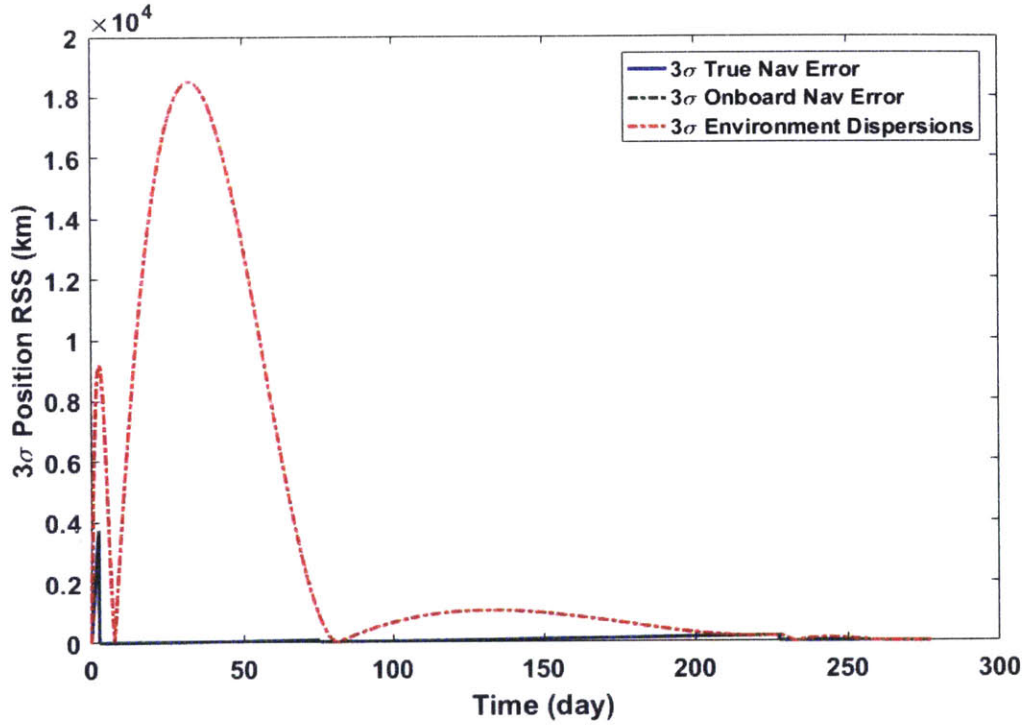

Figure 37: Inertial Position RSS with Long Guidance Segments and Initial Conditions G

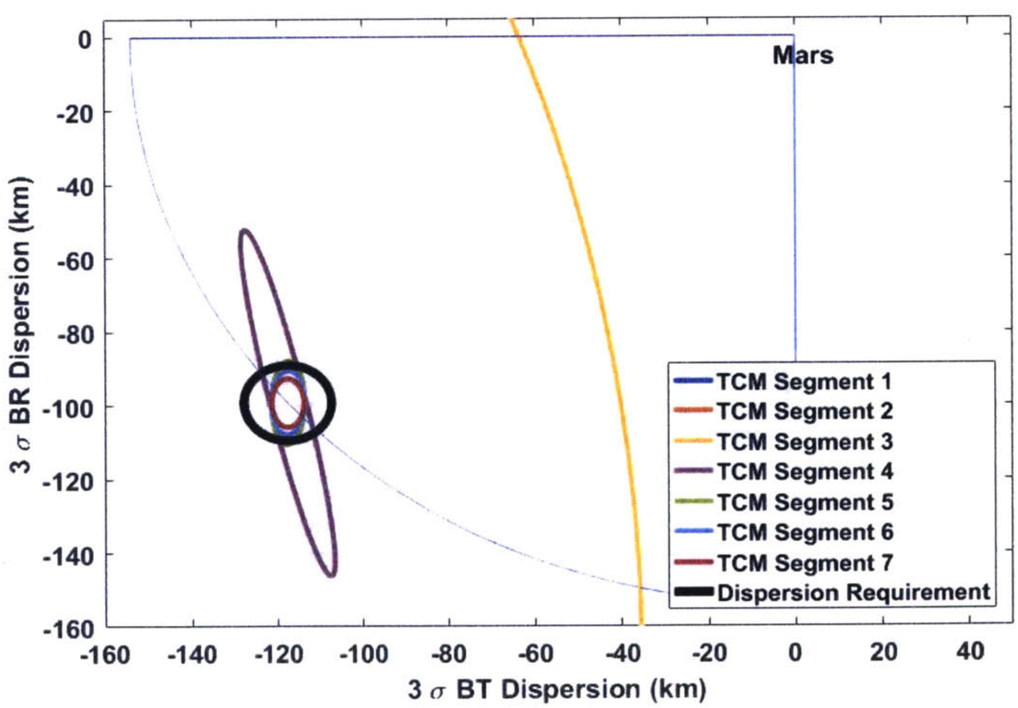

Figure 38: B-Plane Dispersions with Long Guidance Segments and Initial Conditions G

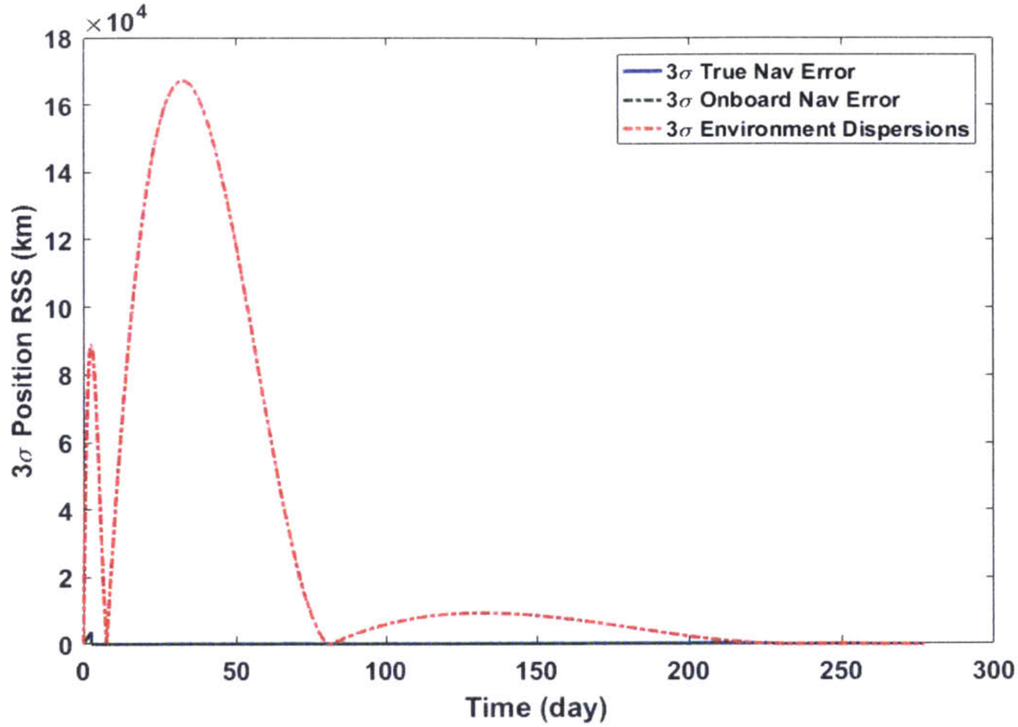

Figure 39: Inertial Position RSS with Long Guidance Segments and Initial Conditions M

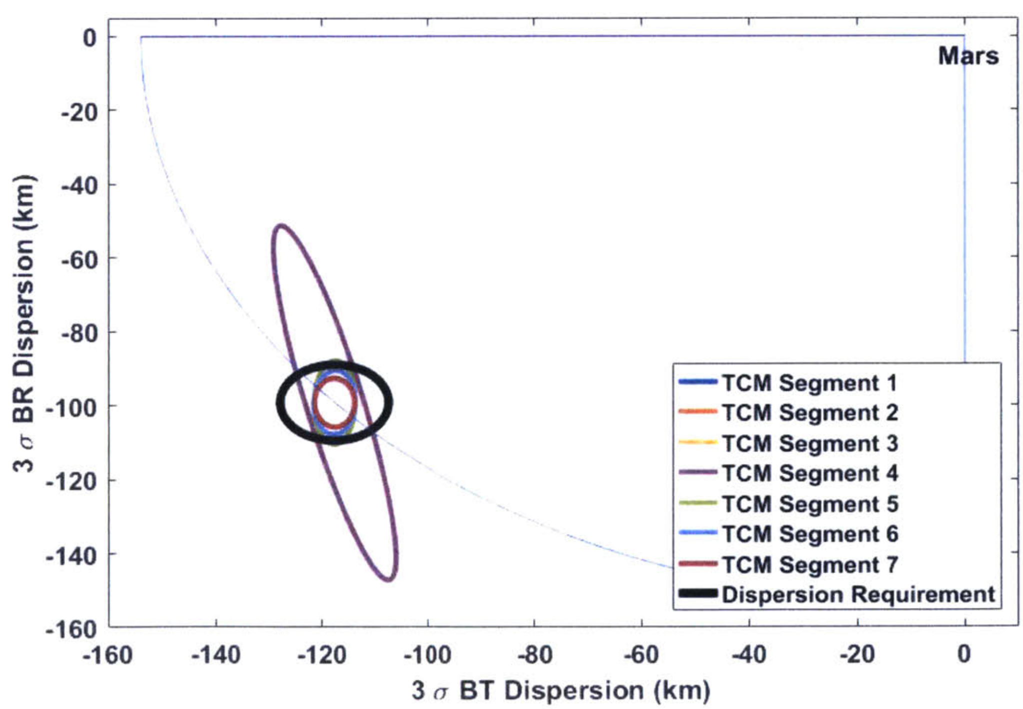

Figure 40: B-Plane Dispersions with Long Guidance Segments and Initial Conditions M

Though Table 65 showed the dispersion values at each trajectory correction maneuver, the figures above provide additional clarity about the differences which result from the initial conditions along the cruise portion of the trajectory. The position RSS figures with long guidance segments compared to Figure 16 highlight the position dispersion differences along cruise when short guidance segments are used. Initial condition A with ground update accuracy from 3 DSN passes per week resulted in both Figure 16 and Figure 35. The only difference between the analysis conditions was that long guidance segments produces the results shown in Figure 35. With short guidance segments the dispersion results very closely follow the navigation error throughout the trajectory. With long guidance segments the dispersion results only follow the navigation results closely at the end of the trajectory near the target. While this report has focused on the dispersion at the target point of interest, it is possible that the dispersions along the trajectory with long guidance segments would be unacceptable. Should that be the case, a new nominal trajectory may need to be provided on the ground if there are not onboard resources that can be trusted to do so. That would possibly entail the need to increase ground based tracking so that a new optimal trajectory can be determined if the original DSN tracking plan was infrequent.

12.3 Expected Errors with Ground Update Accuracy from Standard DSN Tracking Supplemented with Daily Optical Navigation

The same ground update schedule and accuracy which was used in Table 65 is used along with daily optical sightings of Mars. The results of this navigation setup are shown in Table 66.

Table 66: 3σ Dispersion Standard Ground Use with Optical Navigation Supplement

Parameter	TCM-1	TCM-2	TCM-3	TCM-4	TCM-5	TCM-6
			Initial Conditions A			
BT (km)	303.5345	6.729973	1.027628	0.979809	0.978314	0.950621
BR (km)	886.7882	23.15093	5.247577	6.897774	6.723239	5.328306
FPA (°)	4554.992	112.466	24.10858	29.30263	28.46413	27.22309
Altitude (km)	768.0074	14.61142	4.482072	4.045951	3.841627	3.686041
Position (km)	78.57712	14.5791	8.150733	8.709275	8.317877	7.83386
Velocity (km/s)	1.881816	0.054959	0.011577	0.026466	0.032116	0.025538
			Initial Conditions G			
BT (km)	3035.248	62.77769	1.102824	0.980001	0.978332	0.95063
BR (km)	8867.38	183.8283	5.445354	6.990642	6.796819	5.37638
FPA (°)	45547.73	865.0712	24.63739	29.5888	28.69148	27.41218
Altitude (km)	7680.059	145.1415	4.514774	4.065514	3.856964	3.69847
Position (km)	785.322	24.00878	8.249729	8.782814	8.376396	7.881229
Velocity (km/s)	18.81754	0.501002	0.013507	0.026898	0.032505	0.025786
			Initial Conditions M			
BT (km)	29107.51	601.3084	3.596716	0.991422	0.978571	0.950631
BR (km)	82870.65	1712.713	10.71002	7.000689	6.796994	5.376313
FPA (°)	430128.2	8139.507	30.24846	29.58818	28.69098	27.41179
Altitude (km)	76276.6	1441.377	5.478898	4.065384	3.856872	3.698396
Position (km)	7487.511	183.3952	8.597111	8.783655	8.376194	7.881064
Velocity (km/s)	179.8345	4.783321	0.064492	0.027138	0.03251	0.025786

Figure 41, Figure 42, and Figure 43 show the inertial position dispersion, FPA dispersions mapped to entry interface, and the B-Plane dispersions for initial condition A in Table 66.

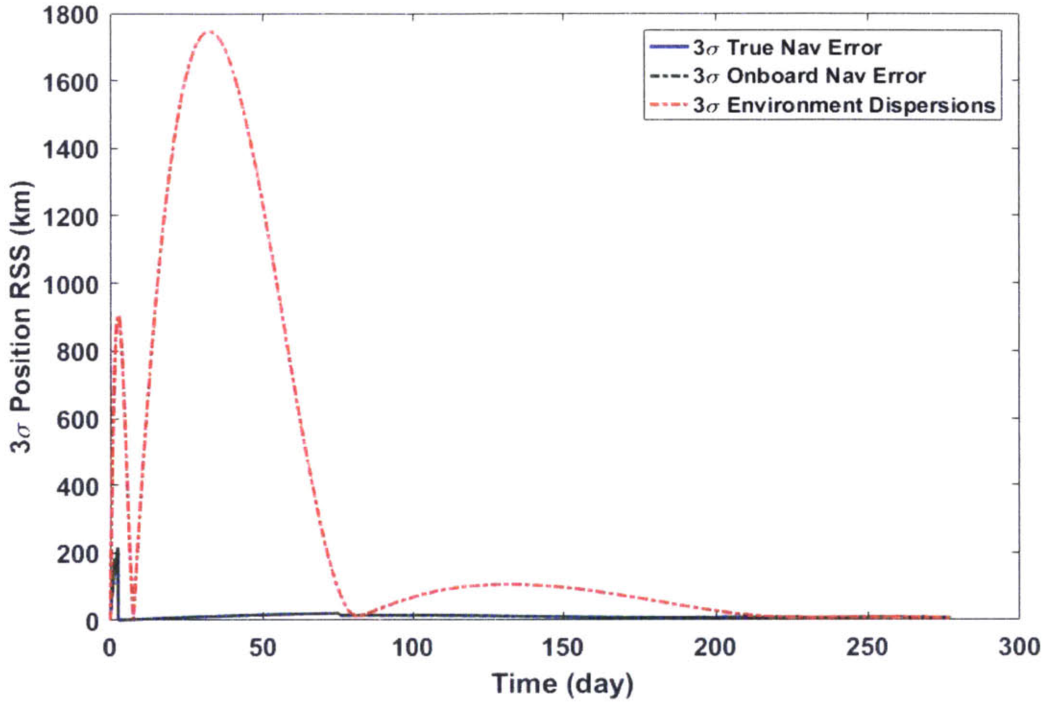

Figure 41: Inertial Position RSS with Long Guidance Segments, Optical Navigation, & Initial Conditions A

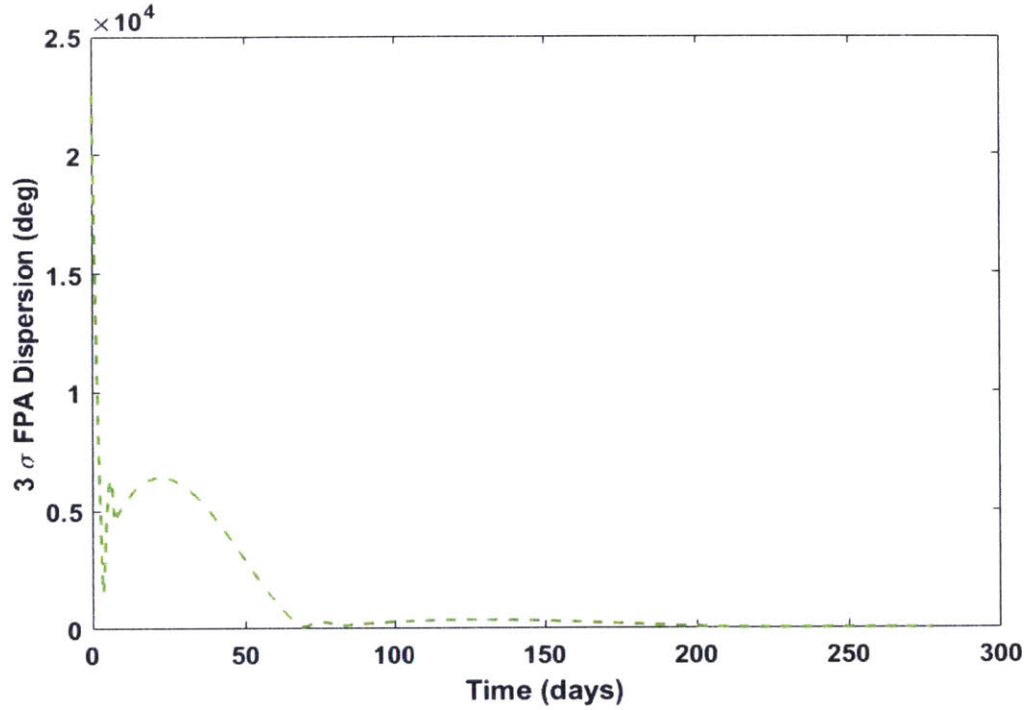

Figure 42: FPA Dispersion Mapped to Entry Interface, Long Guidance Segments, Optical Navigation, & Initial Conditions A

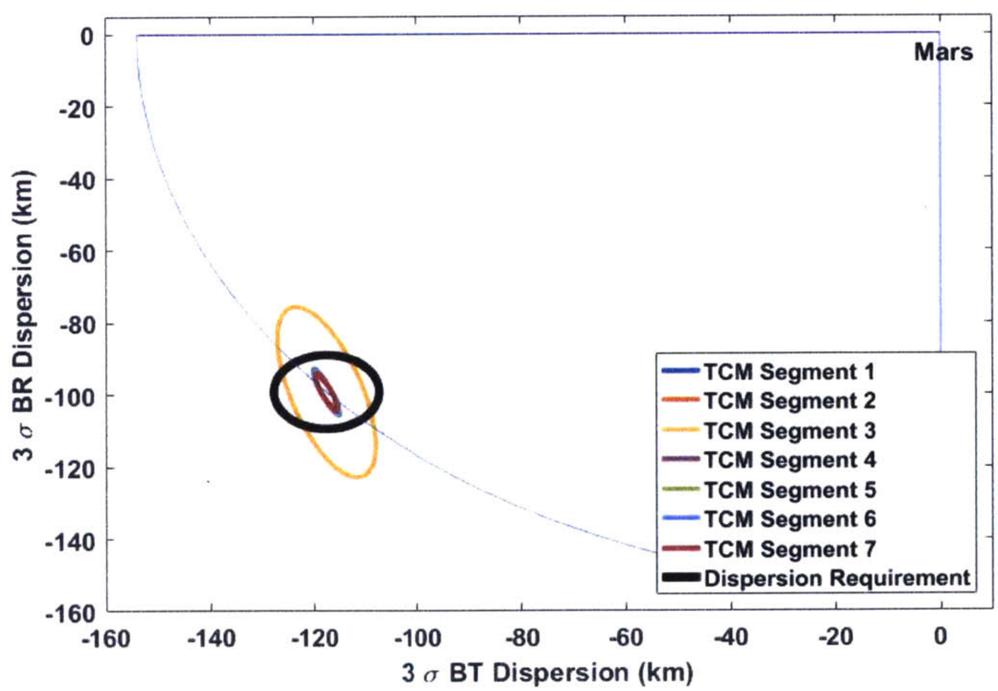

Figure 43: B-Plane Dispersions with Long Guidance Segments, Optical Navigation and Initial Conditions A

Figure 41 can be compared to Figure 35 to see the difference in results from optical navigation inclusion with the same guidance segments and ground update setup without optical navigation. In addition, Figure 41 can be compared to Figure 19, with the same ground update accuracy, optical navigation, and initial conditions but with shorter FTOA guidance segments. With longer guidance segments the position dispersions remain high for a significantly longer amount of time compared to Figure 19. The mapped FPA dispersion of Figure 42 also stays higher for much longer than in Figure 20. With long guidance segments the B-Plane dispersions of Figure 36 without optical navigation are larger and outside of the delivery requirement while those with optical navigation in Figure 43 meet the B-Plane dispersion requirement early and with a much wider margin.

12.4 Analysis of Implication of Computational Results

The difference between the initial condition settings of A, G, and M is the initial position and velocity dispersion and navigation error. The translational process error was constant for each, as well as the timing and accuracy of the ground updates and the guidance segments.

While the dispersions resulting from the standard ground update baseline across cases A, G, and M, as shown in Table 65, show noticeable differences for the first three trajectory correction maneuvers, those differences become much less significant for the subsequent trajectory correction maneuvers. By the final maneuver there is effectively no difference in the values. The implication is that when holding other factors constant, the differences in the initial position and velocity shown in Table 64 are not a major drivers of final B-Plane, FPA, Altitude, Position, and Velocity dispersions for an interplanetary trajectory to Mars.

The dispersions resulting from use of the standard DSN use supplemented with optical navigation, as shown in Table 66, have the same trends as seen in Table 65. However, the B-Plane, altitude, position, and velocity dispersions also all decrease with the optical navigation supplement compared to when only the ground update data is used. The most significant decrease is across the last three parameters shown in the tables. Table 67 compares these results to that of prior missions at similar points in their trajectory.

Table 67: Final TCM Dispersions Result Comparison Between Prior Mars Missions and the Analyzed Initial Condition Cases

Mission	BR (km)	BT (km)	FPA (°)	Altitude (km)
Prior Mission Final TCM Dispersions				
Pathfinder (3σ) [10]	23	17.4	0.83	N/A
Surveyor (3σ) [9]	2.262	6.052	0.24	N/A
Spirit (1σ) [11]	1.5	1.53	0.056	N/A
Opportunity (1σ) [11]	2.38	2.49	0.096	N/A
Odyssey (1σ) [39]	8.3	5.3	N/A	0.063
3σ Large Guidance Segment Baseline Final TCM Dispersions				
Ground A	6.076765	3.657769	43.52055	12.28974
Ground G	6.085254	3.673865	43.53713	12.29727
Ground M	6.085257	3.673866	43.53713	12.29727
Ground A W/ Optical	5.328306	0.950621	27.22309	3.686041
Ground G W/ Optical	5.37638	0.95063	27.41218	3.69847
Ground M W/ Optical	5.376313	0.950631	27.41179	3.698396

As can be seen in Table 67, with initial conditions A, G, and M the B-Plane dispersions at the final trajectory correction segment are better than that of prior missions with or without optical navigation included. The FPA dispersions of the analyzed cases are well beyond that needed for entry-interface. The altitude dispersions are larger than the prior orbiter dispersions, but are still within the orbit insertion requirements.

A consideration regarding the prior mission B-Plane errors seen in Table 67 is that they did not require better B-Plane accuracy for their goals and thus did not attempt to achieve them. For each of the identified prior landing missions, the FPA error was a primary concern because of its impact on entry/descent/landing performance requirements. The arrival state error requirements detailed for Pathfinder [9], the Surveyor Lander [10], Spirit [11],and Opportunity [11] focus only on the FPA error, not the B-Plane errors. Phoenix requirements [8] did provide reference to B-Plane errors as they related to the acceptable FPA uncertainty. The value of the noted Phoenix B-Plane error is based on the acceptable FPA uncertainty along the particular B-Plane error vector magnitude. Here, if a particular FPA error bound is desired for a CubeSat platform utilizing low-thrust propulsion, fixed time of arrival guidance, and the designated translational process noise, then the B-Plane requirements must be much tighter than prior missions to meet the required FPA dispersions limits. As orbit insertion does not have an FPA requirement, the results show that it should be possible to loosen some of the baseline parameter error bounds despite the expected increase in resulting arrival FPA error. Associated differences in navigation use, guidance use, and translational process noise are investigated in subsequent sections.

13 Long Guidance Navigation Study

As in Section 9 where a navigation comparison is performed for the use of short FTOA guidance segments, this section investigates the results of the same navigation cases but with long FTOA guidance segments. The same initial conditions and translational process noise are also used, as in Section 9. The results for the dispersions are shown in Table 68 and the navigation errors are shown in Table 69. In each table the result at the final trajectory correction maneuver is compared to the prior mission results defined in Table 50 and Table 51.

Table 68: Long Guidance Segments 3σ Dispersions at TCM-6

Ground Updates Only									
Case	BT (km)		BR (km)		FPA (°)	Altitude (km)		Position (km)	Velocity (m/s)
GU1	PAN	3.65777	SUR	6.07677	41.8270	SUR	12.2897	18.8629	0.07689
GU2	PAN	6.69822	PAN	11.9819	82.6455	ODR	23.6059	35.8490	0.09938
GU3	PAN	9.84921		17.9243	122.604		35.1089	53.1886	0.14832
GU4		32.3239		59.6284	405.236		116.269	175.808	0.49251
GU5		64.5391		119.233	809.814		232.357	351.270	0.98417
GU6	SPN	1.49450	SUR	3.30442	9.90248	ODN	2.84176	4.09341	0.05115
GU7	PAN	4.89588	PAN	10.9967	32.7946	SUR	9.44006	13.5561	0.16939
GU8	PAN	9.77383		21.9892	65.5347	SUR	18.8674	27.0863	0.33847
GU9	SPN	1.52284	SUR	3.36792	10.5703	ODN	2.92664	4.26434	0.05146
GU10	PAN	4.90468	PAN	11.0159	33.0025	SUR	9.46597	13.6087	0.16949
Ground Updates and Daily Optical Sightings									
Case	BT (km)		BR (km)		FPA (°)	Altitude (km)		Position (km)	Velocity (m/s)
GU1	SPN	0.95062	SUR	5.32831	27.2231	ODN	3.68604	7.83386	0.02554
GU2	SPN	0.96234	PAN	8.51609	40.2795	ODN	4.81061	11.3866	0.03525
GU3	SPN	0.96456	PAN	10.2166	48.1850	ODN	5.53252	13.5520	0.03588
GU4	SPN	0.96611	PAN	12.4305	59.7341	ODN	6.62359	16.7235	0.02273
GU5	SPN	0.96622	PAN	12.6590	61.0289	ODN	6.7479	17.0793	0.01869
GU6	OPA	0.14517	SPN	1.58477	2.95156	ODN	0.34922	0.87587	0.01702
GU7	OPA	0.14533	SPN	1.84450	3.39245	ODN	0.39415	1.00567	0.01954
GU8	OPA	0.14534	SPN	1.86948	3.43511	ODN	0.39854	1.01824	0.01979
GU9	OPA	0.22177	SPN	1.66030	3.92858	ODN	0.58062	1.21254	0.01801
GU10	OPA	0.22187	SPN	1.90981	4.26981	ODN	0.60872	1.30941	0.02042

Table 69: Long Guidance Segments 3σ Navigation Error at TCM-6

Ground Updates Only										
Case	BT (km)		BR (km)		FPA (°)		Altitude (km)		Position (km)	Velocity (m/s)
GU1	PAN	3.65777	SUR	6.07677		11.8597	SUR	14.9186	18.3084	0.00208
GU2	PAN	6.69822	PAN	11.9819		79.2724	ODR	22.7102	34.7435	0.00374
GU3	PAN	9.84921		17.9243		117.546		33.7523	51.5286	0.00546
GU4		32.3239		59.6284		388.377		111.714	170.270	0.01785
GU5		64.5391		119.233		776.116		223.249	340.200	0.03562
GU6	SPN	1.49450	SUR	3.30442	SUN	0.18141	ODA	0.03274	0.05636	0.00011
GU7	PAN	4.89588	PAN	10.9967	SUN	0.18141	ODA	0.03274	0.05636	0.00011
GU8	PAN	9.77383		21.9892	SUN	0.18141	ODA	0.03274	0.05636	0.00011
GU9	SPN	1.52284	SUR	3.36792		3.40797	ODN	0.63567	1.08438	0.00019
GU10	PAN	4.90468	PAN	11.0159		3.40889	ODN	0.63577	1.08457	0.00019
Ground Updates and Daily Optical Sightings										
Case	BT (km)		BR (km)		FPA (°)		Altitude (km)		Position (km)	Velocity (m/s)
GU1	SPN	0.95062	SUR	5.32831		26.6723	ODN	3.64217	7.66132	0.00096
GU2	SPN	0.96234	PAN	8.51609		39.5774	ODN	4.74937	11.1471	0.00126
GU3	SPN	0.96456	PAN	10.2166		47.5695	ODN	5.47736	13.3098	0.00145
GU4	SPN	0.96611	PAN	12.4305		59.5000	ODN	6.60404	16.5267	0.00175
GU5	SPN	0.96622	PAN	12.6590		60.8564	ODN	6.73435	16.8909	0.00178
GU6	OPA	0.14517	SPN	1.58476	SUN	0.17239	ODA	0.02211	0.04551	0.00009
GU7	OPA	0.14533	SPN	1.84450	SUN	0.17239	ODA	0.02211	0.04551	0.00009
GU8	OPA	0.14534	SPN	1.86948	SUN	0.17239	ODA	0.02211	0.04551	0.00009
GU9	OPA	0.22177	SPN	1.66030		2.37031	ODN	0.42285	0.76023	0.00015
GU10	OPA	0.22187	SPN	1.90981		2.37038	ODN	0.42286	0.76027	0.00015

With long FTOA guidance segments the dispersions are worse than the short FTOA guidance segments with all other variables held constant. Unlike in Section 9, the FPA dispersions in Table 68 are larger than even the broadest prior mission, even with optical navigation utilized. The altitude dispersions are also worse, but either meet the same prior mission accuracy as in Section 9 or are minimally within a desirable dispersion range. Unsurprisingly, the navigation error in Section 9 is nearly identical to the navigation error shown in Table 69. This makes sense as trajectory dispersions do not affect navigation error and the same ground update accuracy and optical navigation system was used in the analysis.

14 Long Guidance Segments: Process Noise Trade Study

14.1 Important Settings

The prior results had varied initial position and velocity dispersions and knowledge but had the translational process noise held constant. As such, the results shown so far may be limited to a thrusting model of that accuracy. Checking to make sure the observed trends hold for varied process noise conditions is important as the accuracy of the propulsion models for CubeSat low-thrust propulsion is an area of on-going development itself. Table 70 shows the Translational Process Noise values (TPN) values investigated here. TPN-1 is the translational process noise value which the prior trade study sections used as their baseline.

Table 70: Translational Process Noise (TPN) Versions

Version	TPN-1	TPN-2	TPN-3	TPN-4	TPN-5	TPN-6
Value	4.802E-15	4.802E-14	4.802E-13	4.802E-12	4.802E-11	4.802E-10

14.1.1 Navigation

A standard ground frequency of 3/Week is considered first, then the standard ground update frequency supported by optical navigation of looking to Mars once a day is addressed. The ground updates occur at the baseline times. The navigation details are the same as those in Table 62 and Table 63. Afterwards, comparison to the lower-frequency DSN tracking cases are plotted along the translational process noise versus the dispersion of the parameters of interest.

14.1.2 Initial Conditions

The A, G, and M initial trajectory dispersion and navigation error settings are used. For each, all of the TPN values of Table 70 are plotted but only TPN-1 values are captured in tables addressing varied navigation conditions.

14.1.3 Guidance Correction Scheduling

The baseline guidance correction schedule is used with fixed time of arrival guidance, shown in Table 61.

14.2 Baseline Guidance and Navigation Comparison

First, a comparison to the baseline conditions must be examined for each of the translational process noise values. This includes the initial conditions of A, G, and M. Table 71 and Table 72 capture the dispersion results of the parameters of interest at the final TCM for each TPN value for ground updates and ground updates supplemented with optical navigation, respectively.

Table 71: TPN Effects Comparison for Standard Ground Navigation Update Frequency

Parameter	TPN-1	TPN-2	TPN-3	TPN-4	TPN-5	TPN-6
Initial Condition A TCM-6						
BT (km)	3.657769	5.157696	6.812014	7.900498	8.582514	10.15445
BR (km)	6.076765	6.954752	9.835452	14.59517	19.27059	25.58086
FPA (°)	43.52055	57.38897	84.88322	111.0449	129.6185	149.8419
Altitude (km)	12.28974	15.33981	20.42837	23.52774	25.38805	28.06645
Position (km)	18.86285	24.44894	33.34384	39.09191	42.71371	47.85329
Velocity (km/s)	0.076893	0.097457	0.150401	0.189382	0.220396	0.294538
Initial Condition G TCM-6						
BT (km)	3.673865	5.160532	6.812096	7.9005	8.582514	10.15445
BR (km)	6.085254	6.960592	9.835865	14.59517	19.27059	25.58086
FPA (°)	43.53713	57.39262	84.88361	111.045	129.6185	149.8419
Altitude (km)	12.29727	15.34166	20.42841	23.52774	25.38805	28.06645
Position (km)	18.895	24.45896	33.34431	39.09192	42.71371	47.85329
Velocity (km/s)	0.076949	0.097497	0.150404	0.189382	0.220396	0.294538
Initial Condition M TCM-6						
BT (km)	3.673866	5.160533	6.812097	7.9005	8.582514	10.15445
BR (km)	6.085257	6.960595	9.835867	14.59517	19.27059	25.58086
FPA (°)	43.53713	57.39262	84.88361	111.045	129.6185	149.8419
Altitude (km)	12.29727	15.34166	20.42841	23.52774	25.38805	28.06645
Position (km)	18.895	24.45896	33.34431	39.09192	42.71371	47.85329
Velocity (km/s)	0.076949	0.097497	0.150404	0.189383	0.220396	0.294538

Figures 44-48 show the progression of the inertial position dispersions over the course of the trajectory when applying the translational process noise values of Table 70. The resulting dispersion at the target is shown in Table 71. Though the same ground update accuracy was used to produce the results captured in the figures, higher translational process noise values are shown to have a negative effect on both the navigation error and subsequently the trajectory dispersions.

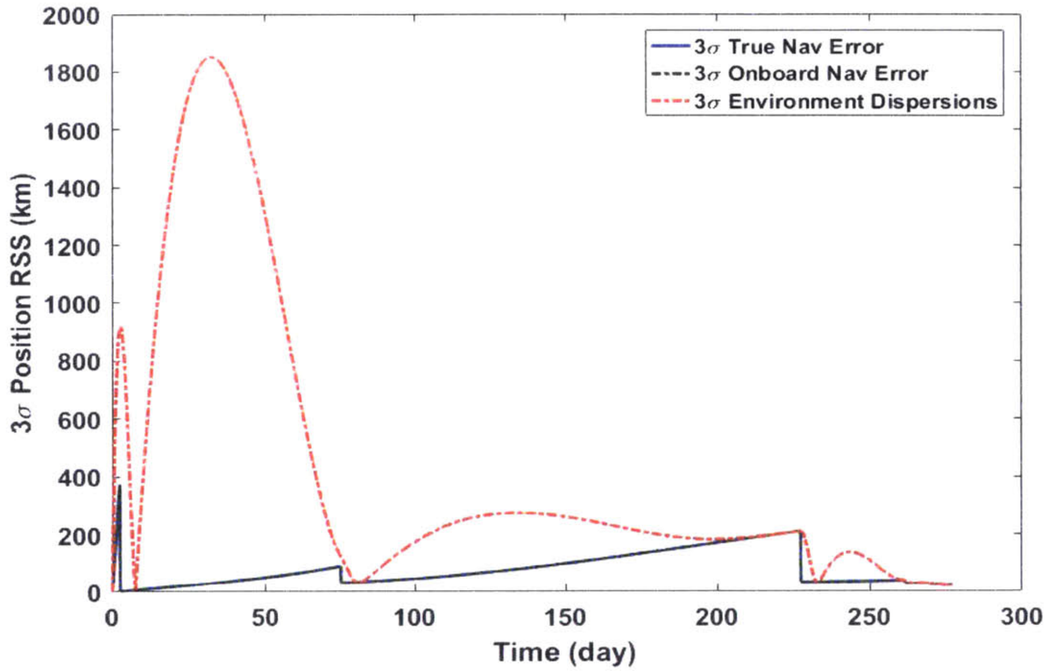

Figure 44: Inertial Position RSS with Long Guidance Segments, Initial Conditions A and 4.802E-14 Translational Process Noise

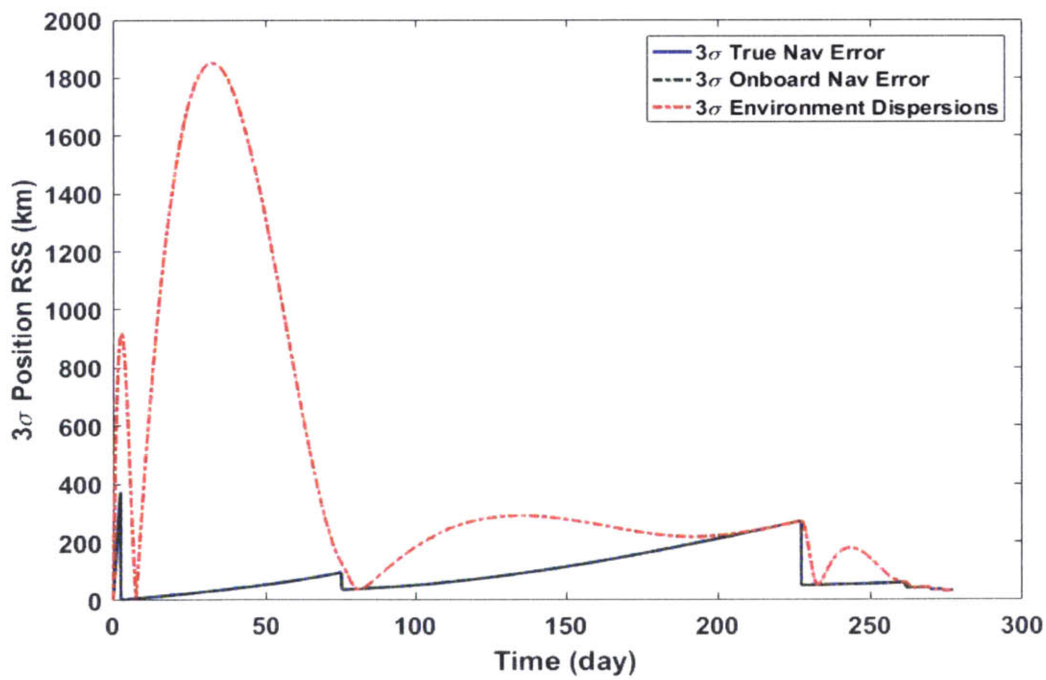

Figure 45: Inertial Position RSS with Long Guidance Segments and Initial Conditions A and 4.802E-13 Translational Process Noise

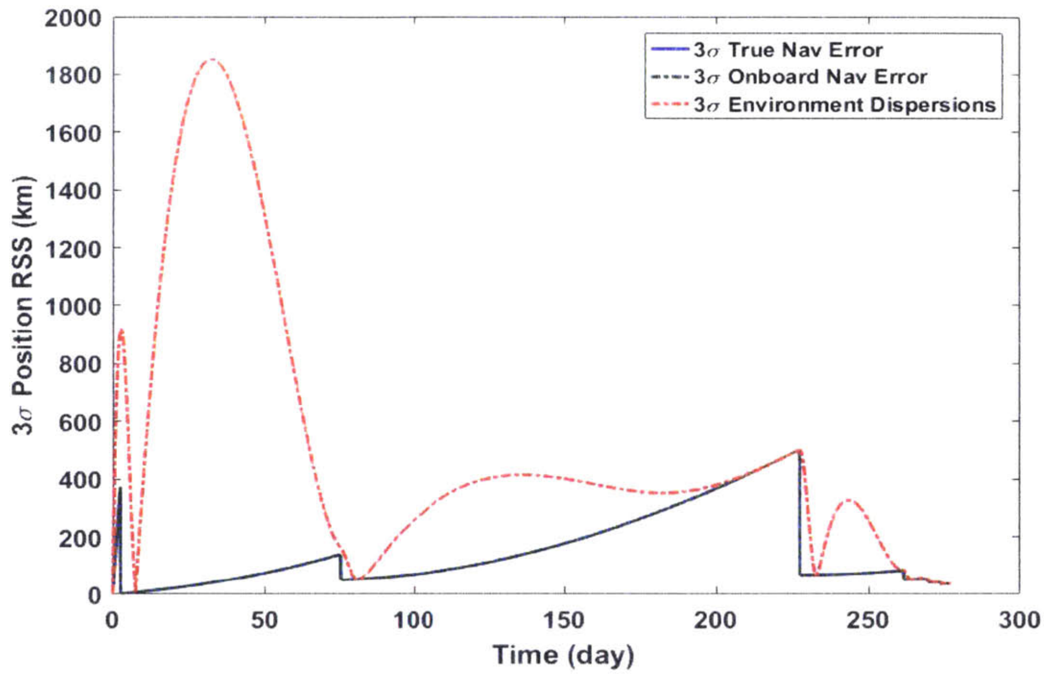

Figure 46: Inertial Position RSS with Long Guidance Segments and Initial Conditions A and 4.802E-12 Translational Process Noise

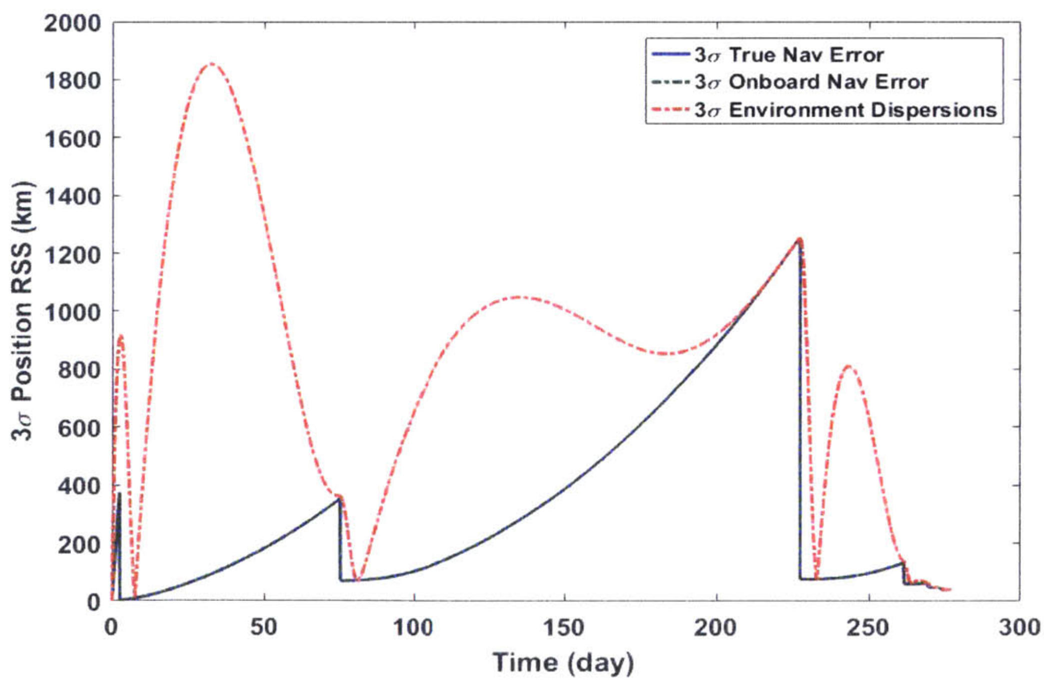

Figure 47: Inertial Position RSS with Long Guidance Segments and Initial Conditions A and 4.802E-11 Translational Process Noise

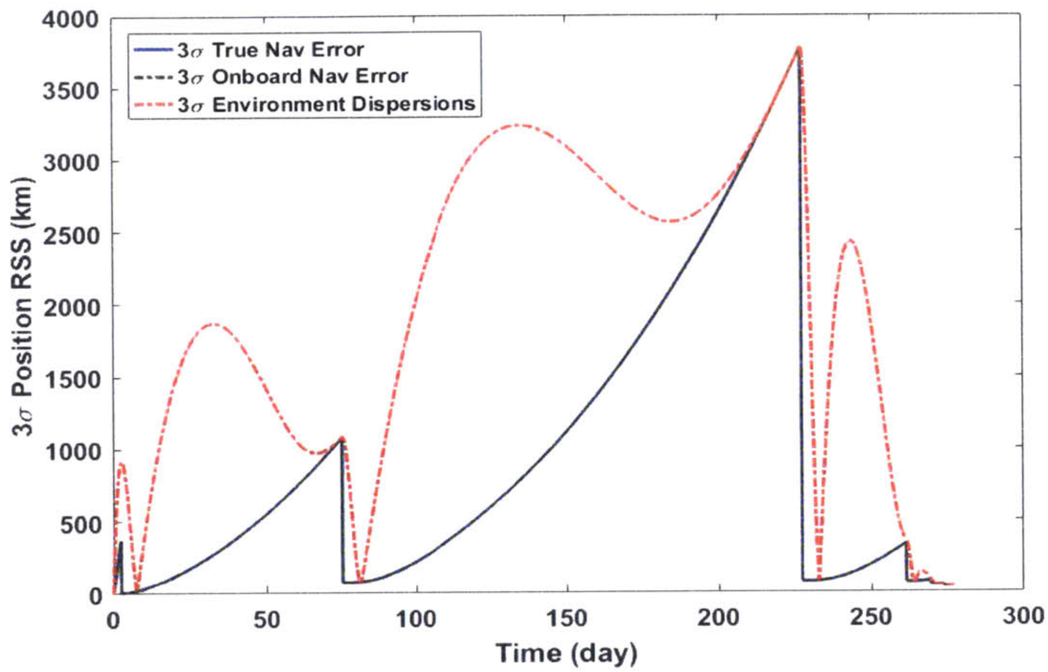

Figure 48: Inertial Position RSS with Long Guidance Segments and Initial Conditions A and 4.802E-10 Translational Process Noise

Figure 49 shows the B-Plane dispersions from the highest translational process noise value of initial conditions A. These results are compared to the B-Plane dispersions of Figure 36, which is the result of the same FTOA guidance segments, initial conditions, and ground update accuracy with the only difference being that the smallest translational process noise. The B-Plane dispersion requirement is met early in Figure 36 but not at all in Figure 49. Figure 50 offers a direct comparison of the effects on the B-Plane dispersions at TCM-None1 from increasing the translational process noise. After a TPN of 4.802E-13, even with the most frequent DSN tracking available the B-Plane dispersions are outside of the requirements.

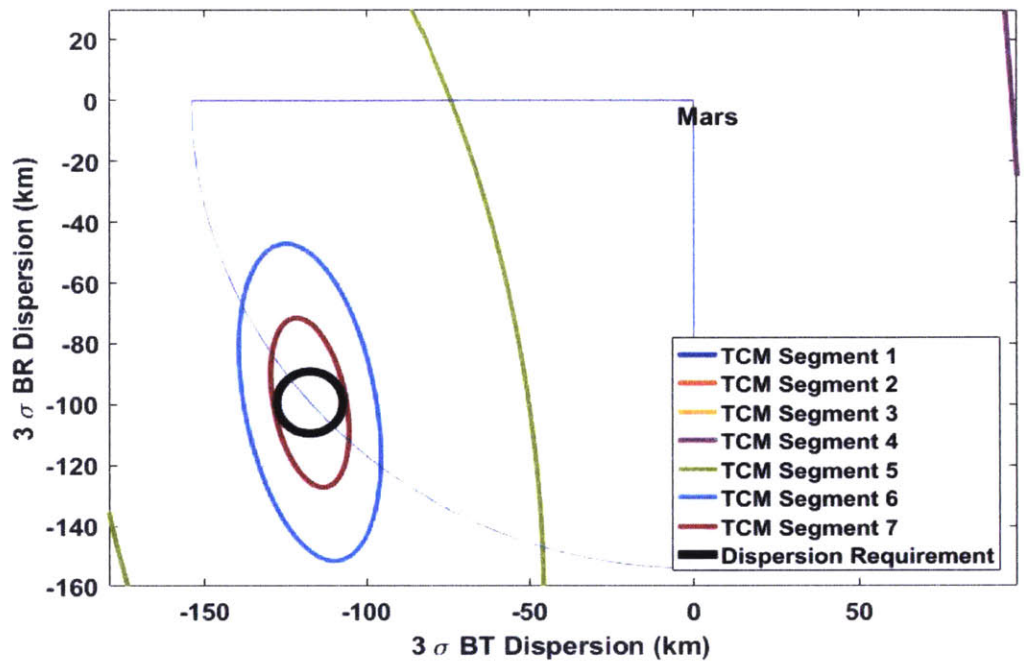

Figure 49: B-Plane Dispersions with Long Guidance Segments and Initial Conditions A and 4.802E-10 Translational Process Noise

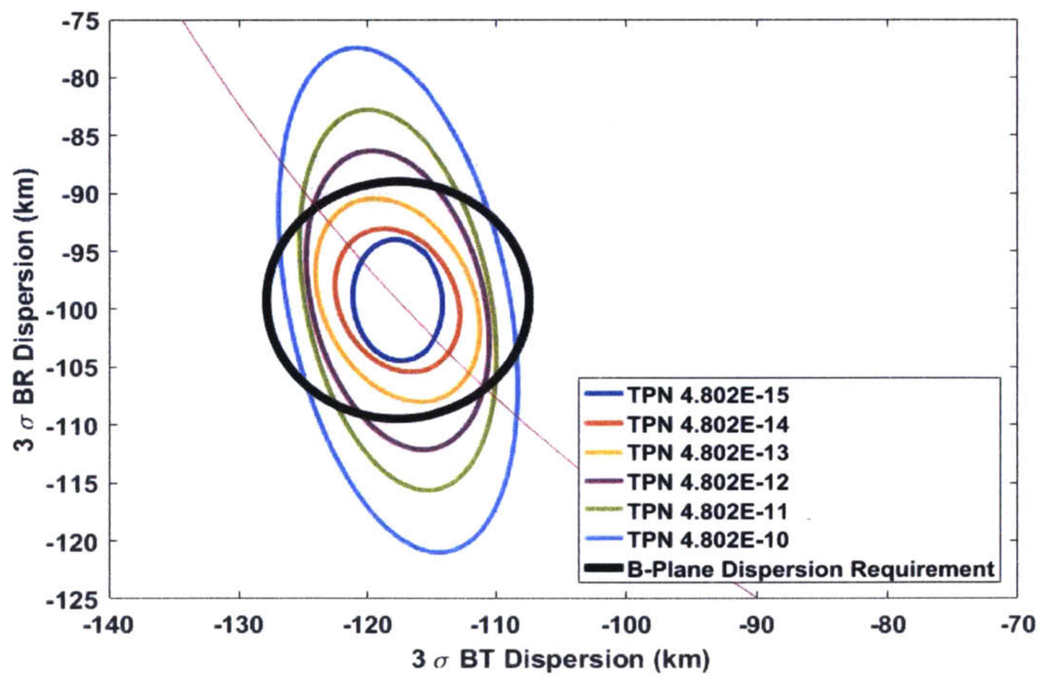

Figure 50: 3σ B-Plane Dispersions from Long Guidance Segments and Initial Conditions A Translational Process Noise Comparison

Table 72: TPN Effects for Standard Ground Navigation Update Frequency Supplemented with Optical Navigation

Parameter	TPN-1	TPN-2	TPN-3	TPN-4	TPN-5	TPN-6
Initial Condition A TCM-6						
BT (km)	0.950621	2.625417	4.574107	5.215984	5.607893	6.802576
BR (km)	5.328306	6.830222	9.344706	11.94028	15.0192	21.99244
FPA (°)	27.22309	49.45473	75.79582	86.08401	98.99038	130.0555
Altitude (km)	3.686041	8.17134	13.16264	15.03061	16.03561	17.87457
Position (km)	7.83386	14.75434	23.07277	26.62709	29.51042	35.59287
Velocity (km/s)	0.025538	0.045416	0.099253	0.127364	0.151013	0.220422
Initial Condition G TCM-6						
BT (km)	0.95063	2.625423	4.57411	5.215984	5.607893	6.802576
BR (km)	5.37638	6.835797	9.345034	11.94029	15.0192	21.99244
FPA (°)	27.41218	49.473	75.79648	86.08401	98.99038	130.0555
Altitude (km)	3.69847	8.172267	13.16271	15.03061	16.03561	17.87457
Position (km)	7.881229	14.75865	23.07299	26.62709	29.51042	35.59287
Velocity (km/s)	0.025786	0.045427	0.099253	0.127364	0.151013	0.220422
Initial Condition M TCM-6						
BT (km)	0.950631	2.625424	4.574111	5.215984	5.607893	6.802576
BR (km)	5.376313	6.835799	9.345036	11.94029	15.01921	21.99244
FPA (°)	27.41179	49.473	75.79648	86.08401	98.99038	130.0555
Altitude (km)	3.698396	8.172268	13.16271	15.03061	16.03561	17.87457
Position (km)	7.881064	14.75865	23.07299	26.62709	29.51042	35.59287
Velocity (m/s)	0.025786	0.045427	0.099253	0.127364	0.151013	0.220422

Figure 51, Figure 52, and Figure 53 show the dispersions through the trajectory for the initial condition A with the target dispersion accuracy detailed in Table 72 for the position dispersion, mapped FPA dispersion and the B-Plane dispersions when optical navigation is included and the highest translational process noise. Comparison of Figure 51 with Figure 48 shows that with the high translational process noise, optical navigation significantly improves the navigation error and the trajectory dispersions experienced in position. Figure 41 shows the results from all of the same conditions which produced Figure 51 except that in Figure 41 a much lower translational process noise was used. Figure 41 shows much better performance than Figure 51. This is especially the case during the middle of the cruise segment. Similarly, in Figure 52 the middle segment of the trajectory has much worse FPA dispersions than Figure 42 though the only difference is that Figure 52 was produced with the highest translational process noise and Figure 42 with the lowest. The individual B-Plane dispersions of Figure 53 are only slightly improved from the results in Figure 49 but still outside of the B-Plane dispersion requirements.

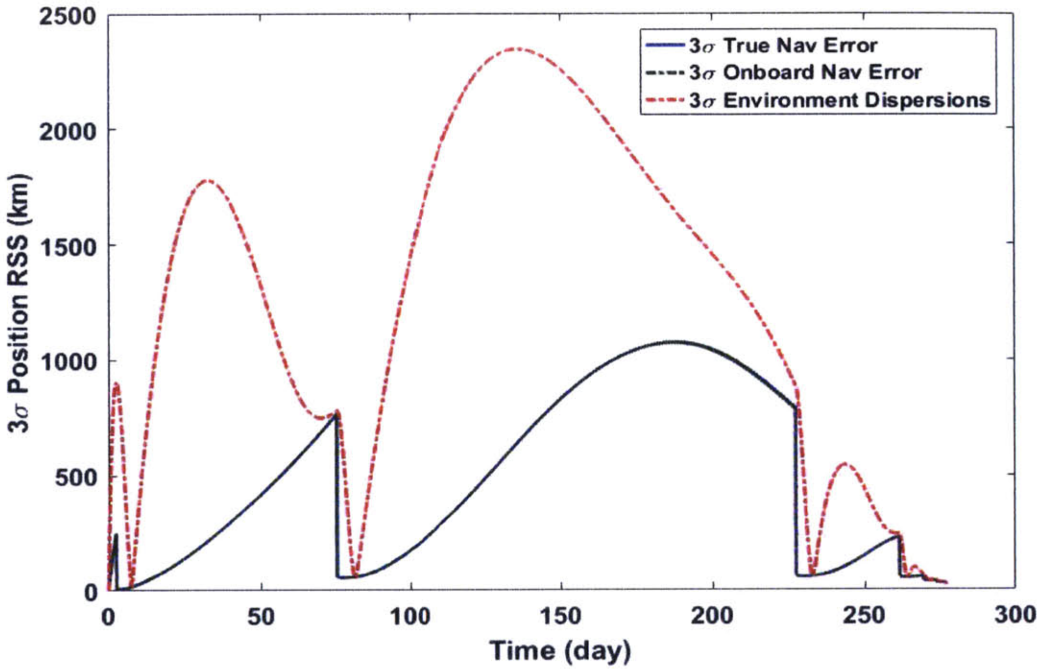

Figure 51: Inertial Position RSS with Long Guidance Segments, Optical Navigation, and Initial Conditions A and 4.802E-10 Translational Process Noise

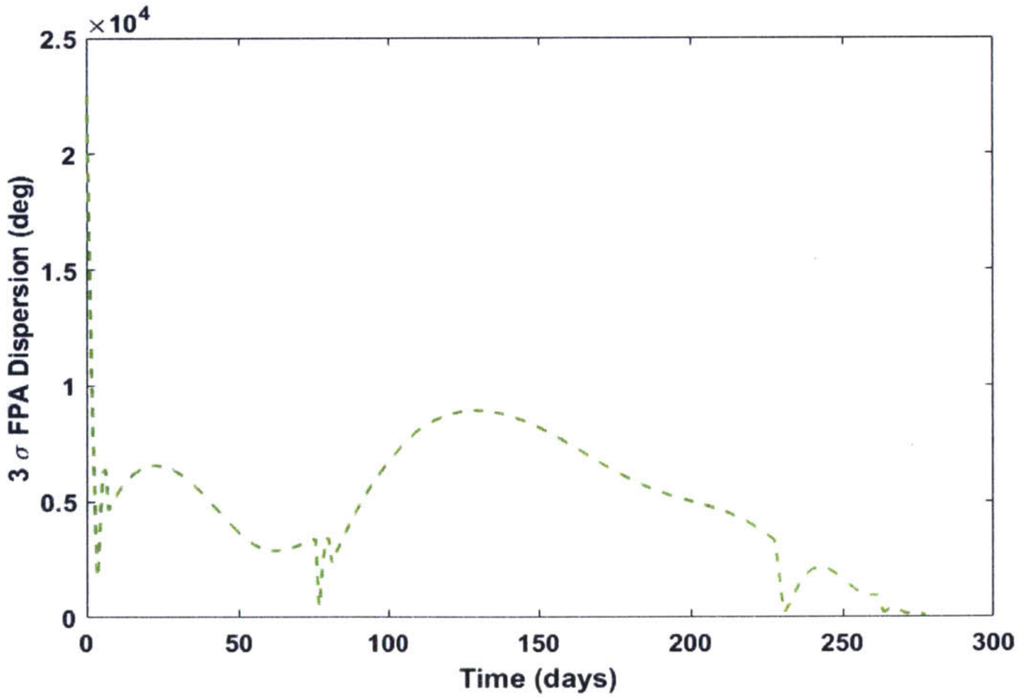

Figure 52: Mapped FPA Dispersions to Entry-Interface with Long Guidance Segments, Optical Navigation and Initial Conditions A and 4.802E-10 Translational Process Noise

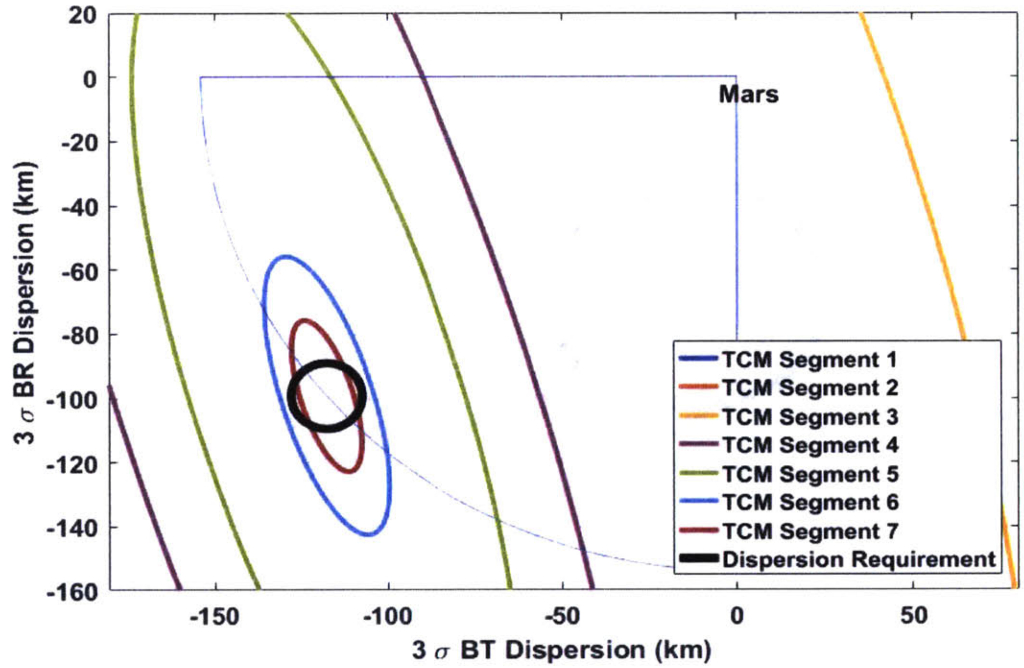

Figure 53: 3σ B-Plane Dispersions with Long Guidance Segments, Optical Navigation, and Initial Conditions A and 4.802E-10 Translational Process Noise

Figure 54 shows a direct comparison of the TPN effects on the B-Plane dispersions when optical navigation is included at TCM-None1. Compared to Figure 50, though some of the smaller TPN cases with optical navigation result in small B-Plane dispersions compared to ground updates only, the shape and orientation of the dispersion with optical navigation violate the B-Plane requirements at the same TPN 4.802E-13. Figure 55 shows the B-Plane dispersions, with and without optical navigation, for the highest and lowest TPN values at TCM-None1. Figure 55 makes it obvious that while including optical navigation at lower TPN values is noticeably beneficial, at higher TPN values optical navigation could cause the B-Plane dispersions to increase. This needs to be weighed against the improvements seen for other parameters of interest under the same conditions.

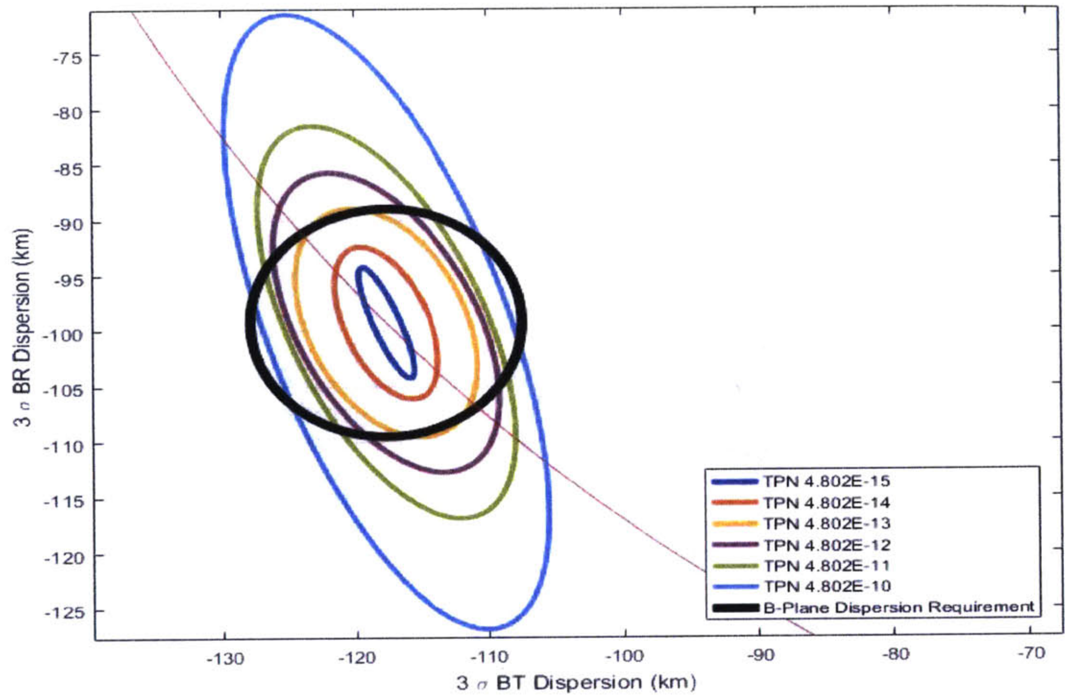

Figure 54: 3σ B-Plane Dispersions from Long Guidance Segments, Optical Navigation, Initial Conditions A Translational Process Noise Comparison

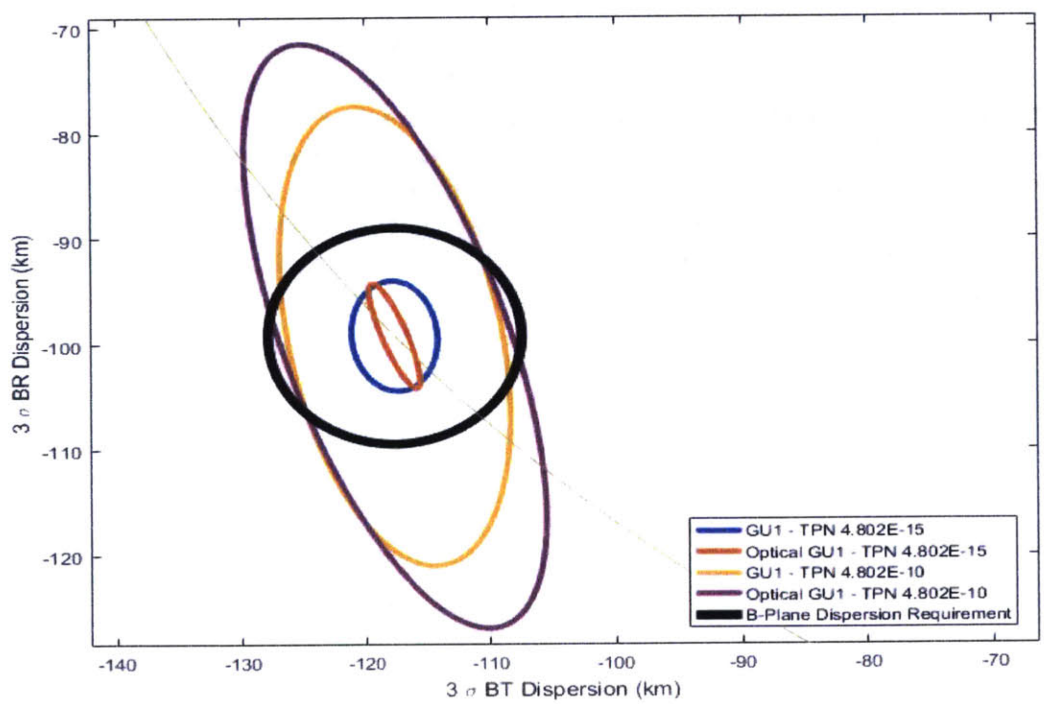

Figure 55: 3σ B-Plane Dispersions from Long Guidance Segments Initial Conditions A Worst and Best Case Translational Process Noise with and without Optical Navigation Comparison

Figures 56-59 compare the dispersion results for each of the parameters of interest with initial condition A and long FTOA guidance segments with and without optical navigation over the translational process noise. The X-axis of each of the figures are logarithmic. The figures show which of the parameters benefit to a greater degree than others with optical navigation included. Significantly, the target dispersion results for altitude are much better with optical navigation even at higher translational noise levels. The figures compare the results to the same prior mission results referenced in Table 50 and Table 51.

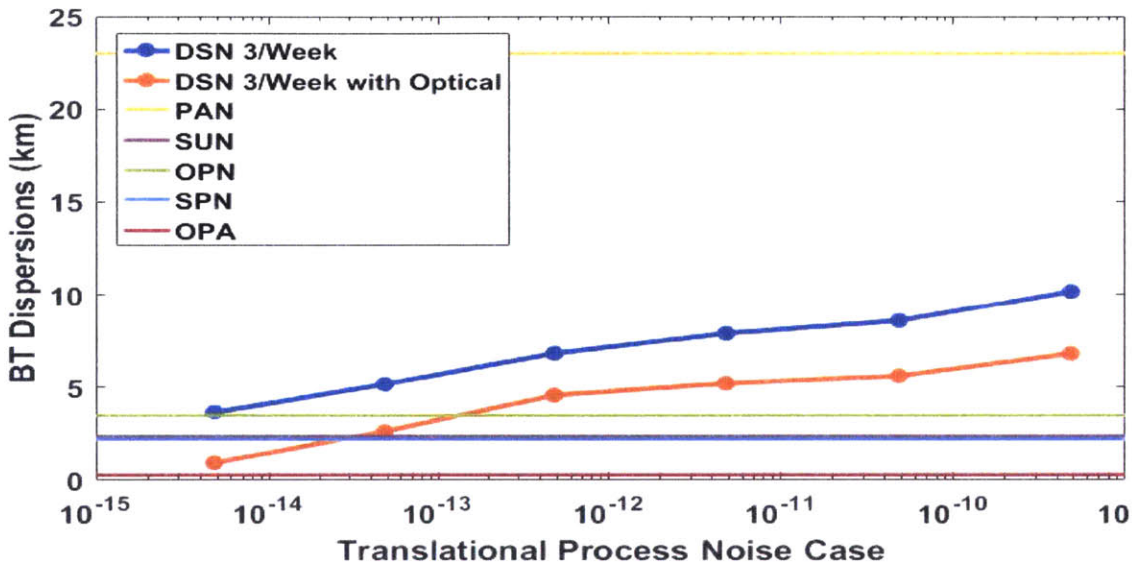

Figure 56: Translational Process Noise Effect on BT Dispersions with Long FTOA Guidance Segments and Initial Conditions A

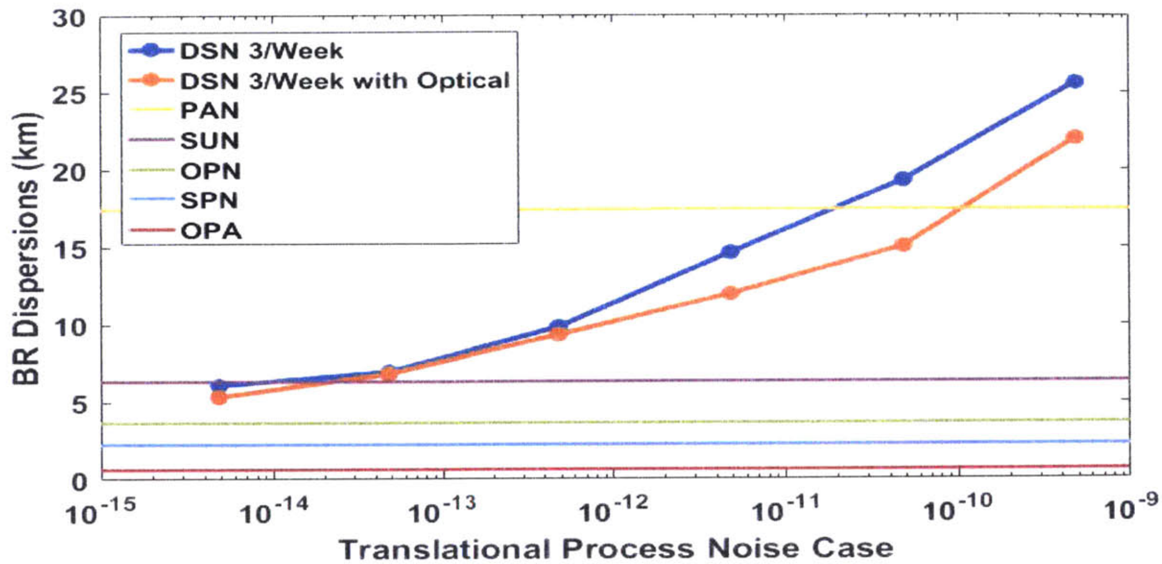

Figure 57: Translational Process Noise Effect on BR Dispersions with Long FTOA Guidance Segments and Initial Conditions A

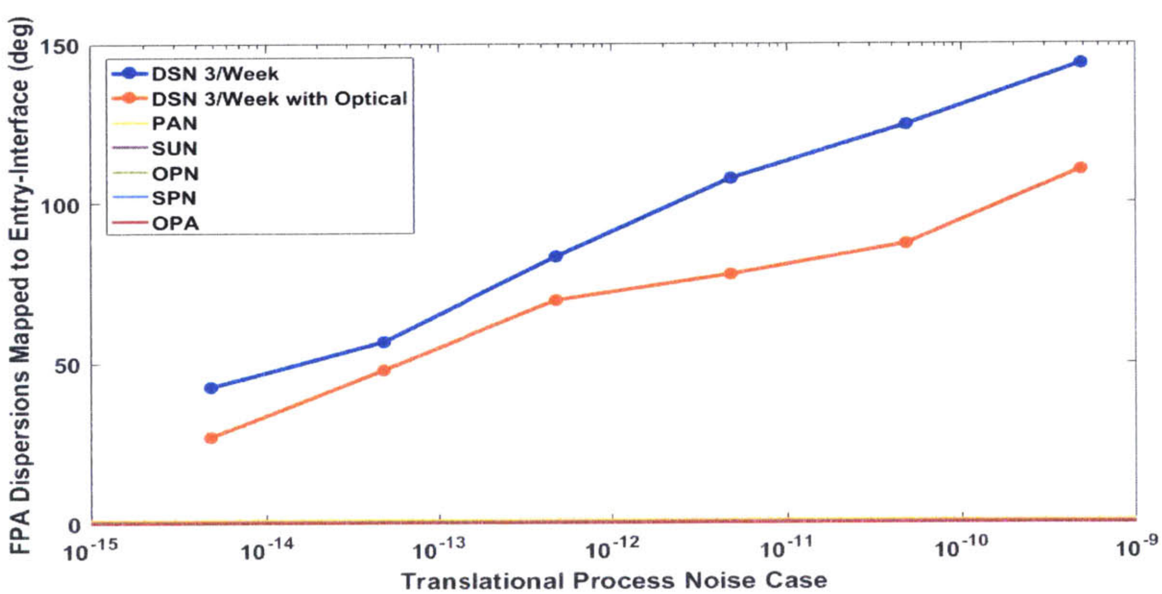

Figure 58: Translational Process Noise Effect on FPA Dispersions Mapped with Entry-Interface with Long FTOA Guidance Segments and Initial Conditions A

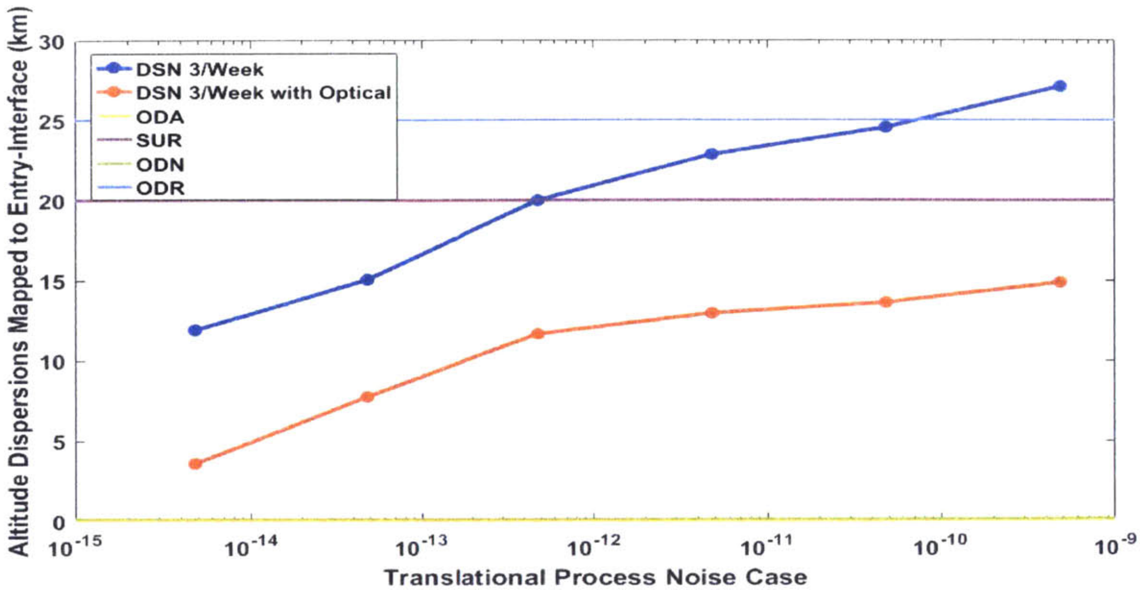

Figure 59: Translational Process Noise Effect on Altitude Dispersions Mapped to Entry-Interface with Long FTOA Guidance Segments and Initial Conditions A

14.3 Mission Suggestions

This section points to the translational process noise in the thrusting model as the driver to the FPA dispersions. The prior sections, which explored different ground update accuracy levels, different lengths of guidance segments, and different initial conditions showed minimal changes for FPA between them. While the thrusting model accuracy does affect the other parameters of interest, it has no more of an affect than the other variables examined. For any one TPN value, the relationships between the initial conditions of A, G, and M hold where there is a noticeable and significant difference towards the beginning of the trajectory which decreases by the end of the trajectory. This is shown in Tables 65-72. All of the parameters of interest experience increase in dispersions as the TPN value increases. The use of optical navigation allows the Odyssey dispersion requirement to be met even at the highest translational process noise. Without optical navigation, even the highest ground update accuracy cannot produce desirable altitude dispersions with midrange translational process noise. The FPA dispersions increases more rapidly than any other parameter as the translational process noise is increased. At no point is the FPA dispersion acceptable to attempt entry interface.

15 Mission Planner Example

Sections 8- 14 were focused on providing details which could be used in the preliminary design of the new deep space low-thrust CubeSat platform. An important aspect of each section was the exploration of different levels of ground update accuracy. These results can be used regardless of whether AGNC capabilities are utilized. Without AGNC, the ground update points represent the position and velocity accuracy the ground orbit determination team used to define maneuver sequences to uplink to the craft. With AGNC, the ground update information and accuracy can be used to determine guidance maneuver over the segments the program preset for consideration. The optical navigation demonstrations in each section are only applicable to AGNC scenarios as the measurements are used to update the navigation covariance immediately and are propagated in-between measurements onboard. Again, these measurements occur exclusively at the preset rate and to the preset targets. The results with optical navigation can be used by a program to decide the amount to increase autonomy and lessen the responsibilities of the ground team as well as the amount of DSN tracking needed to meet desirable target corridors. These results can all be used at the start of a program to scope the system guidance and navigation plans to best suit the mission needs.

This section is different from those addressing ground-based and AGNC capabilities because it moves beyond standard DSN and ground team interactions, beyond autonomy, and into intelligent programs. The difference between autonomy and intelligence was defined in Section 4.3 as well as examples highlighting the difference between the focus and purpose of each. LinCov as a basic OMP can calculate the effects of different guidance and navigation plans and then set the commands onboard the vehicle for the AGNC programs to apply. As such, the OMP can only calculate different onboard navigation and guidance options for the conditions experienced based on its understanding of the system characteristics. It is assumed that the LinCov OMP would be aware of when a ground update is expected as well as its realizable accuracy. The LinCov OMP would also be aware of the nominal trajectory so that a variety of guidance options could be explored. The OMP would not be able to consider solutions with more frequent or more accurate ground updates as this is not an onboard feature. Also, the OMP would not be able to consider guidance options for trajectory segments smaller than supplied to represent the nominal trajectory.

The OMP program would need to be supplied top-level mission goals to choose between the different guidance and navigation scenarios assessed by a LinCov function. These goals can include reaching the target within certain dispersion bounds. The dispersion bounds could be physical, but acceptable bounds on the time of arrival can also be set. A standard mission goal is the minimization of fuel consumed which is typically achieved with VTOA guidance at the cost of increased arrival time dispersions. In addition to mission goals at the target, there could also be goals with respect to different segments of the cruise. The high-level goals would be mission dependent, but the ability of the LinCov OMP to calculate a swath of acceptable guidance and navigation solutions is only dependent on the available processing capability.

To replicate an onboard mission planner, different guidance options are compared for particular ground update scenarios with the same initial conditions. Several potential mission goals are used as an example of the decision making process. The first mission goal would be to meet the altitude dispersion bounds of a prior orbiter mission at the target. Should more than one scenario examined fall within the same range of altitude dispersion accuracy, secondary mission goals would then be considered. The secondary mission goal here is that the difference between the position trajectory dispersion and navigation error at the 200-day mark to be less than 200 km. If needed, the third mission goal would be that the altitude dispersions mapped to entry-interface be robust to the loss of ground update 2 which nominally occurs 75 days into the heliocentric trajectory.

15.1 Initial Conditions

The optical navigation system accuracy is defined in Table 43 for each of the cases examined. The ground update schedule is shown in Table 42, but the accuracy of the ground updates depends on the case examined. The ground update cases were tracked in Table 49. The initial dispersions, navigation error, and translational process noise are detailed in Table 44.

15.2 Mission Planner Options

The navigation options for this onboard mission planner example includes whether or not to provide daily optical sightings to supplement the expected ground updates. The guidance options examined involve short guidance segments of two weeks with FTOA or VTOA, or long FTOA guidance segments coordinated with the ground updates. The prior mission accuracy reference codes are maintained in Table 50 and Table 51 with the accuracy values in Tables 23-26.

15.3 Results

Table 73 compares the results of the three guidance options and two navigation options for ground updates from DSN measurements 3/week.

Table 73: GU1 3σ Dispersion Comparison

Parameter	DS1 FTOA		DS1 VTOA		Phoenix FTOA	
Ground Only						
BT (km)	OPN	3.45611	OPN	3.60262	PAN	3.65777
BR (km)	SUN	5.24995	PAN	6.46993	SUR	6.07677
FPA (°)		42.5978		42.5953		41.8270
Altitude (km)	SUR	11.9198	SUR	13.4612	SUR	12.2897
Position (km)		18.5828		19.5531		18.8629
Velocity (km/s)		0.02059		0.03736		0.07689
With Daily Optical						
BT (km)	SPN	0.95012	SPN	1.00752	SPN	0.95062
BR (km)	PAN	7.87738	PAN	8.02336	SUR	5.32831
FPA (°)		39.3928		39.0265		27.2231
Altitude (km)	ODN	4.61697	ODN	4.97329	ODN	3.68604
Position (km)		10.9512		11.0381		7.83386
Velocity (km/s)		0.05352		0.04503		0.02554

Should altitude dispersions to meet the Surveyor orbiter requirements be desired, optical sightings would not be needed to meet the target conditions. Should a more accurate altitude dispersion corridor be desired, optical sightings could be added. Based on the LinCov results shown in Table 73 the OMP would move to examine additional results to compare them to the secondary and if needed final mission goals. Such an examination is shown for GU5. Table 74, shows for the results with 2/month DSN measurement ground update accuracies. For GU4 the inclusion of optical navigation is required to meet the altitude dispersions of any prior mission. Once optical navigation is included, because each case meets the same prior mission accuracies, additional mission goals would need to be considered to finalize GNC plans.

Table 74: GU4 3σ Dispersion Comparison

Parameter	DS1 FTOA		DS1 VTOA		Phoenix FTOA	
Ground Only						
BT (km)		30.8499		32.6258		32.3239
BR (km)		50.6918		62.5318		59.6284
FPA (°)		394.484		394.471		405.236
Altitude (km)		112.159		128.200		116.269
Position (km)		172.732		182.987		175.808
Velocity (km/s)		0.19826		0.37068		0.49251
With Daily Optical						
BT (km)	SPN	0.95539	SPN	1.01542	SPN	0.96611
BR (km)	PAN	12.2604	PAN	12.5361	PAN	12.4305
FPA (°)		56.6233		55.2785		59.7341
Altitude (km)	ODN	6.14029	ODN	6.62870	ODN	6.62359
Position (km)		15.5039		15.4783		16.7235
Velocity (km/s)		0.11611		0.09908		0.02273

Table 75 provides the dispersion results at the target for GU5, with 1/Month DSN measurement for the ground updates. Figure 60-65 show the position dispersion results throughout the trajectory with the same conditions of Table 75.

Table 75: GU5 3σ Dispersion Comparison

Parameter	DS1 FTOA		DS1 VTOA		Phoenix FTOA	
Ground Only						
BT (km)		61.6032		65.1609		64.5391
BR (km)		101.351		124.992		119.233
FPA (°)		788.299		788.272		809.814
Altitude (km)		224.135		256.201		232.357
Position (km)		345.117		365.62		351.270
Velocity (km/s)		0.39617		0.74089		0.98417
With Daily Optical						
BT (km)	SPN	0.95555	SPN	1.01561	SPN	0.96622
BR (km)	PAN	12.5507	PAN	12.8385	PAN	12.6590
FPA (°)		57.7062		56.2695		61.0289
Altitude (km)	ODN	6.23920	ODN	6.73742	ODN	6.7479
Position (km)		15.7882		15.7516		17.0793
Velocity (km/s)		0.12091		0.10322		0.01869

When only focusing on the dispersions for any at the target, the differences between the alternate guidance options with the same navigation considerations do not seem significant. Position dispersions over the course of the trajectory are the most intuitive to understand out of the parameters tracked. When compared over the course of the interplanetary cruise, it appears that the short VTOA guidance segments with optical navigation, shown in Figure 64, is the best case for position dispersions and should be selected. While this is the case for position dispersions, other mission goals could lead to the selection of a different guidance and navigation combination.

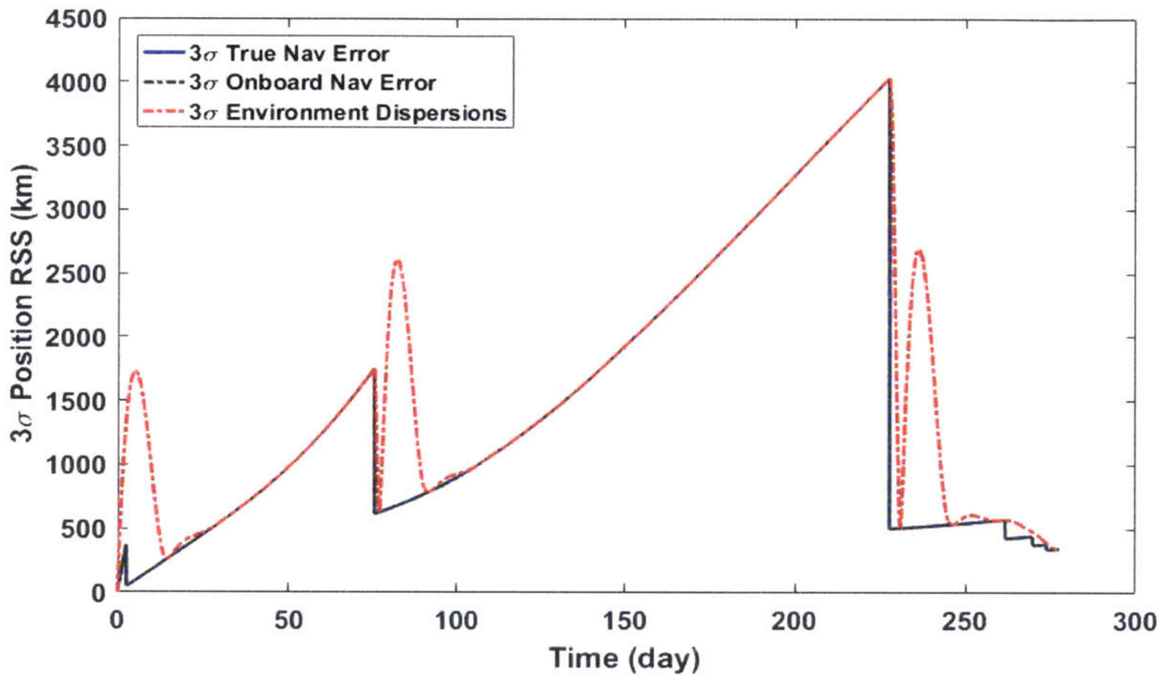

Figure 60: Inertial Position RSS with Short FTOA Guidance Segments with Ground Update Accuracy of DSN Accuracy of 1/Month

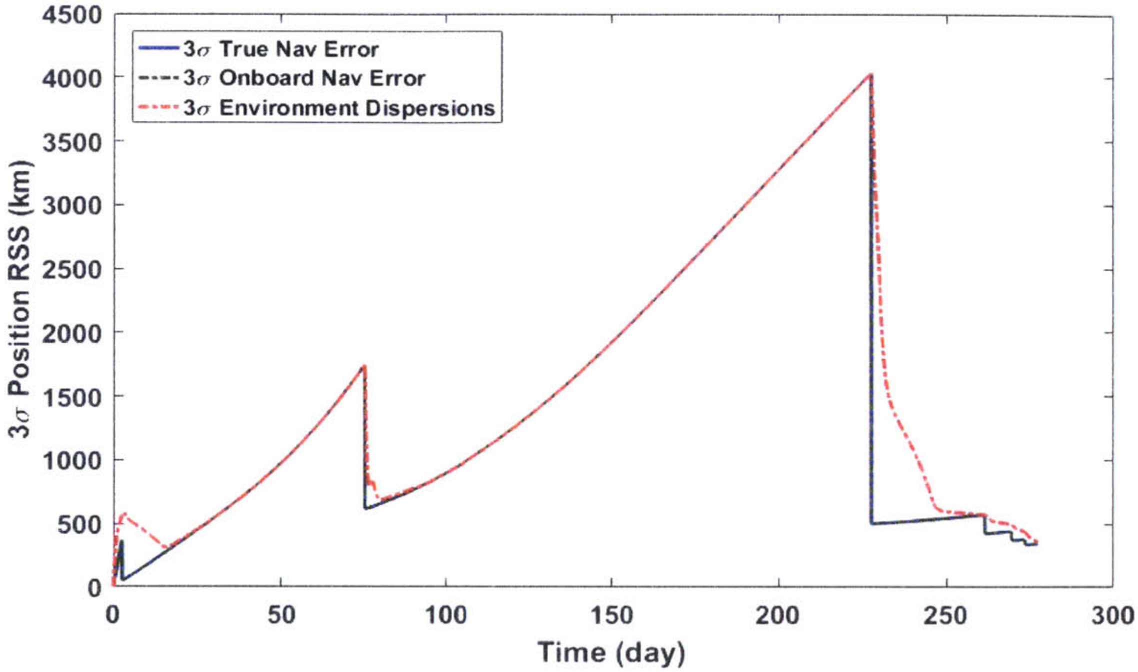

Figure 61: Inertial Position RSS with Short VTOA Guidance Segments with Ground Update Accuracy of DSN Accuracy of 1/Month

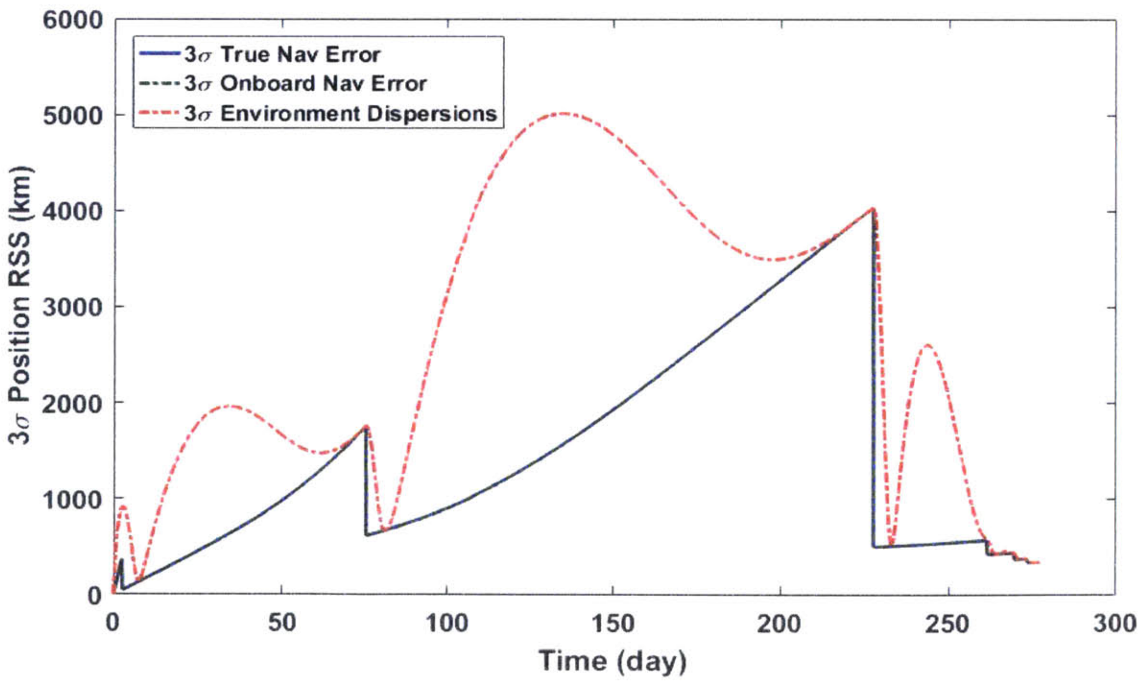

Figure 62: Inertial Position RSS with Long FTOA Guidance Segments with Ground Update Accuracy of DSN Accuracy of 1/Month

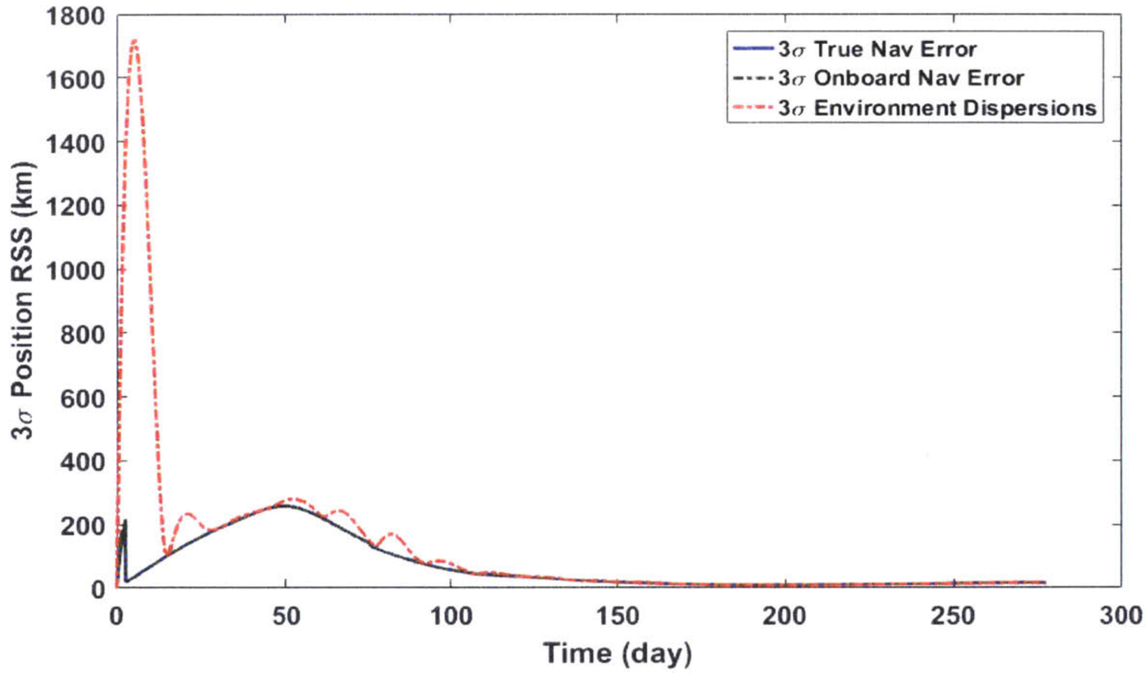

Figure 63: Inertial Position RSS with Short FTOA Guidance Segments with Ground Update Accuracy of DSN Accuracy of 1/Month and Optical Navigation

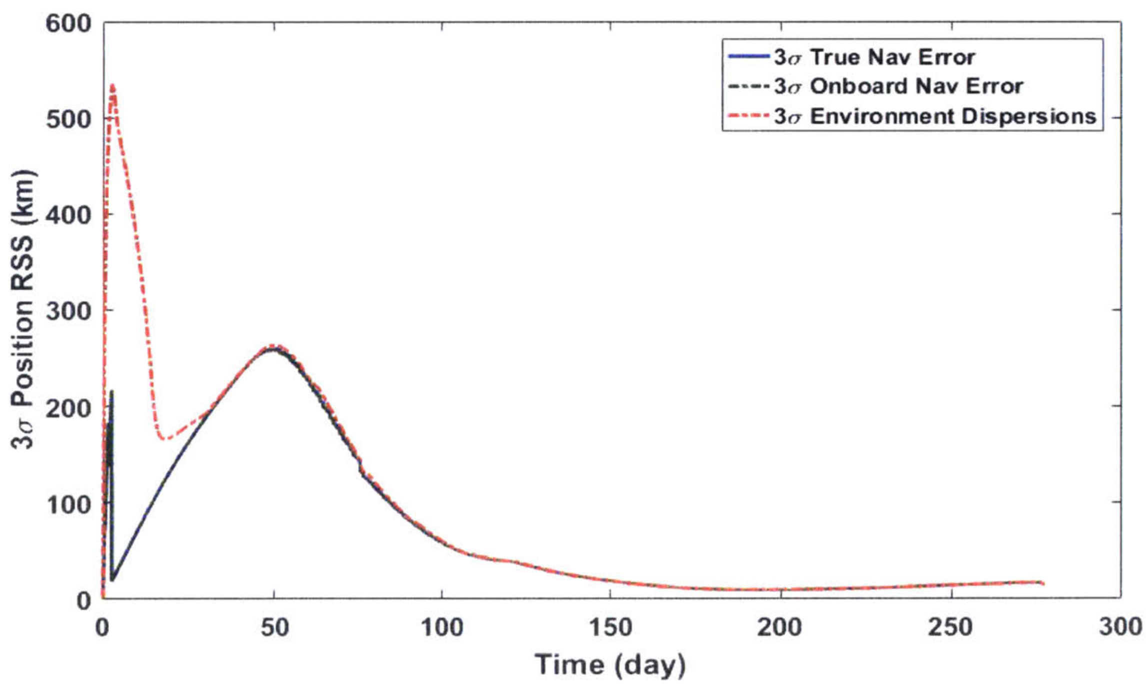

Figure 64: Inertial Position RSS with Short VTOA Guidance Segments with Ground Update Accuracy of DSN Accuracy of 1/Month and Optical Navigation

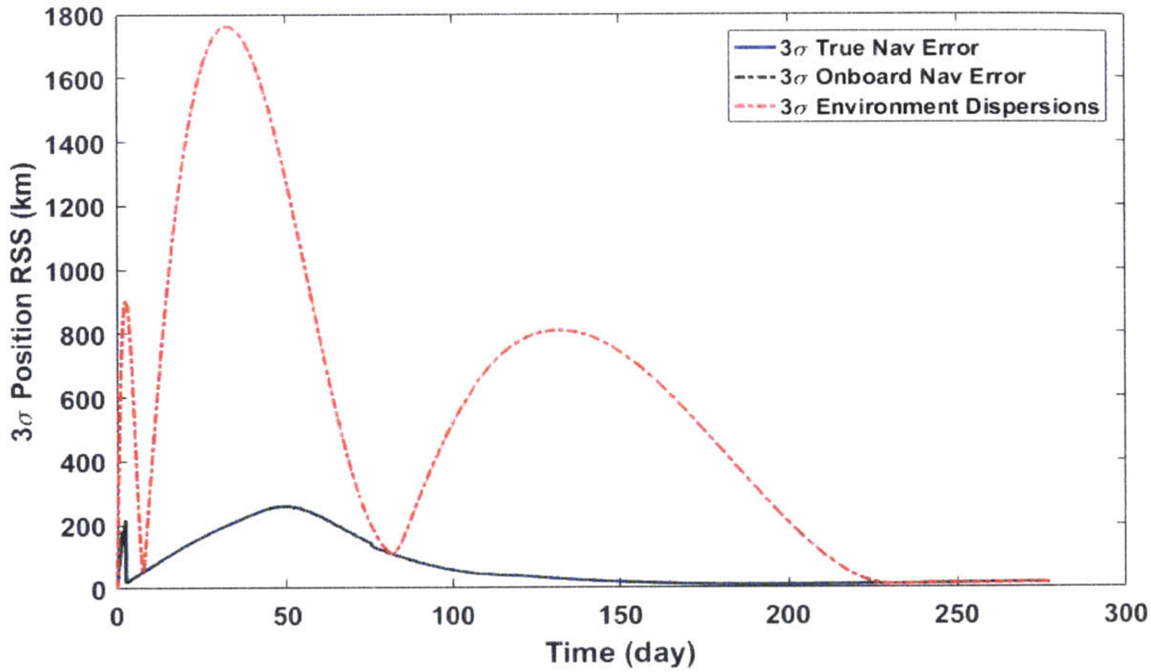

Figure 65: Inertial Position RSS with Long FTOA Guidance Segments with Ground Update Accuracy of DSN Accuracy of 1/Month and Optical Navigation

Table 75 target results reduce the viable GNC options to those with optical daily cases to meet the primary mission goal - of having the altitude dispersions of a prior orbiter mission at the target. Figure 65 removes Phoenix FTOA with optical navigation as an option due to the secondary mission goal of less than 200km difference between the trajectory dispersion and navigation error at the 200-day mission mark. This reduces the choices further to DS1 FTOA optical and DS1 VTOA optical. Figure 66 is used to compare the two options for the third mission goal of altitude dispersions mapped to entry-interface robust to the loss of ground update 2. The VTOA results between 40 – 110 days into the heliocentric trajectory are worse than the FTOA results for altitude dispersions mapped to entry-interface. After this point the difference in the results range from tens of meters to hundreds of meters. The loss of ground update 2 is likely to have a larger impact if VTOA is used than if FTOA is used.

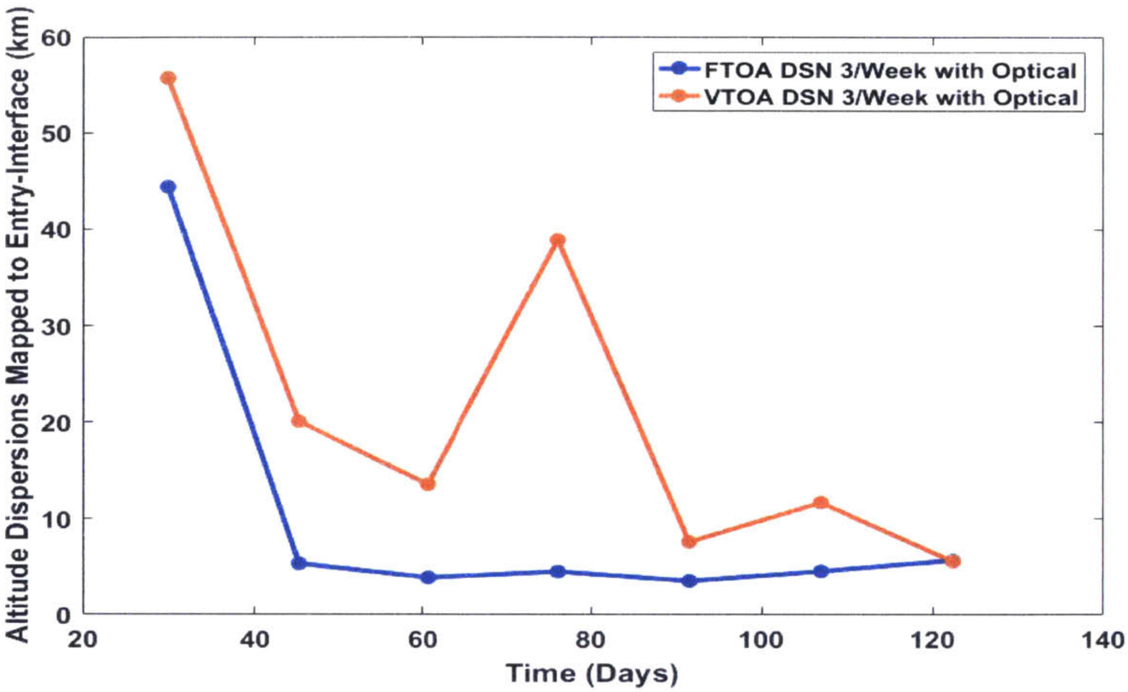

Figure 66: Altitude Dispersions Mapped to Entry-Interface at Ground Update 2

Based on the LinCov results the onboard mission planner described would opt to use the short guidance segments coupled with optical navigation as it meets the most mission goals out of the guidance and navigation scenarios examined for GU5 – ground update accuracy based on DSN tracking 1/month.

Table 76 shows the LinCov results of the three guidance options when the approach ground updates are extremely accurate. If only an orbit insertion is desired, DS1 FTOA with no optical navigation would be selected by the Onboard Mission Planner. Though the dispersion level could be decreased for this parameter if optical navigation was included, as the mission goal was satisfied it would not be needed. If the mission goal involved producing the lowest FPA dispersions at entry-interface possible, DS1 VTOA with optical navigation would be selected. LinCov provides the information needed by the Onboard Mission Planner to select the guidance and navigation options based on the ability of the intelligent system to account for the priority levels of different mission goals of which it is aware.

Table 76: GU8 3σ Dispersion Comparison

Parameter	DS1 FTOA		DS1 VTOA		Phoenix FTOA	
Ground Only						
BT (km)	PAN	11.3524	OPA	0.03911	PAN	9.77383
BR (km)		27.2165		61.3038		21.9892
FPA (°)		14.4731		26.8861		65.5347
Altitude (km)	ODN	4.12348		139.273	SUR	18.8674
Position (km)		4.25951		135.474		27.0863
Velocity (km/s)		0.25405		0.8292		0.33847
With Daily Optical						
BT (km)	OPA	0.17251	OPA	0.01000	OPA	0.14534
BR (km)	SPN	2.15769	SPN	1.27444	SPN	1.86948
FPA (°)	PAN	0.77883	PAN	0.59207		3.43511
Altitude (km)	ODN	0.08904	ODN	2.88532	ODN	0.39854
Position (km)		0.16704		2.807		1.01824
Velocity (km/s)		0.00943		0.01718		0.01979

Table 77: GU9 3σ Dispersion Comparison

Parameter	DS1 FTOA		DS1 VTOA		Phoenix FTOA	
Ground Only						
BT (km)	OPN	1.74712	OPA	0.22694	SPN	1.52284
BR (km)	SUN	4.11541	PAN	9.25219	SUR	3.36792
FPA (°)		4.02953		5.27615		10.5703
Altitude (km)	ODN	0.89295	ODR	20.9899	ODN	2.92664
Position (km)		1.26423		20.4367		4.26434
Velocity (km/s)		0.03844		0.12491		0.05146
With Daily Optical						
BT (km)	OPA	0.20779	OPA	0.14838	OPA	0.22177
BR (km)	SPN	1.87252	SPN	1.21910	SPN	1.66030
FPA (°)		2.46320		2.42609		3.92858
Altitude (km)	ODN	0.43099	ODN	2.62550	ODN	0.58062
Position (km)		0.77284		2.63251		1.21254
Velocity (km/s)		0.00827		0.01543		0.01801

Table 78: GU10 3σ Dispersion Comparison

Parameter	DS1 FTOA		DS1 VTOA		Phoenix FTOA	
Ground Only						
BT (km)	PAN	5.69018	OPA	0.22770	PAN	4.90468
BR (km)	PAN	13.6187		30.6801	PAN	11.0159
FPA (°)		7.99417		13.8714		33.0025
Altitude (km)	ODN	2.16057		69.6917	SUR	9.46597
Position (km)		2.39332		67.7963		13.6087
Velocity (km/s)		0.12716		0.41491		0.16949
With Daily Optical						
BT (km)	OPA	0.20793	OPA	0.14839	OPA	0.22187
BR (km)	SPN	2.15786	SPN	1.33111	SPN	1.90981
FPA (°)		2.49003		2.43735		4.26981
Altitude (km)	ODN	0.43274	ODN	2.89028	ODN	0.60872
Position (km)		0.77662		2.88306		1.30941
Velocity (km/s)		0.00943		0.01702		0.02042

With a LinCov-based OMP, the results along the cruise and at the target can be computed, compared, and analyzed against numerous combinations of mission goals. The comparison and subsequent solution selection is what makes an onboard mission planner an intelligent program. The guidance and navigation programs which perform the desired tasks set without further intervention met the criteria for autonomous systems. However, the navigation filtering and the guidance solutions do not deliberate on the merits of the actions requested. That lack of deliberation by the AGNC system makes use of a LinCov OMP as the only onboard intelligent program addressed as part of this research.

Simple mission goals were showcased in part because of the state of the industry when it comes to the use of intelligent systems in space. Another reason is that the current example is focused on the CubeSat platform. As detailed earlier, because it is unlikely a deep space CubeSat would have DSN support to the degree that prior interplanetary missions experienced. A LinCov OMP system on an interplanetary CubeSat is not just in keeping with the spirit of the class to take on the additional risks to offer lessons learned to the broader space community concerning a new technology. Minimally, to the degree shown here, the simple AGNC & OMP combination offers additional robustness if used as a backup system should a program miss an originally scheduled opportunity to interface with a spacecraft. Ideally, the use of such a LinCov OMP as a primary system would be planned from the start of a program to reduce the cost of extended DSN use compared to traditional missions.

16 Cost Estimates for the Proposed DSN Tracking Cases

The DSN aperture fee, Equation (1), is based on the number of contacts per week. This means that when calculating the aperture fee for hour of use the minimum value which can be selected for that parameter is 1. When a tracking segment is only desired on a monthly basis is reflected in the hours of use the aperture fee is applied. Table 79 captures the aperture fee for the DSN tracking passes of Table 47 assuming 8 hour segments.

Table 79: Aperture Fee of the DSN Tracking of Interest

Tracks	70-m Antenna	34-m Antenna
3 Passes/Week	$5073.60	$1268.40
2 Passes/Week	$4650.80	$1162.70
1 Pass/Week	$4228.00	$1057.00
2 Passes/Month	$4228.00	$1057.00
1 Pass/Month	$4228.00	$1057.00

The accuracies represented in Table 47 are generalized to the amount of passes used to form the ground orbit determination solution and are not antenna size specific. How the distance to the target, overall geometry between Earth and the target spacecraft, resources claimed by other missions, reliability of operations, or any Doppler or range measurement accuracies affect the choice of antenna used are not examined at this time. It is known that the 70-m antennas are not required throughout average mission operations but are typically used for high profile missions during important events.

Because DSN use must be negotiated based on the mission program desires and the availability of resources Table 80 lists the price of both the 70-m and 34-m antennas by the weeks of use for different frequency of passes, assuming 8 hour passes.

Table 80: DSN Antenna Cost by Weeks of Use

Tracking Frequency	70-m Antenna	34-m Antenna
10 Weeks of Use (25% of Examined Mission Trajectory)		
3 Passes/Week	$1,217,664.00	$304,416.00
2 Passes/Week	$744,128.00	$186,032.00
1 Pass/Week	$338,240.00	$84,560.00
2 Passes/Month	$169,120.00	$42,280.00
1 Pass/Month	$84,560.00	$21,140.00
20 Weeks of Use (50% of Examined Mission Trajectory)		
3 Passes/Week	$2,435,328.00	$608,832.00
2 Passes/Week	$1,488,256.00	$372,064.00
1 Pass/Week	$676,480.00	$169,120.00
2 Passes/Month	$338,240.00	$84,560.00
1 Pass/Month	$169,120.00	$42,280.00
30 Weeks of Use (75% of Examined Mission Trajectory)		
3 Passes/Week	$3,652,992.00	$913,248.00
2 Passes/Week	$2,232,384.00	$558,096.00
1 Pass/Week	$1,014,720.00	$253,680.00
2 Passes/Month	$507,360.00	$126,840.00
1 Pass/Month	$253,680.00	$63,420.00
40 Weeks of Use (100% of Examined Mission Trajectory)		
3 Passes/Week	$4,870,656.00	$1,217,664.00
2 Passes/Week	$2,976,512.00	$744,128.00
1 Pass/Week	$1,352,960.00	$338,240.00
2 Passes/Month	$676,480.00	$169,120.00
1 Pass/Month	$338,240.00	$84,560.00

The trajectory from the Earth's SOI to the Mars' target point of interest takes nearly 40 weeks. Table 80 shows that the most expensive antenna use cost as $4,870,656.00 for 3 passes/week with the 70-m antenna for 8 hours and the least expensive as $84,560.00 for 1 pass/month with the 34-m antenna for the entire 40 weeks. While there are a multitude of potential combinations for both the antenna used and the amount of passes of each antenna in a given week, not all are explicitly detailed here. Table 81 represents a subset of the possible combinations, where a portion of the trajectory is measured by the 70-m antenna and the 34-m antenna. The numbers of tracks in a week the same for either.

Table 81: Cost Estimates of Antenna Use Case Combinations

		3/Week	2/Week	1/Week	2/Month	1/Month
		70-m Passes				
30 Weeks of 70-m Antenna Use and 10 Weeks of 34-m Antenna Use						
3/Week	34-m Passes	$3,957,408	$2,536,800	$1,319,136	$811,776	$558,096
2/Week		$3,839,024	$2,418,416	$1,200,752	$693,392	$439,712
1/Week		$3,737,552	$2,316,944	$1,099,280	$591,920	$338,240
2/Month		$3,695,272	$2,274,664	$1,057,000	$549,640	$295,960
1/Month		$3,674,132	$2,253,524	$1,035,860	$528,500	$274,820
20 Weeks of 70-m Antenna Use and 20 Weeks of 34-m Antenna Use						
3/Week	34-m Passes	$3,044,160	$2,097,088	$1,285,312	$947,072	$777,952
2/Week		$2,807,392	$1,860,320	$1,048,544	$710,304	$541,184
1/Week		$2,604,448	$1,657,376	$845,600	$507,360	$338,240
2/Month		$2,519,888	$1,572,816	$761,040	$422,800	$253,680
1/Month		$2,477,608	$1,530,536	$718,760	$380,520	$211,400
10 Weeks of 70-m Antenna Use and 30 Weeks of 34-m Antenna Use						
3/Week	34-m Passes	$2,130,912	$1,657,376	$1,251,488	$1,082,368	$997,808
2/Week		$1,775,760	$1,302,224	$896,336.00	$727,216	$642,656
1/Week		$1,471,344	$997,808	$591,920.00	$422,800	$338,240
2/Month		$1,344,504	$870,968	$465,080.00	$295,960	$211,400
1/Month		$1,281,084	$807,548	$401,660.00	$232,540	$147,980

Recall, as detailed in Section 4.1.1.1, that the aperture fee for the amount of DSN antenna time is only one of several costs required to utilize the antenna. The cost estimates shown in Tables 79-81 are only estimates based on amount of tracking expected for the desired ground update accuracies in Table 47. It is known that traditionally the 70m antennas are reserved for critical events. The ground update values of the report do not reflect the use of the two antenna types in this manner or for the durations of the above tables. Information about the accuracy of orbit determination from use of DSN in the manner above is not readily available as prior missions were able to reserve and afford DSN use as needed for a Mars mission. Table 81 shows that there are cross over points where the number of weeks that the 70m antenna is used at certain rate can be less expensive despite more weeks of use depending on how it is combined with the 34m antenna. As more information becomes available for how deep space CubeSats will be supported by DSN, expected orbit determination accuracy is critical to refine expected mission capabilities and the associated cost.

17 Conclusions

17.1 General Summary

The key navigation question was how the navigation plan affected the dispersions. By varying the expected orbit determination accuracy based on different levels of DSN tracking and by allowing for onboard optical navigation at specified accuracies, it was possible to show how different navigation options affected the vehicle dispersions upon arrival at Mars.

The key trajectory concern was whether the arrival dispersions were acceptable. By comparing to prior missions, both their requirements and experiences, the analysis results were able to be deemed appropriate or not.

The key onboard mission planning issue was how well the Planner/Scheduler of DS1 be can be replicated on CubeSats so high-level mission goals could be met with onboard decisions. It was found that the DS1 Planner Scheduler demonstration was extremely limited, but that the AutoNav demonstration was more thorough and considered a success. LinCov as an onboard mission planner would be able to compare the effects of different navigation and guidance sequences. A LinCov onboard mission planner coupled with a program such as AutoNav would allow real -time selection of navigation and guidance options to best meet mission goals, thereby realizing a goal not met by actual DS1 flight experience.

The input parameters of the analysis done under this research were specified with respect to a CubeSat platform. An examination of the desired CubeSat capabilities, current hardware options, and expected hardware advancements showed that LinCov would be viable option as an onboard mission for the platform. In the near term, missions which provide lessons learned for the refinement of the onboard mission planner software would be worthwhile. In the meantime, LinCov can be used to determine the expected navigation error and trajectory dispersions expected for deep space CubeSats missions.

The report contributions were tracked in Section 3. The specifics for the navigation and guidance contributions are detailed in the findings of the cases examined.

17.1.1 The State of Industry Review

Section 4.3.1 summarized the needed advancements to accomplish onboard autonomy. The focus of this report was on a subset of industry-requested features to advance the confidence in automated guidance and navigation.

There are several major reasons why automated capabilities are suggested for the CubeSat platform. Section 4.1 detailed the motivation for including AGNC on deep space CubeSats, the primary reasons being the expense associated with traditional use of DSN and limited availability of expert ground support teams that determine spacecraft maneuvers. Regardless of the expense, the plans to support CubeSats with DSN does not include tracking them the same way as for prior missions. Instead, the DSN CubeSat plans assume that some onboard AGNC capabilities would be available so that missions are robust to lessened DSN use. Also, the science capabilities desired for deep space CubeSats require an increase in AGNC.

Only a subset of deep space missions have utilized AGNC. Of these, Deep Space 1 was the most relevant to this investigation as it used optical navigation during cruise and low-thrust propulsion. Some optical navigation methods were shown in Section 5.1 as well as use cases. Optical navigation has been refined over the past decades and is a cornerstone of onboard navigation. Onboard mission planning has even less inflight demonstration experience than AGNC.

It was shown that industry desires CubeSats with increased AGNC capabilities and that a number of prior missions have utilized optical navigation with and without onboard autonomy. Given this insight, comparison was performed of available commercial off-the-shelf CubeSat components to the features needed for AGNC. The methods and assumptions of the analysis, detailed in Section 7, reflect these examples. Current navigation and control components for CubeSats have been developed to a point where more difficult GNC missions can be attempted with reasonable confidence. The same hardware that was previously used for attitude determination could be used for optical navigation without an overhaul to the hardware. Some planned CubeSat missions include limited optical navigation capabilities, as shown in Section 2.

More CubeSat hardware is under development and coming online, which increases the ability to demonstrate onboard mission planning. Performing mission planning as well as guidance and navigation responsibilities onboard the vehicle requires increased storage and processing capabilities. The advancement of FPGAs means some calculations previously performed on the ground can now be performed onboard CubeSats. In 2008 NASA selected to fund an investigation for onboard processing algorithms on a high-end FPGA for use by an imaging system. The results showed "a proof-of-concept of the capabilities of the Virtex-5 FPGA to support the on-board processing requirements of future Interplanetary CubeSat missions" [59]. Additional hardware, including one-way radiometric and optical sensors can provide the navigation measurements needed for onboard orbit determination. "For a Mars orbiter, DSAC enabled one-way tracking on an uplink coupled with an on-board GNC system makes it possible to conduct autonomous operations and significantly reduce the ground support operations. [60]"

The concept of deep space CubeSats has, in part, been advanced by the development of electric thrusters for the platform. Due to the limited size of the CubeSat platform, electric thrusters are of extreme interest because they are very efficient. Applicable thruster technology for CubeSats are still under development, so their use on long-duration missions has not yet occurred. Because of this, information on how they perform during extended use is not available.

17.2 Cases Examined and Findings

Linear covariance analysis has historically been used prior to the preliminary vehicle design definition review to provide initial information to help define GNC system requirements, after PDR to confirm the results of nonlinear GNC system analysis, and during missions for orbit determination in order to select maneuver sequences to uplink to spacecraft. The generic setup for a linear covariance analysis was shown in Section 7.7.

Because deep space CubeSats are a new platform class which will utilize new technologies, the use of linear covariance to guide initial mission definition and selection is natural. Because linear covariance is computationally efficient, it has the potential to be used as an onboard mission planner. This bodes well for use on a CubeSat platform due to its limited resources and the previously stated desire to increase AGNC. As the linear assumption is valid so long as a system performs as expected and orbital dynamics typically keep objects near a nominal trajectory, LinCov is a reasonable method for a simple onboard mission planner. The analysis guidance and navigation methods are shown in Section 7.8.1 and Section 7.8.2, respectively. Section 7.8.4 provided a simple example of LinCov as an onboard mission planner to keep in mind while reviewing the analysis results. The nominal trajectory for a low-thrust CubeSat was defined in Section 7.9.

Examined first in Section 8 was the use of fixed time of arrival (FTOA) to target waypoints separated by two-week intervals. The ground updates accuracy assumed 3 DSN passes per week, the amount typically used during deep space cruise. The translational process noise is on the order of e-15. Including daily sighting of Mars in the navigation solution reduces the dispersion of BT and altitude by about half compared to use of ground updates exclusively. In either case the results are sufficient for attempting to target orbit insertion. The FPA dispersions are extremely poor, prohibiting any attempt to use these methods to achieve entry interface conditions needed for a successful landing.

Section 9 compares the dispersion and navigation error of the final trajectory correction segment for different ground update accuracies. The relationship between the amount of DSN tracking during cruise and approach and the ground update accuracies were defined. FTOA guidance over two week segments, with and without daily optical sightings, with the same translational process noise is used. Here it was shown that, with other factors held constant, reducing the amount of DSN tracking during cruise followed by increased DSN tracking during approach produced better results than higher amounts of DSN tracking during cruise that is not increased during approach. The analysis results were compared with the navigation uncertainty, achieved uncertainty, and requirements of prior landing and orbital Mars missions. Only when the approach ground updates were extremely accurate could prior FPA dispersions be met. The majority of the other ground update cases stayed within prior mission navigation and achieved uncertainty bounds, with optical navigation providing significant accuracy improvement. If the approach ground accuracy is not increased, the inclusion of daily optical sightings was still able to reach desirable dispersions, except for FPA, despite low ground update accuracy. The analysis results showed little difference between the dispersion and navigation error. This indicates the settings for the translational process noise and guidance segments were a good combination.

Section 10 compared the final segment results between FTOA and VTOA guidance for different ground update accuracies. When the approach ground update accuracy is not increased from the cruise ground update accuracy, there is minimal difference between the final guidance segment FTOA and VTOA analysis results. This relationship holds regardless of whether optical navigation is used or not though the inclusion of optical sightings does significantly reduce the dispersion level. When the approach DSN accuracy is increased during approach the VTOA analysis results are better for BT dispersions but FTOA results in better accuracy for the other parameters. Once optical navigation is joined with increased ground update approach accuracy, VTOA final segment results are better than the FTOA final segments in the B-Plane and the FPA dispersions, but are worse than FTOA for the altitude dispersions. The use of FTOA and VTOA are mostly interchangeable, but if lower altitude dispersions are of interest FTOA should be used.

Section 11 was an exploration of the minimization of deep space cruise DSN tracking supported with optical navigation while still meeting prior mission FPA dispersion values. Only with extremely accurate approach accuracy do desirable FPA dispersions and navigation errors result. So long as the ground update approach accuracy is extremely accurate, the deep space cruise portion of the trajectory can be extremely or exclusively dependent on optical navigation with daily sightings of Mars. Backing off to moderately accurate ground update approach accuracy increased the FPA dispersion and navigation error to outside of the desirable range. Other than for the FPA, the dispersion analysis results were within the bounds of the best of prior mission achieved and navigation uncertainty levels. This showed that the cruise segment could be highly dependent on optical navigation, but still match the most accurate of prior mission results so long as the approach applied high-accuracy ground updates.

The cases analyzed in Sections 8, 9, 10, and 11 all used the same initial trajectory dispersion, navigation error, translational process noise, and two-week guidance segments. Section 12 explored the effects of longer guidance segments which were timed to begin shortly after ground updates occur. The ground update accuracy was based on DSN passes at a rate of 3 per week. Different initial conditions for trajectory dispersions and navigation error are compared. The translational process noise was the same in each of the initial condition cases tested. The most accurate initial condition of this section is the same one which was used in prior sections. During the first half of the trajectories the analysis results are extremely different depending on the initial position and velocity dispersions. By the second half of the trajectory the results for each parameter are effectively the same no matter what the initial dispersion values were.

Section 13 compares the final segment results of different ground update accuracy cases when long guidance segments are used. The initial conditions of this section was the most accurate of the previous sections. While the navigation error results are similar to that of Section 9 when two-week guidance segments were used, there are noticeable differences between the dispersion results. When the approach ground update accuracy is increased, the FPA, altitude, and position dispersions are about five times worse when only ground updates are used and about two times worse when daily optical sightings of Mars are included compared to the two-week guidance segment results. When the ground update accuracy is not increased during the approach, the dispersion results when long guidance segments are used are much closer to the results when short guidance segments are used for each ground update accuracy level. That being said, two-week guidance segments still produce results with lower dispersion levels than longer guidance segments.

Section 14 explores the effects of different levels of translational process noise on the final segment dispersion results. When optical navigation is not included in the analysis, translational process noise level of about e-14 produces final segment results outside of the Odyssey altitude requirements for orbit insertion. The B-Plane dispersion corridor is comparable to the size expected for prior missions up to a translation process noise of e-12 with only ground updates. Once optical navigation is included, the final guidance segment meets the Odyssey orbit insertion altitude requirements for even the largest translational process noise of e-10. Only with optical navigation included and the lowest translational process noise is the Odyssey navigation uncertainty met. Compared to the results of Section 13, where it was shown that even with lower ground update accuracy and optical sightings the lowest translational process noise was able to meet the Odyssey navigation uncertainty, it becomes obvious how high translational process noise levels negatively impact the dispersion results. To assure meeting prior mission dispersion requirements, and prior navigation uncertainty levels, higher translational process noise must be avoided.

Section 15 included the Mission Planner example. Typically, the three guidance structures examined, 2-week segment FTOA, 2-week segment VTOA, and longer cruise segments FTOA experience the same dispersion levels. This pattern is kept except when the approach ground update accuracy is increased. When the same accuracy levels are met for each guidance type, the onboard mission planner would be able to consider secondary mission goals when down-selecting to the guidance type that should be applied.

The potential financial benefits from lowered DSN use is examined in Section 16. Unsurprisingly, the longer the mission, the greater the cost savings from decreased DSN use. For a 40-week mission to Mars, like the one examined in this report, hundreds of thousands to millions of dollars could be saved per mission.

Overall, it was found that FPA dispersions were extremely poor and outside of the bounds for standard entry-interface accuracy prior to EDL. It is not likely that with the ground approach accuracy and daily optical Mars sightings examined here that EDL entry-interface would be successful. Other parameters, such as B-Plane and altitude dispersions were much more robust so missions which do not have critical FPA dispersion requirements will likely be well supported by the platform. The overall trade explored was the cost savings from reduced DSN tracking versus the dispersions experienced at the target. It was found that the increased affordability from less DSN use was worthwhile as desirable dispersions at the target still occurred for orbit insertion.

17.3 Mission Recommendations

Section 5.1.2.1 showed an overview of the progression of optical navigation spacecraft experiments starting from the 1970s to today. There has not been much use of autonomous guidance and navigation aboard spacecraft during cruise since the DS1 demonstration. Though the algorithms, referred to as AutoNav, have been refined, they have not been coupled with an intelligent decision making program such as an onboard mission planner. The recommended missions follow the incremental progression of more complex mission demonstrations which occurred with optical navigation. This is to increase knowledge on the performance of low-thrust propulsion, the performance of AGNC during a low-thrust cruise, and the benefits and capabilities of a rudimentary onboard mission planner. Section 0 summarized the prior Mars landing and orbiter mission requirements, navigation uncertainty, and achieved uncertainty. More recent missions had tighter requirements and better than expected performance compared to earlier missions. In the same manner, useful demonstration of CubeSat missions with AGNC capabilities should initially have larger dispersion requirements which are decreased as missions are successfully completed.

Any new AGNC and OMP software should first run in a background of a mission which uses traditional DSN tracking and ground support. The results of the software would be downlinked so that issues with the software could be identified before a mission wholly dependent on it occurs. Such an experiment could occur on a low-thrust CubeSat demonstration so that concurrently the new propulsion technology would also increase its flight heritage and be better understood. There is a two-fold benefit here: 1) better modeling of the low-thrust propulsion would be possible thus decreasing the translational process noise, 2) better onboard processing hardware under development could become available by the end of the preliminary mission allowing more onboard software useful to an OMP to be demonstrated.

Section 14 showed that with ground updates accuracies associated with traditional levels of DSN tracking of 3/Week, the low-thrust system could meet orbit insertion requirements if the translational process noise was low. With optical navigation capabilities, prior mission orbit insertion requirements could be met for scenarios with the translational process noise spanning the range considered and with standard ground update accuracies. The caveat with this is that the optical navigation system accuracy utilized assumed the use of an extremely well characterized camera where no issues are experienced during the mission. Section 5.1.2 detailed several types of camera issues which can occur that decrease the optical navigation solution accuracy. In addition, as mentioned previously, it is unlikely a CubeSat mission will have access to DSN tracking at the standard rate. For these reasons, an initial demonstration should likely only seek to achieve a broad target corridor.

For any mission, a nominal trajectory robust to mild modifications is suggested. This is in part due to the state of the CubeSat platform capabilities. CubeSat hardware is still being refined and differences between expected performance and actual performance have been relatively commonplace. Utilizing a nominal trajectory that is dependent on nearly ideal component performance could easily result in additional complications likelihood of necessitating mid-flight a new nominal trajectory to be determined on the ground and uplinked to the craft. The need to determine a new trajectory on the ground for early CubeSat missions would be expected due to the limited processing capabilities. In addition, it is important that a missed ground update or ground update at a decreased accuracy level should not be catastrophic to mission success. While the proposed ground team structure of Section 7.2 was defined to lower their responsibilities for a CubeSat mission utilizing AGNC, it is possible that even the proposed, reduced level of ground support could be disrupted and reduced in favor of priorities driven by the needs of other missions.

17.4 Significance

This report met key recommendations of the Autonomy GNC Industry Survey of [23]. First, this is a study of GNC system level analysis not overly focused on individual algorithms or hardware for the new mission type that would apply deep space CubeSats. The derived results enable better deep space CubeSat mission planning as limited GNC information was previously available for this platform class, especially when considering use of low-thrust propulsion.

LinCov was used here not just for navigation analysis but for guidance analysis as well. As such, this was a closed loop demonstration. This facilitated examination of the limitations of poor propulsion system modeling and the benefits of refined propulsion system modeling on mission capabilities. As more is learned about the capabilities of CubeSat components now available and under development, the LinCov analysis can be refined to reflect these changes, increasing resulting analysis fidelity. Consequently, LinCov analysis meets the recommendation for a system analysis capability that can account for the latest advancements of the desired platform.

The recommendation which drove the primary focus of the report was to "[invest] in autonomous GN&C capability, with parallel investments in innovative architectures, innovative and optimized algorithms, advanced sensors and actuators, and system-level demonstrations with relevant physical dynamics and environment conditions. [23] " This report hit all of these key points, including showing benefits from the inclusion of AGNC and optical navigation, and demonstrating that a new ground support architecture could be successfully applied that would allow ground team members to spend less time on individual CubeSat missions. The research also considered sensor and propulsion characteristics advancements expected for CubeSat hardware as part of a system level demonstration to show the benefits of integrating all of these features.

This report provided an assessment of the OD accuracy which could be expected for deep space CubeSats with application of the proposed level of DSN tracking. A starting point for the spacing of trajectory correction maneuvers for new deep space CubeSat missions was also included. Regardless of whether AGNC or an onboard mission planner is used, the analysis provided new information about how the planned DSN CubeSat support can impact a mission's capability to enable better structuring of deep space CubeSat concepts of operation to reflect what capability and performance a CubeSat mission should expect. The literature lacks thorough studies of guidance and navigation in line with NASA's plans and desires for CubeSat missions. In addition, the GNC development which has occurred for CubeSats has typically focused on the construction of individual hardware components rather than realizable mission performance. This study bridges the gap between NASA's plans and desires and the hardware development which has occurred for CubeSats.

This work is significant because it has a system focus and also because it shows the LinCov software program can have multiple uses for CubeSat mission including: preliminary design requirement recommendations; covariance and dispersion analysis during missions for maneuver planning; providing an important part of an OMP capability applicable to the needs of the deep space platform and able to function within current processing capabilities. Combined with nominal flight plans and mission goals onboard the craft, LinCov analysis can provide the GNC analysis capabilities needed by an onboard mission planner. During CubeSat missions, LinCov could also be used on the ground (manually) to compare action plans and to finalize the maneuver sequence to uplink to crafts. Because of the computational efficiency of LinCov, this would be a rapid comparison method.

This work is also significant because it provides a jumping off point for higher fidelity, future AGNC and OMP work. Selecting an action plan by comparing different guidance and navigation setups for the same conditions at a given time was possible because of the numerous dispersion and navigation results derived with LinCov. Minimally, the implementation of a LinCov OMP could be a suitable backup program should a mission experience any unexpected decrease of ground support or DSN measurements

Without some AGNC backup the dispersions experienced by a mission could diverge, necessitating a significantly altered nominal trajectory or resulting in the loss of the mission. This report has shown that basic optical navigation such as the sighting of one target throughout the mission is extremely beneficial, and that use of LinCov results for a mission highly dependent on optical navigation throughout cruise can meet orbit insertion target dispersion bounds. This finding is contingent on use of ground support when the vehicle is near the target on par with that applied during approach for prior missions. As backup, AGNC/OMP system capabilities are valuable for deep space CubeSats which may have limited ground support nominally. This report has shown a LinCov to be a viable option for such a purpose as a CubeSat backup or primary system which could offer lessons learned to more advanced intelligent/autonomous programs under development.

This research has touched on several industry requests so that CubeSats can be utilized to accomplish significant science in deep space. The LinCov analysis can be used to provide new CubeSat programs with more expected guidance and navigation performance information than was previously possible. This research found that with an onboard, LinCov-based OMP alterations to the current ground support practices can be made that lessen the workload for CubeSat missions, thereby allowing new mission types and increased mission numbers. The analysis showed the ability to accomplish desirable missions with lessened use of DSN compared to traditional methods; in turn, the identified cost savings increases the viability of deep space CubeSats with the adoption of minimally AGNC but preferably the capabilities shown of LinCov OMP.

18 Recommendations for Future Work

The recommendations for future work fall into three categories:

1. Increasing the fidelity of the LinCov analysis for deep space CubeSat platforms
2. Additional software programs beneficial to the increased autonomy desired by industry
3. Desirable closed-loop GNC system analyses

18.1 Increasing LinCov Deep Space CubeSat Analysis Fidelity

One of the primary areas which needs improvement is the characterization and modeling of new low-thrust propulsion for CubeSat systems. Trajectory dispersion results can be very different with minor changes in the translational process noise. Information such as expected propulsion system degradation over time could be within LinCov analysis to represent resulting trajectory stochastic characteristic trends. While information about the nominal performance of some CubeSat thrusters can be found, details regarding their performance variances are harder to come by.

Another important investigation area is optical navigation options. This research analysis only showed the effects from using one particular optical target throughout the mission. An alternative approach would be to observe the geometry expected by sighting different targets (e.g., other planets, moons, and asteroids with known ephemeris characteristics). Consideration of use of this alternative approach would involve a trade regarding any navigation performance gains against the challenges (and mission mass penalties) of enabling observation of multiple targets. More advanced optical navigation could enable account for the diameter of a body when it can be resolved, which could be extremely beneficial during the approach phase to a target. While the accuracy of the optical navigation considered in this research was deemed reasonable based on currently available hardware and processing algorithms, coordination with optical component manufactures to get the best possible hardware performance models (including for off-nominal conditions) to use in updated analysis would increase confidence in the use of optical navigation.

While the nominal trajectory used in this report included changes to the power available and therefore to the propulsion system thrust output, it would be of interest to enable onboard account for a degraded thrusting system performance effective for part of the trajectory to represent possible component condition changes. This could be done with a timed trigger as described earlier (e.g., based on expected propulsion system degradation effects with use). The generation of a new nominal trajectory would also be of interest. A new nominal trajectory could be required due to performance perturbation issues with the propulsion system, an evolving understanding of how a propulsion system is actually performing in flight, or due to altered mission objectives.

The ground update accuracies resulting from different frequencies of DSN tracking that were discussed in the thesis were based on prior mission tracking, prior mission results and professional recommendations. DSN tracking measurements are put into the orbit determination programs available to the ground team. An analysis should be performed with the orbit determination programs used on an actual mission to check how the results would change if only a subset of the measurements were used. Previously, there has not been a reason to perform such an analysis; but, as more interplanetary CubeSats come online, the resulting orbit determination accuracy from decreased DSN measurement availability will be vital to representing the realizable navigation system performance with increased confidence. With a refined ground update accuracy estimate available, the cost associated for subsequent missions could be refined as well. The final refinement associated with DSN for CubeSats is the initial trajectory dispersions and navigation error that can be expected when the CubeSats are not the primary mission, but an ability to check out the satellite and provide an optimal nominal trajectory is still needed.

18.2 Additional Software Programs of Interest

A flight software version of LinCov OMP needs to be developed based on the desktop analysis version used in this report. LinCov OMP has been shown to be a viable option to increase onboard mission management robustness it would need further development to be suitable for onboard use.

Fault Detection Isolation and Recovery (FDIR) capabilities could be used to provide additional inputs to an OMP. Information about the state of sensors and actuator performance as they are altered is essential for an OMP to be able to select the best course of action. Without such information, the performance characterization derived from LinCov results would not be accurate. Even if the LinCov analysis covers a variety of scenarios, some of which represent potential degraded or failed component, if the OMP does not have FDIR information readily available, it may lead to choosing a correct action based on resulting expectations but not based on what is actually occurring onboard.

Though the optical navigation hardware available for CubeSats is already suitable for use, the advancement of optical navigation algorithms is desirable. Optical navigation requires a variety of filtering and calculations to perform orbit determination. Optimizations of the algorithms for use on a CubeSat platform that account both or the current limitations in processing and expected advancements would enable deep space CubeSats to evolve their use of optical navigation in a manner similar to prior, larger platform missions.

Development of a targeting scheme that is robust and also able to be represented in LinCov is needed for deep space CubeSats. As LinCov requires a nominal trajectory, a targeting scheme that at least checks the viability of the current trajectory and provides a feasible option until an optimal one can be provided from the ground would increase the assurance of mission success.

18.3 Desirable Closed-Loop GNC System Analyses

Though low-thrust propulsion is of primary interest for the CubeSat platform, an investigation that assumes impulsive propulsion is also desired. The benefit of low-thrust propulsion is that it affords many opportunities to refine the trajectory. Impulsive cases have a few extremely critical usage points for missions similar to the ones considered here. Though prior deep space missions have generally used impulsive propulsion, these missions all relied on extensive support from DSN. With the uncertain reliability of DSN tracking for low priority CubeSat missions, it would be of interest to check on the ability to accommodate likely dispersions effects and altered navigation system needs for CubeSats using impulsive propulsion.

Additional LinCov analysis cases should be assessed for low-thrust deep space CubeSats. This should include varying ground update accuracy conditions. More optical navigation accuracy cases should be evaluated to help refine sensor and algorithm development needs. Another hardware area of interest is one-way radio navigation. Unlike traditional radio navigation, one-way radio navigation could take advantage of DSN tracking in a more passive manner and then use the measurements to calculate onboard state information. Finally, a more thorough LinCov OMP demonstration would be beneficial as the simple LinCov OMP deserve considerations for a flight demonstration.

19 Works Cited

[1] S. Spangelo and D. Dalle, "Integrated Vehicle and Trajectory Design of Small Spacecraft with Electric Propulsion for Earth and Interplanetary Missions," in *29th Annual AAA/USU Conference on Small Satellites*, Logan, Utah, 2015.

[2] A. Klesh and J. Krajewski, "MarCO: CubeSats to Mars in 2016," in *29th Annual AIAA/USU Conference on Small Satellites*, Logan, Utah, 2015.

[3] L. McNutt, L. Johnson, D. Clardy, J. Castillo-Rogez, A. Frick and L. Jones, "Near-Earth Asteroid Scout," in *AIAA Space 2014 Conference and Exposition*, San Diego, 2014.

[4] W. Huffman, *Autonomous Science Applications on Robotic Spacecraft,* Cambridge, MA: JPL, 2015.

[5] R. L. Staehle and e. al, "Interplanetary CubeSats: Opening the Solar System to a Broad Community at Lower Cost," *Journal of Small Satellites,* pp. 161-186, 2013.

[6] S. Chien and e. al., "Flight Validating the Proposed HypIRI Intelligent Payload Module: Results from Intelligent Payload EXperment (PEX) CubeSat Operations," in *JPL Symposium Day 2*, LA, 2014.

[7] S. Spangelo and e. al., "JPL's Advanced Interplanetary CubeSat Concepts for Science and Technology Demonstrations," in *Interplanetary Small Satellite Conference*, Santa Clara, CA, 2015.

[8] M. S. Ryne, E. Graat, R. Haw, G. Kruizinga, E. Lau, T. Martin-Mur, T. McElrath, S. Nandi and B. Prtock, "Orbit Determination for the 2007 Mars Phoenix Lander," in *AIAA/AAS Astrodynamics Specialist Conference and Exhibit*, Honolulu, Hawaii, 2008.

[9] P. Kallemeyn, D. Spencer, R. Vaughan and C. Helfrich, "The Mars Pathfinder Navigation System," in *AIAA/AAS Astrodynamics Conference*, Reston, VA, 1996.

[10] P. H. J. Kallemeyn, P. C. Knocke, P. D. Burkhart and S. W. Thurman, "NAVIGATION AND GUIDANCE FOR THE MARS SURVEYOR '98 MISSION," *American Institute of Aeronautics and Astronautics,* pp. 471-481, 1998.

[11] L. A. D'Amario, "Mars Exploration Rovers Navigation Results," in *AIAA/AAS Astrodynamics Specialist Conference and Exhibit*, Providence, RI, 2004.

[12] T. J. Martin-Mur, G. L. Kruizinga, P. D. Burkhart, F. Abilleira, M. C. Wong and J. A. Kangas, "Mars Science Laboratory Interplanetary Navigation," *Journal of Spacecraft and Rockets,* pp. 1014-1028, 2014.

[13] Jet Propulsion Laboratory, "DSN Mission Support Definition & Commitments : Mission Introduction to the DSN," National Aeronautics and Space Administration , California, 2015.

[14] NASA, "NASA's Mission Operations and Communication Services," NASA, 2009.

[15] P. G. Antreasian, R. M. Beswick, K. E. Criddle, R. Ionasescu, R. A. Jacobson, J. B. Jones, R. A. MacKenzie, D. W. Parcher, F. J. Pelletier, D. C. Roth, P. F. Thompson and A. T. Vaughan, "Orbit Determination Processes for the Navigation of the Cassini-Huygens Mission," *SpaceOps 2008 Conference,* pp. 1-18, 2008.

[16] G. Elliott, March 2016. [Online]. Available: http://deepspace.jpl.nasa.gov/files/dsn/DSN%20Current%20Mission%20Set%209_30_15.pdf.

[17] L. Deutsch, "IND Communications Policy," in *IND CubeSat Briefing/Technical Exchange*, California Institute of Technology, 2015.

[18] E. Basillio, "Mission System Overview," in *IND CubeSat Briefing/Technical Exchange*, California Institute of Technology, 2015.

[19] D. Abraham, "Stratefy for Cubesats and the DSN," in *IND CubeSat Briefing/Technical Exchange*, Califaornia Institute of Technology, 2015.

[20] F. Manshadi and F. Mogan, "Spectrum Management," in *IND CubeSat Briefing/Technical Exchange*, California Institute of Technology, 2015.

[21] J. Berner, "DSN Approach and Anomoly Response," in *IND CubeSat Briefing/Technical Exchange*, California Institute of Technology, 2015.

[22] M. B. Quadrelli, L. J. Wood, J. E. Riedel, M. C. McHenry, M. Aung, L. A. Cangahuala, R. A. Volpe, P. M. Beauchamp and J. A. Cutts, "Guidance, Navigation, and Control Technology Assessment for Future Planetary Science Missions," *Journal of Guidance, Control, and Dynamics,* vol. 38, no. 7, pp. 1165-1186, July 2015.

[23] J. E. Riedel and M. Aung, "Guidance, Navigation, and Control Technology Assessment for Future Planetary Science Missions Part 2: Onboard Guidance, Navigation, and Control (GN&C)," Pasadena, 2013.

[24] D. B. LaVallee, J. F. Jaconsohn, C. D. Olsen and J. Schmoll, "Autonomous Spacecraft Control - An Industry Survey Update," in *AIAA 2007 Conference and Exhibit*, Rohnert Park, CA, 2007.

[25] N. Muscettola, B. Smith, C. Fry, S. Chien, K. Rajan, G. Rabideau and D. Yan, "On-Board Planning for New Millennium Deep Space One Autonomy," *IEEE,* pp. 303-318, 1997.

[26] S. Bhaskaran and e. al, "Orbit Determination Performance Evalutation of the Deep Space 1 Autonomous Navigation System".

[27] S. Bhaskaran, "Autonomous Navigation for Deep Space Missions," *American Institute of Aeronautics and Astronautics,* 2012.

[28] V. H. Adams and M. Peck, "Interplanetary Optical Navigation," in *AIAA Guidance, Navigation, and Control Conference*, San Diego, 2016.

[29] W. M. Owen Jr, "Methods of Optical Navigation," in *AIAA/AAS Spaceflight Mechanics Conference*, New Orleans, 2011.

[30] M. Vasile, F. Sironi and F. B. Zazzera, "Deep Space Autonomous Orbit Determination Using CCD," in *AIAA/AAS Astrodynamic Specialist Conference*, Monterey, 2002.

[31] J. D. Vedder, "Autonomous Position and Velocity Determination in Interplanetary Space," 1992.

[32] E. Riedel, "NASA Experience with Automated and Autonomous Navigation in Deep Space," in *WE-Heraeus Seminar*, Physikzentrum Bad Honnef Germany, 2015.

[33] R. M. Vaughan, J. E. Riedel, R. P. Davis, W. M. Owen and S. P. Synnott, "Optical Navigation for the Galileo Gaspra Encounter," *AIAA,* pp. 361-369, 1992.

[34] R. Ionasescu, "Orbit Determination Covariance Analysis for the Cassini Solstice Mission," in *AIAA/AAS Astrodynamic Specialist Conference*, Toronto, 2010.

[35] JPL, "Mission: Optical Camera," [Online]. Available: http://mars.nasa.gov/mro/mission/instruments/opticalnav/. [Accessed 21 2 2016].

[36] R. J. Cesarone, "Voyager 1 Saturn Targeting Strategy," in *AIAA/AAS Astrodynamics Conference*, Danvers, MA, 1980.

[37] S. Bhaskaran, "Autonomous Navigation for Deep Space Missions," *Cal Tech,* 2012.

[38] P. J. Neirinckx, "Autonomous Onboard Guidance and Navigation Performance for Earth to Mars Transfer Missions," Massachusetts Institute of Technology, Cambridge, MA, 1992.

[39] P. G. Antreasian, D. T. Baird, J. S. Border, P. D. Burkhart, E. J. Grant, M. K. Jah, R. A. Mase, T. P. McElrath and B. M. Portock, "2001 Mars Odyssey Orbit Determination During Interplanetary Cruise," in *AIAA/AAS Astrodynamics Specialist Conference and Exhibit*, Moneterey, CA, 2002.

[40] F. J. Hale, Introduction to Space Flight, Upper Saddle River, NJ: Prentice Hall, 1994.

[41] C. D'Souza, "Hyperbolic (B-Plane) Parameters and Partials for the Orion Earth-Moon Missions (Document # FltDyn-CEV-15-27)," NASA JSC, Houston, 2015.

[42] I. Alizadeh and B. F. Villac, "Sensitivity Reduction and Lifetime Extension of Power-Limited Low-Thrust Trajectories," *Journal of Guidance, Control, and Dynamics,* vol. 36, no. 1, pp. 218-228, Jan-Feb 2013.

[43] J. Gil-Fernandez and M. A. Gomez-Tierno, "Optimal Guidance of Low-Thrust Trajectories," *Journal of Guidance, Control, and Dynamics,* vol. 33, no. 6, pp. 1913-1917, Nov-Dec 2010.

[44] "BCT XACT Lite Datasheet," Blue Canyon Technologies, [Online]. Available: http://bluecanyontech.com/wp-content/uploads/2015/12/BCT-XACT-Lite-Datasheet.pdf. [Accessed 16 4 2016].

[45] "BCT Extended Nano Star Tracker," Blue Canyon Technology, [Online]. Available: http://bluecanyontech.com/wp-content/uploads/2015/12/Ext-Baffle-NST-Data-Sheet_1.1.pdf. [Accessed 16 4 2016].

[46] D. N. Sinclair, "Second Generation Star Tracker (ST-16RT)," Sinclair Interplanetary, [Online]. Available: http://www.sinclairinterplanetary.com/startrackers. [Accessed 16 4 2016].

[47] "ECAM Imaging System," Malin Space Science Systems, [Online]. Available: http://www.msss.com/brochures/ecam.pdf. [Accessed 16 4 2016].

[48] D. K. Geller, "Linear Covariance Techniques for Orbital Rendezvous Analysis and Autonomous Onboard Mission Planning," *AIAA,* 2006.

[49] D. Woffinden, "LinCov Training: How to Build a Simple LinCov Simulation," Draper Laboratory, Houston, 2015.

[50] B. A. Smith, C. A. Vanelli and A. Y. Lee, "Understanding Spacecraft Agility for Orbit Transfers on the Dawn Low-Thrust Mission," in *Guidance and Control 2012 - Advances in Astronautical Sciences: Proceedings of the 35th Annual AAS Rocky Mountain Section Guidance and Control Conference*, 2012.

[51] A. E. Bryson Jr and Y.-C. Ho, Applied Optimal Control, Revised ed., Washington DC: Hemisphere Publishing Corporation, 1975.

[52] D. Fiehler and C. Kluever, "Compensaor Design for Low-Thrust Interplanetary Missions," in *AIAA/AAS Astrodynamics Specialist Conference and Exhibit*, Monterey, CA, 2002.

[53] B. A. Steinfeldt and P. Tsiotras, "A State-Dependent Riccati Equation Approach to Atmospheric Entry Guidance," in *AIAA Guidance, Navigation, and Control Conference*, Toronto, 2010.

[54] B. Polle, B. Frapard, J. Gil-Fernandez, M. Grazano, J. Rebordao and P. Motrena, "Autonomous Navigation For Interplanetary Missions Performance Achievements based on Real and Flight imag," in *Proceedings of the 6th International ESA Conference on Guidance, Navigation and Control Systems*, Loutraki, Greece, 2005.

[55] C. D'Souza, "Terminal Guidance Controllers," Houston, 2006.

[56] D.-H. Cho, H. Bnag and H.-D. Kim, "Trajectory Correction Maneuver Design based on B-plane Targeting for Low-thruster," in *International Conference on Control, Automation and Systems*, Gwangju, Korea, 2013.

[57] R. H. Battin, An Introduction to the Mathematics and Methods of Astrodynamics, Revised Edition, Reston, VA: AIAA, 1999.

[58] D. H. Ellison, J. Englander and B. Conway, "Numerical Computation of a Continuous-Thrust State Transition Matrix Incorporating Accurate Hardware and Ephemeris Models," in *AAS/AIAA Space Flight Mecanics Meeting; 25th*, Williamsburg, VA, 2015.

[59] R. L. Staehle, D. Blaney, H. Hemmati, D. Jones, A. Klesh, P. Liewer, J. Lazio, M. Wen-Yu Lo, P. Mouroulis, N. Murphy, P. J. Pingree and T. Wilson, "Interplanetary CubeSat Architecture and Missions," in *AIAA Space 2012 Conference & Exposition*, Pasadena, CA, 2012.

[60] T. A. Ely and J. Seubert, "One-Way Radiometric Navigation with the Deep Space Atomic Clock," in *AAs/AIAA Space Flight Mechanics Meeting*, Napa, CA, 2015.